Addendum D

Final Remedial Action Plan
DOE-EM/GJ1547
July 2008

Final Design Calculations

Number	Title	
C-02	Disposal Cell Erosion Protection	
C-03	Wedge Longevity	
C-04	Area Between Cell and Wedge	
C-05	Radon Barrier Evaluation	
C-06	Drainage During First Phase of Construction	
C-10	Slope Stability of Crescent Junction Disposal Cell	
C-11	Settlement Analysis of Uranium Mine Tailings at Crescent Junction, UT	
C-12	Liquefaction Analysis of Uranium Mine Tailings Repository at Crescent Junction, UT	
C-13	Frost Penetration Depth at Crescent Junction Disposal Site	
C-15	Analysis for Cover Cracking of the Crescent Junction Disposal Cell	

JACOBS	Calculation No: C-02	Page 1 of 17 – Plus Appendices 40 Pgs
Calculation Cover Sheet	Rev. No.: 0	Revision Date:
(Ref. FOWI 116 Design Calculations)	Previous Revision Date:	Current Revision Date:1/09/08
Issuing Department: *Federal Operations Design Engineering*	Supersedes:	
Client: Energy solutions Project Title: Moab UMTRA Project Number: 35DJ2600 System:	Engineering Discipline: Civil	
Calculation Title: Disposal cell Erosion Protection		

Purpose:

Determine the rock protection required to protect the cover of the Crescent Junction disposal cell from erosion due to precipitation directly on the cell to meet the specifications of the *Code of Federal Regulations* (CFR) (40 CFR part 192).

NQA-1 QUALITY LEVEL: 2

Prepared by: Bob Yager Robert E. Yager Date: 1/09/08

Checked by: Bill Barton Bill Barton Date: 1/25/08

Engineering Managers Approval: Bill Barton Date: 1/25/08

The current applicable version of this publication resides on Jacobs' Intranet. All copies are considered to be uncontrolled.
Copyright© Jacobs Engineering Group Inc., 2007

Revision History:

Pages Affected By Revision	Revised/Added/Deleted	Description of Revision
All		

The current applicable version of this publication resides on Jacobs' Intranet. All copies are considered to be uncontrolled.
Copyright© Jacobs Engineering Group Inc., 2007

Description of Calculation:

- Determine the peak unit discharge from the Probable Maximum Precipitation (PMP) using methods given in the UMTRA TAD (DOE 1989).
- Calculate the required rock size (D50) on the top slope of the disposal cell using the Safety Factor method (Nelson et al. 1986).
- Calculate the required rock size (D50) on the side slopes of the disposal cell using Abt and Johnson method (Abt and Johnson 1991).
- Calculate the required rock size (D50) for the toe apron to accommodate flow transitioning from cell slope to native ground using the method proposed by Abt et al. (1998).
- Evaluate the scour potential of flow from the toe apron using methods in NUREG 1623 (Johnson 2002) and U.S. Department of Transportation (1983).
- Evaluate the need for a bedding layer between cover soils and erosion protection material by estimating interstitial pore velocities using the method proposed by Abt and Johnson (1991).

Assumptions:

- The PMP precipitation event is applicable for long-term erosional stability analyses.
- The 1-hour PMP event is estimated to be 8.2 inches, ("Site Drainage—Hydrology Parameters" calculation, Draft RAP Attachment 1, Appendix E).
- Rock available for erosion protection will be angular, have a specific gravity of 2.65, and will meet Nuclear Regulatory Commission (NRC) durability requirements.
- For the PMP precipitation event, all the rainfall runs off during the peak rainfall intensity (C=1.0 for the Rational Method).

The current applicable version of this publication resides on Jacobs' Intranet. All copies are considered to be uncontrolled.
Copyright© Jacobs Engineering Group Inc., 2007

Design Inputs:

Software:

Title	Developer	Versions	Revision Level
EXCEL	Microsoft	2002	

The current applicable version of this publication resides on Jacobs' Intranet. All copies are considered to be uncontrolled.
Copyright© Jacobs Engineering Group Inc., 2007

Calculation Section:

See Following text

The current applicable version of this publication resides on Jacobs' Intranet. All copies are considered to be uncontrolled.
Copyright© Jacobs Engineering Group Inc., 2007

Conclusions/Recommendations:

See following text.

Reference:

See following text.

The current applicable version of this publication resides on Jacobs' Intranet. All copies are considered to be uncontrolled.
Copyright© Jacobs Engineering Group Inc., 2007

DESCRIPTION OF CALCULATION:

Determine the rock protection required to protect the cover of the disposal cell from erosion due to precipitation directly on the cell to meet the specifications of the *Code of Federal Regulations* (CFR) (40 CFR part 192).

METHOD OF SOLUTION:

- Determine the peak unit discharge from the Probable Maximum Precipitation (PMP) using methods given in the UMTRA TAD (DOE 1989).
- Calculate the required rock size (D50) on the top slope of the disposal cell using the Safety Factor method (Nelson et al. 1986).
- Calculate the required rock size (D50) on the side slopes of the disposal cell using Abt and Johnson method (Abt and Johnson 1991).
- Calculate the required rock size (D50) for the toe apron to accommodate flow transitioning from cell slope to native ground using the method proposed by Abt et al. (1998).
- Evaluate the scour potential of flow from the toe apron using methods in NUREG 1623 (Johnson 2002) and U.S. Department of Transportation (1983).
- Evaluate the need for a bedding layer between cover soils and erosion protection material by estimating interstitial pore velocities using the method proposed by Abt and Johnson (1991).

ASSUMPTIONS:

- The PMP precipitation event is applicable for long-term erosional stability analyses.
- The 1-hour PMP event is estimated to be 8.2 inches, ("Site Drainage—Hydrology Parameters" calculation, Draft RAP Attachment 1, Appendix E).
- Rock available for erosion protection will be angular, have a specific gravity of 2.65, and will meet Nuclear Regulatory Commission (NRC) durability requirements.
- For the PMP precipitation event, all the rainfall runs off during the peak rainfall intensity (C=1.0 for the Rational Method).

The current applicable version of this publication resides on Jacobs' Intranet. All copies are considered to be uncontrolled.
Copyright© Jacobs Engineering Group Inc., 2007

Figure 1. Disposal Cell Layout

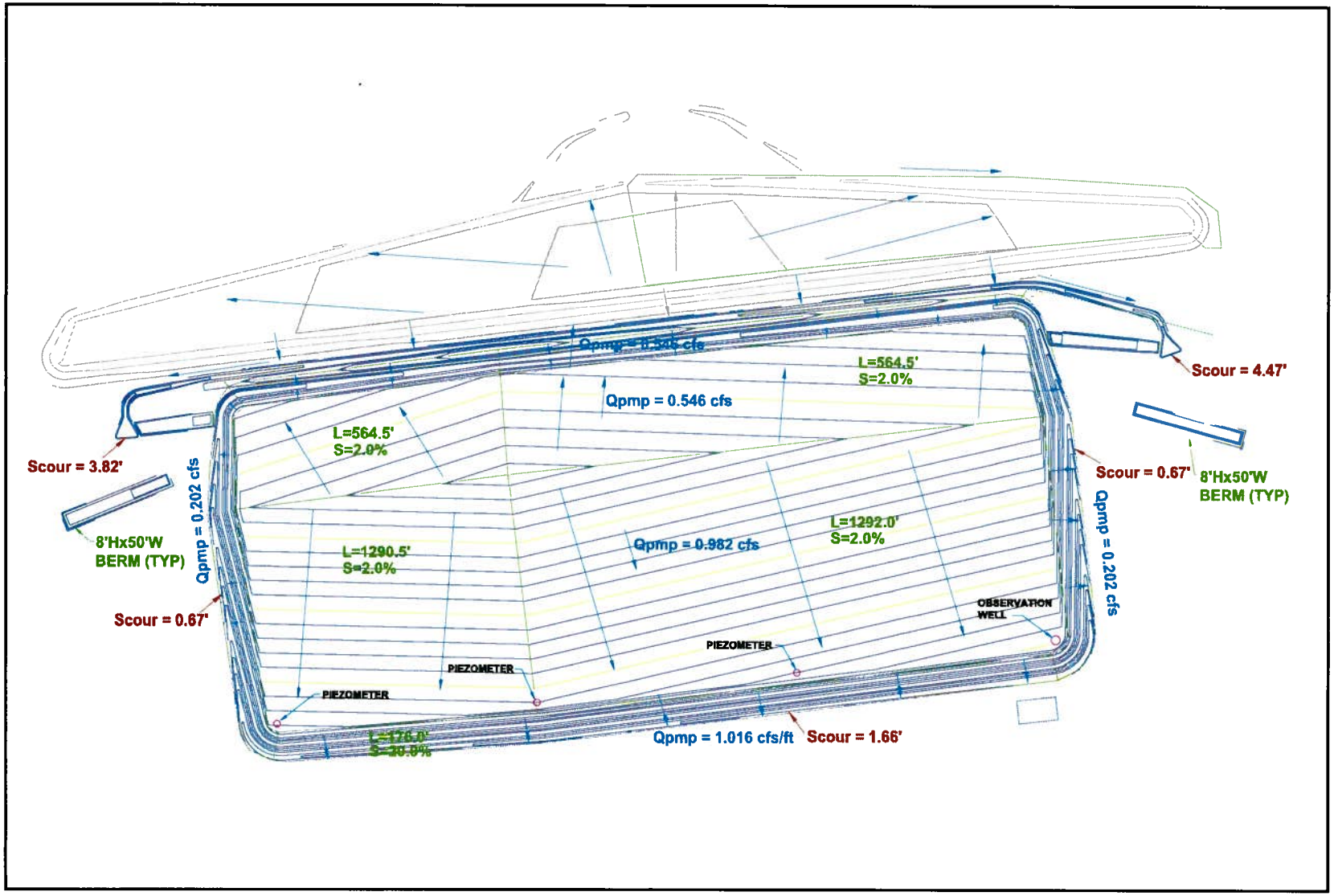

CALCULATION SECTION:

SPREADSHEETS WHERE CALCULATIONS WERE PERFORMED INCLUDED IN THIS CALCULATION PACKAGE ARE. CELLRIPRAP.XLS AND APRONSCOUR.XLS.

Drainage Area Characteristics

The layout of the disposal cell is shown in Figure 1. A cross section from the top to the apron on the south side is shown in Figure 2. The cell will have a 2 percent top slope, 5:1 (horizontal:vertical) side slopes, and a total footprint area of 251 acres.

Six drainage areas were delineated on the cover of the disposal cell, as shown in Figure 1. The area and flow length of these drainage areas were calculated using computer-aided design (CAD) tools.

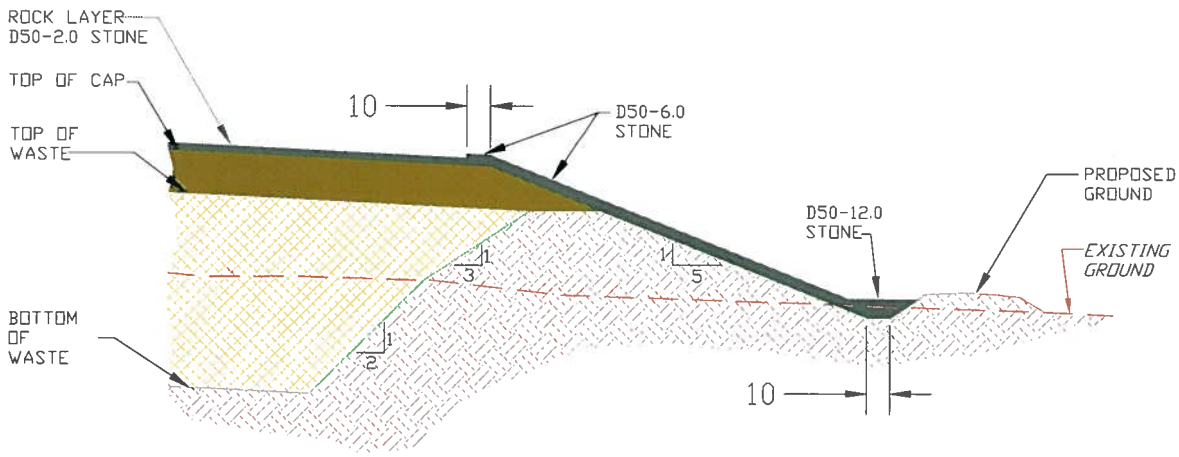

Figure 2 Cross section of the south slope of the waste cell.

Peak flows occurring within each drainage area are calculated using a rainfall duration equivalent to the time of concentration for each drainage basin. The time of concentration is a characteristic of the geometry and slopes of the drainage areas, and is computed by three different methods, with the average of the three methods used to calculate peak discharges. The three methods used to calculate the time of concentration are described below. The mean of the three times calculated was used as the time of concentration in runoff calculations.

1) The Kirpich equation as presented in NUREG/CR-4620 (Nelson et al. 1986):

$$T_c = 0.0078 \frac{L^{0.77}}{S^{0.385}}$$

The current applicable version of this publication resides on Jacobs' Intranet. All copies are considered to be uncontrolled.
Copyright© Jacobs Engineering Group Inc., 2007

where:

T_c = time of concentration (minutes),

L = slope length (feet [ft]), and
S = slope (ft/ft).

2) The Soil Conservation Service (SCS) Triangular Hydrograph Theory, as presented in NUREG/CR-4620 (Nelson et al. 1986):

$$T_c = \left(\frac{11.9L^3}{H}\right)^{0.385}$$

where:

T_c = time of concentration (hours),
L = slope length (miles), and
H = slope height (ft).

3) The Brant and Oberman equation as presented in the Uranium Mill Tailings Remedial Action Project (UMTRA) Technical Approach Document (TAD) (DOE 1989):

$$T_c = C\left(\frac{L}{Si^2}\right)^{\frac{1}{3}}$$

where:

T_c = time of concentration (minutes),
C = coefficient = 1.0 for bare earth,
S = slope (ft/ ft), and
i = one-hour rainfall intensity (inches/hour).

As specified in UMTRA TAD (DOE 1989), T_c is limited to a minimum of 2.5 minutes. Because precipitation falling on the top of the cover flows to the north and south slopes, the time of concentration for each of these side slopes is equivalent to the time of concentration for precipitation on the top slope plus the time of concentration for precipitation on the side slope. The characteristics of the drainage areas on the disposal cell are summarized in Table 1. Where there is some variation of slope length within an area, the maximum slope length was used in the calculation.

Table 1. Drainage Area Characteristics

Drainage Area	Slope (ft/ft)	Slope Length (ft)	Time of Concentration (min)			
			Kirpich	SCS	Brant and Oberman	Mean
South Top Slope	0.02	1292.0	8.75	8.76	9.87	9.12
North Top Slope	0.02	564.5	4.62	4.63	7.49	5.58
South Side Slope	0.2	176.0	9.52	9.53	12.22	10.43
North Side Slope	0.2	42.0	4.88	4.89	8.95	6.24
East Side Slope	0.2	164.0	0.74	0.74	2.30	2.5*
West Side Slope	0.2	164.0	0.74	0.74	2.30	2.5*

*Time of concentration is limited to a minimum of 2.5 minutes.

The current applicable version of this publication resides on Jacobs' Intranet. All copies are considered to be uncontrolled.
Copyright© Jacobs Engineering Group Inc., 2007

Peak Discharge

One of the technical criteria for the stability of the disposal cell is acceptable erosional stability from extreme storm events (10 CFR 40, Appendix A). NRC has interpreted this criterion to be able to safely pass the peak runoff from storms up to the PMP event (Johnson 2002). The PMP event has a 1-hour depth of 8.2 inches, and a 15-minute depth of 7.1 inches ("Site Drainage—Hydrology Parameters" calculation, Draft RAP Attachment 1, Appendix E). For events with durations less than 15 minutes, precipitation depths as a percent of the 1-hour PMP are estimated using the following formula, as given in Table 4.1 of the UMTRA TAD (DOE 1989):

$$\%PMP_{1-hour} = \frac{RD}{0.0089RD + 0.0686}$$

where: RD = rainfall duration (minutes).

The precipitation depth of any given storm duration is then calculated as:

$$PD_{PMP} = \%PMP_{1-hour} \times PMP_{1-hour}$$

where: PD_{PMP} = precipitation depth of the PMP storm with duration equivalent to the time of concentration (inches).

The rainfall intensity is calculated for a rainfall duration equivalent to the time of concentration for the drainage basin. Rainfall intensity (inches per hour) is calculated as follows:

$$I = \frac{\Pr ecDepth(in) \times 60}{\Pr ecDur(\min)}$$

Peak flow per unit width was calculated as specified in the UMTRA TAD.

$$q = \frac{CIL}{43200}$$

where:

q = unit discharge (cubic feet per second per foot [cfs/ft]),
C = runoff coefficient = 1.0,
I = rainfall intensity (inches per hour), and
L = slope length (ft).

A runoff coefficient of 1.0 is used for PMP conditions, as discussed in UMTRA TAD (section 4.1.3).

Table 2 shows the results of the PMP unit discharge calculations in cubic feet per second per foot (cfs/ft) for the areas shown in Figure 1.

The current applicable version of this publication resides on Jacobs' Intranet. All copies are considered to be uncontrolled.
Copyright© Jacobs Engineering Group Inc., 2007

Table 2 Results of PMP Unit Discharge Calculation

Drainage Area Description	Average T_c (min)	Percent $PMP_{1\text{-}hr}$	Prec D (inches)	Intensity (inches/hr)	Unit Discharge, q (cfs/ft)
South Top Slope	9.12	60.9	5.0	32.8	0.98
North Top Slope	5.58	47.2	3.9	41.6	0.54
South Side Slope	10.43	64.6	5.3	30.5	1.02
North Side Slope	6.24	50.3	4.1	39.6	0.55
East Side Slope	2.5*	27.5	2.3	54.2	0.20
West Side Slope	2.5*	27.5	2.3	54.2	0.20

Rock Size (D50) Calculation:

The required rock size on the top slopes was calculated using the Safety Factor method, as recommended in NUREG/CR-4620 (Nelson et al. 1986) and NUREG-1623 (Johnson 2002) for slopes less than 10 percent. The safety factor against erosion for any given rock is calculated as:

$$SF = \frac{\cos\alpha \times \tan\phi}{\eta \times \tan\phi + \sin\alpha}$$

where:

α = angle of slope measured from horizontal,
ϕ = angle of repose of rock, and
η = stability number.

The stability number is calculated as:

$$\eta = \frac{21\tau_o}{(S_s - 1)\gamma D}$$

where:

τ_o = bed shear stress (psf),
S_s = specific weight of the rock,
γ = specific weight of water,
D = representative rock size (ft),

and:

$$\tau_o = \gamma d s$$

where:

d = depth of flow (ft), and
s = slope (ft/ft).

The depth of flow is calculated using Manning's equation

$$q = \frac{1.486 d R^{\frac{2}{3}} \sqrt{S}}{n}$$

The current applicable version of this publication resides on Jacobs' Intranet. All copies are considered to be uncontrolled.
Copyright© Jacobs Engineering Group Inc., 2007

where:

q = unit flow (cfs/ft),
d = depth of flow (ft),
R = hydraulic radius = d for wide channels,
S = slope (ft/ft), and
n = Manning's n

Manning's *n* is computed using procedures discussed by Abt et al. (1987) as follows:

$$n = 0.0456 * (D_{50} * S)^{0.159} \qquad (1)$$

where: *n* is Manning's *n*,
D_{50} is the mean riprap diameter in inches, and
S is the channel slope (ft/ft).

For a PMP event, a factor of safety slightly greater than 1.0 is recommended (Nelson et al. 1986). A factor of safety of 1.01 was used in these calculations. The method assumes uniform sheet flow across the entire drainage basin. The peak unit discharges due to the PMP (Table 2) were used to represent flow conditions on the top slope. The flow per unit width was multiplied by 3 to account for potential flow channelization. The angle of repose of 37° and specific gravity of rock (2.65) were assumed. The minimum thickness of rock on the top slope should be 2 times the D50 (Johnson, 2002).

The rock size (D50) required on the side slopes was calculated using the Abt and Johnson (1991) method, as discussed in NUREG-1623 (Johnson 2002). This method is recommended for slopes greater than 10 percent. The D_{50} rock size using the Abt and Johnson method is calculated as:

$$D_{50} = 5.23 S^{0.43} q^{0.56}$$

where:

q = design unit discharge (cfs/ft), and
S = Slope (ft/ft).

The method assumes uniform sheet flow across the entire drainage basin. The peak unit discharges due to the PMP (Table 2) were used to represent flow conditions on the top slope. This flow was multiplied by a concentration factor of 3 to account for flow channelization and by 1.35 to account for the ratio of stone movement to stone failure (Abt and Johnson, 1991). The angle of repose and specific gravity of rock were assumed and will need to be adjusted (if necessary) with actual source characteristics.

The rock protection layer thickness should be at least 1.5 to 2 times the median rock size.

Rock Size (D50) on Cell Aprons

Additional erosion protection will be provided for runoff from the side slopes of the disposal cell with rock aprons. The perimeter apron will: (1) serve as an impact basin and provide for energy dissipation of runoff, (2) provide erosion protection, and (3) transition flow from side slopes to natural ground. The median rock size required in the perimeter apron was calculated using the equations derived by Abt et al. (1998) as outlined in NUREG 1623 (Johnson 2002) as follows:

$$D_{50} = 10.46 S^{0.43} q_d^{\ 0.56}$$

The current applicable version of this publication resides on Jacobs' Intranet. All copies are considered to be uncontrolled.
Copyright© Jacobs Engineering Group Inc., 2007

where S is the side slope above the apron, and q_d is the design unit discharge. The computed unit discharge was multiplied by three to account for potential flow channelization and by 1.35 to protect against rock movement as well as catastrophic failure (Johnson, 2002 and Abt et.al. 1998) The thickness of the rock apron should be at least three times the D50 (Johnson, 2002) and the width of the apron at least 15 times the D50.

Scour at Aprons:

The maximum scour depth for a PMP storm was calculated using procedures outlined in NUREG 1623 (Johnson 2002) and U.S. Department of Transportation (DOT 1983). For discharge from a rock apron onto natural ground the scour depth is computed as:

$$D_s = \alpha_e y_e \left[\frac{\rho V^2}{\tau_c}\right]^{\beta} \left[\frac{t}{t_o}\right]^{\theta}$$

where

Ds = scour depth (ft)
α_e = 1.37
τ_c = critical tractive shear
β = 0.18
θ = 0.10
t = time duration of peak flow duration or 30 minutes if unknown
t_o = base time used in the experiments to determine the coefficients (316 minutes is the default)
$y_e = (A/2)^{1/2}$ where A is the cross sectional area of flow

and $\tau_c = 0.001(S_v + 8618)\tan(30 + 1.73 * PI)$

where

S_v = saturated shear strength (assumed 1.4 for native soils)
PI = plasticity index (5 for native soils)

For these calculations, the flow per unit width was multiplied by 3 to account for potential flow concentration. This design flow was assumed to exit the apron in a v-shaped channel with side slopes of 2H to 1V. The Manning n value was computed from the D50 of the rock on the apron using the equation from Abt et. al. (1987) as follows:

$$n = 0.0456 * (D_{50} * S)^{0.159} \qquad (1)$$

where: *n* is Manning's *n*,
D_{50} is the median riprap diameter in inches, and
S is the channel slope (ft/ft).

The results of these calculations are summarized in Table 3.

The current applicable version of this publication resides on Jacobs' Intranet. All copies are considered to be uncontrolled.
Copyright© Jacobs Engineering Group Inc., 2007

Table 3 Calculated rock sizes and thickness for erosion protection.

Drainage Area	Unit PMP Discharge (cfs/ft)	Conc Factor	Stone Movement Ratio	D50 (in)	Min Layer Thickness (in)	Min Apron Width (ft) 10 ft min.	Scour Depth (ft)
South Top Slope	0.98	3		1.8	3.6		
North Top Slope	0.54	3		1.2	2.4		
South Side Slope	1.02	3	1.35	5.8	11.6		
North Side Slope	0.55	3	1.35	4.1	8.2		
East Side Slope	0.20	3	1.35	2.3	4.6		
West Side Slope	0.20	3	1.35	2.3	4.6		
South Apron	1.02	3	1.35	11.6	34.7	15	1.66
North Apron	0.55	3	1.35	8.2	24.5	10	1.18
East Apron	0.20	3	1.35	4.7	14.0	10	0.67
West Apron	0.20	3	1.35	4.7	14.0	10	0.67

Over sizing may be required for rounded rock or for durability considerations. The width of the apron should be a minimum of 15 times the median rock size or construction width. Rock apron thickness should be a minimum of 3 times the median rock size or greater than the calculated scour depth. (Johnson, 2002)

Bedding Requirements

NUREG-1623, Appendix D (Johnson 2002), recommends a filter or bedding layer be placed under erosion protection if interstitial velocities are greater than 1 ft/sec, in order to prevent erosion of the underlying soils. Bedding is not required if interstitial velocities are less than 0.5 ft/sec, and recommended depending on the characteristics of the underlying soil if velocities are between 0.5 and 1 ft/sec.

Interstitial velocities are calculated by procedures presented by Abt and Johnson (1991) as given by the following equation:

$$V_i = 0.23 * (g * D_{10} * S)^{\frac{1}{2}}$$

where:

V_i = interstitial velocities (ft/s),
g = acceleration of gravity (ft/s^2),
D_{10} = stone diameter at which 10 percent is finer (inches), and
S = gradient in decimal form.

The current applicable version of this publication resides on Jacobs' Intranet. All copies are considered to be uncontrolled.
Copyright© Jacobs Engineering Group Inc., 2007

The D10 is still to be determined, but assuming it will be equal to ½ the D50, the following results are obtained. These results will be refined when the source and size distribution of the rock is determined, but it is expected that a bedding layer will be required at least on the north and south side slopes and probably on the east and west.

Table 4. Results of Bedding Requirements

Location	D10 (in)	Slope	Interstitial Velocity (fps)
South Top Slope	0.9	0.02	0.18
North Top Slope	0.6	0.02	0.14
South Side Slope	2.9	0.2	0.99
North Side Slope	2.05	0.2	0.84
East Side Slope	1.15	0.2	0.63
West Side Slope	1.15	0.2	0.63
South Apron	5.8	0.02	0.44
North Apron	4.1	0.02	0.37
East Apron	2.35	0.02	0.28
West Apron	2.35	0.02	0.28

The current applicable version of this publication resides on Jacobs' Intranet. All copies are considered to be uncontrolled.
Copyright© Jacobs Engineering Group Inc., 2007

References:

10 CFR 40. U.S. Nuclear Regulatory Commission (NRC), "Domestic Licensing of Source Material," Appendix A, *Code of Federal Regulations*, February 2007.

40 CFR 192. U.S. Environmental Protection Agency (EPA) "Health and Environmental Protection Standards for Uranium and Thorium Mill Tailings," *Code of Federal Regulations*, February 2007.

Abt, S.R., M.S. Khattak, J.D. Nelson, J.F. Ruff, A. Shaikh, R.J. Wittler, D.W. Lee, and N.E. Hikle, 1987. *Development of Riprap Design Criteria by Riprap Testing in Flumes: Phase I*, NUREG/CR-4651.

Abt, S.R., and T.L. Johnson, 1991. "Riprap Design for Overtopping Flow", *Journal of Hydraulic Engineering*, 117(8), pp. 959–972.

Abt, S.R., T.L. Johnson, C.I. Thornton, and S.C. Trabant, 1998. "Riprap Sizing at Toe of Embankment Slopes", *Journal of Hydraulic Engineering*, 124(7), July.

Abt, S.R., J.F. Ruff, and R.J. Wittler, 1991. "Estimating Flow Through Riprap", *Journal of Hydraulic Engineering*, 117(5), pp. 670–675.

Chow, V.T., 1964. *Handbook of Applied Hydrology*, McGraw-Hill Book Company, New York, New York.

DOE (U.S. Department of Energy), 1989. *Technical Approach Document, Revision II*, UMTRA-DOE/AL 050424.0002, December.

DOT (U.S. Department of Transportation), 1983. *Hydraulic Design of Energy Dissipaters for Culverts and Channels*, Hydraulic Engineering Circular No. 14, September.

Geotechnical Engineering Group, Inc. (GEG), 2005. Technical Testing, Crescent Junction, GEG Job No. 2165, December 22.

Johnson, T.L., 2002 *Design of Erosion Protection for Long-Term Stabilization*, Final Report, NUREG-1623, U.S. Nuclear Regulatory Commission, September.

Nelson, J.D., S.R. Abt, R.L. Volpe, D. van Zyl, N.E. Hinkle, W.P. Staub, 1986. *Methodologies for Evaluating Long-Term Stabilization Design of Uranium Mill Tailings Impoundments*, NUREG/CR-4620, U.S. Nuclear Regulatory Commission, June.

Temple, D.M., K.M. Robinson, R.M. Ahring, and A.G. Davis, 1987. *Stability Design of Grass-Lined Open Channels*, U.S. Department of Agriculture Handbook No. 667, September.

USDA (U.S. Department of Agriculture), 1994. "Gradation Design of Sand and Gravel Filters", *National Engineering Handbook*, Part 633, Chapter 26, October.

The current applicable version of this publication resides on Jacobs' Intranet. All copies are considered to be uncontrolled.
Copyright© Jacobs Engineering Group Inc., 2007

Appendix A

Sample Calculations

Rock D50 on the South Top, Side , and Apron

Scour Depth on the South

Size side slope riprap using the Abt and Johnson Method (1991)
For the PMP, the requirement is that the safety factor, S, by greater than 1.
The top slope RipRap is sized with the safety factor method.
Only marginal exceedance is required for safety factor.

Enter Data Here		Then
Maximum Flow Length on Top (ft)	1292	
Slope on the Top of Cell (ft/ft)	0.02	
Length of the Side Slope (ft)	176	
Side Slope (ft/ft)	0.2	

Results are Below

Don't enter any data below this point !!!

Maximum Flow Length on Top (ft)	1292	Length of the Side Slope (ft)	176
Slope on the Top of Cell (ft/ft)	0.02	Side Slope (ft/ft)	0.2

	Top Tc(minutes)	Side Tc(minutes)	
Kirpich	8.75	0.78	
SCS	8.76	0.78	
B&O	9.87	2.36	
Mean	9.12	1.30	
Top + Side	10.43		
q Top(cf/ft-sec)	0.982	x3	2.95
q Side(cf/ft-sec)	1.016	x3	3.05

Use Angular Riprap with a D50 of	**1.8**	inches on the top slope
Use Angular Riprap with a D50 of	**5.8**	inches on the side slope
Use Angular Riprap with a D50 of	**11.6**	inches on the apron.
Minimum apron rock depth is	**34.7**	inches
and minimum width of apron is	**9.6**	feet

For flow in cfs/ft width use with i(inches/hr), L(ft) is the flow path length

$$q = \frac{CiL}{43{,}200}$$

This is almost the rational formula but is more theoretically based.

Find the time of concentration using three formulas and take the mean.

	Tc for Top of Cell Feet	Miles	Tc for Side Slope Feet	Miles
Maximum Flow Length	1292	0.2447	176	0.0333
Slope of watershed =	0.02		0.2	
Delta H =	25.8	feet	35.2	feet
Kirpich(1940) $T_c = \frac{0.0078L^{0.377}}{S^{0.385}}$	8.75	minutes	0.78	minutes
SCS $T_c = \left[\frac{11.9L^3}{H}\right]^{0.385}$	8.76	minutes	0.78	minutes
Brant & Oberman $T_c = C\left[\frac{L}{Si^2}\right]^{(1/3)}$	9.87	minutes	2.36	minutes
Mean Tc	9.12	minutes	1.30	minutes
Combined Tc Top and Side	10.43	minutes		

Unit Weight of Water	62.4
Specific Gravity of Rock	2.65

1 Hour PMP = 8.2 inches for 1 square mile watershed

9.12	minute PMP =	60.9%	of 1 hour =	4.99 inches
10.43	minute PMP =	64.6%	of 1 hour =	5.30 inches

For Rock on top Slope
Rainfall Intensity = 32.84 inches/hour

Max Q/ft width = 0.982 cfs/ft
Multiply by Concentration Factor of 3 2.95 cfs/ft

Rock size on top slope by Safety Factor Method

$$S = \frac{\cos\alpha \tan\phi}{\eta \tan\phi + \sin\alpha}$$ where $$\eta = \frac{21\tau_o}{(S_s - 1)\gamma D}$$ and $$\tau_o = \gamma S y$$

Set up Solver			
D_{50}	1.8	inches	0.1468 feet
Ss	2.65	specific gravity	
Gamma	62.4	lb/cf	
Safety Factor	1.01		
Alpha	1.146	degrees	
Phi	37	degrees	
n	0.0268	manning	
y	0.556	ft	
q	2.95	cfs	
Tau_0	0.6934406		
Slope	0.02	ft/ft	
Eta	0.9634		
Velocity (fps)	5.30		

For Rock on Side Slope
Rainfall Intensity = 30.48 inches/hour

Max Q/ft width = 1.016 cfs/ft
Multiply by Concentration Factor of 3 3.05 cfs/ft
Multiply by stone movement to stone failure ratio = 1.35 4.11 cfs/ft
For side Slope D50 = 5.8 inches

				Tc =	10.43	minutes			
	Fluid Density	1.94	slugs/ft^2						
	Q	1.016	cfs						
	Concentration Factor	3	for overland sheet flow concentrating				Use solver to find y		
	Design Flow	3.048	cfs				Assume V Shaped Channel		
	G	32.2					Rh =	0.33	
	Time t	10.43	p. 73 HEC14 - 30 min or peak flow duration				Area =	1.10	
	Base Time to	316	from HEC14 after eq 5-1				Q =	3.05	
	D50	Native Soil					y =	0.74	
	Apron slope	0.02					WP =	3.31	
	RipRap D50	11.6	inches				Solve Q by varying y		
	Manning n	0.036					Channel Shape		
							Horizontal	2	
							Vertical	1	
	Hydraulic Radius	0.33				Depth of Scour =		1.66	ft
	Flow Area	1.10							
	Flow Depth	0.74							
	Q	3.048							
	Velocity	2.78							
	PI	5							
	Unconfined Compressive strength(psi)	1.4							
	Critical Tractive Shear	0.145							
	Modified Shear Number	103.49							
	α	0.86							
	β	0.18							
	θ	0.1							
	αe	1.37							
	Equivalent Depth ye =Culvert Diameter	0.74	or sqrt(A/2)						
	Dimensionless Depth	2.25							
	Depth of scour	1.66	ft						

Size side slope riprap using the Abt and Johnson Method (1991)
For the PMP, the requirement is that the safety factor, S, by greater than 1.
The top slope RipRap is sized with the safety factor method.
Only marginal exceedance is required for safety factor.

Enter Data Here		Then
Maximum Flow Length on Top (ft)	1292	
Slope on the Top of Cell (ft/ft)	0.02	
Length of the Side Slope (ft)	176	
Side Slope (ft/ft)	0.2	

Results are Below

Don't enter any data below this point !!!

Maximum Flow Length on Top (ft)	1292	Length of the Side Slope (ft)	176
Slope on the Top of Cell (ft/ft)	0.02	Side Slope (ft/ft)	0.2

Use Angular Riprap with a D50 of	**1.8**	inches on the top slope
Use Angular Riprap with a D50 of	**5.8**	inches on the side slope
Use Angular Riprap with a D50 of	**11.6**	inches on the apron.
Minimum apron rock depth is	**34.7**	inches
and minimum width of apron is	**9.6**	feet

	Top Tc(minutes)	Side Tc(minutes)	
Kirpich	8.75	0.78	
SCS	8.76	0.78	
B&O	9.87	2.36	
Mean	9.12	1.30	
Top + Side	10.43		
q Top(cf/ft-sec)	0.982	x3	2.95
q Side(cf/ft-sec)	1.016	x3	3.05

For flow in cfs/ft width use with i(inches/hr), L(ft) is the flow path length

$$q = \frac{CiL}{43{,}200}$$

This is almost the rational formula but is more theoretically based.

Find the time of concentration using three formulas and take the mean.

		Tc for Top of Cell		Tc for Side Slope	
		Feet	Miles	Feet	Miles
Maximum Flow Length		1292	0.2447	176	0.0333
Slope of watershed =		0.02		0.2	
	Delta H =	25.8	feet	35.2	feet
Kirpich(1940) $T_c = \frac{0.0078L^{0.377}}{S^{0.385}}$		8.75	minutes	0.78	minutes
SCS $T_c = \left[\frac{11.9L^3}{H}\right]^{0.385}$		8.76	minutes	0.78	minutes
Brant & Oberman $T_c = C\left[\frac{L}{Si^2}\right]^{(1/3)}$		9.87	minutes	2.36	minutes
	Mean Tc	9.12	minutes	1.30	minutes
Combined Tc Top and Side		10.43	minutes		

Unit Weight of Water	62.4
Specific Gravity of Rock	2.65

1 Hour PMP = 8.2 inches for 1 square mile watershed

9.12	minute PMP =	60.9%	of 1 hour =	4.99	inches
10.43	minute PMP =	64.6%	of 1 hour =	5.30	inches

For Rock on top Slope
Rainfall Intensity = 32.84 inches/hour

Max Q/ft width = 0.982 cfs/ft
Multiply by Concentration Factor of 3 2.95 cfs/ft

Rock size on top slope by Safety Factor Method

$$S = \frac{\cos\alpha \tan\phi}{\eta \tan\phi + \sin\alpha}$$ where $$\eta = \frac{21\tau_o}{(S_s - 1)\gamma D}$$ and $$\tau_o = \gamma S y$$

For Rock on Side Slope
Rainfall Intensity = 30.48 inches/hour

Max Q/ft width = 1.016 cfs/ft
Multiply by Concentration Factor of 3 3.05 cfs/ft
Multiply by stone movement to stone failure ratio = 1.35 4.11 cfs/ft
For side Slope D50 = 5.8 inches

Set up Solver

D_{50}	1.8	inches	0.1468	feet
Ss	2.65	specific gravity		
Gamma	62.4	lb/cf		
Safety Factor	1.01			
Alpha	1.146	degrees		
Phi	37	degrees		
n	0.0268	manning		
y	0.556	ft		
q	2.95	cfs		
Tau_0	0.6934406			
Slope	0.02	ft/ft		
Eta	0.9634			
Velocity (fps)	5.30			

Appendix B

Reference Material

Safety Factors Method

Overtopping Flow

Toe of Embankments

Culvert Scour

Interstitial Flow

12115 MAY 1976 HY5

JOURNAL OF THE HYDRAULICS DIVISION

Safety Factors for Riprap Protection[a]

By Michael A. Stevens,[1] Daryl B. Simons,[2] F. ASCE, and Gary L. Lewis,[3] A. M. ASCE

Introduction

The safety factor for rock riprap is defined as the ratio of the moments of forces resisting rotation of the rock particle out of the riprap blanket to the moments tending to dislodge the particle out of the riprap layer into the flow. The critical condition is the flow for which incipient motion occurs. At the critical condition, the riprap particles have a safety factor of unity. If the safety factor is greater than one, the riprap is considered safe from failure; if the safety factor is less than one, rocks are washed from the riprap layer and failure of the protection may occur. The safety factor for riprap protection is analogous to the safety factor employed in structural design. Incipient motion conditions for rock riprap correspond to yield stress conditions in structural members.

The equations describing safety factors for riprap protection are based on theoretical considerations and existing empirical information. Shield's criteria for incipient particle motion as modified by Gessler (9) is employed. Hydrodynamic drag of the fluid on the rock is considered in the same manner as employed by Lane (12). The hydrodynamic lift of the fluid on the rock (5,8) is included in the analysis. The magnitude of the lift force is proportional to the magnitude of the drag force, but the lift force acts normal to the drag force. This difference in direction of force is important in analyzing stability of particles on side slopes (6). The stability of the particle is obtained from its submerged weight and the angle of repose. The particle stability analysis is similar to that made by Campbell (3) except that, herein, the safety factor term is added.

Safety factors in riprap protection design are employed for two purposes:

Note.—Discussion open until October 1, 1976. To extend the closing date one month, a written request must be filed with the Editor of Technical Publications, ASCE. This paper is part of the copyrighted Journal of the Hydraulics Division, Proceedings of the American Society of Civil Engineers, Vol. 102, No. HY5, May, 1976. Manuscript was submitted for review for possible publication on November 26, 1974.

[a] Presented at the July 15–19, 1974, ASCE/EIC/RTAC Joint Transportation Engineering Meeting, held at Montreal, Canada.

[1] Assoc. Prof., Dept. of Civ. Engrg., Colorado State Univ., Fort Collins, Colo.

[2] Assoc. Dean for Research, and Prof. of Civ. Engrg., Colorado State Univ., Fort Collins, Colo.

[3] Assoc. Prof., Dept. of Civ. Engrg., Univ. of Nebraska, Lincoln, Neb.

(1) The safety factor can be used to assess the merits of a particular riprap design; and (2) the safety factor can be used to evaluate different riprap design methods that have been recommended in the technical literature. Illustrations of riprap design and comparisons with recommended design methods are presented.

Riprap Stability Analysis

In the absence of waves and seepage, the stability of rock riprap particles on a side slope is a function of: (1) The magnitude and direction of the stream velocity in the vicinity of the particles; (2) the angle of the side slope; and (3) the characteristics of the rock including the geometry, angularity, and density.

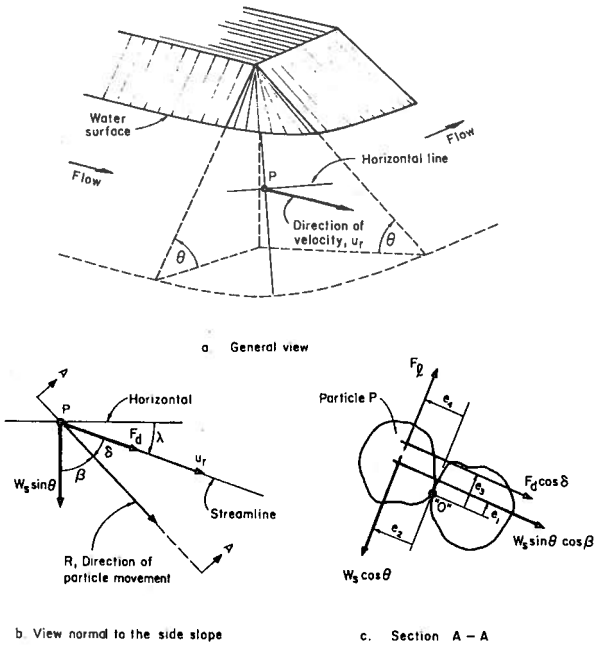

FIG. 1.—Diagrams for Riprap Stability Analysis

The functional relations between the variables are developed subsequently. This development closely follows those given by Stevens and Simons (20) and Lewis (13).

Oblique Flow on Side Slope.—Consider flow along an embankment as shown in Fig. 1. The fluid forces on a rock particle identified as P in Fig. (1a) result primarily from fluid pressures around the surface of the particles. Lift force, F_l, is defined herein as the fluid force normal to the plane of the bank. The lift force is zero when the fluid velocity is zero. Drag force, F_d, is defined as the fluid force acting on the particle in the direction of the velocity field in the vicinity of the particle. The drag force is normal to the lift force and

is zero when the fluid velocity is zero. The remaining force is the submerged weight of the rock particle, W_s.

Rock particles on side slopes tend to roll rather than slide, so it is appropriate to consider the stability of rock particles in terms of moments about the point of rotation. In Fig. 1(b) the direction of movement is defined by vector **R**. The point of contact about which rotation in the **R** direction occurs is identified as point "0" in Fig. 1(c).

Forces acting in the plane of the side slope are F_d and $W_s \sin\theta$ as shown in Fig. 1(b). The angle θ is the side slope angle. The lift force acts normal to the side slope and the component of submerged weight $W_s \cos\theta$ acts in the direction as shown in Fig. 1(c).

At incipient motion, there is a balance of moments about the contact point "0" such that

$$e_2 W_s \cos\theta = e_1 W_s \sin\theta \cos\beta + e_3 F_d \cos\delta + e_4 F_l \quad (1)$$

Moment arms e_1, e_2, e_3, and e_4 are defined in Fig. 1(c) and angles δ and β are defined in Fig. 1(b).

The factor of safety, S, of particle P against rotation is defined as the ratio of the moments resisting particle rotation out of the bank to the submerged weight and fluid force moments tending to rotate the particle out of its resting position. Accordingly

$$S = \frac{e_2 W_s \cos\theta}{e_1 W_s \sin\theta \cos\beta + e_3 F_d \cos\delta + e_4 F_l} \quad (2)$$

If there is no flow and the side slope angle is increased to the angle of repose ϕ for the rock particles, the safety factor becomes unity. Then, $S = 1.0$; $\theta = \phi$; $\beta = 0°$; $\lambda = 0°$; and $\delta = 90 - \lambda - \beta = 90°$ [see Fig. 1(b)]. With these values, Eq. 2 reduces to

$$\tan\phi = \frac{e_2}{e_1} \quad (3)$$

that is, the ratio of the moment arms, e_2/e_1, is characterized by the natural angle of repose, ϕ. Further, it is assumed that the ratio, e_2/e_1, is invariant to the direction of particle motion indicated by angle β.

Dividing both numerator and denominator by $e_1 W_s$, Eq. 2 is transformed to

$$S = \frac{\cos\theta \tan\phi}{\eta' \tan\phi + \sin\theta \cos\beta} \quad (4)$$

$$\text{in which} \quad \eta' = \frac{e_3 F_d}{e_2 W_s} \cos\delta + \frac{e_4 F_l}{e_2 W_s} \quad (5)$$

The variable η' is called the stability number for particles on the embankment side slope.

The angle λ shown in Fig. 1(b) is the angle between the horizontal and the velocity vector (or drag force) measured in the plane of the side slope. Then

$$\delta = 90 - \lambda - \beta \quad (6)$$

It is assumed that moments of the drag force, F_d, and the component of

submerged weight, $W_s \sin\theta$, normal to path R are balanced so that the direction of particle motion will be along R. Thus

$$e_3 F_d \sin\delta = e_1 W_s \sin\theta \sin\beta \quad (7)$$

It follows then from Eqs. 6 and 7 that

$$\sin\beta = \frac{e_3 F_d \sin\delta}{e_1 W_s \sin\theta} = \frac{e_3 F_d (\cos\lambda \cos\beta - \sin\lambda \sin\beta)}{e_1 W_s \sin\theta} \quad (8)$$

$$\text{or} \quad \tan\beta = \frac{\cos\lambda}{\frac{e_1 W_s}{e_3 F_d}\sin\theta + \sin\lambda} \quad (9)$$

The stability number η for particles on a plane bed ($\theta = 0$) with $\delta = 0$ would be

$$\eta = \frac{e_3 F_d}{e_2 W_s} + \frac{e_4 F_l}{e_2 W_s} \quad (10)$$

according to Eq. 5. Also, Eq. 4 becomes

$$S = \frac{1}{\eta} \quad (11)$$

for flow over a plane flat bed.

Both the hydrodynamic drag and lift on the particle are related to the square of the fluid velocity in the vicinity of the particle and to the exposed area of the particle (8,20). The tractive force on the bed is also directly related to the square of the fluid velocity, or

$$F_l = c_1 k^2 \tau_s \quad (12)$$

$$\text{and} \quad F_d = c_2 k^2 \tau_s \quad (13)$$

in which τ_s = the average tractive force on the plane containing the particle, P; and k = the diameter of the rock particle. Coefficients c_1 and c_2 are dependent on the exposed area of the particle, the coefficients of drag and lift, and the relation between velocity and tractive force.

The submerged weight of the particle can be written (20) as

$$W_s = c_3 (S_s - 1)\gamma k^3 \quad (14)$$

in which c_3 is a coefficient depending only on the shape of the particle; P; S_s = the specific weight of the rock; and γ is the unit weight of water.

Substitution of Eqs. 12, 13 and 14 into Eq. 10 we obtain

$$\eta = \frac{c_1 e_4 + c_2 e_3}{c_3 e_2} \frac{\tau_s}{(S_s - 1)\gamma k} \quad (15)$$

The term $\tau_s/(S_s - 1)\gamma k$ is known as Shield's parameter.

Incipient motion conditions for flow over a plane flat bed give $S = 1.0$ by definition so from Eq. 11, $\eta = 1.0$. When flow along the bed is fully turbulent, Shield's parameter for incipient motion has the value 0.047 according to Gessler

(9). It follows then that

$$\frac{c_1 e_4 + c_2 e_3}{c_3 e_2} = \frac{1}{0.047} = 21 \quad (16)$$

For flow conditions other than incipient Eq. 15 becomes

$$\eta = \frac{21\tau_s}{(S_s - 1)\gamma k} \quad (17)$$

For convenience, let

$$M = \frac{e_4 F_l}{e_2 W_s} \quad (18)$$

$$\text{and} \quad N = \frac{e_3 F_d}{e_2 W_s} \quad (19)$$

In terms of these new variables, Eq. 5 becomes

$$\eta' = M + N\cos\delta \quad (20)$$

and Eq. 10 becomes

$$\eta = M + N \quad (21)$$

Thus η' and η are related by

$$\frac{\eta'}{\eta} = \frac{\frac{M}{N} + \cos\delta}{\frac{M}{N} + 1} \quad (22)$$

The problem is to select the proper value of the ratio M/N so that the stability factor on a slide slope η' can be related to the stability factor on a plane horizontal bed, η, which in turn is related to the Shield's parameter. The assumption that the drag force, F_d, is zero means M/N is infinite, β is zero, and $\eta' = \eta$. The assumption of zero lift force F_l means M/N is zero and $\eta'/\eta = \cos\delta$. For finite values of lift and drag forces, stability factor ratios are between the limits 0 and $\cos\delta$.

In considering incipient motion of riprap particles, the ratios, F_l/F_d and e_4/e_3, depend on the turbulent conditions of the flow and the interlocking arrangement of the rock particles. To facilitate the analysis, the product of F_l/F_d and e_4/e_3 is assumed to be

$$\frac{M}{N} = \frac{e_4}{e_3}\frac{F_l}{F_d} \simeq 1 \quad (23)$$

This value was chosen by Stevens and Simons (20) after considering the range of possible values for F_l/F_d and e_4/e_3 and the effect of M/N on the value of the safety factor, S. The safety factor, S, depends on the value of M/N only for flow on side slopes. Otherwise, the value of S is independent of the value chosen for M/N. With $M/N = 1$, Eq. 22 becomes

$$\frac{\eta'}{\eta} = \frac{1 + \cos\delta}{2} \quad (24)$$

or by using Eq. 6

$$\frac{\eta'}{\eta} = \frac{1 + \sin(\lambda + \beta)}{2} \quad (25)$$

In Eq. 9, the term $e_1 W_s / e_3 F_d$ can be written

$$\frac{e_1 W_s}{e_3 F_d} = \frac{e_2}{e_3}\frac{W_s}{F_d}\frac{e_1}{e_2} = \frac{1}{N}\frac{1}{\tan\phi} \quad (26)$$

according to Eqs. 3 and 19. For $M/N = 1$, Eq. 21 becomes

$$N = \frac{\eta}{2} \quad (27)$$

If we substitute Eqs. 26 and 27 into Eq. 9, the expression for β becomes

$$\beta = \tan^{-1}\left(\frac{\cos\lambda}{\dfrac{2\sin\theta}{\eta\tan\phi} + \sin\lambda}\right) \quad (28)$$

In summary, the safety factor for rock riprap on side slopes where flow has a nonhorizontal velocity vector is related to properties of the rock, side slope, and flow by Eqs. 4, 17, 25, and 28.

Given a rock size k of specific weight S_s and angle of repose ϕ and given a velocity field at an angle λ to the horizontal producing a tractive force τ_s on the side slope of angle θ, the set of four equations (Eqs. 4, 17, 25, and 28) can be solved to obtain the safety factor, S. If S is greater than unity, the riprap is safe from failure; if S is unity, the rock is at the condition of incipient motion; and if S is less than unity, the riprap will fail.

Horizontal Flow on Side Slope.—In many circumstances, the flow angularity with the horizontal is small, i.e., $\lambda \simeq 0$. Then Eqs. 25 and 28 reduce to

$$\beta = \tan^{-1}\left(\frac{\eta\tan\phi}{2\sin\theta}\right) \quad (29)$$

and $$\eta' = \left(\frac{1 + \sin\beta}{2}\right) \quad (30)$$

When Eqs. 29 and 30 are substituted into Eq. 4, the expression for the safety factor for horizontal flow along a side slope is

$$S = \frac{S_m}{2}\left[(\xi^2 + 4)^{1/2} - \xi\right] \quad (31)$$

in which $$\xi = S_m \eta \sec\theta \quad (32)$$

and $$S_m = \frac{\tan\phi}{\tan\theta} \quad (33)$$

If we solve Eqs. 32 and ~~33~~ 31 for η, then

$$\eta = \left(\frac{S_m^2 - S^2}{S S_m^2}\right)\cos\theta \quad (34)$$

The term, S_m, is the safety factor for riprap on a side slope with no flow. Unless flow is up the slope, the safety factor for the riprap cannot be greater than S_m.

Flow on Plane Sloping Bed.—Flow over a plane bed at a slope of α degrees in the downstream direction is equivalent to oblique flow on a side slope with $\theta = \alpha$ and $\lambda = 90°$.

Then, according to Eq. 28, $\beta = 0°$ and from Eq. 25, $\eta' = \eta$. It follows from Eq. 4 that

$$S = \frac{\cos\alpha\tan\phi}{\eta\tan\phi + \sin\alpha} \quad (35)$$

for flow on a plane bed sloping α degrees to the horizontal. Alternatively, solving for η in Eq. 35, we obtain

$$\eta = \cos\alpha\left(\frac{1}{S} - \frac{\tan\alpha}{\tan\phi}\right) \quad (36)$$

Flow on Horizontal Bed.—For fully developed rough turbulent flow over a plane horizontal bed ($\alpha \doteq 0$) of rock riprap, Eq. 35 reduces to

$$S = \frac{1}{\eta} \quad (37)$$

If the riprap particles are at the condition of incipient motion, $S = 1$ so $\eta = 1$ and we revert back to Shield's expression for incipient motion (Eq. 17 with $\eta = 1$).

Relation Between Shear and Velocity.—In order to compare the equations previously developed with those employed by others to design riprap, it is necessary to relate tractive forces acting on the riprap bed or bank to fluid velocities in the vicinity of the riprap. For fully turbulent flow, the relation between the local velocity, u, at distance y above the bed is

$$u = 2.5\, u_* \ln\left(30.2\frac{y}{k}\right) \quad (38)$$

in which u_* is the shear velocity defined as

$$u_* = \left(\frac{\tau_s}{\rho}\right)^{1/2} \quad (39)$$

This velocity distribution equation was derived by Keulegan (11) and was employed by Einstein (7) in his bed-load function research.

If we select the velocity at a distance $y = k$ above the bed as a reference velocity, u_r, then

$$u_r = 2.5\, u_* \ln 30.2 = 8.5\, u_* \quad (40)$$

The value of the reference velocity, u_r, given by Eq. 40 is the same as that employed by Campbell (3) in the Corps of Engineers' studies of the hydraulic design of rock riprap.

From Eqs. 39 and 40, the relation between u_r and τ_s is

$$\rho u_r^2 = 72\,\tau_s \qquad (41)$$

This relation is strictly valid only for uniform flow in wide prismatic channels in which flow is fully turbulent. For purposes of riprap design, Eq. 41 can be employed when flow is accelerating, e.g., on the nose of a spur dike. The equation should not be used in areas where the flow is decelerating or below energy dissipating structures. In these areas, the shear stress is larger than would be calculated by Eq. 41 because of turbulence in the flow.

Substitution of Eq. 41 into Eq. 17 gives the stability factor

$$\eta = \frac{0.30\,u_r^2}{(S_s - 1)gk} \qquad (42)$$

The average velocity in the vertical U is given by

$$U = 2.5\,u_* \ln\left(12.3\frac{y_0}{k}\right) \qquad (43)$$

in which y_0 = the depth of flow. This equation is the companion to Eq. 38 and was also obtained by Keulegan (11). The ratio of the reference velocity, u_r, to the depth-averaged velocity is

$$\frac{u_r}{U} = \frac{2.5\,u_* \ln(30.2)}{2.5\,u_* \ln\left(12.3\frac{y_0}{k}\right)} = \frac{3.4}{\ln\left(12.3\frac{y_0}{k}\right)} \qquad (44)$$

Now the expression for the stability factor, η, can be written in terms of the depth-averaged velocity. From Eqs. 42 and 44

$$\eta = \frac{\epsilon\,U^2}{(S_s - 1)gk} \qquad (45)$$

$$\text{in which} \quad \epsilon = 0.30\left[\frac{3.4}{\ln\left(12.3\frac{y_0}{k}\right)}\right]^2 \qquad (46)$$

In his study, Search (16) gives the expression

$$\frac{v_s}{V} = \frac{1}{0.958\log\left(\frac{y_0}{k}\right) + 1} \qquad (47)$$

in which v_s = the velocity against the stone; and V = the mean velocity in the channel. This equation can be closely approximated by dividing Eq. 38 by Eq. 43, using the assumption that $u = v_s$ when $y = 0.39k$. The velocity against the stone can, therefore, be considered as the velocity from Eq. 38 at a distance $y = 0.39k$ above the bed.

In wide channels, the depth-averaged velocity and the mean velocity in the channel are nearly equal, i.e., $U \simeq V$. Then the velocity against the stone is related to the reference velocity by the expression

$$\frac{u_r}{v_s} = \frac{u_r}{U}\frac{U}{v_s} = \frac{3.4\left[0.958\log\left(\frac{y_0}{k}\right) + 1\right]}{\ln\left(12.3\frac{y_0}{k}\right)} \qquad (48)$$

according to Eqs. 44 and 47. For values of y_0/k between 1×10^0 and 1×10^6, the value of the u_r/v_s is nearly 1.4. Finally, by letting $u_r/v_s = 1.4$ the expression for the stability factor η (Eq. 42) becomes

$$\eta = \frac{0.60\,v_s^2}{(S_s - 1)gk} \qquad (49)$$

Representative Grain Size.—In studies of scour below culvert outlets, Stevens (21) was able to consolidate a wide range of scour data by employing the expression

$$k = \left(\frac{\sum_{i=1}^{10} d_i^3}{10}\right)^{1/3} \qquad (50)$$

for the effective or representative grain size of graded materials. Here: d_i $(i = 1) = (d_0 + d_{10})/2$; d_i $(i = 2) = (d_{10} + d_{20})/2$; ... d_i $(i = 10) = (d_{90} + d_{100})/2$. The terms, d_0, d_{10}, ... d_{100}, are sieve diameters of the riprap for which 0%, 10%, ..., 100% of the material (by weight) is finer. Eq. 50 is equivalent to determining the arithmetic average of the sum of weights of individual particles. In Stevens' studies (21), the ratio k/d_{50} varied from 1.005–2.25, but normally $k \leq d_{67}$.

Safety Factors for Existing Design Methods

Many methods of designing riprap are available. The developed equations are compared subsequently with methods developed by the Bureau of Public Roads, the Corps of Engineers, the California Division of Highways, the ASCE Task Committee on Sedimentation, the Bureau of Reclamation, and Lane's and Campbell's methods.

Bureau of Public Roads.—Searcy (16) used the 1948 ASCE Subcommittee's summary on slope protection (15) to adopt Fig. 2. The relations shown in Fig. 2 require the velocity against the stone given by Eq. 47 and the median spherical diameter of the rock. Searcy recommended a gradation specification for riprap patterned after gradations recommended by Murphy and Grace (14). These gradations were called the A-rock for which $k/d_{50} = 1.08$ and the B-rock for which $k/d_{50} = 1.36$. Searcy chose the A-rock gradation in formulating his specifications.

Safety factors for the curves in Fig. 2 can be determined in the following manner. The recommended equivalent spherical diameter of the d_{50} rock is 3.75 ft (1.14 m) for v_s = 24 fps (7.3 m/s) on a horizontal bed. This diameter

corresponds to $k = 5.1$ ft (1.56 m) if we use the B-rock gradation. The stability factor for this rock and velocity is given by Eq. 49 or $\eta = 1.28$ and from Eq. 37, the safety factor is $S = 0.78$.

If Searcy's recommended gradation (A-rock) is used, $k = 4.1$ ft (1.25 m)

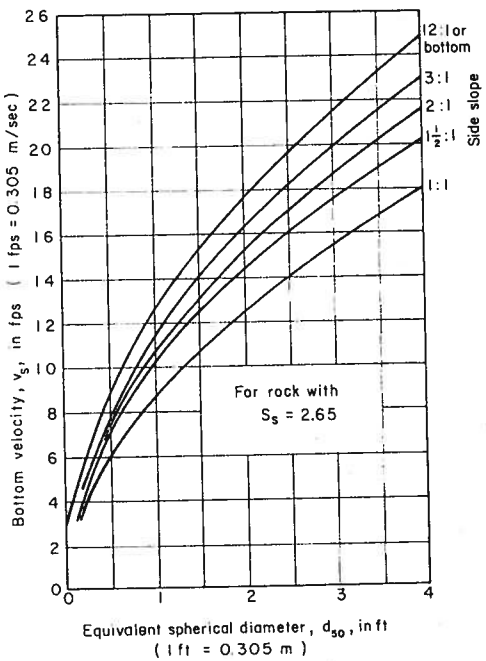

FIG. 2.—Rock Size for Bureau of Public Roads Design

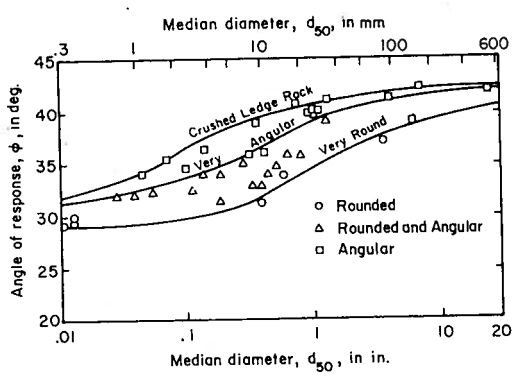

FIG. 3.—Angle of Repose for Dumped Riprap (15)

and $S = 0.63$. For either gradation, the rock sizes obtained from Fig. 2 for flow on a horizontal bed are considered "unsafe" according to the equations presented herein.

On a 2:1 side slope, the B-rock gradation has a safety factor of 0.76 which is obtained in the following manner. For a velocity v_s of 20 fps (6.1 m/s), Fig. 2 specifies a rock size d_{50} of 3.4 ft (1.04 m). With the B-rock gradation $k = 4.6$ ft (1.40 m) and from Eq. 49, $\eta = 0.98$. On a 2:1 side slope with horizontal flows ($\lambda = 0°$), the safety factor is given by Eq. 31. An estimate of the angle of repose can be made by extrapolating information obtained by Simons (18) and given in Fig. 3. With $\phi \simeq 42°$, from Eq. 33 $S_m = 1.80$, from Eq. 32 $\xi = 1.97$, and from Eq. 31 $S = 0.76$. Again, the safety factor is less than unity indicating that rock selected from Fig. 2 is undersized.

In order to have a safety factor greater than unity for the 1:1 side slope curve shown in Fig. 2, the angle of repose for the riprap must be very large. From the 1:1 curve in Fig. 2, a 2.5-ft (0.76-m) diam rock should withstand a bottom velocity of 14 fps (4.3 m/s) on a 1:1 side slope. With the B-rock gradation $k = 3.4$ ft (1.04 m). From Eq. 34, $\eta = 0.65$, and by solving Eq. 34 with $S = 1.0$ we obtain $S_m = 3.52$. As $\tan \phi = S_m \tan \theta$ (from Eq. 33), $\phi = 74°$. To obtain a ϕ this large, the riprap would have to be placed piece by piece by crane or by some other mechanical means. An alternative would be to grout the riprap or to place smaller rock in baskets.

In conclusion, safety factors for the design curves in Fig. 2 are less than unity.

U.S. Army Corps of Engineers Waterways Experiment Station.—The riprap design criteria adopted by the Corps of Engineers (22) is based on Isbash's equation for the movement of stone in flowing water. The equation can be written

$$\frac{U^2}{(S_s - 1)\, g d_{50}} = 2C^2 \qquad (51)$$

and is applicable for flow on plane flat beds. Here C is Isbash's turbulence coefficient.

By comparing this expression with Eq. 45, it is found that

$$\eta = 2\epsilon C^2 \frac{d_{50}}{k} \qquad (52)$$

According to the gradation criteria recommended by the Corps of Engineers (22), the representative grain size, k, is not more than 5% greater than d_{50}. Therefore, $k \simeq d_{50}$ and $S = 1/2\epsilon C^2$.

The Corps of Engineers uses $C = 1.20$ for applications in which the turbulence level is low. Accordingly, $S = 0.347/\epsilon$. The coefficient ϵ is a function of y_0/k (Eq. 46), and the relation between S and y_0/k for the design equation recommended by the Corps of Engineers is shown in Fig. 4. The safety factor is less than unity for very shallow flows and increases to unity when $y_0/k = 1.92$. For relative depths greater than 1.92, the safety factor is greater than unity.

California Division of Highways.—The California expression (1) for sizing riprap is

$$W = \frac{2 \times 10^{-5} S_s V^6}{(S_s - 1)^3 \sin^3 (70° - \theta)} \qquad (53)$$

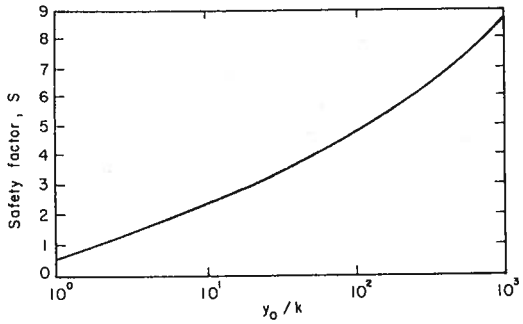

FIG. 4.—Safety Factors for Corps of Engineer's Riprap Design

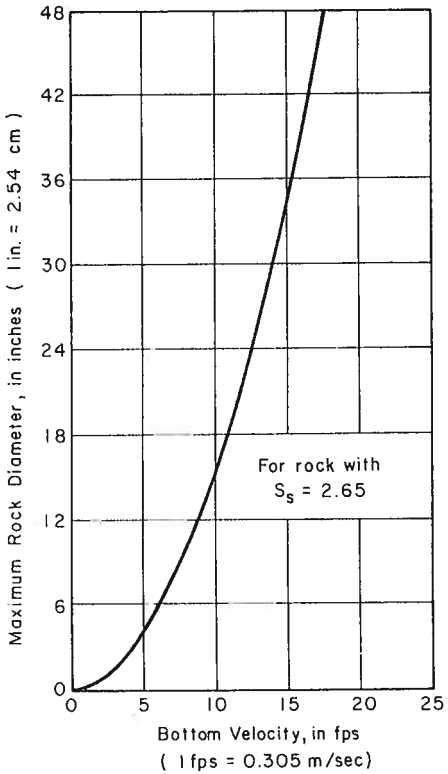

FIG. 5.—Rock Size for Bureau of Reclamation Design

in which W = the minimum weight, in pounds, of the outside stone; and V = the average stream velocity, in feet per second. If we assume $S_s = 2.65$ and that the particles are spheres with diameter d_{50}, then Eq. 53 reduces to

$$\frac{0.27\ V^2}{(S_s - 1)gd_{50}} = \sin(70° - \theta) \quad (54)$$

for horizontal flow on side slopes. For flow on level beds, Eq. 54 reduces to

$$\frac{0.29\ V^2}{(S_s - 1)gd_{50}} = 1 \quad (55)$$

Eq. 55 can be compared directly with Eq. 45 if it is assumed the channel is wide so that $V \simeq U$. Then

$$\eta = 3.45\epsilon \frac{d_{50}}{k} \quad (56)$$

$$\text{so} \quad S = \frac{0.29}{\epsilon}\frac{k}{d_{50}} \quad (57)$$

For comparison purposes, if we make $k = 1.2\ d_{50}$, then $S = 0.347/\epsilon$ which is the same expression as was obtained in the analysis of the Corps of Engineers' method. The safety factors are given in Fig. 4.

For horizontal flows on side slopes, the comparison is more difficult. The relation between the mean channel velocity and the shear stress or velocity on the side slopes must be established to obtain a safety factor. This relation has been established by Lane (12) and others and depends on the geometry of the channel. As Eq. 54 is based on an average stream velocity, some simplifying assumptions must have been made about the ratio of side slope shear to average shear. The analysis of these assumptions are outside the scope of this paper.

ASCE Task Committee on Preparation of Sedimentation Manual.—This committee (17) has recommended Isbash's formula

$$W_{50} = \frac{4.1 \times 10^{-5} S_s V^6}{(S_s - 1)^3 \cos^3\theta} \quad (58)$$

for riprap design. Here W_{50} is the weight of the rock with an equivalent spherical diameter d_{50}. Eq. 58 reduces to

$$\frac{0.347\ V^2}{(S_s - 1)g\,d_{50}} = \cos\theta \quad (59)$$

For flow on a horizontal bed ($\theta = 0°$), Eq. 59 becomes

$$\frac{0.347\ V^2}{(S_s - 1)g\,d_{50}} = 1 \quad (60)$$

Eq. 60 can be compared directly with Eq. 45, if it is assumed the channel is wide so that $V \simeq U$. Accordingly

$$\eta = 2.88\,\epsilon \frac{d_{50}}{k} \quad (61)$$

$$\text{so} \quad S = \frac{0.347}{\epsilon}\frac{k}{d_{50}} \quad (62)$$

For comparison purposes, if we make $k = 1.2\ d_{50}$, then $S = 0.416/\epsilon$. This

safety factor for Isbash's formula is 20% greater for flow on a horizontal bed than that obtained by the California Division of Highways method (1).

Bureau of Reclamation.—The Bureau of Reclamation (10) developed Fig. 5 to determine the maximum stone size in a riprap mixture downstream from stilling basins. If the bottom velocity is assumed equal to the velocity against the stone, v_s, the curve in Fig. 5 can be closely approximated by

$$V_s^2 = 49.1\,(S_s - 1)\,d_{100} \qquad (63)$$

The stability factor for the curve in Fig. 5 is determined from Eq. 49 or

$$\eta = 0.915\,\frac{d_{100}}{k} \qquad (64)$$

and from Eq. 37, the corresponding safety factor for particles on a horizontal bed is

$$S = 1.09\,\frac{k}{d_{100}} \qquad (65)$$

For comparison purposes, if we make $k = 1.2\,d_{50}$, then

$$S = 1.31\,\frac{d_{50}}{d_{100}} \qquad (66)$$

resulting in the conclusion that the Bureau of Reclamation curve in Fig. 5 provides stable d_{100} riprap sizes on horizontal beds whenever the gradation is selected such that the d_{50} size is greater than 0.76 d_{100}. For cases other than $k = 1.2\,d_{50}$, the riprap is stable when k is greater than 0.92 d_{100}. Riprap designed from Fig. 5 with a uniform gradation ($k = d_{100}$) would have a safety factor of 1.09.

Lane's Design of Stable Channels.—In his method for designing stable channels in noncohesive materials, Lane (12) employed the expression

$$K = \left(1 - \frac{\tan^2\theta}{\tan^2\phi}\right)^{1/2} \cos\theta \qquad (67)$$

to relate the stability of materials on a side slope to those on a horizontal bed. The factor K was defined as ". . . the ratio of the tractive force required to start motion on the sloping sides to that force required, in the same material, to start motion on a level surface." Eq. 67 was developed earlier by Carter, Carlson, and Lane (4).

Because $S_m = \tan\phi/\tan\theta$ the expression for K can be written

$$K = \left(1 - \frac{1}{S_m^2}\right)^{1/2} \cos\theta \qquad (68)$$

Eq. 68 can be obtained in the foregoing theoretical analysis by assuming that the lift force is zero. In other words, Lane's method does not consider fluid lift forces on the particles. With lift forces included, the equation corresponding to Eq. 67 is obtained from Eq. 34 with $S = 1$, i.e.

$$\eta = \left(1 - \frac{1}{S_m^2}\right) \cos\theta \qquad (69)$$

The ratio η/K then reflects the consequence of ignoring lift in a riprap stability analysis. From Eqs. 68 and 69, the ratio is

$$\frac{\eta}{K} = \left(1 - \frac{1}{S_m^2}\right)^{1/2} \qquad (70)$$

for the initiation of motion condition and is

$$\frac{\eta}{K} = \left(\frac{S_m^2 - S^2}{S_m^2}\right)^{1/2} \qquad (71)$$

for other conditions of horizontal flow along a side slope.

For a given rock material on a given side slope, the ratio, η/K, is the ratio of the computed incipient motion tractive force, τ_s, including lift, to the computed incipient motion shear stress, τ_s', ignoring lift or, from Eq. 70

$$\frac{\tau_s}{\tau_s'} = \left(1 - \frac{1}{S_m^2}\right)^{1/2} \qquad (72)$$

Eq. 72 indicates that neglecting the lift force for flow along a horizontal bed is of no consequence. On a horizontal bed, $S_m = \infty$ and $\tau_s = \tau_s'$. On steep side slopes, S_m is small and Eq. 72 shows that the allowable shear stress would be much lower when lift is included than when lift is ignored.

The conclusion is that lift is an important factor in the stability analysis of particles on steep side slopes. For flow on a level bed, Lane (12) recommended an allowable shear stress

$$\tau_s = 4.8\,d_{75} \qquad (73)$$

in which d_{75} = the rock size, in feet, for which 75% of the material (by weight) is finer. The units of shear stress are pound per square foot. Eq. 73 was recommended for rock with $S_s = 2.56$, but can be written

$$\tau_s = 0.049\,(S_s - 1)\,\gamma d_{75} \qquad (74)$$

for rock with any specific weight. Substitution of Eq. 74 into Eq. 32, the stability number becomes $\eta = 1.03\,d_{75}/k$. Using Lane's recommended shear stress, the safety factor on a level bed becomes $S = 0.97\,k/d_{75}$. As k is usually slightly less than d_{75}, the safety factor is slightly less than unity. For horizontal flow along a side slope, the safety factor for Lane's design criteria is given by

$$S = \frac{S_m}{2}\left[(\Omega^2 + 4)^{1/2} - \Omega\right] \qquad (75)$$

in which $$\Omega = 1.03\,\frac{d_{75}}{k}\,(S_m^2 - 1)^{1/2} \qquad (76)$$

The value of the safety factor as determined by Eq. 75 is generally less than unity.

According to the stability analysis presented herein, Lane's design criteria for stable channels yields designs in which particle motion would likely occur on the banks.

Calculation C-02 Project 35DJ2600 Appendix B Page B-9 of 37

Campbell's Analysis.—Campbell (3) employed a reference velocity $u_r = 8.5u_*$ and Isbash's equation to develop the relation

$$\frac{u_r^2}{(S_s - 1)gd_{50}} = 2.94 \quad (77)$$

for stable rock sizes. Eq. 77 corresponds to $\eta = 0.882\ d_{50}/k$ and the safety factor for flow on a plane flat bed becomes $S = 1.13\ k/d_{50}$. As $k \geq d_{50}$, Campbell's safety factor is always greater than unity for flow on a plane flat bed.

Campbell (3) also derived a method of sizing riprap for side slopes. The derivation is similar to that employed herein. His relations are complex so that no direct comparison can be made. However, according to his example calculation a 1.25-ft (0.38-m) diam riprap size is required on a 6:1 side slope in which $u_r = 14.4$ fps (4.39 m/s). Assuming that flow velocity along the bankline is horizontal, then from Eq. 42, $\eta = 0.937$. The angle of repose for dumped riprap of diameter 1.25 ft (0.38 m) is approx 42° (from Fig. 3). Therefore, from Eqs. 31, 32, and 33, $S_m = 5.40$, $\xi = 5.13$, and $S = 1.015$. That is, the 1.25-ft (0.38-m) diam rock is at the condition of incipient motion.

Riprap Design with Safety Factors

The set of equations describing stability of rock riprap permits the use of four possible design options for a fixed set of flow conditions on a side slope or on a plane bed. The options are: (1) For a given rock size and side slope or bed slope, the safety factor can be computed and the design accepted or rejected on the basis of the value of the safety factor; (2) for a given rock size, the side slope or bed slope can be chosen so as to provide a preselected safety factor; (3) for a given side slope or bed slope, the rock size which gives a preselected safety factor can be computed; and (4) for a given safety factor, the proper combinations of rock size and side slope or bed slope can be computed.

Suppose for Option 1 that the flow at point P on the nose of the embankment in Fig. 1 has a velocity $u_r = 6$ fps (1.8 m/s) and is directed down the slope so that $\lambda = 20°$. The embankment side slope is 3:1 or $\theta = 18.4°$. If the embankment is covered with dumped rock having a specific weight, $S_s = 2.65$, and an effective rock size, $k = 1.0$ ft (0.3 m), the safety factor is determined in the following manner.

From Eq. 42, $\eta = 0.203$, and according to Fig. 3 this dumped rock has an angle of repose of approx 35°. Therefore, from Eq. 28, $\beta = 11°$ and from Eq. 25, $\eta' = 0.154$. The safety factor for the rock is given by Eq. 4 or $S = 1.59$. Thus, this rock is more than adequate to withstand the flow velocity.

Because it is easier to compute the safety factor given rock size and side slope, Option 3 is best accomplished by repeating Option 1 over the range of interest for k. The results of such computations (with $\phi = 35°$) are given in Fig. 6 which shows that the incipient motion rock size is approx 0.35 ft (0.11 m) and that the maximum safety factor is less than 2.0 on the 3:2 side slope.

The safety factor of a particular side slope riprap design can be increased by decreasing the side slope angle, θ. If the side slope angle is decreased to

0°, then Eq. 37 is applicable and $S = 4.93$. The curve in Fig. 7 relates the safety factor and side slope angle of the embankment shown in Fig. 1 [for $\lambda = 20°$, $k = 1.0$ ft (0.305 m) and $u_r = 6.0$ fps (1.8 m/s)]. The curve can be employed to obtain Option 2.

Design Option 4 is difficult to use for oblique flow on side slopes and is,

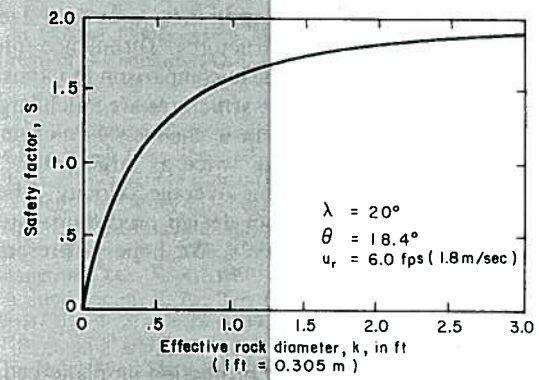

FIG. 6.—Safety Factors for Various Rock Sizes on Side Slope

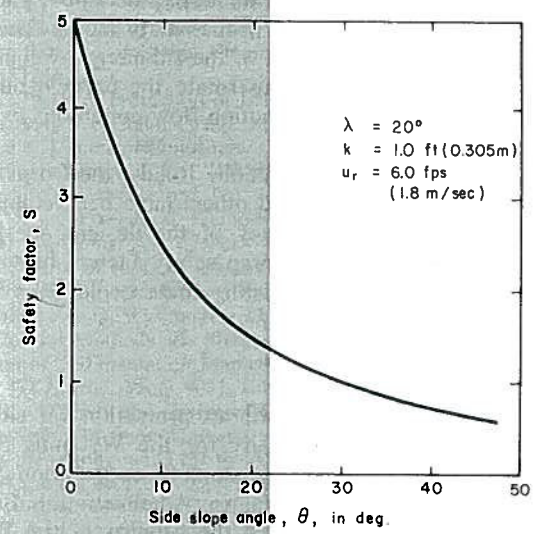

FIG. 7.—Safety Factors for Various Side Slopes

therefore, recommended only if the flow velocity vector on the side slope is nearly horizontal.

The developed equations deal with average values of shear stress and local velocity. Instantaneous values of the shear stress, τ_s, or local velocity, u_r, may be as much as two or three times greater or less than the average value. The fact that instantaneous shear stress at the bed could be varying greatly

is accounted for in Shield's criteria for incipient motion if turbulence is generated at the channel boundary. However, if turbulence is being generated in some other manner (e.g., by a hydraulic jump), then the average boundary shear stress is more closely related to the turbulence intensity of the flow than to the velocity gradients.

As there are very few measurements of turbulence intensities in flow fields over riprap below energy dissipators, riprap in these areas are sized from model studies and from experience with field structures. Turbulence intensities below energy dissipating structures are very large in comparison to intensities in normal channels. Rock sizes required below these structures are much larger than would be needed for the same mean velocity in a channel. For example, the U.S. Army Engineers (22) specify a rock size twice as large below stilling basins as in normal turbulent flow with the same average velocity. The writers have had the opportunity to confirm the riprap design procedures presented herein by experimentation with large-scale models. We hope to present these model data in the future.

Summary and Conclusions

Stability equations for design of riprap protection on plane beds, side slopes, and embankment slopes have been formulated from theoretical considerations and existing empirical information. The relative importance of the magnitude and direction of the velocity vector, the angle of side slope, and the size and angle of repose for riprap, are reflected in the safety factor. The safety factor is formulated as the ratio of the moment of the submerged weight of a particle to the lift and drag moments tending to rotate the particle out of the bed. The safety factor is unity for incipient-motion flow conditions over riprap, and is greater than unity for stable riprap.

The design criteria of the Bureau of Public Roads, the Corps of Engineers, the California Highway Department, and others have been compared with the developed stability criteria. The adequacy of the designs are judged on the basis of the computed values of the riprap safety factor. In some cases, the safety factors are less than unity indicating there could be a loss of riprap material when the design flows are obtained.

Acknowledgments

The problem of safety factors for riprap protection on side slopes was investigated by Colorado State University for the Wyoming State Highway Department, Planning and Research Division, in cooperation with the U.S. Department of Transportation, Federal Highway Administration, Bureau of Public Roads. The writers wish to acknowledge the support of the Wyoming State Highway Department and the Federal Highway Administration and the technical help of Mainard Wacker and his staff in the Hydraulic Design Office of the Wyoming Highway Department. The opinions, findings, and conclusions in this publication are those of the writers and not necessarily those of the State Highway Commission of Wyoming or the Federal Highway Administration.

Appendix.—References

1. "Bank and Shore Protection in California Highway Practice," California Division of Highways, Department of Public Works, Sacramento, Calif., Nov., 1970.
2. Brooks, N. H., discussion of "Boundary Shear Stresses in Curves Trapezoidal Channels," By A. T. Ippen and P. A. Drinker, *Journal of the Hydraulics Division*, ASCE, Vol. 89, No. HY3, Proc. Paper 3529, May, 1963, pp. 327–333.
3. Campbell, F. B., "Hydraulic Design of Rock Riprap," *Miscellaneous Paper No. 2-777*, Office, Chief of Engineers, U.S. Army, Waterways Experiment Station, Vicksburg, Miss., Feb., 1966.
4. Carter, A. C., Carlson, E. J., and Lane, E. W., "Critical Tractive Forces on Channel Side Slopes in Coarse Noncohesive Material," *Hydraulic Laboratory Report No. Hyd.-366*, Bureau of Reclamation, U.S. Department of the Interior, Washington, D.C., 1953.
5. Cheng, E. D. H., and Clyde, C. G., "Instantaneous Hydrodynamic Lift and Drag Forces on Large Roughness Elements in Turbulent Open Channel Flow," *Sedimentation*, published by Hsieh Wen Shen, ed., Fort Collins, Colo., 1972, pp. 3-1 to 3-20.
6. Christensen, B. A., "Incipient Motion on Cohesionless Channel Banks," *Sedimentation*, published by Hsieh Wen Shen, ed., Fort Collins, Colo., 1972, pp. 4-1 to 4-22.
7. Einstein, H. A., "The Bed-Load Function for Sediment Transportation in Open Channel Flows," *Technical Bulletin No. 1026*, U.S. Department of Agriculture, Soil Conservation Service, Washington, D.C., Sept., 1950.
8. Einstein, H. A., and Samni, E. A., "Hydrodynamic Forces on a Rough Wall," *Review of Modern Physics*, Vol. 21, No. 3, 1949, pp. 520–524.
9. Gessler, J., "Beginning and Ceasing of Sediment Motion," *River Mechanics*, Vol. 1, published by Hsieh Wen Shen, ed., Fort Collins, Colo., 1971, pp. 7-1 to 7-22.
10. "Hydraulic Design of Stilling Basins and Energy Dissipators," *Engineering Monograph No. 25*, U.S. Bureau of Reclamation, Technical Information Branch, Denver Federal Center, Denver, Colo., 1958.
11. Keulegan, G. H., "Laws of Turbulent Flow in Open Channels," *Journal of Research*, Vol. 21, National Bureau of Standards, Washington, D.C., 1938, pp. 701–741.
12. Lane, E. W., "Design of Stable Channels," *Transactions*, ASCE, Vol. 120, Paper No. 2776, pp. 1234–1260.
13. Lewis, G. L., "Riprap Protection of Bridge Footings," thesis presented to Colorado State University, at Fort Collins, Colo., in 1972, in partial fulfillment of the requirements for the degree of Doctor of Philosophy.
14. Murphy, T. E., and Grace, J. L., "Riprap Requirements for Overflow Embankments," *Highway Research Board Record, No. 30*, Washington, D.C., 1963, pp. 47–55.
15. "Review of Slope Protection Methods," by the ASCE Subcommittee on Slope Protection, *Transactions*, ASCE, Vol. 74, 1948, pp. 845–866.
16. Searcy, J. K., "Use of Riprap for Bank Protection," *Hydraulic Engineering Circular No. 11*, Hydraulics Branch, Bridge Division, Office of Engineering and Operations, Bureau of Public Roads, Washington, D.C., June, 1967.
17. "Sediment Control Methods: B. Stream Channels," by the ASCE Task Committee on Preparation of Sedimentation Manual, *Journal of the Hydraulics Division*, ASCE, Vol. 98, No. HY7, Proc. Paper 9071, July, 1972, pp. 1295–1326.
18. Simons, D. B., "Theory and Design of Stable Channels in Alluvial Materials," thesis presented to Colorado State University, at Fort Collins, Colo., in 1957, in partial fulfillment of the requirements for the degree of Doctor of Philosophy.
19. Simons, D. B., and Lewis, G. L., "Flood Protection at Bridge Crossings," *CER71-72DBS-GLL10*, Colorado State University, Fort Collins, Colo., 1971.
20. Simons, D. B., and Stevens, M. A., "Stability Analysis for Coarse Granular Material on Slopes," *River Mechanics*, Vol. 1, published by Hsieh Wen Shen, ed., Fort Collins, Colo., 1971, pp. 17-1 to 17-27.
21. Stevens, M. A., "Scour in Riprap at Culvert Outlets," thesis presented to Colorado State University, at Fort Collins, Colo., in 1968, in partial fulfillment of the requirements of the degree of Doctor of Philosophy.
22. "Stone Stability—Velocity vs Stone Diameter," Sheet 712-1, Civil Works Investigations, *Hydraulic Design Criteria*, U.S. Army Engineers, Waterways Experiment Station, Vicksburg, Miss., Revised, Aug., 1970.

Estimating Probabilities of Extreme Rainfalls. Thomas A. Fontaine and Kenneth W. Potter.
By George A. Harper. Closure by authors 1092

Riprap Design for Overtopping Flow

By Steven R. Abt[1] and Terry L. Johnson,[2] Members, ASCE

Abstract: Near-prototype flume studies were conducted in which riprap-protected embankments were subjected to overtopping flows. Embankment slopes of 1, 2, 8, 10, and 20% were covered with riprap layers with median stone sizes of 1, 2, 4, 5, and/or 6 in. Each riprap layer was tested by slowly increasing the discharge to failure. Riprap design criteria for overtopping flows were developed for estimating incipient stone movement and riprap layer failure as a function of the unit discharge, stone shape, median stone size, and embankment slope. Incipient stone movement occurred at approximately 74% of the riprap layer failure unit discharge. It was determined that rounded shape stone should be oversized approximately 40% to provide comparable protection of an angular shape stone. Flow channelization was observed to occur at approximately 88% of the unit discharge at failure. A flow concentration factor of approximately 1 to 3 was introduced for sizing stone.

Introduction

The erosion potential of dams, levees, roadways, and other embankment structures resulting from overflows during flood events has become an important aspect of assessing structure stability and safety. The technology and procedures developed for evaluating embankment safety have also been applied to the capping and sealing of waste disposal impoundments that have been legislated to be stable for periods of up to 1,000 years. Therefore, understanding the mechanics of erosion due to overtopping and providing alternative design measures for preventing erosion are vital steps in providing the engineer the tools to insure embankment stability.

The mechanics of erosion on embankments due to overtopping were reviewed by Powledge et al. (1989b), in which information was presented based on research and case studies of embankment overtopping. In addition, alternative methods for embankment protection systems were summarized to include vegetation, geotextiles, mat and block systems, gabions, and riprap. Powledge et al. evaluated the various embankment protective systems by relating the flow depth over the embankment, flow duration, and soil composition, where applicable, to the extent of erosive damage to the embankment.

One embankment protective system investigated and reported by Powledge et al. was the placement of a riprap layer over the embankment downstream face. It was indicated that riprap can provide suitable overtopping protection. However, undersizing of the riprap or layer thickness may result in a fluidizing of the protective layer subjecting the embankment to severe erosive processes. Powledge et al. did not specifically present a method(s) of sizing riprap for preventing fluidizing of the riprap layer.

The objective of this investigation is to develop riprap design criteria ap-

[1]Prof. and Dir., Hydr. Lab., Dept. of Civ. Engrg., Colorado State Univ., Fort Collins, CO 80523.
[2]Sr. Hydr. Engr., U.S. Nuclear Regulatory Commission, Washington, DC 20555.

Note. Discussion open until January 1, 1992. To extend the closing date one month, a written request must be filed with the ASCE Manager of Journals. The manuscript for this paper was submitted for review and possible publication on December 28, 1989. This paper is part of the ***Journal of Hydraulic Engineering***, Vol. 117, No. 8, August, 1991. ©ASCE, ISSN 0733-9429/91/0008-0959/$1.00 + $.15 per page. Paper No. 26038.

plicable to overtopping flow conditions to prevent fluidization of the protective riprap layer. If riprap is to be a viable, long-term alternative for protecting embankments from erosion, engineering design criteria must be formulated to prevent stone movement and riprap layer failure.

Background

One of the classic studies of rockfill design and placement was conducted by Isbash (1935). Isbash investigated the construction of dams by dumping rounded stones into flowing rivers. His investigation focused on:

1. Sizing individual stones located on the downstream dam slope to resist displacement due to overtopping flow and percolation through the dam body.
2. Estimating spillway discharge coefficients of the dam for various stages of completion.
3. Characterizing percolated flow through the coarse-grained material from the dam.

Isbash also conducted a series of experiments that yielded an expression indicating the critical transport velocity for displacing rounded stones as:

$$V = Y\psi(d)^{1/2} \quad (1)$$

where

$$\psi = \left[2g\left(\frac{\Delta_s - \Delta_w}{\Delta_s}\right)\right]^{1/2} \quad (2)$$

and V = the velocity acting against the individual stones, d = the stone size reduced to the equivalent sphere, Δ_s = the unit weight of the stone, Δ_w = the unit weight of water, Y = a coefficient, and g = the acceleration of gravity. Further, he expressed the percolation velocity, V_p, through the rock layer as:

$$V_p = C_0 P(dI)^{1/2} \quad (3)$$

where I = the average hydraulic gradient, P = the natural porosity or void ratio of rockfill, and C_0 = a coefficient. Based upon these relationships, Isbash formulated a procedure for dumping and stabilizing stones in flowing water.

A comprehensive investigation was conducted by Olivier (1967) on the flow through and over rockfill dams. A series of laboratory experiments were performed to evaluate how rockfill could be safely overtopped by floods both during and after construction without risk of failure. Olivier carried out his experiments in flumes 22-in. (56-cm) wide and 5-ft (152-cm) long on slopes ranging from 8 to 45%. Median stone sizes ranged from 0.51 in. (1.3 cm) to 2.33 in. (6 cm) for crushed granite and from 0.63 in. (1.6 cm) to 1.01 in. (2.6 cm) for pebbles and gravel.

Olivier observed two distinct stages during each test, threshold flow, and collapse flow. Threshold flow was defined when incipient stone movement occurs. Collapse flow is the final stage where stone failure results. Olivier was the first to recognize that channelization occurred between the threshold and collapsing stages.

Olivier empirically derived an expression for overtopping flow linking the design parameters of unit flow, slope, and median rock size for crushed or rough stones to threshold flow. The unit discharge at stone movement is:

$$q_{0t} = 0.423 d_s^{3/2}\left[\frac{(w_s - w)}{w}\right]^{5/3} i^{-7/6} \quad (4)$$

where q_{0t} = the unit discharge in cfs per foot, d_s = the median stone size in feet, w_s = the unit weight of the stone, w = the unit weight of water, and i = the embankment gradient.

Hartung and Scheuerlein (1970) performed a series of overflow tests in a steep flume simulating steep open channels with natural roughness. They determined that the maximum unit discharge, q_{max}, that would resist stone movement can be expressed as:

$$q_{max} = T \cdot Y_m \cdot V_c \quad (5)$$

where

$$V_c = 1.2\left[\frac{2g(\gamma_s - \gamma_w)}{T \cdot \gamma_w}\right]^{1/2} (d_s \cos\phi)^{1/2} \quad (6)$$

and

$$T = \frac{\gamma_{wl}}{\gamma_w} \quad (7)$$

or

$$T = 1 - 1.3 \sin\phi + 0.08\frac{Y_m}{\theta_m} \quad (8)$$

where Y_m = the mean water depth, θ_m = the mean roughness height ($\sim d_s/3$), d_s = the equivalent diameter of the stones, ϕ = the angle of slope, T = the aeration factor, V_c = the critical velocity at which the stone begins to move, γ_w = the specific weight of water, γ_{wl} = the specific weight of the air-water mixture, γ_s = the specific weight of the stone, and g = the acceleration of gravity.

Stephenson (1979) performed a stability analysis for stones placed on the downstream face of a rockfilled embankment subjected to overtopping. His analysis of the hydraulic reaction on the resisting stones related the stone size to the slope angle and flow rate. Stephenson derived an equation to determine median stone size, d, for the threshold flow expressed as:

$$d = \left[\frac{q\,(\tan\theta)^{7/6} n^{1/6}}{C g^{1/2}[(1-n)(S-1)\cos\theta\,(\tan\phi - \tan\theta)]^{5/3}}\right]^{2/3} \quad (9)$$

where q = the threshold unit discharge, n = the porosity, s = the relative density of the stone, C = a coefficient, θ = the slope angle, ϕ = the angle of friction, and g = the gravitational acceleration. The coefficient, C, is derived from Olivier (1967) and reported to be 0.22 for gravel and pebbles, and 0.27 for crushed stone. Complete collapse of the riprap will occur when the unit discharge is increased 120% for gravel and 108% for crushed stone.

Knauss (1979) performed a comparison of the Olivier expression, (4), and

the Hartung and Scheuerlein expression, (5), for overtopping flow conditions. He determined that both equations were valid for crushed stone with angular shapes. However, Knauss recommended the Hartung and Scheuerlein equation for the design of overflowed rockfill dams with steep downstream slopes ranging from 20 to 67%.

Powledge and Dodge (1985) conducted a series of small-scale overtopping tests using riprap as embankment protection on the downstream face. Since the tests were to evaluate embankment protection and not to provide riprap design criteria, the riprap fluidized and eroded the embankment. Powledge and Dodge determined that improperly designed riprap did not provide erosive protection to the embankment from overtopping flow.

It is evident that riprap design to resist overtopping flow is a function of the representative stone size, the hydraulic gradient, and the discharge. Further, riprap design should be directed toward preventing stone movement and to insure the riprap layer does not fail or collapse.

Testing Facilities

An experimental program (Abt et al. 1987, 1988) was conducted in two flume facilities located at the Engineering Research Center of Colorado State University (CSU). An outdoor flume was utilized for simulating steep embankment slopes ($\geq$0.10) while an indoor laboratory flume was used for simulating flatter slopes ($\leq$0.10). Each flume was modified to enable prototype testing of stone-covered embankments in order to evaluate flow conditions and stone movement.

The outdoor facility is a concrete flume that is 180-ft (54.9-m) long, 20-ft (6.1-m) wide, and 8-ft (2.4-m) deep. The flume was modified to where the upper 20 ft (6.1 m) served as a holding basin and inlet to the test section. A headwall was constructed 20 ft (6.1 m) downstream of the inlet. The embankment was constructed downstream of the headwall. The throat of the test section containing the embankment was 12-ft (3.7-m) wide to concentrate flow onto the slope. Fig. 1 depicts the outdoor facility.

The test embankment was constructed of a moistened, compacted sand in the throat of the test section. The initial 15 ft (4.6 m) of embankment, downstream of the headwall, was horizontally placed to simulate the embankment crest and to fully develop flow approaching the slope. The embankment transitioned to a designated slope. A geofabric covered and stabilized the sand. The geofabric allowed the embankment face to be saturated and flex under a variety of loading conditions. However, the geofabric prevented the sand from massive failure, thereby minimizing turn-around time between experiments. A 6-in.- (0.15-m-) thick sand/gravel bedding was placed on top of the geofabric as specified by the bedding design criteria suggested by Sherard et al. (1984). Riprap was placed on top of the bedding material.

The indoor facility, located in the CSU Hydraulics Laboratory, is a steel, tilting flume that is 200-ft (61-m) long, 8-ft (2.4-m) wide, and 4-ft (1.2-m) deep. The flume was modified to enable the embankment slope to vary from 0.01 to 0.10. The flume inlet was modified to where flows entered the head box, discharged through a diffuser, and transitioned into the flow development section. Rock was placed in the upstream 80 ft of the flume to establish uniform approach flow conditions. A 20-ft (6.1-m) transition section was constructed linking the approach to the riprap test section. The riprap test

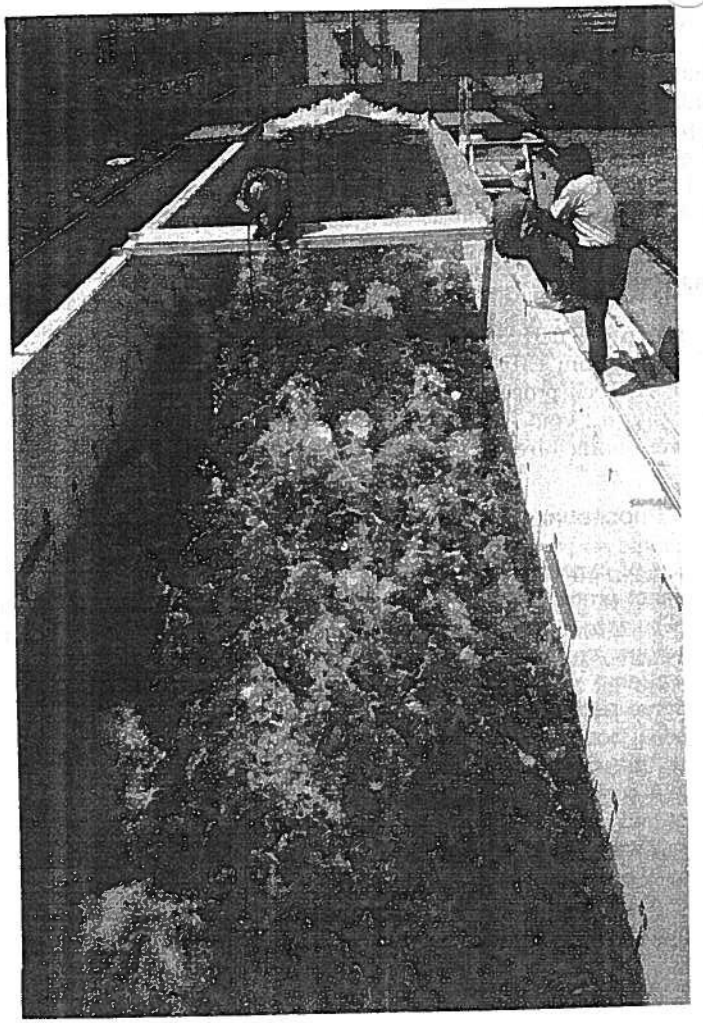

FIG. 1. Test Facility with Riprap-Protected Embankment

section extended 50 ft (15.2 m). The remainder of the flume served as the tailwater control and material recovery basin. The test embankment consisted of a moistened, compacted 4-in. (0.10-m) sand layer. A geofabric covered and stabilized the sand bed. An appropriately sized sand/gravel bedding was placed on the geofabric to a thickness of approximately 6 in. (0.15 m). Riprap was placed on top of the bedding material.

The instrumentation used in both facilities consisted of the equipment and materials necessary to monitor the discharge, water surface elevation, and flow velocity over the riprap layer. Surface velocities were recorded using a Marsh-McBirney® magnetic flowmeter and discharges were measured with a sonic flowmeter in the outdoor flume. A pitot tube was used to determine

the velocity profiles and orifice plates measured discharges entering the headbox in the indoor flume.

Water-surface elevations were monitored using manometer taps installed beneath the bedding of the embankment of both flumes. The manometer taps were placed at sections near the transition, at the upper one-third point of the slope, and at the lower one-third point of the slope. The taps were equally spaced across the embankment at the quarter points of each section to monitor potential differences in the flow distribution.

Riprap Properties

The riprap was derived from a limestone quarry. Median stone sizes, D_{50}, tested ranged from 1.02 in. (2.59 cm) to 6.2 in. (15.75 cm) as summarized in Table 1. Rock properties of gradation, unit weight, γ, specific gravity, G_s, porosity, n_p, void ratio, e, and friction angle, ϕ, were determined using procedures outlined by the American Society for Testing Materials (ASTM).

Testing Procedure

A series of experiments were conducted in which riprap was placed as an embankment protective material and subjected to an overtopping flow until failure. The experimental variables encompassed the median stone diameter, channel slope, unit surface discharge, surface flow velocity, and water surface elevation.

The riprap testing and failure procedures were similar for all experiments conducted in both indoor and outdoor facilities. The riprap was dump-placed. However, the stone surface was leveled to avoid the occurrence of man-made flow concentrations. Once the riprap was placed and the instrumentation set and checked, the flume inlet valves were opened, initiating flow. The riprap was inundated and the bed was allowed to adjust and/or settle. The flow was increased until flow over the riprap surface was observed. Once the flow stabilized, the discharge was determined and localized velocities and water surface elevations were obtained through the upper third and lower third of the embankment when and where possible. Since the depth of surface flow could not be directly measured due to cascading flow conditions, the depth of flow along the slope was determined by monitoring

TABLE 1. Riprap Properties

Shape (1)	D_{50} (in.) (2)	D_{50} (cm) (3)	C_u (d_{60}/d_{10}) (4)	σ (d_{84}/d_{16}) (5)	γ (6)	G_s (7)	n_p (8)	ϕ (9)
Subangular	1.02	2.59	1.75	1.79	94	2.72	0.44	40
Angular	2.2	5.59	2.09	2.09	92	2.72	0.45	41
Angular	4.1	10.41	2.15	2.16	92	2.65	0.44	42
Angular	5.1	12.95	1.62	1.87	90	2.65	0.46	42
Angular	6.2	15.75	1.69	1.86	90	2.65	0.46	42
Angular	2.0	5.08	2.14	2.50	92	2.72	0.45	41
Angular	4.0	10.16	2.30	2.72	92	2.65	0.44	42
Round	2.0	5.03	2.14	5.70	92	2.72	0.45	37
Round	4.0	10.16	2.12	2.24	90	2.50	0.45	38

the manometers placed in the bed. The flow depths presented are an average value derived from the six manometers along the embankment slope. After recording the data and documenting observations, the flow was increased. The procedure was repeated until stone movement and/or riprap layer failure occurred.

The failure criterion of the riprap layer was when the filter blanket, or more often, the geofabric, was exposed. In many cases, concentrated flows would scour a localized zone along the embankment. However, rock movement from up slope would subsequently fill and stabilize the scour area. When rock movement could no longer adequately replenish rock to the scour or failure zone, catastrophic failure was observed. Therefore, catastrophic failure could occur prior to geofabric exposure due to the dynamic rock movement along the bed and due to poor conditions for observing the bedding resulting from the significant turbulence, bubbles, and air entrainment of the cascading flows. The times from the initiation of flow to the rock layer failure ranged from 2 to 4 hours depending upon riprap size.

Results

Twenty-six flume tests were conducted with riprap placed on embankment slopes of 0.01 to 0.20 and subjected to overtopping flows until riprap failure, or collapse, occurred. Twenty-one tests were performed using angular shaped stones and five tests evaluated rounded shaped stones. In 15 tests, the unit discharge at stone movement, or threshold flow, and riprap channelization was recorded. A summary of the test parameters measured for each test is presented in Table 2.

It was observed in the early stages of each test that the smaller stones on the riprap surface were often washed out, leaving the upper layer of larger stones to armor the remainder of the embankment. On slopes greater than 0.02, cascading flows resulted. The plunging and impacting flow conditions often caused the larger stones to move and/or adjust until interlocking, wedging, and/or packing occurred between adjacent stones, particularly during discharges approaching the failure discharge on the steeper embankment slopes. During the adjustment process, stones often penetrated the water surface, thereby increasing the white water appearance. When the riprap layer failed, a catastrophic failure was observed on all slopes greater than 0.02.

Angular-Stone Failure

Riprap specifications have traditionally stipulated that a high-quality, angular-shaped stone (preferably crushed) be used for placement in the field. Angular stone tends to interlock or wedge and subsequently resist sliding and rolling. In addition, fewer fines are required to fill the voids of crushed material compared with a similarly graded rounded stone.

In an attempt to determine the riprap layer stability for angular shaped stones when subjected to overtopping flow, the riprap layer median stone size, D_{50}, was correlated to the overtopping unit discharge at failure, q_f, for the angular shaped stones, as presented in Fig. 2. It is observed in Fig. 2 that the data represent a family of parallel relationships that correlates the unit discharge at failure to the embankment slope, S, and median stone size. A composite relationship was formulated collapsing the data presented in

TABLE 2. Data Summary

Run (1)	Flume (2)	Stone shape (3)	Riprap D^{50} (in.) (4)	Riprap D^{50} (cm) (5)	Riprap thickness (in.) (6)	Layer (r) (cm) (7)	Slope (8)	q failure (cfs/ft) (9)	q failure (m^3/s-m) (10)	t/D^{50} (11)	q move/ q failure (12)	q channel/ q failure (13)
7	Outdoor	Angular	4.1	10.4	12	30.5	0.20	1.81	0.17	2.9	0.77	0.90
10A	Outdoor	Angular	5.1	13.0	12	30.5	0.20	3.56	0.33	2.4	0.79	0.88
15	Outdoor	Angular	6.2	15.7	12	30.5	0.20	4.43	0.41	1.9	0.75	0.85
18	Outdoor	Angular	2.2	5.6	6	15.2	0.20	0.50	0.05	2.7	0.73	0.93
21	Outdoor	Rounded	4.0	10.2	12	30.5	0.20	0.95	0.09	3.0	0.79	0.88
22	Outdoor	Rounded	4.0	10.2	12	30.5	0.20	0.95	0.09	3.0	0.80	0.89
29	Outdoor	Angular	2.0	5.1	4	10.2	0.10	0.85	0.08	2.0	0.66	0.85
31	Outdoor	Angular	2.0	5.1	6	15.2	0.10	1.00	0.09	3.0	0.62	0.82
32	Outdoor	Angular	2.0	5.1	6	15.2	0.10	1.11	0.10	3.0	0.76	0.86
36	Outdoor	Rounded	4.0	10.2	6	15.2	0.10	1.99	0.18	1.5	0.76	0.84
38	Outdoor	Rounded	4.0	10.2	12	30.5	0.10	2.09	0.19	3.0	0.66	0.86
42	Outdoor	Angular	4.0	10.2	8	20.3	0.10	3.51	0.33	2.0	0.77	0.92
44	Outdoor	Angular	4.0	10.2	12	30.5	0.10	3.79	0.35	3.0	0.78	0.86
46	Outdoor	Rounded	2.0	5.1	6	15.2	0.10	0.69	0.06	3.0	0.67	0.83
51	Outdoor	Angular	4.0	10.2	12	30.5	0.10	4.12	0.38	3.0	0.75	0.89
107	Indoor	Angular	2.2	5.6	6	15.2	0.02	4.53	0.42	2.7	—	—
111	Indoor	Angular	1.02	2.6	3	7.6	0.02	1.11	0.10	2.9	—	—
120	Indoor	Angular	1.02	2.6	3	7.6	0.01	1.50	0.14	2.9	—	—
125	Indoor	Angular	1.02	2.6	3	7.6	0.10	0.36	0.03	2.9	—	—
126	Indoor	Angular	1.02	2.6	3	7.6	0.10	0.34	0.03	2.9	—	—
127	Indoor	Angular	1.02	2.6	3	7.6	0.10	0.31	0.03	2.9	—	—
128	Indoor	Angular	1.02	2.6	3	7.6	0.10	0.42	0.04	2.9	—	—
129	Indoor	Angular	2.2	5.6	6	15.2	0.10	1.12	0.10	2.7	—	—
130	Indoor	Angular	2.2	5.6	6	15.2	0.10	1.25	0.12	2.7	—	—
131	Indoor	Angular	2.2	5.6	6	15.2	0.10	1.25	0.12	2.7	—	—
132	Indoor	Angular	2.2	5.6	6	15.2	0.08	1.81	0.17	2.7	—	—

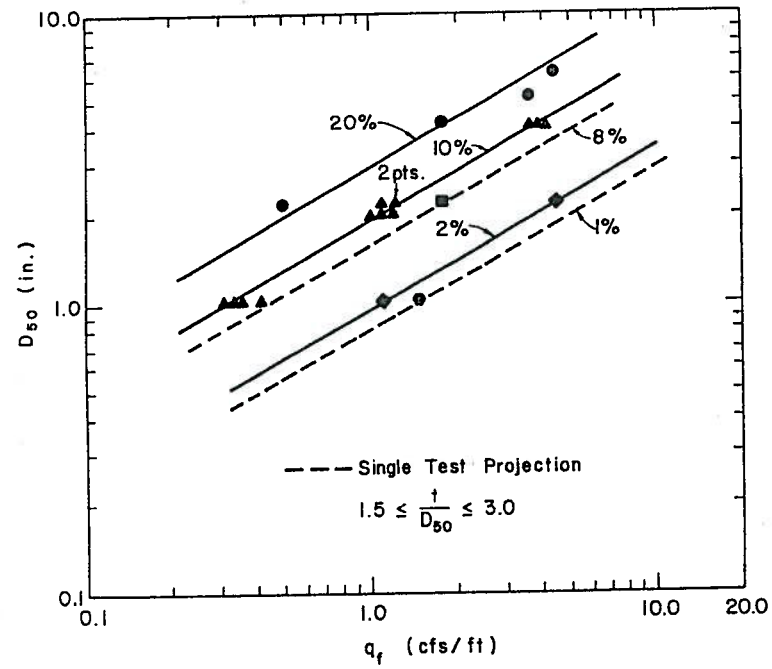

FIG. 2. Unit Discharge at Failure versus Median Stone Size

Fig. 2 into single envelope for angular stones as shown in Fig. 3. A power regression was performed on the parametric expression relating median stone size to the embankment slope and overtopping unit discharge at failure. The results are expressed as:

$$D_{50} = 5.23S^{0.43}q_f^{0.56} \quad (10)$$

Eq. (10) provides the user a means to estimate the minimum median stone size required to withstand a design overtopping unit discharge on an embankment with specific design slope. However, (10) indicates the riprap layer failure criteria and should be adjusted to prevent stone movement.

A safety factor may be derived for adjusting the stone size by enveloping the scattered data shown in Fig. 3. The maximum deviation about the power regression fit, (10), is approximately 20%. Therefore, a safety factor of 1.20 is recommended.

It is observed in (10), that the median stone size is determined independent of the rock specific gravity. Since (10) is an empirical relationship derived from riprap with the same specific gravity, $\gamma = 2.65$, the affect of variable specific gravity on stone sizing could not be evaluated.

The writers acknowledge that the empirical curves representative of 1, 2, and 8% embankment slopes are based on only four failure tests. However, the extensive costs associated with near prototype experimentation significantly limited the extent of the testing program. The relationship for angular-shaped stones presented in Fig. 3 provide a means for confidently estimating

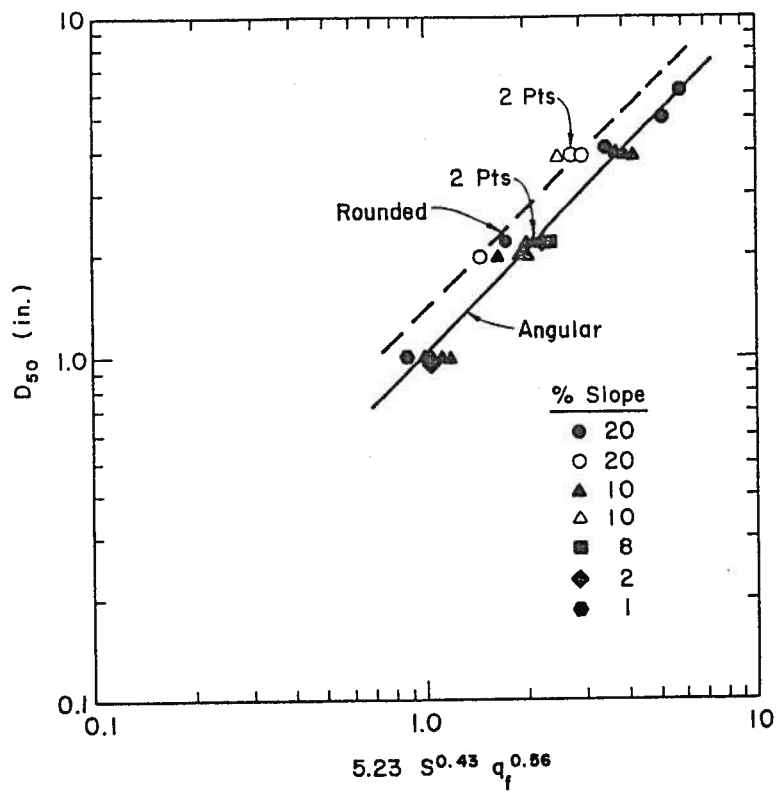

FIG. 3. Composite Riprap Layer Failure Envelope

the median stone size necessary for stabilizing an embankment of 1 to 20% subjected to overtopping flow conditions. Application of this stone sizing relationship beyond the test parameters presented are at the users' risk.

Rounded-Stone Failure

A series of five failure tests were conducted evaluating the stability of rounded-shaped stones with median diameters of 2 and 4 in., placed on 10 and 20% slopes as presented in Table 2. Test procedures were identical for both angular- and rounded-shaped riprap layers. Round rock was defined as rock with no intersecting surfaces, but rather a single, continuous, smooth-curved surface. During mining, transport, and handling, a portion of the rock fractured and became faced. The faced rock comprised approximately 5% of the rounded rock tested.

To compare the stability of rounded stone with the angular stone, the unit discharges at failure for 2- and 4-in. rounded and 2- and 4-in. angular-shaped stones were compared for a 10% slope with 3 D_{50} layer thickness. It was determined from the results in Table 2 that the rounded stones failed at a unit discharge 32 and 45% lower than the angular stone for the 2- and 4-

in. stone sizes, respectively. Although these results represent only one set of test conditions, they are indicative of the stability relationship between angular and rounded stones.

The five rounded-stone failure points were plotted in Fig. 3 adjacent to the angular-stone failure relationship. It is observed that the rounded stones reflect a linear relationship parallel to the regression curve for the angular-shaped stone. The rounded-shape riprap fails at a unit discharge of approximately 40% less than angular-shaped stones of the same median stone size.

Usually, when angular stones moved, they traveled a short distance and wedged into other stones. When the rounded stones moved, they often rolled down the entire embankment without intermediate lodging. Stone shape appears to significantly affect riprap layer stability for overtopping conditions.

The suggested relationship between angular- and round-shaped stones is based on limited data. The rounded stone relationship presented in Fig. 3 is not recommended for design. However, the angular- and round-shaped stone relationships appear to be indicative of how shape influences embankment stability.

Stone Movement

The unit discharge at stone movement, q_m, was recorded in 14 of the failure tests as indicated in Table 2. Stone movement observations were verified with videotape recordings. The stone movement was normalized by dividing the unit discharge at movement by the unit discharge at failure. The unit discharge at movement to unit discharge at failure ratio ranged from 0.62 to 0.79 with a mean value of 0.74 for both angular and rounded stone.

Since it is imperative that the riprap layer be designed to prevent failure, the median stone size should be sized to resist stone movement. Therefore, the failure unit discharge, q_f, must be adjusted by the stone movement to stone failure ratio where

$$q_{design} = \frac{q_f}{0.74} = 1.35 q_f \qquad (11)$$

Eq. (10) is modified such that the riprap median stone size is designed to resist stone movement using the design unit discharge as:

$$D_{50} = 5.23 S^{0.43} q_{design}^{0.56} \qquad (12)$$

Eq. (12) is applicable to angular-shaped riprap.

Channelization

In 15 of the 26 tests, channels formed in the riprap layer, as shown in Fig. 4, conveying unit discharges greater than expected under sheet flow conditions. The channels appeared to form as flows were diverted around the larger stones and directed into areas or zones of the smaller stones. The smaller stones were moved, creating a gap or notch between the larger stones. The flow concentrated into these notches, thereby increasing the localized unit discharge. The newly formed subchannel would quickly migrate downstream. Flow channelization occurred after stone movement and immediately prior to collapse of the riprap layer.

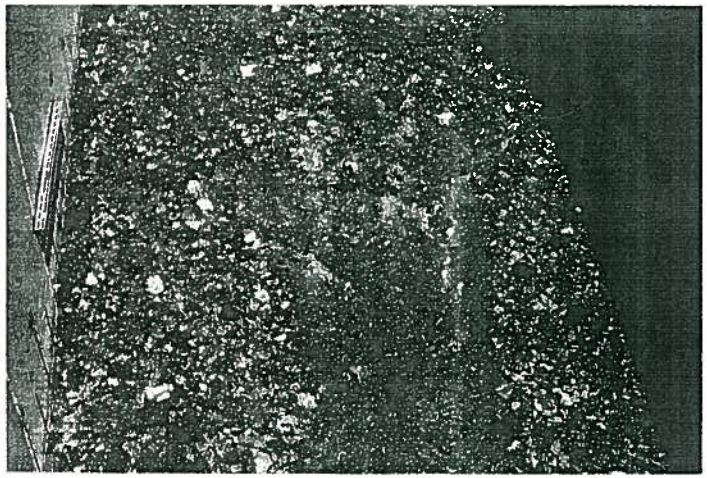

FIG. 4. Flow Channelization in 2-in. Layer of Angular Riprap on 10% Slope

During four tests, 7, 10A, 15, and 18, the subchannel depth and width were measured and localized velocities were taken when initially observed. The sheet flow unit discharge at the time of subchannel development was compared to the unit discharge estimated in the subchannel. The ratio of the subchannel flow unit discharge to the sheet flow unit discharge was 3.33, 2.24, 1.67, and 1.33 for the 2.2-, 4.1-, 5.1-, and 6.2-in. stones, respectively. The results indicate that flows can concentrate and form subchannels in the riprap layer. Therefore, flow concentrations of 3 are possible and may need to be incorporated into the design process.

The flow concentration factor may be incorporated into the stone size analysis by multiplying the failure unit discharge, q_f in (11), by the flow concentration factor, which ranges from 1 to 3. An increase of the flow concentration factor of 100% (i.e., 1 to 2) will result in a stone size increase of approximately 50%. The selection of a flow concentration factor is dependent upon the hazard level of the protected surface.

Incipient channelization was documented during 15 of the tests and verified with videotape recordings. The incipient channelization unit discharge, q_c, was normalized to the unit discharge at failure, q_f, for each test. The q_c/q_f ratios are presented in Table 2. The average point of incipient subchannel formation occurs at approximately 88% of the unit discharge at failure. Therefore, it is possible to predict the unit discharge at which channelization will occur on a riprap layer subjected to overtopping.

Comparison of Design Alternatives

The stone sizing procedures presented in (12) Olivier (1967), and Stephenson (1979) were compared by applying the appropriate stone sizing equations to the same design conditions. Stone sizing computations were conducted for unit discharges of 1.25 cfs (0.035 m^3/s) and 4.0 cfs (0.113 m^3/s) on embankment slopes of 0.10 and 0.20. The stones were assumed

TABLE 3. Design Comparison

Procedure (1)	Unit (cfs) (2)	Discharge, q (m^3/s) (3)	Embankment slope (4)	Median rock (in.) (5)	Size (cm) (6)
Eq. (12)[a]	1.25	0.035	0.10	2.6	6.6
	1.25	0.035	0.20	3.5	8.9
	4.0	0.113	0.10	5.0	12.7
	4.0	0.113	0.20	6.7	17.0
Olivier	1.25	0.035	0.10	2.4	6.1
	1.25	0.035	0.20	4.0	10.2
	4.0	0.113	0.10	5.1	13.0
	4.0	0.113	0.20	8.8	22.4
Stephenson[b]	1.25	0.035	0.10	2.9	7.4
	1.25	0.035	0.20	5.5	14.0
	4.0	0.113	0.10	6.3	16.0
	4.0	0.113	0.20	11.9	30.2

[a]Safety factor not incorporated in rock sizing.
[b]Assumes $n_p = 0.40$, $\phi = 40°$, $C = 0.27$.

to be angular in shape, with a porosity of 0.40, friction angle of 40°, and stone specific weight of 2.65. The resulting stone sizes for each procedure is presented in Table 3.

It is observed that for the flatter embankment slope (0.10) and low unit discharge (1.25 cfs), the three procedures determine similar median stone sizes ranging from 2.4 to 2.9 in. However, as the slope steepens and the unit discharge increases, the Stephenson procedure yields conservative results compared to both the proposed procedure and the Olivier procedure. The Stephenson procedure was extremely sensitive to the porosity of the stone layer.

Summary and Conclusions

A series of 26 laboratory flume tests was conducted in which riprap protected embankments were subjected to overtopping flows until the riprap layer failed. Embankment slopes of 1, 2, 8, 10, and 20% were covered with riprap layers of median stone sizes of 1, 2, 4, 5, and/or 6 in. The results of these test provided the following findings:

1. A unique riprap design relationship was developed to determine median stone size on the basis of a design unit discharge and embankment slope for overtopping flows.
2. A criterion was developed to compare the stability of round-shape riprap with angular-shape riprap. The rounded riprap appears to require oversizing of about 40% to provide a similar level of protection as angular riprap. Additional testing is required to substantiate these initial findings.
3. The median stone size should be increased by increasing the design unit discharge by 35% to prevent stone movement.
4. Flow channelization occurred along the riprap-protected embankment when the unit discharge approached 88% of the unit discharge at failure.

5. Flow concentration can occur on riprap-protected embankments. Flow concentrations of 1.33 to 3.33 were observed.

6. Riprap design criteria for sizing riprap subjected to overtopping flow conditions is presented based on near-prototype test data.

Acknowledgments

The research reported was sponsored by the office of Nuclear Material Safety and Safeguards, U.S. Nuclear Regulatory Commission.

Appendix. References

Abt, S. R., Khattak, M. S., Nelson, J. D., Ruff, J. F., Shaikh, A., Wittler, R. J., Lee, D. W., and Hinkle, N. E. (1987). "Development of riprap design criteria by riprap testing in flumes: Phase I." *NUREG/CR-4651*, U.S. Nuclear Regulatory Commission, Washington, D.C., May, 111.

Abt, S. R., Wittler, R. J., Ruff, J. F., LaGrone, D. L., Khattak, M. S., Nelson, J. D., Hinkle, N. E., and Lee, D. W. (1988). "Development of riprap design criteria by riprap testing in flumes: Phase II." *NUREG/CR-4651*, U.S. Nuclear Regulatory Commission, Washington, D.C., May, 113.

Hartung, F., and Scheuerlein, H. (1970). "Design of overflow rockfill dams." *Proc. Tenth Int. Congress of Large Dams*, 1, 587–598.

Isbash, S. (1935). *Construction of dams by dumping stones into flowing water*. U.S. Army Engrg. District, Eastport, Me.

Knauss, J. (1979). "Computation of maximum discharge at overflow rockfill dams." *Proc. 13th Congress of Int. Commission of Large Dams*, 143–159.

Olivier, H. (1967). "Through and overflow rockfill dams—new design techniques." *Proc.*, Institution of Civil Engineers, Mar., 36, 433–471.

Powledge, G. R., and Dodge, R. A. (1985). "Overtopping of small dams—an alternative for dam safety." *Proc. Hydr. and Hydro. in Small Computer Age*, ASCE, 2, Aug., 1071–1076.

Powledge, G. R., Ralston, D. C., Miller, P., Chen, Y. H., Clopper, P. E., and Temple, D. M. (1989a). "Mechanics of overflow erosion and embankments I: Research activities." *J. Hydr. Engrg.*, ASCE, 115(8), 1040–1055.

Powledge, G. R., Ralston, D. C., Miller, P., Chen, Y. H., Clopper, P. E., and Temple, D. M. (1989b). "Mechanics of overflow erosion and embankments II: Hydraulics and design considerations." *J. Hydr. Engrg.*, 115(8), 1056–1075.

Sherard, J. C., Dunnigan, L. P., and Talbot, J. R. (1984). "Basic properties of sand and gravel filters." *J. Geotech. Engrg.*, 110(6), 684–700.

Stephenson, D. (1979). *Rockfill in hydraulic engineering*. Elsevier Scientific Publishing Co., New York, N.Y., 215.

Comparisons of Selected Bed-Material Load Formulas

By Chih Ted Yang,[1] Fellow, ASCE, and Schenggan Wan[2]

Abstract: Comparisons are made of the overall accuracy as well as the accuracy within different ranges of sediment concentration, Froude number, and slope for seven bed-material load formulas. Four formulas that can compute bed-material load transport by size fraction are used to determine the particle size distribution of the bed materials in transportation. One-thousand, one-hundred-nineteen sets of laboratory data and 319 sets of river data in the sand size range are used to evaluate and compare the accuracy of these formulas. The overall accuracy of formulas in descending order are those of Yang, Engelund and Hansen, Ackers and White (d_{50}), Laursen, Ackers and White (d_{35}), Colby, Einstein, and Toffaleti formulas when applied to laboratory flumes. The accuracy in descending order when applied to natural rivers are the formulas by Yang, Toffaleti, Einstein, Ackers and White (d_{50}), Colby, Laursen, Engelund and Hansen, and Ackers and White (d_{35}). However, these ratings may vary depending on the values of sediment concentration, Froude number, and slope of the data used in the comparison. The study also indicates that Yang's formula by size fraction can accurately predict the size distribution of bed material in transportation, while Einstein's hiding and lifting correction factors overcorrected the effect of nonuniform size distribution of bed material on total bed-material transport.

Introduction

There are numerous sediment transport formulas developed by different investigators for the prediction of bed load, suspended load, and total bed-material load in alluvial channels. Comparisons of the accuracy of these formulas were made by Yang and Stall (1973), White et al. (1975), Yang (1976), Alonso (1980), Brownlie (1981), Yang and Molinas (1982), the ASCE Task Committee ("Relationships between Morphology" 1982), Yang (1988), Vetter (1989), and the German Association for Water Resources and Land Improvement (1990), among others. These comparisons emphasize the overall accuracy of formulas without given detailed information of the hydraulic and sediment conditions under which measurements were made. Depending on the conditions under which data were collected for comparisons, the same formula could have different ratings of accuracy. This often causes confusion in the profession in the selection of formulas for solving engineering problems.

Measured sediment concentration, Froude number, and slope are used as parameters to define the hydraulic and sediment conditions. The analyses in this paper are limited to total bed-material load formulas due to the lack of general criteria to separate bed load from suspended load. Comparisons between computed bed-material size distribution and size distribution of bed materials in bed and in transportation are also made in this paper. The computer programs published by Stevens and Yang (1989) are used herein for

[1]Int. and Special Proj. Coordinator, U.S. Bureau of Reclamation, Denver, CO 80225.

[2]Sr. Engr., Nanjing Hydr. Res. Inst., Nanjing, China.

Note. Discussion open until January 1, 1992. To extend the closing date one month, a written request must be filed with the ASCE Manager of Journals. The manuscript for this paper was submitted for review and possible publication on June 14, 1990. This paper is part of the ***Journal of Hydraulic Engineering***, Vol. 117, No. 8, August, 1991. ©ASCE, ISSN 0733-9429/91/0008-0973/$1.00 + $.15 per page. Paper No. 26039.

Riprap Sizing at Toe of Embankment Slopes

By Steven R. Abt,[1] Fellow, ASCE, T. L. Johnson,[2] Member, ASCE, Christopher I. Thornton,[3] and Stuart C. Trabant[4]

Abstract: A pilot study was conducted to evaluate existing rock-sizing techniques for stabilizing transition toes of embankments. The U.S. Bureau of Reclamation and the U.S. Army Corps of Engineers (Campbell) procedures were applied and determined to be conservative in sizing riprap. Embankment-overtopping tests were conducted placing 8.9, 13.0, and 19.8-cm-diameter stones at the slope transition. An alternative method was developed for sizing toe rock based upon the unit discharge, embankment slope, and flow concentration. The results indicate that an embankment toe can be stabilized with a smaller median stone size than previously anticipated. These results were verified for unit discharges of 0.54 $m^3/s/m$ or less.

INTRODUCTION

Rock toes, or toe basins, are often placed at the base of sloped embankments to stabilize and/or anchor rock placed on the side slope; serve as a toe drainage channel; serve as an impact basin and provide for energy dissipation from tributary flow; and provide erosion protection at the toe, transition flow from the side slope to adjacent properties, and/or provide gully intrusion protection to the embankment. Therefore, proper rock sizing is an imperative element of the design process to meet the project requirements while minimizing project costs.

Rock-sizing procedures have been developed by Isbash (1935), Olivier (1967), Hartung and Scheuerlein (1970), Stephenson (1979), and Abt and Johnson (1991) that can be applied for protecting embankment top slopes and side slopes for parallel flow conditions. However, these procedures were derived from through-flow and overtopping-flow conditions and are not considered applicable to flow transitioning from a side slope onto a horizontal or near-horizontal toe. In most cases, riprap placed at the toe of an embankment slope must be sized to ensure stability as runoff transitions from the embankment slope to the toe.

The U.S. Bureau of Reclamation (USBR) developed a riprap design procedure for applications in stilling basins (USDOI 1978) founded on the work of Berry (1948). The USBR procedure is empirically based from extensive laboratory testing and field observations. The procedure estimates the median stone size as a function of the localized bottom velocity (in feet per second) of the flow, V_b, at the location where the flow transitions onto a stone-filled basin. If the bottom velocity cannot be determined, the local average velocity may be substituted to size the rock. The local average velocity can be determined using the U.S. Army Corps of Engineers procedures (USACE 1991). The stone size and/or stone weight can be determined from Fig. 1 (developed in English units).

Campbell (1966) presented a velocity-based riprap design procedure for stone placed in channels for bank stability and in stilling basin applications. Using the Isbash approach to rock sizing and applying the logarithmic law velocity distribution, Campbell developed a series of relationships between velocity and stone size as presented in Fig. 2. Campbell presented velocity in feet per second, stone diameters in feet, and stone weights in pounds.

The USBR and Campbell rock-sizing procedures were developed to dissipate energy and provide a stable toe as flow transitions into a stilling basin or similar structure. The rock was sized to resist movement on a flat toe in the hydraulic jump development region of flow. These procedures are difficult to apply for relatively small rock requirements (<0.3 m). Both procedures have been routinely applied in engineering practice for sizing rock placed at the transitions of compound slopes (i.e., toe rock at the base of a slope) because alternative procedures have not yet been formulated. Interestingly, both procedures are perceived to yield conservative rock sizes.

A pilot program was performed to test and evaluate the USBR and Campbell rock-sizing procedures when applied to flow transitioning from an embankment side slope onto a rock toe. The experimental program was designed to observe and document rock movement and/or failure of riprap placed at the toe of an embankment and subjected to flow parallel to the embankment, thereby, transitioning into a rock toe.

TEST PROGRAM

Facility

An outdoor, concrete facility was used to accommodate a pilot, near-prototype experimental program. The model consisted of a supply pipeline with a control valve, a headbox with a manifold, an embankment, a rock toe, and an outlet sluice. A schematic profile of the test section is presented in Fig. 3.

The embankment was constructed in the test section with dimensions of 29.3 m (96.2 ft) long and 2.4 m (7.8 ft) wide. The embankment consisted of a moistened sand-fill material placed to a height of 1.83 m (6 ft). The top slope was 4.6 m (15 ft) long with a slope of 0.5%. The side slope was approximately 4.6 m (15 ft) long with a slope of 20%. The toe-of-the-slope (rock toe) basin was approximately 4.9 m (16 ft) in length with a rock depth transitioning from 0.91 m (3 ft) to 0.61 m (2 ft) as indicated in Fig. 3. A sand/clay soil was placed adjacent to the toe rock outlet extending downstream approximately 12.2 m (40 ft) at a slope of approximately 3% to simulate adjacent field conditions.

The embankment top slope and side slope were covered with a stabilized riprap layer of 8.9 cm (3.5 in.) diameter rock with a minimum depth of 1.5 times the median rock D_{50}. Rock was placed at the toe and smoothly transitioned the embankment side slope to the toe as indicated in Fig. 3.

Riprap

The riprap placed at the toe for each of three tests had median stone sizes of 8.9 cm (3.5 in.), 13.0 cm (5.1 in.), and

[1]Prof., Dept. of Civ. Engrg., Colorado State Univ., Ft. Collins, CO 80523.

[2]Sr. Hydr. Engr., Ofc. of Nuclear Mat. Safety and Safeguards, U.S. Nuclear Regulatory Commission, Washington, DC 20555.

[3]Res. Assoc., Dept. of Civ. Engrg., Colorado State Univ., Ft. Collins, CO.

[4]Hydr. Engr., Mussetter Engineering Inc., Ft. Collins, CO 80524.

Note. Discussion open until December 1, 1998. To extend the closing date one month, a written request must be filed with the ASCE Manager of Journals. The manuscript for this paper was submitted for review and possible publication on December 3, 1996. This paper is part of the ***Journal of Hydraulic Engineering***, Vol. 124, No. 7, July, 1998. ©ASCE, ISSN 0733-9429/98/0007-0672–0677/$8.00 + $.50 per page. Paper No. 14718.

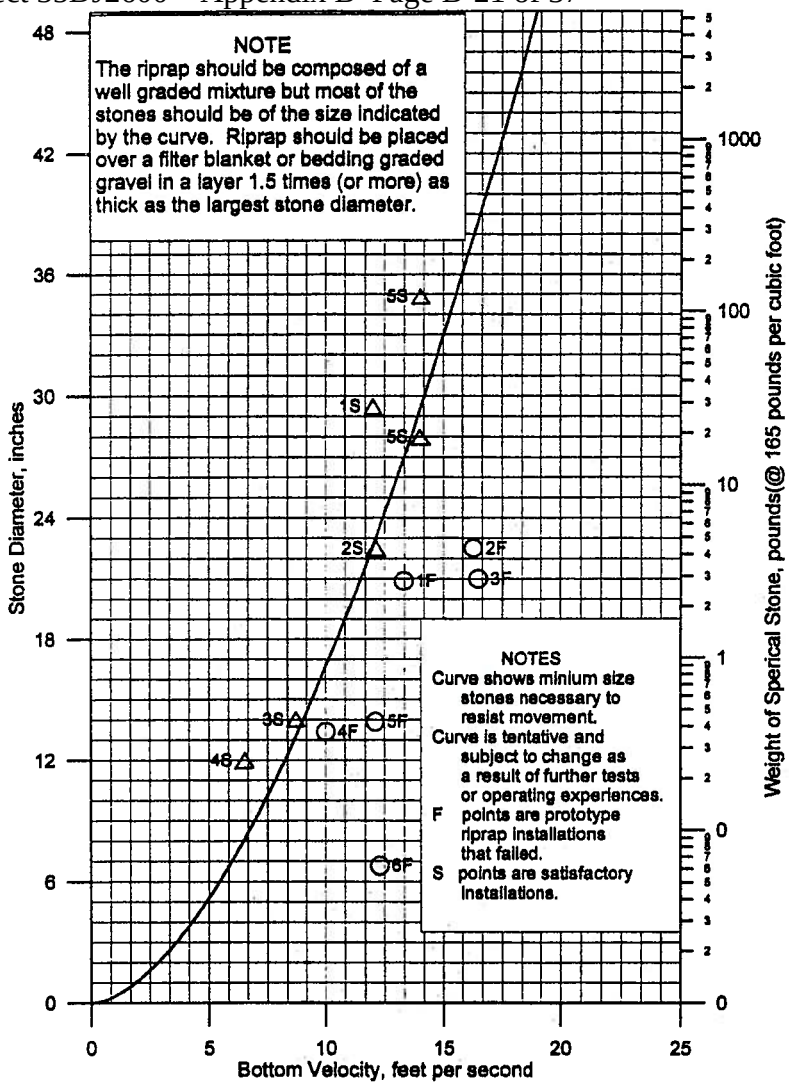

FIG. 1. Parametric Curve Used To Determine Maximum Stone Size in Riprap Mixture as Function of Channel Flow (USDOI 1978)

19.8 cm (7.8 in.), respectively. The stones were angular in shape with a specific gravity of 2.63. The coefficients of uniformity of the riprap ranged from 1.13 to 1.25 and are considered uniform.

Instrumentation

Instrumentation used to document the rock performance included a point gauge for monitoring the water surface on the top slope and slide slope of the embankment and a total station survey instrument with prism for monitoring the bed elevations at and near the toe. Velocities were measured using a Marsh-McBirney magnetic flowmeter, which was calibrated immediately prior to its use. Videotape and still photographs were used to visually document each test.

Test Procedure and Program

Once the embankment was constructed, a detailed survey was performed to document the pretest stone surface elevations. A 0.3-m grid was established throughout the toe basin area. The grid elevations served as the base elevations for monitoring riprap movement during and after each flow increment.

Each rock toe was tested in the same manner. The flow to the facility was initiated, and the headbox was slowly filled. Care was taken to prevent surging or pulsation of the flow as it first overtopped the embankment and entered the test section. The discharge was increased to a flow of approximately 0.028 $m^3/s/m$ (1 cfs/ft). Flow was allowed to stabilize; then data were collected at four locations throughout the test section. Flow velocities were recorded at the embankment crest (Section 1), midslope (Section 2), toe of the slope immediately upstream of the hydraulic jump (Section 3), and 1.5-m downstream of the toe in the basin as indicated in Fig. 3. Point velocity measurements were taken at 0.6 times the flow depth from the surface at quarter intervals across the flume. Bed elevations were determined at the toe of the slope each time velocity measurements were obtained. After the velocity and bed elevations were recorded, the flow was increased and the data collection repeated. The process continued until the rock toe failed. The test was then terminated, the toe basin documented, and the embankment and/or toe basin reconstructed.

The testing program consisted of three tests; each test using one of the rock sizes (8.9, 13.0, and 19.8 cm) in the toe. The program test focused on the rock placed at and immediately downstream of the location where the flow transitioned from the side slope to the rock toe. It is acknowledged that the flow turbulence at the impact zone made direct observation difficult. Therefore, observations of the rock included monitoring audible vibrations of the stone. In addition to the vibrations, the point gauge and survey rod with base plate were used to monitor vertical displacement prior to stone entrainment or horizontal dislodgment. Rock movement was defined to be when stone was horizontally dislodged at the toe. Toe failure oc-

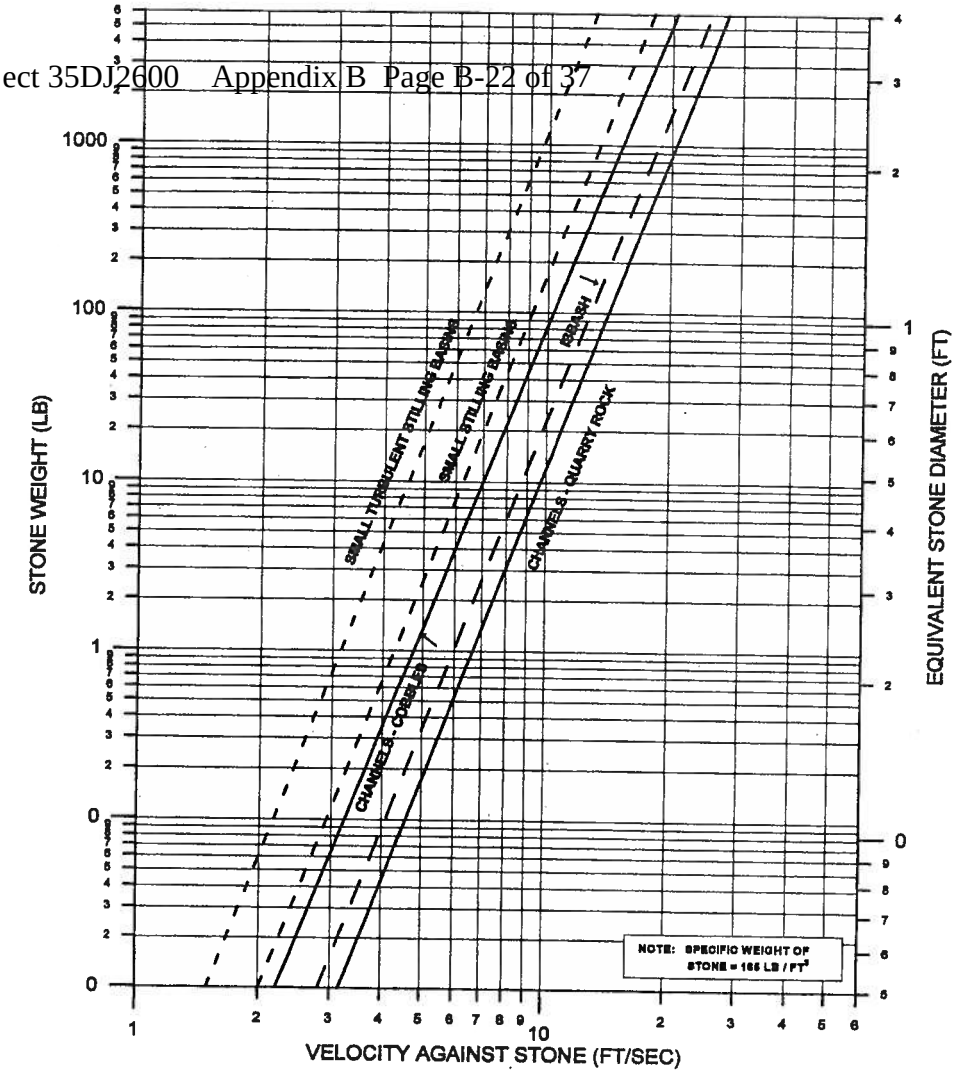

FIG. 2. Campbell Velocity–Stone-Sizing Relationships (Campbell 1966)

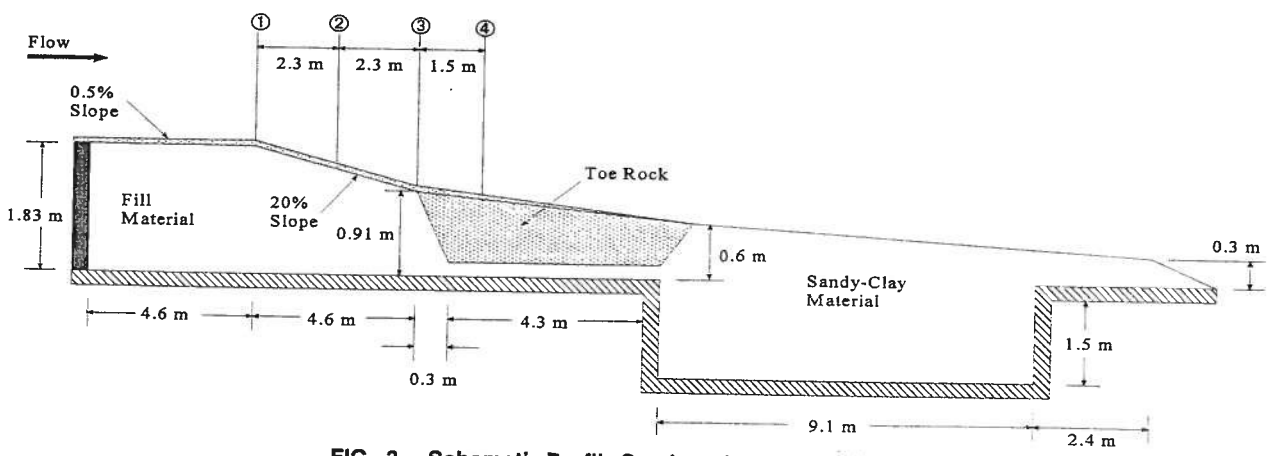

FIG. 3. Schematic Profile Section of Test Embankment

curred when the elevation of the toe degraded the equivalent of one median stone size. Although this is not a conservative definition of failure, it provides measurable criteria during testing.

RESULTS

When overtopping began, flow was conveyed down the embankment slope and transitioned onto the toe. Rock usually settled and/or adjusted to resist the impinging forces. Rock adjustment to incremental flow increases was not considered a state of rock movement. As the flow increased, a point was attained where individual stones began to vibrate and/or vertically displace. Rock vibrations would eventually transition to rock entrainment and/or displacement. In some instances, the rock displaced a short distance across the toe basin and then settled and/or lodged into other rocks in the basin. The flow eventually entrained the rock and completely transported the rock out of the basin. Identifying the exact point of rock movement was difficult (horizontal displacement) due to the turbulent conditions.

TABLE 1. Summary of Velocities

Test (1)	D_{50} (cm) (2)	q ($m^3/s/m$) (3)	Average Velocity (m/s) Section 1 (4)	Section 2 (5)	Section 3 (6)	Section 4 (7)	Comment (8)
1	19.8	0.08	1.22	1.58	1.25	0.52	
	19.8	0.18	1.54	2.61	2.38	1.04	
	19.8	0.26	1.73	2.73	3.00[a]	0.81	
	19.8	0.36	1.87	3.01	3.26	0.96	
	19.8	0.44	2.02	3.15	3.50	0.94	
	19.8	0.54	2.15	3.43	3.65	—	Failure
2	13.0	0.09	1.09	1.65	1.98[a]	0.92	
	13.0	0.18	1.50	3.15	3.05	0.83	
	13.0	0.26	1.72	3.36	2.36	1.11	
	13.0	0.36	1.83	2.99	3.20	1.32	Failure
3	8.9	0.08	—	—	1.05[a]	—	
	8.9	0.08	1.49	1.75	—	—	
	8.9	0.18	1.56	2.04	1.78	1.78	
	8.9	0.26	1.69	2.18	2.85	1.81	Failure

[a]Rock begins to vibrate/vertically translate based on visual and auditory observations.

A summary of the test measurements indicating the unit discharge and average velocities at each of the four monitoring sections is presented in Table 1. Incipient rock vibration and/or vertical displacement was detected based upon visual observations, videotapes, and auditory assessments as annotated in Table 1. Rock movement was monitored in Sections 3 and 4 based upon periodic bed elevation contouring. It is observed that the maximum flow velocities were measured at the toe of the slope adjacent to Section 3; velocities ranged from 2.85 m/s (9.34 ft/s) to 3.65 m/s (11.97 ft/s).

The flow impinged on the rock toe and transitioned into a hydraulic jump to dissipate the energy of the flow. The data demonstrate that the velocity was significantly slowed at the jump downstream of the toe by 50–70%.

ANALYSIS

During the low-flow segments of each test, flow conditions permitted the observation (visual and auditory) of rock vibration and/or vertical displacement (incipient movement). The 8.9 cm (3.5 in.), 13 cm (5.1 in.), and 19.8 cm (7.8 in.) stones were observed to vibrate/vertically displace at velocities of approximately 1.05 m/s (3.43 ft/s), 1.98 m/s (6.48 ft/s), and 3.0 m/s (9.84 ft/s), respectively. The incipient values were plotted on the USBR (USDOI 1978) rock-sizing design curve as presented in Fig. 4. The incipient movement measurements appear to agree closely with the data used to establish the USBR criteria. These results imply that the USBR used a conservative definition of rock movement.

Traditional procedures such as the USBR (USDOI 1978) and Campbell (1966) utilize the flow velocity estimated at the transition to determine the median rock size of the riprap in the stilling area (toe basin). These procedures are empirically based and determine rock sizes based upon flow impingement at the toe. The point velocities measured at stone failure are plotted with the USBR relation as presented in Fig. 5. A relation is projected through the test results to allow a comparison of these test results with the USBR procedure. When a flow velocity of 3.65 m/s (12.0 ft/s) transitions onto the rock toe, the USBR yields a median rock size of approximately 53.3 cm (21 in.). The initial results of these flume tests indicate that a 20.3 cm (8 in.) rock would fail at the same 3.65 m/s velocity (Section 3). The USBR rock size is larger than 260% of those indicated in Fig. 5. The Campbell procedure prescribes a stable rock size of 55.9 cm (22.0 in.) at a transition velocity of 3.65 m/s. It is important to note that flow velocities depicted in the USBR and Campbell procedures is measured immediately downstream of the jump transition, whereas the velocity presented herein is measured immediately upstream of the jump transition.

The USBR and Campbell procedures apparently provide a conservative approach to stone sizing in stilling basins and for rock placed at the toe of a slope. Although the rock size derived from the flume tests requires adjustment (increased) from the failure condition to reflect a nonmovement condition, considerable differences exist between these procedures.

An analysis was performed to evaluate how the unit dis-

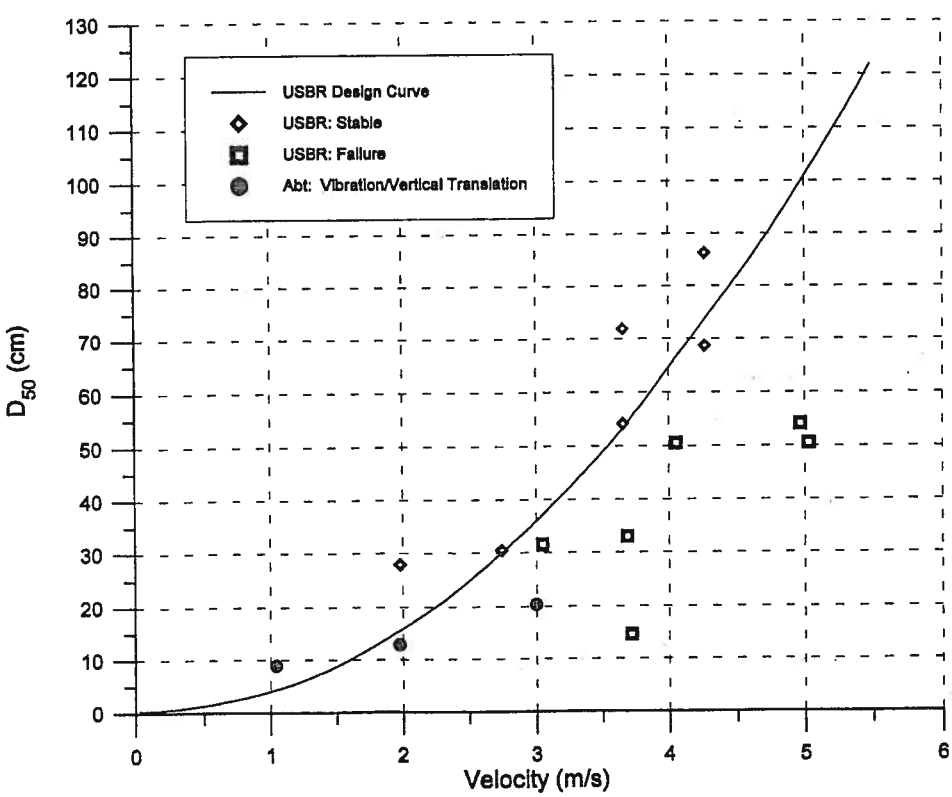

FIG. 4. Comparison of USBR Design Relation with Rock Movement Results

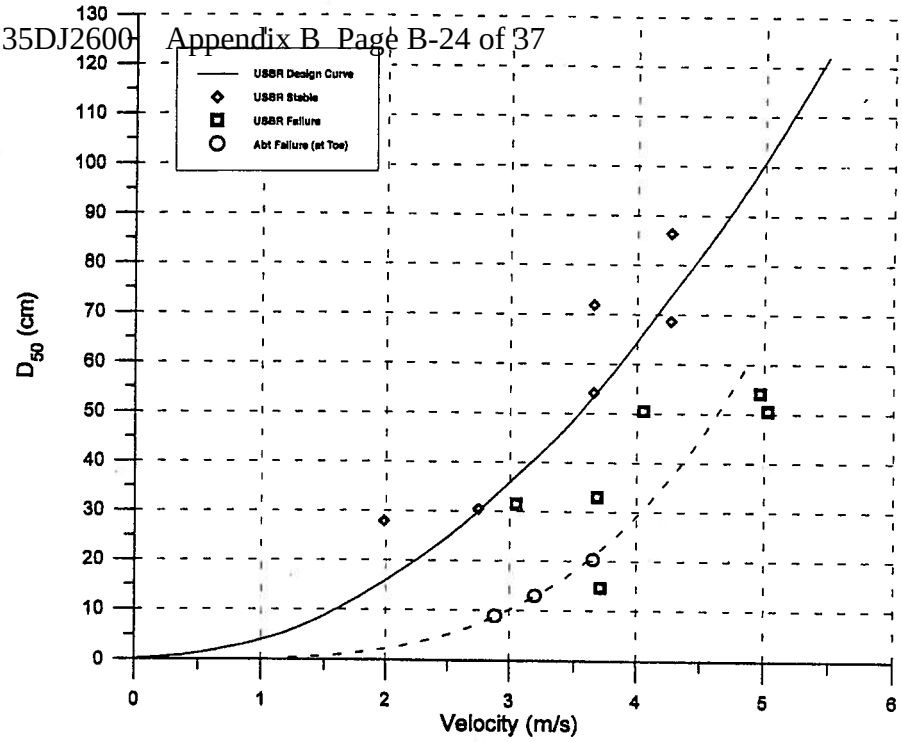

FIG. 5. Comparison of USBR Design Relation with Rock Failure Results

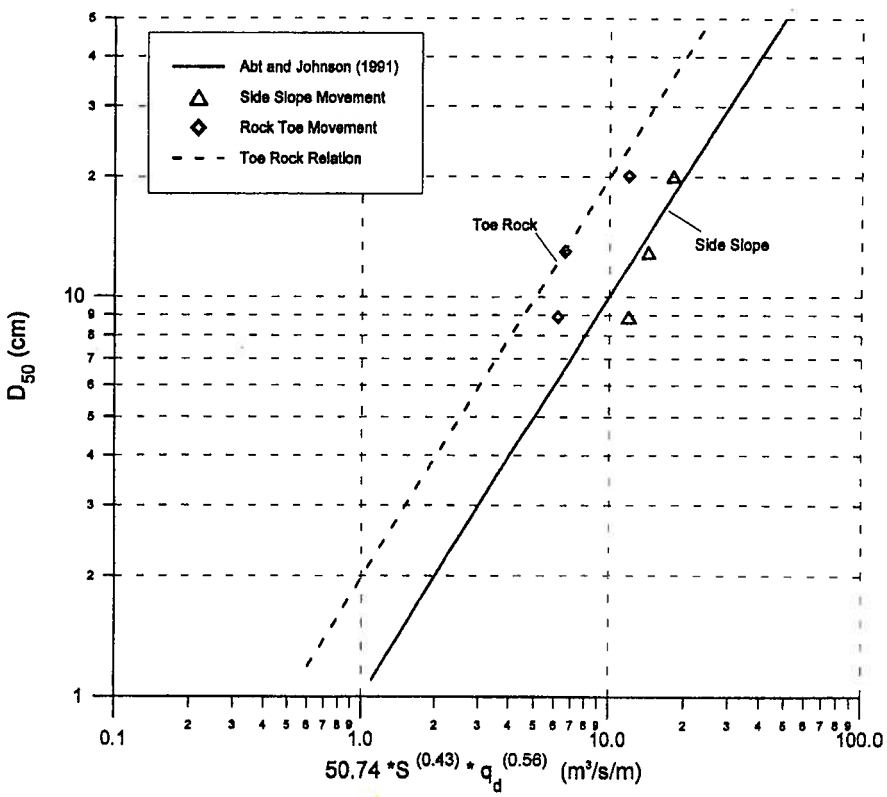

FIG. 6. Toe Rock Relations

charge affects the median rock size at the toe. Abt and Johnson (1991) formulated an expression for sizing the median rock, D_{50}, for top and side slopes of embankments as a function of the estimated design unit discharge, q_d, and the slope, S. Utilizing the unit discharge instead of the flow velocity relieves the designer from estimating the resistance to flow parameter as well as rectifying the differences between average, bottom, and point velocities. The median stone size (Abt and Johnson 1991) designed to resist stone movement on embankment slopes is expressed as

$$D_{50} = 5.23 \times S^{0.43} q_d^{0.56} \quad (1)$$

where q_d is in cubic feet per second per foot; and D_{50} is in inches. Eq. (1), expressed in SI units is

$$D_{50} = 50.74 \times S^{0.43} \times q_d^{0.56} \quad (2)$$

where D_{50} is in centimeters; and q_d is in cubic meters per second per meter.

Stone movement, upstream of Section 3, was documented and plotted in Fig. 6. The stone movement of the embankment slope reasonably agrees with the Abt and Johnson relation. The data indicate that the Abt and Johnson relation, plus 100%, envelops the rock toe size for unit discharges $\leqq 0.54$ m^3/s/m (5.77 cfs/ft).

An expression can be derived to size the median rock size based upon the toe rock relation presented in Fig. 6. The modified expression should incorporate (1) the rock size differential between the two relations portrayed in Fig. 6; and (2) the flow concentration, C_f, aspect of flow discussed by Abt and Johnson. Abt et al. (1988) and Abt and Johnson (1991) reported that flow channelization develops on uniformly graded slopes. Flow concentrations, or areas where flow was diverted around larger stones and directed into zones of smaller stones, created subchannels. The unit discharge in the subchannels was documented to be at least three times ($1 < C_f < 3$) the uniform unit discharge before channelization. The magnitude of C_f should depend upon the hazard level of the protected surface. For example, a C_f of 1.0 should be used for low-hazard applications, whereas a C_f of 2–3 should be used for high-hazard conditions. Therefore, the inclusion of a flow concentration factor for rock toe sizing is warranted.

Eq. (1) may be shifted such that the median stone size is designed to resist stone movement rather than failure at the transition of the toe as

$$D_{50} = 10.46 \times S^{0.43} \times (C_f \times q_d)^{0.56} \quad (3)$$

where q_d = design unit discharge in cubic feet per second; D_{50} is in inches, and C_f = flow concentration factor. Eq. (3) expressed in SI units is

$$D_{50} = 100.5 \times S^{0.43} \times (C_f \times q_d)^{0.56} \quad (4)$$

where q_d is in cubic meters per second per meter; and D_{50} is in centimeters. Extrapolation of Eqs. (3) and (4) beyond unit discharges of 0.54 m^3/s/m are not recommended without further testing.

These flow tests indicate that the rock toe may be sized based upon the unit discharge and the embankment slope transitioning into the rock basin. The rock toe should minimally extend 10-stone-diameters downstream of the toe and the stone layer should be a minimum of 3-stone-diameters thick. It is recognized that these few data points do not necessarily define a definitive relation. Further, it is noted that (3) and (4) are applicable to a small range of flows (<0.54 m^3/s/m) and do not incorporate a factor of safety. However, (3) and (4) provide the user a unit discharge rather than velocity-based approach, accounts for concentrated flows, and reduces the conservatism of design.

CONCLUSIONS

A few methods or procedures exist that size riprap placed at the toe of a slope. Existing rock-sizing methods are velocity based, focus on energy dissipation, and are extremely conservative. A near-prototype, pilot flume study was performed where flow overtopped an embankment and transitioned into a rock toe comprised of 8.9, 13.0, and 19.8 cm (median stone diameter). The test results indicate that the stone size required to stabilize the riprap layer at the toe is approximately 100% larger than the rock size required to stabilize embankment side slopes. A method was developed for sizing rock placed at an embankment toe based upon the embankment slope and unit discharge at the compound slope transition. Although the unit discharge approach to rock sizing is based upon a limited database, the results indicate that a less conservative rock size may be sufficient to stabilize the embankment toe. It is acknowledged that the database must be expanded.

ACKNOWLEDGMENT

This project was sponsored by the Office of Nuclear Material Safety and Safeguards, U.S. Nuclear Regulatory Commission. The findings and opinions expressed are those of the writers and do not necessarily represent the U.S. Nuclear Regulatory Commission or Colorado State University.

APPENDIX. REFERENCES

Abt, S. R., et al. (1988). "Development of riprap design criteria by riprap testing in flumes: Phase II—Follow-Up Investigations." *NUREG/CR-4651, ORNL/TM-10100/V2*, U.S. Nuclear Regulatory Commission, Washington, D.C., 2, 85.

Abt, S. R., and Johnson, T. L. (1991). "Riprap design for overtopping flow." *J. Hydr. Engrg.*, ASCE, 117(8), 959–972.

Berry, N. K. (1948). "The start of bed load movement," MS thesis, Univ. of Colorado, Boulder, Colo.

Campbell, F. B. (1966). "Hydraulic design of rock riprap." *Misc. Paper No. 2-777*, Ofc. of the Chf. of Engrs., U.S. Army Wtrwy. Experiment Station, Vicksburg, Miss.

Hartung, F., and Scheuerlein, H. (1970). "Design of overflow rockfill dams." *Proc., 10th Int. Congr. of Large Dams*, 1, 587–598.

Isbash, S. (1935). "Construction of dams by dumping stones into flowing water." *Rep.*, U.S. Army Engrg. Dist., U.S. Army Corps of Engrs., Eastport, Maine.

Olivier, H. (1967). "Through and overflow rockfill dams—New design techniques." *Proc., Instn. of Civ. Engrs.*, 36, 433–471.

Stephenson, D. (1979). *Rockfill in hydraulic engineering*. Elsevier Scientific Publishing Co., New York, N.Y., 215.

USACE. (1991). "Hydraulic design of flood control channels." *EM1110-2-1601*, Dept. of the Army, U.S. Army Corps of Engineers, Washington, D.C.

USDOI. (1978). "Hydraulic design of stilling basins and energy dissipators." *Engrg. Monograph No. 25*, U.S. Bureau of Reclamation, U.S. Department of the Interior, Washington, D.C.

CHAPTER V

ESTIMATING EROSION AT CULVERT OUTLETS

Estimating erosion at culvert outlets is difficult because of the many complex factors affecting erosion. Some of these factors are the discharge, culvert diameter, soil type, duration of flow and tailwater depth. In addition, the magnitude of the total erosion can consist of local scour and channel degradation, the two types of erosion discussed in Chapter II-B. Maintenance history, site reconnaissance and data on soils, flows and flow duration provide the best estimate of the potential erosion hazard at a culvert outlet.

The objective of this chapter is to present a method for predicting local scour at the outlet of structures based on soil and flow data and culvert geometry. This scour prediction is intended to serve together with the maintenance history and site reconnaissance information for determining energy dissipator needs.

Investigations (1), (3), indicate that the scour hole geometry varies with tailwater conditions with the maximum scour geometry occuring at tailwater depths less than half the culvert diameter (1); and that the maximum depth of scour (h_s) occurs at a location approximately 0.4 L_s downstream of the culvert outlet (3) where L_s is the length of scour.

Empirical equations defining the relationship between the culvert discharge intensity, time, and the length, width, depth, and volume of scour hole are presented for the maximum or extreme scour case.

Cohesionless Material

The general expression for determining scour geometry in a cohesionless soil for a circular pipe flowing full is

$$\text{Dimensionless Scour Geometry} = \alpha\left(\frac{Q}{\sqrt{g}\,D^{5/2}}\right)^{\beta}\left(\frac{t}{t_o}\right)^{\theta} \qquad \text{(V-1)}$$

where:

Dimensionless Scour Geometry is $\frac{h_s}{y_e}$, $\frac{W_s}{y_e}$, $\frac{L_s}{y_e}$, or $\frac{V_s}{y_e}$

h_s, W_s, L_s, and V_s are depth, width, length and volume of scour respectively.

D is the diameter of the culvert

Q is the discharge, g is the acceleration of gravity

t is the time in minutes

t_o is a base time used in the experiments to derive coefficients (316 minutes unless specified otherwise).

For noncircular or part full culverts, the diameter D can be replaced by a n equivalent depth y_e, where y_e is defined as

$$y_e = (A/2)^{1/2}$$

and A is the cross sectional area of flow. Modifying Equation (V-1) to include the equivalent depth results in the general expression.

$$\text{Dimensionless Scour Geometry} = \alpha_e \left(\frac{Q}{\sqrt{g}\, y_e^{5/2}}\right)^{\beta} \left(\frac{t}{t_o}\right)^{\theta} \qquad \text{(V-2)}$$

where:

$$\alpha_e = \alpha\, 0.63^{2.5\,\beta-1} \text{ for } h_s,\ W_s, \text{ and } L_s$$

$$\alpha_e = \alpha\, 0.63^{2.5\,\beta-3} \text{ for } V_s$$

The values of the coefficients α_e, β, and θ in Equations V-1 and V-2 are given in Table V-1.

Gradation

The cohensionless bed materials presented in Table V-1 are categorized as either uniform (U) or graded (G). The grain size distribution is determined by performing a sieve analysis (ASTM DA22-63). The standard deviation (σ) is computed as:

$$\sigma = \left(\frac{d_{84}}{d_{16}}\right)^{1/2}$$

where the values of d_{84} and d_{16} are extracted from the grain size distribution. If ≤ 1.5, the material is considered to be uniform; if ≥ 1.5, the material is classified as graded.

Cohesive Soils

If the cohesive soil is a sandy clay similar to the one tested at Colorado State University by Abt et al (8), Equation (V-1) or (V-2) and the appropriate coefficients in Table V-1 can be used to estimate the scour hole dimensions. The sandy clay tested had 58 percent sand, 27 percent clay, 15 percent silt and 1 percent organic matter; had a mean grain size of 0.15 mm and had a plasticity index, PI, of 15.

Since Equations V-1 and V-2 do not include soil characterisitcs, they can only be used for soils similar to the ones tested. Shear number expressions, that related scour to the critical shear stress of the soil, were derived to have a wider range of applicability for cohesive soils besides the one specific sandy clay that was tested. The shear number expressions for circular culverts are:

$$\left[\frac{h_s}{D}, \frac{W_s}{D}, \frac{L_s}{D}, \text{ or } \frac{V_s}{D}\right] = \alpha\left(\frac{\rho V^2}{\tau_c}\right)^{\beta}\left(\frac{t}{t_o}\right)^{\theta} \qquad \text{(V-3)}$$

and for other shaped culverts:

$$\left[\frac{h_s}{y_e}, \frac{W_s}{y_e}, \frac{L_s}{y_e}, \text{ or } \frac{V_s}{y_e}\right] = \alpha_e\left(\frac{\rho V^2}{\tau_c}\right)^{\beta}\left(\frac{t}{t_o}\right)^{\theta} \qquad \text{(V-4)}$$

where: $\frac{\rho V^2}{\tau_c}$ is the modified shear number

V = outlet mean velocity

τ_c = critical tractive shear stress

ρ = fluid density

$\alpha_e = \frac{\alpha}{.63}$ for h_s, W_s, and L_s

$\alpha_e = \frac{\alpha}{(.63)^3}$ for V_s

The values of the coefficients α, β, θ, and α_e in Equations V-4 and V-5 are presented in Table V-1. The critical tractive shear stress (2) is defined as

$$\tau_c = 0.0001\ (S_v + 180)\ \tan\ (30 + 1.73\ PI) \qquad \text{(V-5)}$$

where S_v is the saturated shear strength in pounds per square inch and PI is the Plasticity Index from the Atterberg Limits.

It is recommended that Equations V-3 and V-4 be limited to sandy clay soils with a plasticity index of 5-16.

Time of Scour

The time of scour is estimated based upon a knowledge of peak flow duration. Lacking this knowledge, it is recommended that a time of 30 minutes be used in Equations V-1, V-2, V-3, and V-4. The tests indicate that approximately 2/3 to 3/4 of the maximum scour occurs in the first 30 minutes of the flow duration.

It should be noted that the exponents for the time parameter in Table V-1 reflect the relatively flat part of the scour-time relationship and are not applicable for the first 30 minutes of the scour process.

Headwalls

Installation of headwalls (6) flush with the culvert outlet moves the scour hole downstream. However, the magnitude of the scour geometries remain essentially the same as for the case without the headwall. If the culvert is installed with a headwall, the headwall should extend to a depth equal to the maximum depth of scour.

SUMMARY

The prediction equations presented in this chapter are intended to serve along with field reconnaissance as guidance for determining the need for energy dissipators at culvert outlets. It should be remembered that the equations do not include long-term channel degradation of the downstream channel. The equations are based on tests which were conducted to determine maximum scour for the given condition and therefore represent what might be termed worst case scour geometries. The equations were derived from tests conducted by the Corps of Engineers (1), and Colorado State University (5), (6), (7), (8) and (9).

Design Procedure

1. Perform a hydrologic analysis of the drainage in which the culvert is located or to be placed. Estimate the magnitude and duration of the peak discharge. Express the discharge in cfs and the duration in minutes.

   The discharge intensity is

$$D.I. = \frac{Q}{\sqrt{g}\ D^{5/2}} \text{ for circular culverts flowing full}$$

$$D.I. = \frac{Q}{\sqrt{g}\ y_e^{5/2}} \text{ for other shapes}$$

where $y_e = \left(\frac{A}{2}\right)^{1/2}$

FOR COHESIONLESS MATERIALS, OR THE 0.15mm SANDY CLAY

2. Compute the discharge intensity when the culvert is flowing at the peak discharge.

3. Determine scour coefficients from Table V-1.

4. Compute the scour hole dimensions from

$$\left[\frac{h_s}{D}, \frac{W_s}{D}, \frac{L_s}{D}, \text{ or } \frac{V_s}{D^3}\right] = \alpha\left(\frac{Q}{\sqrt{g}\ D^{5/2}}\right)^{\beta}\left(\frac{t}{316}\right)^{\theta} \qquad \text{(V-1)}$$

or

$$\left[\frac{h_s}{y_e}, \frac{W_s}{y_e}, \frac{L_s}{y_e}, \text{ or } \frac{V_s}{y_e}\right] = \alpha_e\left(\frac{Q}{\sqrt{g}\ y_e^{5/2}}\right)^{\beta}\left(\frac{t}{316}\right)^{\theta} \qquad \text{(V-2)}$$

FOR OTHER COHESIVE MATERIALS WITH PI FROM 5 TO 16

a. Compute the culvert outlet velocity in feet/sec.

b. Obtain a soil sample at the proposed culvert location.

c. Perform Atterberg limits tests and determine the plasticity index, PI (ASTM D423-36).

d. Saturate a sample and perform an unconfined compressive test (ASTM D211-66-76) to determine the saturated shear stress, Sv, in pounds per square inch.

e. Compute the critical tractive shear strength, τ_c, from equation V-5.

f. Compute the modified shear number $\frac{\rho V^2}{\tau_c}$

3. Determine scour coefficients from Table V-1.

4. Compute the desired scour hole dimensions from

$$\left[\frac{h_s}{D}, \frac{W_s}{D}, \frac{L_s}{D}, \text{ or } \frac{V_s}{D}\right] = \alpha \left(\frac{V^2}{\tau_c}\right)^{\beta} \left(\frac{t}{316}\right)^{\theta}$$

for circular culvert

or

$$\left[\frac{h_s}{y_e}, \frac{W_s}{y_e}, \frac{L_s}{y_e}, \frac{V_s}{y_e^3}\right] = \alpha_e \left(\frac{V^2}{\tau_c}\right)^{\beta} \left(\frac{t}{316}\right)^{\theta}$$

for noncircular culverts.

Example Problem Cohesionless Material

Determine the scour geometry--maximum depth, width, length and volume of scour--for a proposed circular 30-inch C.M.P. discharging an estimated 50 cfs when flowing full. The downstream channel is composed of a graded gravel material.

1. The duration of the peak discharge of 50 cfs is not known. Therefore, a peak flow duration of 30 minutes will be estimated.

2. The circular, 30-inch C.M.P. at 50 cfs will have a discharge intensity of

$$D.I. = \frac{50}{\sqrt{g}\,\left(\frac{30}{12}\right)^{5/2}} = \frac{50}{(5.67)(2.5)^{5/2}} = 0.89$$

3. The coefficients of scour obtained from Table V-1 are:

	α	β	θ
Depth of Scour	1.49	.50	.03
Width of Scour	8.76	0.89	.10
Length of Scour	13.09	0.62	.07
Volume of Scour	42.31	2.28	.17

4. Scour hole dimensions:

depth: $$\frac{h_s}{D} = \alpha\left(\frac{Q}{\sqrt{g}\ D^{2.5}}\right)^{\beta}\left(\frac{t}{316}\right)^{\theta}$$

$$= 1.49\ (0.89)^{0.50}\ (0.09)^{.03};\ h_s = 3.27\ \text{ft}$$

width: $$\frac{W_s}{D} = 8.76(0.89)^{0.89}\ (.09)^{.10};\ W_s = 15.5\ \text{ft}$$

Length: $L_s = 13.09(0.89)^{0.62}\ (.09)^{.07};\ L_s = 25.72$ ft

Volume: $V_s = 42.31(0.89)^{2.28}\ (.09)^{.17};\ V_s = 335.79\ \text{ft}^3$

5. The location of the maximum scour (Figure V-2)

$0.4\ (L_s) = .4\ (25.72) = 10.3$ ft downstream of the culvert outle

Example Problem Cohesive Material

Determine the scour geometry-maximum depth, width, length and volume of scour for an existing circular 24-inch C.M.P. discharging an estimated 40 cfs when flowing full. The downstream channel is composed of a sandy-clay material.

1. The duration of the peak discharge of 40 cfs is not known. Therefore, a peak flow duration of 30 minutes will be estimated.

2. a. The average velocity at the culvert outlet is:

$$V = \frac{Q}{A} = \frac{40.0}{3.14} = 12.74 \text{ fps}$$

b-e. The sandy-clay material was tested and found to have a Plasticity Index (PI) of 12 and a saturated shear strength (Sv) of 240 psi.

The critical tractive shear can be estimated by substituting into Equation V-5

$$\tau_c = 0.001\ (240 + 180)\ \tan\ (30 + 1.73(12))$$

$$0.001(420)\ \tan\ (50.76) = 0.51\ \text{lb/ft}^2$$

f. The modified shear number $S_{n_{mod}} = \frac{(\rho V^2)}{\tau_c}$ is:

$$S_{n_{mod}} = \frac{1.94\ (12.74)^2}{0.51} = 617.4$$

3. The experimental coefficients α, β and θ from Table V-1 are

	α	β	θ
Depth	.86	.18	.10
Width	3.55	.17	.07
Length	2.82	.33	.09
Volume	.62	.93	.23

4. The scour hole dimensions are:

$$\frac{h_s}{D} = \alpha \left(\frac{\rho V^2}{\tau_c}\right)^{\beta} \left(\frac{t}{316}\right)^{\theta}$$

$$= .86(617.4)^{.18}\ (.09)^{.10}; \quad h_s = 2.14 \times 2 = 4.30 \text{ ft}$$

$$\frac{W_s}{D} = 3.55(617.4)^{.17}\ (.09)^{.07}; \quad W_s = 8.94 \times 2 = 27.9 \text{ ft}$$

$$\frac{L_s}{D} = 2.82(617.4)^{.33}\ (.09)^{.09}; \quad L_s = 18.92 \times 2 = 37.8 \text{ ft}$$

$$\frac{V_s}{D^3} = .62(617.4)^{.93}\ (.09)^{.23}; \quad V_s = 140.3 \times 23 = 1122.5 \text{ ft}^3$$

5. Location of maximum depth of scour (Figure V-2)

$0.4\ L_s = 0.4(37.8) = 15.1$ ft downstream of culvert outlet

... THROUGH RIPRAP

By Steven R. Abt,[1] James F. Ruff,[2] Members, ASCE, and Rodney J. Wittler,[3] Associate Member, ASCE

Introduction

Estimating flow through rockfill and protective rock covers can be a useful procedure for designing or evaluating flood control, waste repository, and waterways structures. Often, a knowledge of rockfill and rock cover transmissibility and the effect of through-flow forces on the stone are needed for structural stability analyses. Through-flow velocity is defined as the average velocity of water flow through rock voids. An understanding of turbulent flow in a rock medium is needed for through-flow analyses.

Numerous investigators have analyzed turbulent through flow, including Weiss (1951), Escande (1953), Olivier (1967), and Stephenson (1979). Wilkins (1956, 1963) performed laboratory transmissivity tests on cylindrical specimens, resulting in the relation

$$V_v = 32.9m^{0.5}i^{0.54} \quad (1)$$

where V_v = the average velocity of water through rock voids in inches per second; i = the hydraulic gradient; and m = the hydraulic mean radius of rock voids in inches (volume of voids divided by total surface area of the particles).

Parkin (1963; Parkin et al. 1966) performed tests on clean, angular gravel (3/8–3/4 in.). Parkin derived the expression

$$i = 1.86V_v^{1.86} \quad (2)$$

where i = the hydraulic gradient and V_v = the average velocity of flow through the rock voids in feet per second.

Leps (1973) consolidated the concepts of Escande, Wilkins, and Parkin and presented an expression for the average flow through rockfill for turbulent conditions as

$$V_v = Wm^{0.5}i^{0.54} \quad (3)$$

where V_v = the average velocity of water in rockfill voids in inches per second; W = an empirical constant; m = the hydraulic mean radius in inches; and i = the hydraulic gradient. The average through-flow velocity is estimated by obtaining the appropriate value from Table 1 and inserting it into Eq. 3. Leps' relation is applicable to uniformly sized rock with a specific gravity of 2.87.

Wilkins (1956, 1963), Olivier (1967), and Stephenson (1979) reported that

[1]Prof., Dept. of Civ. Engrg., Colorado State Univ., Fort Collins, CO 80523.
[2]Prof., Dept. of Civ. Engrg., Colorado State Univ., Fort Collins, CO.
[3]Res. Hydr. Engr., U.S. Bureau of Reclamation, Denver, CO 80225.

Note. Discussion open until October 1, 1991. To extend the closing date one month, a written request must be filed with the ASCE Manager of Journals. The manuscript for this paper was submitted for review and possible publication on January 23, 1990. This paper is part of the ***Journal of Hydraulic Engineering***, Vol. 117, No. 5, May, 1991. ©ASCE, ISSN 0733-9429/91/0005-0670/$1.00 + $.15 per page. Paper No. 25842.

TABLE 1. Coefficients for Estimating Through Flow (for Eq. 3)

Rock Size in. (1)	Rock Size cm (2)	$Wm^{0.5}$ (3)
0.75	1.9	10
2	5.1	16
6	15.2	28
8	20.3	32
24	61.0	58
48	121.9	84

Note: Adapted from Leps (1971).

the average interstitial, or through-flow, velocity was a function of the riprap properties and the gradient. However, in the preliminary design process, the engineer must assume a representative stone size and gradation before extensive material testing or analysis of a rock source is done. Therefore, a procedure that predicts the average through-flow velocity for riprap and rockfill would be helpful. This note presents a method.

Experimental Program

An experimental program was conducted by Abt et al. (1987, 1988) at Colorado State University in which embankments with slopes ranging from 1–20% were constructed in recirculating flumes. These model embankments were similar to those designed for waste repositories. The embankments consisted of a compacted sand material covered with a geotextile. A 6-in. (0.15-m) sand-gravel bed was placed atop the geotextile. Riprap was placed on top of the bedding material in uniform layer thicknesses ranging from 3 in. (7.6 cm) to 12 in. (30.5 cm). The embankments were constructed horizontally upstream of the crest and transitioned to the desired downstream slope. Water overtopped the embankment crest and flowed through the riprap.

The riprap was obtained from a limestone quarry. Median stone sizes D_{50}, ranged from 1.02 in. (2.6 cm) to 6.2 in. (15.8 cm), as presented in Table 2. The rock specific gravity was 2.65, the gradation d_{84}/d_{16}, ranged from 1.80 to 2.72, and the stones were angular.

A tracer injection and recording system was developed to document the flow velocities through the riprap layer. The system consisted of a pressure-operated tracer injector, tracer-sensitive probes, a multichannel selector, and a multichannel strip chart recorder. Each tracer-sensitive probe was fabricated with three tracer-sensitive elements placed in the lower 8 in. (20.3 cm) of the probe. The tracer injector was fabricated with three injection ports. The injector port spacing was similar to the spacing of the tracer-sensitive elements in the probe; the spacing was 3 in. Fig. 1 shows a schematic of the injector and sensor in the rock layer. A salt solution was used as the tracer.

The injector ports were approximately aligned in the riprap layer with the elements in the tracer-sensitive probe. The lowest injector was approximately 1 in. (2.54 cm) above the riprap-bedding interface. The injector was placed 10–12 in. (25.4–30.5 cm) upstream from the first tracer-sensitive probe.

TABLE 2. Interstitial Velocity Summary

Test number (1)	Median Stone Size, D_{50} in. (2)	Median Stone Size, D_{50} cm (3)	D_{10} in. (4)	D_{10} cm (5)	Riprap Layer Thickness in. (6)	Riprap Layer Thickness cm (7)	Embankment slope (8)	Average Interstitial Velocity V_i fps (9)	Average Interstitial Velocity V_i cm/s (10)
6I	1.02	2.6	0.6	1.5	3	7.6	0.01	0.10	3.0
7I	1.02	2.6	0.6	1.5	3	7.6	0.02	0.13	4.0
9I	1.02	2.6	0.6	1.5	3	7.6	0.10	0.24	7.3
4I	2.2	5.6	1.1	2.8	6	15.2	0.01	0.15	4.6
3I	2.2	5.6	1.1	2.8	6	15.2	0.02	0.23	7.0
10I	2.2	5.6	1.1	2.8	6	15.2	0.10	0.36	11.0
11I	2.2	5.6	1.1	2.8	6	15.2	0.10	0.37	11.3
3	4.1	10.4	2.0	5.1	12	30.5	0.20	0.72	21.9
4	4.1	10.4	2.0	5.1	12	30.5	0.20	0.97	29.6
8	5.1	13.0	3.45	8.8	12	30.5	0.20	1.04	31.7
9	5.1	13.0	3.45	8.8	12	30.5	0.20	0.86	26.2
14	6.2	15.7	3.8	9.7	12	30.5	0.20	1.47	44.8
26	2.0	5.1	1.03	2.6	3	7.6	0.10	0.46	14.0
28	2.0	5.1	1.03	2.6	4	10.2	0.10	0.50	15.2
30	2.0	5.1	1.03	2.6	6	15.2	0.10	0.54	16.5
39	4.0	10.2	2.0	5.1	6	15.2	0.10	0.62	18.9
41	4.0	10.2	2.0	5.1	8	20.3	0.10	0.66	20.1
47	4.0	10.2	1.2	3.0	12	30.5	0.10	0.48	14.6
50	4.0	10.2	2.38	6.0	12	30.5	0.10	0.66	20.1

The second probe was 20–24 in. (50.3–61.0 cm) downstream from the injector. Velocity measurements were taken in the upper third and lower third segments of the embankment slope.

In each of the 19 tests, flow was established in the flume with the water surface stabilized at a point just above the riprap surface. The tracer was then injected into the rock layer. An event marker on the strip chart recorder indicated when the injector was triggered. Output from the tracer-sensitive probe elements also was recorded on the strip chart so that tracer concentration versus time could be observed and documented. A tracer concentration curve was recorded for each injector port. The peak of the concentration curve was used to estimate the interstitial velocity. Knowing the time of injection, travel time between injector and tracer ports, and the distance between ports, one could compute the average interstitial velocity for each test condition in the rock layer. Each velocity reported in Table 2 represents the average value of one-to-five velocity measurement locations in each profile. The number of velocity measurements taken was a function of the layer thickness; a 3-in. (7.62 cm) layer allowed space for a single velocity measurement.

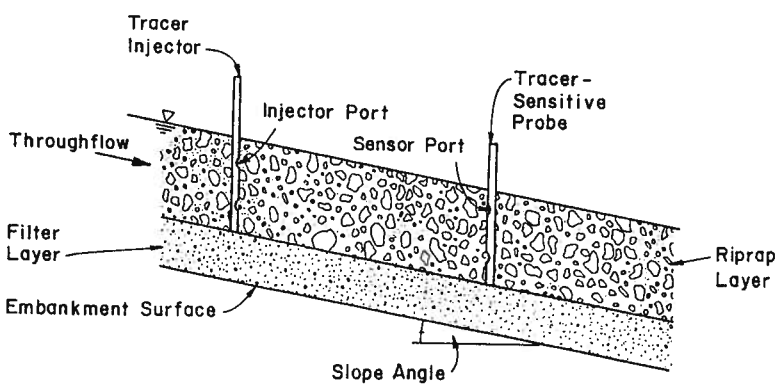

FIG. 1. Schematic of Tracer, Injector, and Sensor in Rock Layer

RESULTS

The average interstitial velocities V_i that resulted from the 19 flume tests are presented in Table 2. Velocities through the rock layers ranged from 3–44.8 cm/s for embankment slopes of 1–20%, respectively. At a constant slope of 10%, average interstitial velocities ranged from 7.3–20.1 cm/s for median stone sizes of 2.6–10.2 cm, respectively.

A sensitivity analysis was performed, relating the rock size and embankment gradient to the average interstitial velocity. Representative stone sizes of D_{50}, D_{40}, D_{30}, D_{20}, D_{15}, and D_{10}, in conjunction with the slope, were correlated with the measured interstitial velocity. The analysis indicated that

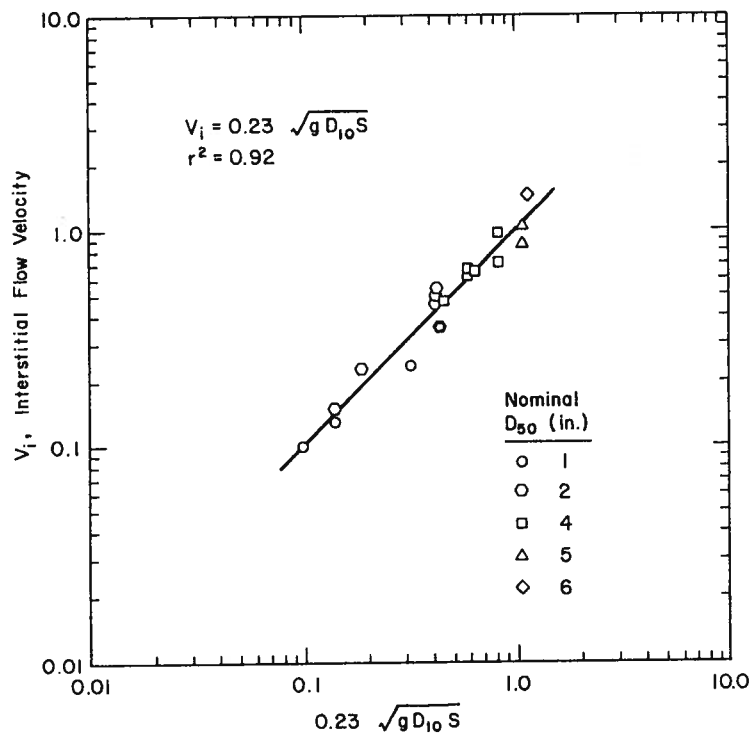

FIG. 2. Average Interstitial Velocity through Riprap as Function of D_{10} and Gradient

t[illegible]$_{10}$ stone diameter (at which 10% of the weight is finer) provided the h[illegible]st coefficient of correlation of the stone sizes tested. The interstitial velocities are shown in Fig. 2, as a function of the rock size D_{10} and the slope. A linear regression analysis yielded the expression

$$V_i = 0.23(gD_{10}S)^{1/2} \quad (4)$$

where V_i = the average interstitial velocity in feet per second; g = the acceleration of gravity in ft/sec^2, D_{10} is in inches, and S = the gradient expressed in decimal form. The correlation coefficient for Eq. 4 is $r^2 = 0.92$. It appears that the D_{10} stone size controls the rate of flow through the stone layer void space. Eq. 4 can be expressed in SI units as

$$V_i = 0.79(gD_{10}S)^{1/2} \quad (5)$$

The flow distance between the injector port and the sensor port was dependent on the probe placement in the rock layer. In some instances, the injector discharged directly into a large stone, resulting in immediate tracer dilution and the tracer taking a sinuous path toward the sensor. In other cases, the injector discharged into a void between the stones, resulting in a shortened path between injector and sensor. Because of the high variability in flow distance, the average interstitial velocities through the rock layer varied ± 40%. Velocity variability was dependent on stone size.

Conclusions

A series of 19 flume tests was conducted, in which flow was routed through a riprap layer, and the average interstitial, or through-flow, velocity was measured and recorded. Flow measurements varied ±40% about the average velocity. A predictive relationship was developed in which the average interstitial velocity was determined to be a function of the embankment slope and rock size D_{10}, as presented in Eq. 4. The predictive relationship provides the designer with a method for estimating through flow based upon a representative stone size, gradation, and embankment slope. The relationship was developed for stone sizes with a D_{50} ranging from 2.6 cm to 15.7 cm, and D_{10} ranging from 1.5 cm to 9.7 cm.

Acknowledgment

This research was sponsored by the Office of Nuclear Material Safety and Safeguards, U.S. Nuclear Regulatory Commission.

Appendix. References

Abt, S. R., Khattak, M. S., Nelson, J. D., Ruff, J. F., Shaikh, A., Wittler, R. J., Lee, D. W., and Hinkle, N. E. (1987). "Development of riprap design criteria by riprap testing in flumes: Phase I." *NUREG/CR-4651*, U.S. Nuclear Regulatory Commission, Vol. 1, 48–53.

Abt, S. R., Wittler, R. J., Ruff, J. F., LaGrone, D. L., Khattak, M. S., Nelson, J. D., Hinkle, N. E., and Lee, D. W. (1988). "Development of riprap design criteria by riprap testing in flumes: Phase II." *NUREG/CR-4651*, U.S. Nuclear Regulatory Commission, Vol. 2, 57–65.

Escande, L. (1953). "Experiments concerning the infiltration of water through a rock mass." *Proc., Minnesota Int. Hydrology Convention.*

ps, T. M. (1973). "Flow through rockfill." *Embankment dam engineering*, Jo Wiley and Sons, 87–107.

Olivier, H. (1967). "Through and overflow rockfill dams—New design techniques." *J. Inst. of Civ. Engrg.*, 36, 433–471.

Parkin, A. K. (1963). "Rockfill Dams with Inbuilt spillway." *Bulletin No. 6*, Water Resources Edn. Australia, Melbourne, Australia.

Parkin, A. K., Trollope, D. H., and Lawson, J. D. (1966). "Rockfill structures subject to water flow." *J. Soil Mech. Found. Div.*, ASCE, (6), 135.

Stephenson, D. (1979). *Rockfill in hydraulic engineering: Developments in geotechnical engineering 27*, Elsevier Scientific Publishing Company, Amsterdam, the Netherlands, 38–60.

Weiss, A. (1951). "Construction technique of passing floods over earth dams." *Trans. ASCE*, 116, 1158–1173.

Wilkins, J. K. (1956). "Flow of water through rockfill and its application to the design of dams." *Proc., Second Australian—New Zealand Soil Conf.*, Mechanics and Foundation Engrg., Christchurch, New Zealand.

Wilkins, J. K. (1963). "The stability of overtopped rockfill dams." *Proc. Fourth Australian Conf. on Soil Mech. Found. Engrg.*, Adelaide, Australia, 1–7.

JACOBS	Calculation No: C-03	Page 1 of 20 – Plus Appendices 53 Pgs
Calculation Cover Sheet	Rev. No.: 0	Revision Date:
(Ref. FOWI 116 Design Calculations)	Previous Revision Date:	Current Revision Date:1/09/08
Issuing Department: *Federal Operations Design Engineering*	Supersedes:	
Client: Energy solutions Project Title: Moab UMTRA Project Number: 35DJ2600 System:	Engineering Discipline: Civil	
Calculation Title: Wedge Longevity		

Purpose:

Runoff from the area between the top of the Book cliffs and the waste cell will diverted around the cell by a wedge constructed of approximately 3,000,000 cubic yards of excavated material placed between the Book Cliffs and the cell. The purpose of this calculation is to analyze the ability of the "wedge" to survive for the 1000 year life of the disposal cell.

NQA-1 QUALITY LEVEL: 2

Prepared by: Bob Yager Robert E. Yager Date: 1/09/08

Checked by: Bill Barton Bill Barton Date: 1/25/08

Engineering Managers Approval: Bill Barton Date: 1/25/08

The current applicable version of this publication resides on Jacobs' Intranet. All copies are considered to be uncontrolled.
Copyright© Jacobs Engineering Group Inc., 2007

Revision History:

Pages Affected By Revision	Revised/Added/Deleted	Description of Revision
All		

The current applicable version of this publication resides on Jacobs' Intranet. All copies are considered to be uncontrolled.
Copyright© Jacobs Engineering Group Inc., 2007

Description of Calculation:

- Determine the runoff from the watersheds between the book cliffs and the wedge and from the top of the wedge for design storms with return intervals from 1 year to the pmp.
- Calculate the potential sediment transport in a hypothetical channel that routes the runoff along the north side of the wedge and around the disposal cell using methods from Johnson, 2002.
- Calculate the sediment yield of the areas between the Book Cliffs and the wedge using the Modified Universal Soil Loss equation (MUSLE) (Nelson, et. al., 1986)
- Calculate the sediment yield from the top of the wedge using the MUSLE to determine the potential reduction in the height of the wedge due to direct rainfall. .
- Compute the net potential sediment addition to or subtraction from the wedge.
- Calculate the potential depth of gullies formed on the top and side slopes of the wedge using the methodology of Johnson, 2002 to determine whether the wedge may be breached by gullying.

Assumptions:

- The 1-hour PMP event is estimated to be 8.2 inches, ("Site Drainage—Hydrology Parameters" calculation, Draft RAP Attachment 1, Appendix E).
- The rainfall frequency-depth-duration data were developed in the Draft RAP. The 1 year rainfall depth was taken from the NOAA Atlas 14 (http://hdsc.nws.noaa.gov/hdsc/pfds/sa/ut_pfds.html).
- Over a period of 1000, years 12.7% of the total rainfall will become runoff (Johnson, 2002).
- The unit weight of compacted soil in the wedge is 103.5 pcf and of undisturbed soil between the Book cliffs and the wedge is 91.3 pcf.
- Since the results of this calculation indicate that most of the erosion of soil in the channel along the north side of the wedge will be uncompacted sediment from the area between the Book Cliffs and the wedge, it has been assumed that the unit weight of all soil transported in the channel is 91.3 pcf. This is a conservative assumption as erosion of compacted soil would result in less volume for a given weight of eroded soil.

The current applicable version of this publication resides on Jacobs' Intranet. All copies are considered to be uncontrolled.
Copyright© Jacobs Engineering Group Inc., 2007

Design Inputs:

See following pages

Software:

Title	Developer	Versions	Revision Level
EXCEL	Microsoft	2002	
HEC-HMS	USACE	3.1.0	

The current applicable version of this publication resides on Jacobs' Intranet. All copies are considered to be uncontrolled.
Copyright© Jacobs Engineering Group Inc., 2007

Calculation Section:

See following pages

The current applicable version of this publication resides on Jacobs' Intranet. All copies are considered to be uncontrolled.
Copyright© Jacobs Engineering Group Inc., 2007

Conclusions/Recommendations:

See following pages

Reference:

See following pages

The current applicable version of this publication resides on Jacobs' Intranet. All copies are considered to be uncontrolled.
Copyright© Jacobs Engineering Group Inc., 2007

DESCRIPTION OF CALCULATION:

Runoff from the area between the top of the Book cliffs and the waste cell will diverted around the cell by a wedge constructed of approximately 3,000,000 cubic yards of excavated material placed as shown in Figure 1. The purpose of this calculation is to analyze the ability of the "wedge" to survive for the 1000 year life of the disposal cell.

METHOD OF SOLUTION:

- Determine the runoff from the watersheds between the book cliffs and the wedge and from the top of the wedge for design storms with return intervals from 1 year to the PMP.
- Calculate the potential sediment transport in a hypothetical channel that routes the runoff along the north side of the wedge and around the disposal cell using methods from Johnson, 2002.
- Calculate the sediment yield of the areas between the Book Cliffs and the wedge using the Modified Universal Soil Loss equation (MUSLE) (Nelson, et. al, 1986)
- Calculate the sediment yield from the top of the wedge using the MUSLE to determine the potential reduction in the height of the wedge due to direct rainfall.
- Compute the net potential sediment addition to or subtraction from the wedge.
- Calculate the potential depth of gullies formed on the top and side slopes of the wedge using the methodology of Johnson, 2002 to determine whether the wedge may be breached by gullying.

ASSUMPTIONS:

- The 1-hour PMP event is estimated to be 8.2 inches, ("Site Drainage—Hydrology Parameters" calculation, Draft RAP Attachment 1, Appendix E).
- The rainfall frequency-depth-duration data were developed in the Draft RAP. The 1 year rainfall depth was taken from the NOAA Atlas 14 (http://hdsc.nws.noaa.gov/hdsc/pfds/sa/ut_pfds.html).
- Over a period of 1000 years, 12.7% of the total rainfall will become runoff (Johnson, 2002).
- The unit weight of compacted soil in the wedge is 103.5 pcf and of undisturbed soil between the Book cliffs and the wedge is 91.3 pcf.
- Since the results of this calculation indicate that most of the erosion of soil in the channel along the north side of the wedge will be uncompacted sediment from the area between the Book Cliffs and the wedge, it has been assumed that the unit weight of all soil transported in the channel is 91.3 pcf. This is a conservative assumption as erosion of compacted soil would result in less volume for a given weight of eroded soil.

The current applicable version of this publication resides on Jacobs' Intranet. All copies are considered to be uncontrolled.
Copyright© Jacobs Engineering Group Inc., 2007

Figure 1. Location and Configuration of the Wedge

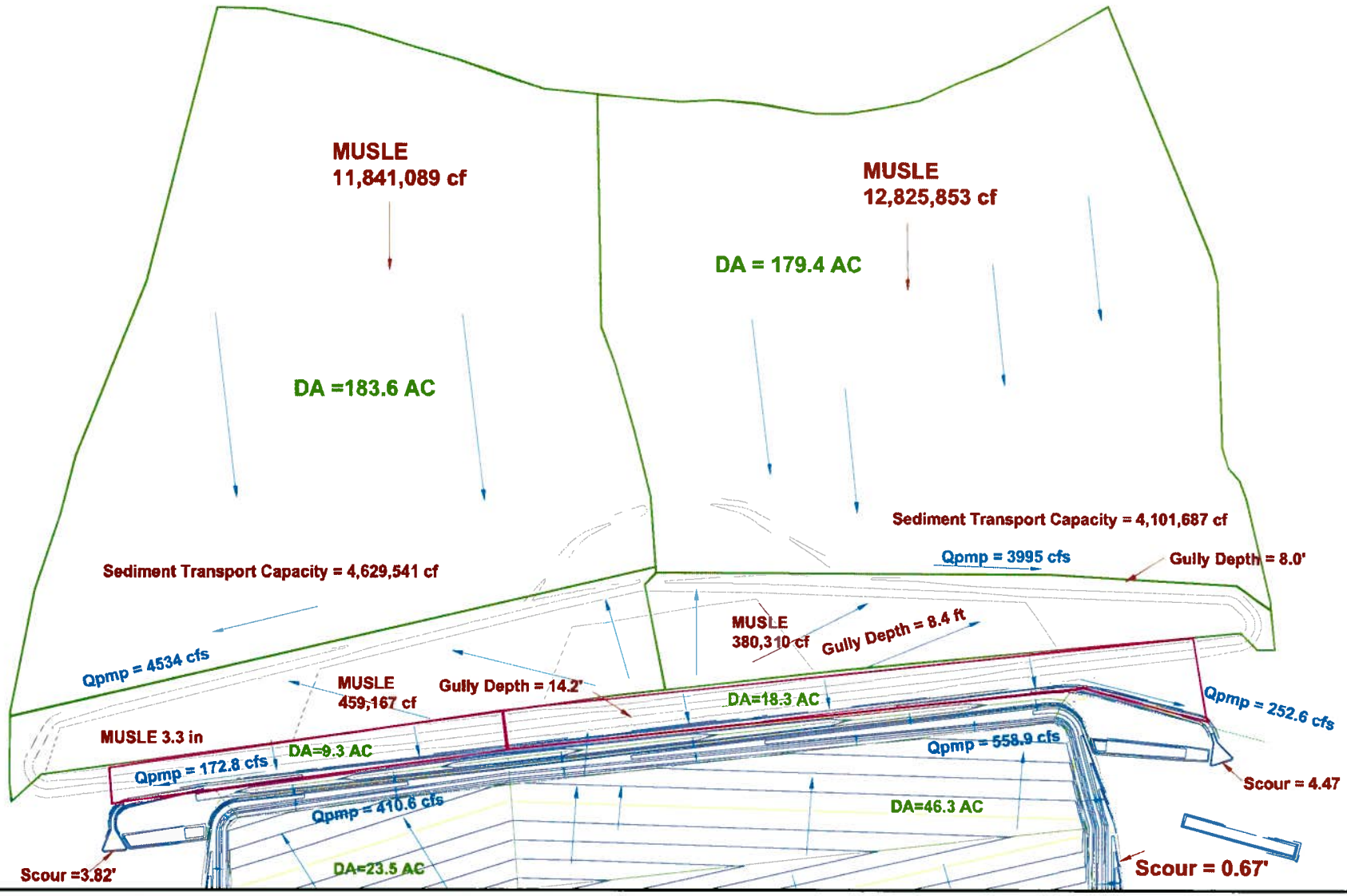

CALCULATION SECTION:

Unit hydrographs for the two drainage areas between the Book Cliffs and the wedge are developed in Unit Hydrographs.xls WedgeErosionEast.xls WedgeErosionWest.xls. Runoff calculations are performed using HEC-HMS using the project: WedgeDrainage.hms Drainage area properties for other watersheds are in WatershedParms.xls

Sediment Transport Capacity

Drainage Area Characteristics

Two drainage areas were delineated between the Book Cliffs and the wedge draining to the southeast and to the southwest. Two more were delineated on top the wedge draining to the northeast and the northwest. These drainage areas are shown in Figure 1.

For the undisturbed watersheds north of the wedge composite curve numbers were developed. The western drainage is approximately 63% Toddler-Ravola-Glenton families association with an HSG of B and a constant infiltration rate of 0.2 – 0.6 inches/hr. The remainder is Hanksville family-Badland complex with an HSG of C and an infiltration rate of 0.0 – 0.06 inches/hr (WEB Soil Survey, http://websoilsurvey.nrcs.usda.gov/app/WebSoilSurvey.aspx, and Appendix B). The Eastern drainage is approximately 49% Toddler-Ravola-Glenton and 51% Hanksville family-Badland complex. The following curve numbers have been assigned, a runoff curve number of 75 to the type B soils for semiarid rangelands with herbaceous cover in fair to poor condition and 87 to the type C soils for the same use in poor condition (TR-55,), composite curve numbers of 79.4 for the western drainage and 81.1 for the eastern. Computing initial abstraction using the NRCS curve number approach yields 0.52 inches for the western drainage and 0.47 for the eastern. The NRCS initial abstraction is

$$I_a = 0.2\left[\frac{1000}{CN} - 10\right]$$

Assuming a constant infiltration of 0.3 inches/hr for the type B soils and 0.03 for type C results in constant infiltration rates of 0.20 in/hr for the western drainage and 0.16 for the eastern . For the compacted soil comprising the wedge an initial abstraction equal to 0.2 inches was assumed with a constant infiltration rate of 0.1 in/hr. These loss values were used for all storms except the PMP for which the initial abstraction was set equal to 0.0.

Pertinent properties of the four drainage areas are computed in UnitHydrographs.xls and WaterShedParms.xls and listed in Table 1. The flow lengths are used to develop a unit hydrograph using the USBR methodology and the Lag time is used in the SCS unit hydrograph method. The mean of the Kirpich and SCS time of concentration formulas is used for the time of concentration.

The Kirpich equation is $T_c = 0.0078\frac{L^{0.77}}{S^{0.385}}$ where

T_c = time of concentration (minutes)
L = slope length (feet [ft])
S = slope (ft/ft).

and the SCS equation is $T_c = \left(\frac{11.9L^3}{H}\right)^{0.385}$ where

The current applicable version of this publication resides on Jacobs' Intranet. All copies are considered to be uncontrolled.
Copyright© Jacobs Engineering Group Inc., 2007

T_c = time of concentration (hours)
L = slope length (miles)
H = slope height (ft).

Table 1. Drainage Area Characteristics

Drainage Area	Area (acres)	Max Flow Length (ft)	Flow Length Opposite Centroid	Time of Conc (min)	Lag = 0.6 Tc	Initial Abstraction (inches)	Const Inf Rate (in/hr)
Northwest of Wedge	183.6	4911	3078	NA	NA	0.52	0.20
Northeast of Wedge	179.4	5126	3309	NA	NA	0.47	0.16
West Side of Wedge	37.1	3140	NA	25.5	15.3	0.30	0.10
East Side of Wedge	31.6	2942	NA	24.5	14.7	0.30	0.10

Runoff Hydrograph Calculations

For the two largely undisturbed drainage areas between the book cliffs and the wedge, unit hydrographs were developed using the methodology of the U S. Bureau of Reclamation (USBR, 1987). These unit hydrographs are computed in UnitHydrographs.xls. For the two drainage areas on top the wedge the SCS unit hydrograph was used. The USBR method was developed for natural areas in the west and is not appropriate for the wedge constructed of compacted soil. The runoff hydrographs were computed using the Computer Program HEC-HMS (USACE 2007).

Rainfall Depths Applied

The series of storms for the runoff calculations was developed from the Hydrology data in the draft RAP and NOAA Atlas 14. The number of storms of each depth was chosen conservatively as follows.

- A storm with rainfall depth equal to or greater than the 1000 year storm occurs on the average once every 1000 years. Since the rainfall depth may be any depth between the 1000 year storm and the PMP, the PMP was used for this storm.
- A storm with rainfall depth equal to or greater than the 500 year storm occurs on the average twice every 1000 years. Since the rainfall depth may be any depth between the 500 year storm and the 1000 year storm, the 1000 year rainfall depth was used for this storm. Since the PMP accounts for one of these storms, only one 1000 year storm was used.
- A storm with rainfall depth equal to or greater than the 200 year storm occurs on the average five times every 1000 years. Since the rainfall depth may be any depth between the 200 year storm and the 500 year storm, the 500 year rainfall depth was used for this storm. Since two larger storms have already been applied, three 500 year storms were used.

Following this logic through storms of all available return periods resulted in the distribution of rainfall depths and number of storms listed in Table 2. All storms represent 24 hour precipitation depth except for the PMP which is a 6 hour depth.

Table 2 Distribution of storms used in computing sediment transport capacity.

Return Interval Represented	Return Interval	Precipitation Depth (inches)	Number of Storms Equal or Greater than	Number of Storms of Depth Employed

The current applicable version of this publication resides on Jacobs' Intranet. All copies are considered to be uncontrolled.
Copyright© Jacobs Engineering Group Inc., 2007

(years)	Employed (years)		Interval Represented	
1000	PMP (6 hour)	9.0	1	1
500	1000	3.73	2	1
200	500	3.15	5	3
100	200	2.58	10	5
50	100	2.35	20	10
25	50	2.12	40	20
10	25	1.91	100	60
5	10	1.63	200	100
2	5	1.42	500	300
1	2	1.16	1000	500
< 1	1	0.93	Unknown	1000

The runoff from each area was computed using HEC-HMS with the results from the wedge and from the book cliffs area flowing to the west combined into one hydrograph and to the east into another. A five minute time step was used.

Sediment Transport Capacity

The capacity of the flow to the east and the flow to the west along the north edge of the wedge (Figure 2) was estimated using a procedure in NUREG 1623 (Johnson 2002).

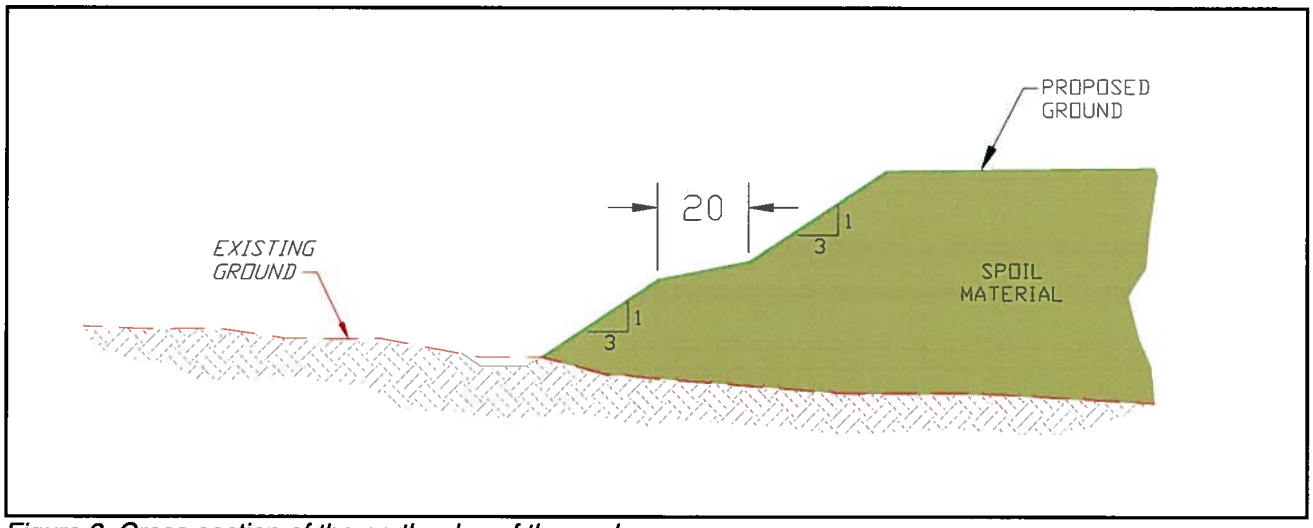

Figure 2 Cross section of the north edge of the wedge.

In this method the sediment transport capacity of a channel can be computed as

$$q_s = c_{s1} h^{c_{s2}} V^{c_{s3}}$$

where
q_s = unit sediment transport rate in ft^2/s (unbulked)
V = velocity in ft/s

The current applicable version of this publication resides on Jacobs' Intranet. All copies are considered to be uncontrolled.
Copyright© Jacobs Engineering Group Inc., 2007

h = flow depth in feet

NUREG 1623 gives the coefficient and exponents as a function of grain size distribution. Those that most closely correspond to the grain size distribution of the native soil are

$C_{s1} = 3.3 \times 10^{-5}$
$C_{s2} = 0.715$
$C_{s3} = 3.30$

A hypothetical trapezoidal channel with a bottom width of 3 feet and a side slope of 1.5 horizontal to 1 vertical was assumed based on field observations of West Kendall Wash. The slope of the channel was assumed to be 0.007 to the east and 0.009 to the west as determined from the topography of the site and the location of the wedge. A table was constructed of sediment transport in cfs as a function of discharge in each channel. The flow in each 5 minute period of a runoff hydrograph was then used to interpolate to find the sediment transport during each 5 minute increment of the hydrograph. The sediment transport of each hydrograph was then computed as the sum of these 5 minute contributions.

For the channel shown below in Figure 3 with a discharge Q, a depth h, and a top width T, the volume of sediment transport capacity in a five minute period was calculated as follows. q_s was computed as above. Since this is the unbulked volume transport rate the unit weight was assumed to be 165 pcf. The value of q_s will vary across the channel as it depends on both the velocity and depth of flow. As a conservative approach, the value q_s computed for the full depth, h, was applied throughout the channel. The total rate of sediment transport in cubic feet/sec (unbulked) was computed as

$$Q_s(unbulked) = q_s T$$

and the rate in cf/5 min (bulked) as

$$Q_s(5\min_bulked) = Qs(unbulked) * (300\sec) * \frac{165\,pcf}{91.3\,pcf}$$

These 5 minute contributions were summed for each of the 5 minute flow periods of a storm hydrograph to compute the total sediment transport potential in cubic feet of the native soil from a single storm.

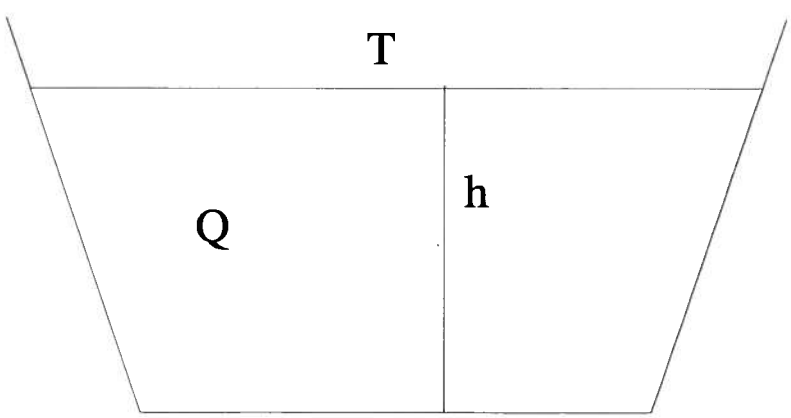

Figure 3 Cross Section of Hypothetical Channel along the North Edge of the wedge.

The current applicable version of this publication resides on Jacobs' Intranet. All copies are considered to be uncontrolled.
Copyright© Jacobs Engineering Group Inc., 2007

This calculation was repeated for all the storms listed in Table 2 and the total potential sediment transport during 1000 years was computed.

Unaccounted for Runoff

The total runoff of water in the listed storms was also computed. Since the annual rainfall at Thompson Springs during the period (1971-2000) was 9.97 inches(reference), and NUREG 1623 states that a reasonable estimate of the ratio of runoff to rainfall in the semi-arid regions of the western United States is 0.127, a volume of total expected runoff during 1000 years was computed. Comparing this volume with that computed from the listed storms indicated that over half the runoff had not been accounted for.

Assuming that the sediment concentration in this additional runoff will be equal to the average concentration in the runoff from the one year storm, an additional volume of sediment transport was added by multiplying the average concentration in the runoff from the one year storm by the volume of additional runoff.

Sediment Supply from the Book Cliffs Area

The runoff from the area between the Book cliffs and the wedge will transport sediment toward the wedge. The total sediment loss from the two watersheds delineated over a 1000 year period can be estimated with the Modified Universal Soil Loss Equation (MUSLE).

The equation is

$$A = R \times K \times LS \times VM$$

where:

A = soil loss in tons per acre per year,
R = rainfall factor,
K = soil erodibility factor,
LS = topographic factor, and
VM = dimensionless erosion control factor relating to vegetative and mechanical factors.

The rainfall factor is 25, as given in NUREG/CR-4620 (Nelson et al. 1986) for the eastern third of Utah. The soil erodibility factor was estimated using the nomograph given in NUREG/CR-4620 (Nelson et al. 1986).

The topographic factor is calculated by the following equation:

$$LS = \frac{650 + 450 \times s + 65 \times s^2}{10{,}000 + s^2} \times \left(\frac{L}{72.6}\right)^m$$

where:

s = slope steepness in percent,
L = slope length in ft, and
m = exponent dependent upon slope steepness.

The dimensionless erosion control factor used for the undisturbed watersheds was 0.4, from Table 5.3 of NUREG/CR-4620 (Nelson et al. 1986), representing seedings of 0 to 60 days to mimic light vegetation in the area. Over an extended period of time, a similar value can be expected to apply on the top of the wedge as some vegetation will develop. A slope of 3.5% was used. This is a representative slope for the area between

The current applicable version of this publication resides on Jacobs' Intranet. All copies are considered to be uncontrolled.
Copyright© Jacobs Engineering Group Inc., 2007

the wedge and the base of the Book Cliffs. Table 3 summarizes the results of the soil loss equation. The soil loss (sediment supply) from the Book cliffs area is most likely underestimated since the slope from the base to the top of the Book Cliffs is 40 – 50% and the erodibility factor of the soil is about the same for the two soil types in the watershed (Web Soil Survey and Appendix B). More sediment than calculated should be eroded from this area, but much of the additional sediment will be deposited as the slope flattens near the wedge.

Table 3. Results of Soil Loss Equation

Soil Cover	Book Cliffs Area (West)	Top of Wedge (West)	Book Cliffs Area (East)	Top of Wedge (East)
Rainfall factor, R	25	25	25	25
Silt and very fine sand (%)	60	60	60	60
Sand (%)	25	25	25	25
Organic matter (%)	2	2	2	2
Soil structure	Very fine granular	Very fine granular	Very fine granular	Very fine granular
Relative permeability	Moderate	Moderate	Moderate	Moderate
Erodibility factor	0.35	0.35	0.35	0.35
Topographic factor, LS	0.911	0.183	0.861	0.178
VM (low density seedings)	0.4	0.4	0.4	0.4
Soil loss (tons/acre/year)	3.19	0.64	3.01	0.62
Soil loss (inches/1,000 years)	19.2	3.4	18.2	3.3
Total sediment loss in 1000 years (cf)	12,825,853	459,167	11,841,089	380,310

The relative sediment yield of a more realistic watershed shape has been assessed with the Revised Universal Soil loss Equation (RUSLE) using the computer program RUSLE2 (USDA 2001). In this simulation three slopes were used, 1000 feet at 40% to represent the book cliffs, 800 feet at 3.5% and 800 feet at 2.5% to represent the area between the base of the Book Cliffs and the wedge. A RUSLE2 simulation was also performed with a the same three segments, but with each having a slope of 3.5%. The rainfall was the long term average at Thompson, about 6 miles east of the site of the waste cell and the other climate factors were those for Grand Junction, Colorado. These input parameters and the results are presented in Table 4 and Appendix C.

Table 4 Input Data and Results of RUSLE2 Estimate of Sediment Yiels from t Yield from Book Cliffs Area

RUSLE2 Sediment Yield				
Segment	**Length(ft)**	**Slope(%)**	**Avg Erosion(T/ac/yr)**	**Sed Delivery(T/ac/yr)**
1	100	3.5		
2	800	3.5		
3	800	3.5		
	Net Erosion		2.6	2.6
1	100	40		
2	800	3.5		
3	800	2.5		
	Net Erosion		28	9.1

These results indicate that the assumption of a single 3.5% slope in the MUSLE calculation was conservative.

The current applicable version of this publication resides on Jacobs' Intranet. All copies are considered to be uncontrolled.
Copyright© Jacobs Engineering Group Inc., 2007

Sediment Budget

The volumes of sediments over a 1000 year period calculated with the MUSLE and the sediment transport potential along the north side of the wedge are summarized in Table 5.

Table 5 Sediment Budget for the North Side of the Wedge

Area	Sediment Transport Capacity (cf)	Sediment Yield from MUSLE (cf)
Channel along wedge to the west	4,629,541	
Channel along wedge to the east	4,101,687	
Western area between Book Cliffs and the wedge		12,825,853
Eastern area between Book Cliffs and the wedge		11,841,089
Western portion of the top of the wedge		459,167
Eastern portion of the top of the wedge		380,310
Total sediment yield toward the west portion of the wedge		13,285,020
Total sediment yield toward the east portion of the wedge		12,221,399
Ratio of sediment supply from Book Cliffs to transport capacity (west)	2.8	
Ratio of sediment supply from Book Cliffs to transport capacity (east)	2.9	

These results indicate that the water flowing along the northern side of the wedge to the west and the east does not have sufficient sediment transport capacity to carry away the supply of sediment from the areas between the Book Cliffs and the wedge. The northern edge of the wedge is expected to expand northward during the 1000 year life of the disposal cell and offer increasingly more protection to the cell as time passes. Even if the sediment supply from the north is discounted, the total sediment transport potential over 100 years is only about 12% of the volume of the wedge.

Erosion from top of Wedge

Due to the flat slope the predicted erosion from the top of the wedge is only 3.3 inches over a 1000 year period. This is a relatively high estimate since the longest flow paths to the east and the west were used in these estimates. Since the height of the wedge ranges from 28 to 48 feet, this is an insignificant depth of erosion.

Gully Formation on Wedge

In addition to potential erosion of the wedge by runoff from the Book cliffs area and sheet and rill erosion from precipitation directly on the top of the wedge, runoff from the top of the wedge is expected to form gullies on the top and on the steep slopes as the runoff from the top of the wedge flows to the northwest and the northeast. The potential depth of these gullies can be estimated with an approach detailed in NUREG 1623. The three types of embankment geometries analyzed in this guidance document as shown in Figure 3. Gullies forming on the top of the wedge are analyzed as a Type 3 embankment and on the steep side slope as a Type 2 embankment. The effective tributary drainage area for each embankment is computed as

The current applicable version of this publication resides on Jacobs' Intranet. All copies are considered to be uncontrolled.
Copyright© Jacobs Engineering Group Inc., 2007

$$A = 0.276[L\cos(\theta)]^{1.636}$$

where L = total length of the flow path. A gully factor depending on the soil type, the height of the embankment and the volume of runoff to the toe of the embankment toe is

$$G_f = \frac{1}{2.80 + \left[0.197\frac{V_r}{H_o^{\,3}}\right]^{-0.70}}$$ for a clay content between 15 and 50%.

The current applicable version of this publication resides on Jacobs' Intranet. All copies are considered to be uncontrolled.
Copyright© Jacobs Engineering Group Inc., 2007

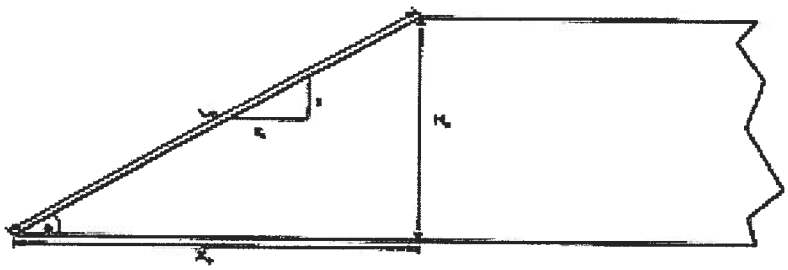

Type 1 Embankment

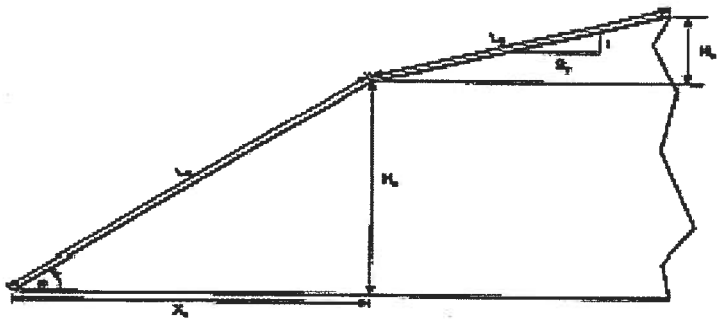

Type 2 Embankment

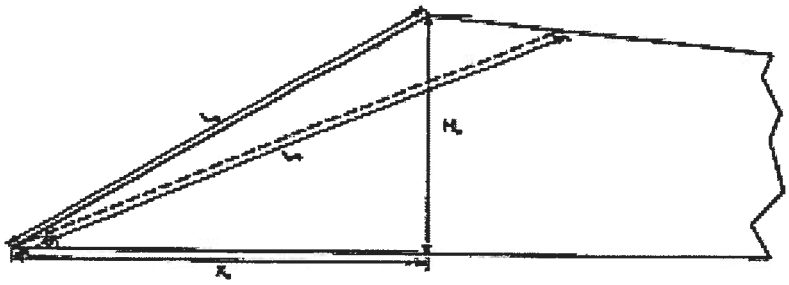

Type 3 Embankment

Figure B-4. Three types of embankment geometry.

NUREG-1623 B-6

Figure 4 Three types of embankment geometry for gully calculations.

The current applicable version of this publication resides on Jacobs' Intranet. All copies are considered to be uncontrolled.
Copyright© Jacobs Engineering Group Inc., 2007

The estimated maximum depth of gully incision is

$$D_{\max} = G_f L_{total} S$$

where S is the original slope of the embankment. The top width of the gully at its deepest point is

$$W = \left[\frac{D_{\max}}{0.61}\right]^{1.149}$$

and the location of the deepest incision measured in units of D_{max} downslope from the crest of the embankment is

$$D_l = 0.713\left[\frac{V_r S}{L_o^{\ 3}}\right]^{-0.415}$$

The results of these calculations are summarized in Table 6. The calculations are performed in metric units and the results converted to English units.

Table 6 Summary of Calculation of Depth of Gullies on the Wedge

Variable	Description	Top Slope West	Side Slope West	Top Slope East	Side Slope East
H_o (ft)	Height of Embankment	10	18	8	22
X_o (ft)	Horizontal Length of Embankment	1339	95	1254	92
L_o (ft)	Length of Embankment along Slope	1339	96.7	1254	94.6
θ (radians)	Embankment Slope Angle (radians)	0.0075	0.1873	0.0064	0.2347
L_2 (ft)	Distance along Top Slope (Type II)	NA	1339	NA	1254
H_2 (ft)	Height of Top Slope (Type II)	NA	10	NA	8
L_t (ft)	Long Term Embankment Slope Length	1573	1436	1473	1349
A (sq ft)	Effective Drainage Area	72,231	60,418	64,882	53,638
V_r (cf)	Rainfall Volume	7,622,392	6,375,820	6,846,885	5,660,312
G_f	Gully Factor	0.36	0.35	0.36	0.35
D_{max} (ft)	Maximum Gully Depth	4.2	6.5	3.4	8.0
W (ft)	Gully Width at Maximum Depth	7.7	12.7	5.9	16.0
D_l (ft)	Distance of D_{max} from Top of Slope	248	4.1	204	4.7

Summary

As shown Figure 1 a wedge of spoil material consisting of approximately 3,000,000 cubic yards of soil excavated from the waste cell will be placed between the Book cliffs and the waste cell to divert runoff from the Book Cliffs area around the waste cell. These calculations have been performed to asses whether the wedge will continue to protect the cell during the 1000 year design life. Three possible processes by which the integrity of the wedge might be compromised have been considered.

The current applicable version of this publication resides on Jacobs' Intranet. All copies are considered to be uncontrolled.
Copyright© Jacobs Engineering Group Inc., 2007

1. Erosion of the wedge by runoff from the area between the Book Cliffs and the wedge will tend to erode the wedge as it is routed to the southwest and northwest around the wedge and the waste cell. The sediment transport capacity of this runoff during the 1000 year design life has been assessed using equations from NUREG 1623. Supply of sediment from the watersheds north of the wedge have been estimated by use of the Modified Universal Soil Loss Equation (MUSLE), as described in NUREG 4620 (Nelson et al. 1986). The assumptions made in the MUSLE have been evaluated using the RUSLE. The results of these calculations indicate that the total sediment carrying capacity of the runoff as it flows around the wedge is slightly more than 10% of the volume of the wedge. In addition, the sediment supply from the Book Cliffs area computed from the MUSLE will be approximately three times the sediment transport capacity of the flow around the wedge resulting in a net gain in the volume of the wedge over the design life of the waste cell. For each storm, the flow in the channels along the north side of the wedge will increase from near zero at the center of the wedge to the full flow calculated at the east and west ends of the channels. This will result in increasingly greater sediment transport as the flow increases along the channel. Since the sediment supply to the north edge of the wedge is expected to be comparatively uniform along the channel, the result will be that the central portion of the north edge of the wedge will migrate further northward than the east and west ends. The slope of the channels will then increase over time and a balance between sediment transport capacity and sediment supply may be achieved during the 1000 year design life of the cell.

2. Precipitation falling directly on the top of the wedge will run off toward the northeast and the northwest. This runoff will erode the wedge from the top. Application of the MUSLE to estimate the volume of sediment lost from the wedge through this mechanism indicate that the wedge will be reduced in average height by about 3 to 4 inches. With a design height ranging from approximately 20 to 48 feet, this loss of soil will not threaten the integrity of the wedge.

3. The third mechanism considered is concentration of flow as it runs off the top of the wedge and the consequent formation of gullies both on the top of the wedge and on the steep slopes to the northwest and the northeast. The depth, width, and location of the deepest portions of these gullies has been estimated with techniques described in NUREG 1623 (Johnson 2002). The results are summarized in Table 6. On top the wedge the deepest gully is estimated to be slightly over 4 feet deep, 8 feet wide, with the deepest part of the gully about 250 feet from the south edge of the wedge. The deepest gully on the steep side slope is anticipated to be about 8 feet deep, 16 feet wide, with the deepest portion about 5 feet below the slope break from the flat top to the steep side of the wedge. Neither of these gullies would pose a serious threat to the integrity of the wedge. It should be noted that because of the time period over which gullies developed that were used in developing the equations, NRC staff recommends the method be used for a design cell life of 200 years. Since the gully depth increases with time, the calculation has been extrapolated to 1000 years as the best available estimate of the extent of potential gully formation over a 1000 year design period.

Based on these calculations, we conclude that the wedge will protect the waste cell from runoff from the areas to the north and continue to function over the 1000 design life.

The current applicable version of this publication resides on Jacobs' Intranet. All copies are considered to be uncontrolled.
Copyright© Jacobs Engineering Group Inc., 2007

References:

10 CFR 40. U.S. Nuclear Regulatory Commission (NRC), "Domestic Licensing of Source Material," Appendix A, *Code of Federal Regulations*, February 2007.

40 CFR 192. U.S. Environmental Protection Agency (EPA) "Health and Environmental Protection Standards for Uranium and Thorium Mill Tailings," *Code of Federal Regulations*, February 2007.

Abt, S.R., and T.L. Johnson, 1991. "Riprap Design for Overtopping Flow", *Journal of Hydraulic Engineering*, 117(8), pp. 959–972.

Abt, S.R., T.L. Johnson, C.I. Thornton, and S.C. Trabant, 1998. "Riprap Sizing at Toe of Embankment Slopes", *Journal of Hydraulic Engineering*, 124(7), July.

Abt, S.R., J.F. Ruff, and R.J. Wittler, 1991. "Estimating Flow Through Riprap", *Journal of Hydraulic Engineering*, 117(5), pp. 670–675.

Chow, V.T., 1964. *Handbook of Applied Hydrology*, McGraw-Hill Book Company, New York, New York.

DOE (U.S. Department of Energy), 1989. *Technical Approach Document, Revision II*, UMTRA-DOE/AL 050424.0002, December.

DOT (U.S. Department of Transportation), 1983. *Hydraulic Design of Energy Dissipaters for Culverts and Channels*, Hydraulic Engineering Circular No. 14, September.

Geotechnical Engineering Group, Inc. (GEG), 2005. Technical Testing, Crescent Junction, GEG Job No. 2165, December 22.

Johnson, T.L., 2002 *Design of Erosion Protection for Long-Term Stabilization*, Final Report, NUREG-1623, U.S. Nuclear Regulatory Commission, September.

Nelson, J.D., S.R. Abt, R.L. Volpe, D. van Zyl, N.E. Hinkle, W.P. Staub, 1986. *Methodologies for Evaluating Long-Term Stabilization Design of Uranium Mill Tailings Impoundments*, NUREG/CR-4620, U.S. Nuclear Regulatory Commission, June.

Temple, D.M., K.M. Robinson, R.M. Ahring, and A.G. Davis, 1987. *Stability Design of Grass-Lined Open Channels*, U.S. Department of Agriculture Handbook No. 667, September.

TR-55, Win TR-55 User Guide, US Department of Agriculture, 2003

USDA (U.S. Department of Agriculture), 1994. "Gradation Design of Sand and Gravel Filters", *National Engineering Handbook*, Part 633, Chapter 26, October.

The current applicable version of this publication resides on Jacobs' Intranet. All copies are considered to be uncontrolled.
Copyright© Jacobs Engineering Group Inc., 2007

Appendix A

Reference Material

NUREG 4620 MUSL

NUREG 1623 Gully Formation

NUREG 1623 Channel Sediment Transport

Two basic approaches exist for the design of suitable erosion-resistant covers for a tailings impoundment surface as originally described by Nelson et al. (1983). The first approach consists of providing a cover material that will resist material transport by flowing water using the concept of critical shear stress. The second approach is based on the Universal Soil Loss Equation, an empirical method originally developed during the 1930's. The methodologies involved with both of these methods are discussed below.

5.1.1 Critical Shear Stress Approach

The critical shear stress approach consists of providing a cover material with a d_{30} grain size (i.e., 70% of the material by weight is coarser than the d_{30}) that will resist movement when subjected to the sheet flow maximum permissible velocity resulting from the application of the PMP over the entire impoundment surface. Minimum d_{30} grain sizes should be determined using the critical shear stress approach similar to the procedures discussed in Simons and Senturk (1977) applicable to overland flow. A numerical solution for selecting an appropriate d_{30} to provide armoring has been developed by Shen and Lu (1983).

The design approach described above, in which the critical grain size is selected to resist the onset of sheet erosion, should evaluate the runoff from PMP storms of different durations, such as 0.5, 1, 2, 4, and 6 hours to select the maximum d_{30} required. Rainfall depths will usually be based on 2.5 to 15 minute durations for small drainage basins as presented in Section 2.1.2. Typically, the minimum construction layer thickness is specified to be at least two times the maximum particle size. If the above approach results in a cover thickness less than about 6 inches, then other considerations - such as nonuniform placement of cover and particle breakdown due to handling, placement and weathering - would suggest that a minimum cover thickness of 10 inches should be considered. If a self-armoring cover can be provided, and there is no major concern for weathering of the cover material, the design is independent of time and the cover should remain intact indefinitely.

5.1.2 Soil Loss Equation Approach

The concept of sheet erosion was recognized by early researchers and the Universal Soil Loss Equation (USLE) was developed in the late 1930's by the Agricultural Research Service to evaluate soil conservation practices for cropland throughout the United States. After its inception, the soil loss procedure was used and modified as field experience and data were obtained incorporating the basic parameters of field slope and length, precipitation, and crop management to estimate soil losses on an annual basis. Application of the USLE to non-cropland areas and specifically for construction sites became feasible when Wischmeier et al. (1971), using basic soil loss characteristics, developed and implemented a soil erodibility factor (K) in the soil loss computation. Subsequent efforts refined the parameters used in the USLE for mining and construction activities in the interior western United States.

The Modified Universal Soil Loss Equation (MUSLE) was developed by the Utah Water Research Laboratory in 1978 for the principal objective of estimating soil losses due to highway construction activities. Alterations were made to the USLE to accomodate unique or special conditions encountered in highway construction, including steep and deep cuts and fill slopes that could cause erosion affecting adjacent or nearby roadways, streams, lakes, or inhabited areas. It is apparent that the modifications made to the USLE extend to many construction and mining sites beyond the scope of highway construction.

The Modified Universal Soil Loss Equation (MUSLE) is a mathematical model based on field determined coefficients and provides the most rational approach to evaluate the long-term erosion potential from an upland area similar to that of the area covering a reclaimed tailings pond. Recent investigations into appropriate methods of modeling major types of sheet erosion (Abt and Ruff, 1978; Nelson et al. 1983; Nyhan and Lane, 1983; and NRC, 1983), indicate that although more rigorous mathematical models are available to simulate erosion as a function of time, the use of the USLE has a strong precedent because it has a 40-year history of runoff and soil loss data.

The MUSLE is used to evaluate average soil losses for certain types of slopes as a function of time. The MUSLE does not consider the potential for gully development or intrusion as discussed in Chapter 4 because the topographic features of the tailings area are assumed to remain constant with time. Also, the MUSLE does not incorporate the concept of the PMP but rather a rainfall factor based on historical rainfall values. The MUSLE is defined by Clyde et al. (1978) as follows:

$$A = R\ K\ (LS)\ (VM) \qquad (5.1)$$

where,

A = the computed loss per unit area in tons per acre per year with the units selected for K and R properly selected;

R = the rainfall factor which is the number for rainfall erosion index units plus a factor for snowmelt, if applicable;

K = the soil erodibility factor, which is the soil loss rate per erosion index unit for a specified soil as measured on a unit plot that is defined as a 72.6-ft length of uniform 9% slope continuously maintained as clean tilled fallow;

LS = the topographic factor, which is the ratio of soil loss from the field slope length to that from a 72.6-ft length under otherwise identical conditions;

VM = the dimensionless erosion control factor relating to vegetative and mechanical factors. This factor replaces the cover management factor (C) and the support factor (P) of the original USLE.

5.1.2.1 The Rainfall and Runoff Factor (R)

As noted by previous research at Los Alamos National Laboratory (Nyhan and Lane, 1983), the R factor as used in the MUSLE is often misinterpreted only as a rainfall factor. In reality, it must quantify both the raindrop impact and provide information on the amount and rate of runoff likely to be associated with the rain. More specifically, the R factor is described in terms of a rainfall storm energy (E) and the maximum 30-minute rainfall intensity (I_{30}). Generalized R factors applicable to the interior western United States are given in Table 5.1. For R factors in specific areas of the United States, it is recommended that erosion index distribution curves be obtained from local SCS offices.

Table 5.1. Generalized Rainfall and Runoff (R) Values.

State	Eastern Third	Central Third	Western Third
N. Dakota	50 - 75	40 - 50	40
S. Dakota	75 - 100	50	40
Montana	30 - 40	20	20 - 50
Wyoming	30 - 50	15 - 30	15 - 25
Colorado	75 - 100	40 - 50	20 - 40
Utah	20 - 30	20 - 50	15 - 40
New Mexico	75 - 100	40 - 50	20 - 40
Arizona	20 - 50	20 - 50	25 - 40

5.1.2.2 The Soil Erodibility Factor (K)

The soil erodibility factor (K) recognized the fact that the erodibility potential of a given soil is dependent on its compositional makeup, which in turn reflects the grain size distribution of the soil. To predict soil erodibility, five soil characteristics that include the percent silt and fine sand, percent sand greater than 0.1 mm, percent organic material, general soil structure and general permeability are determined. The K factor is then found by using the Wischmeier nomograph presented in Figure 5.1.

The makeup of the various soil fractions presented in Figure 5.1 is based on separating sand and silt at the 0.1 mm size. This differs from the Unified Soil Classification System which uses the No. 200 sieve size (0.075 mm) for the separation between sand and silt. The value to enter Figure 5.1 with should be the percentage of material finer than 0.1 mm in size, not the percentage passing the No. 200 sieve. Also, the determination of the Soil Erodibility Factor (K) as shown on Figure 5.1 does not specifically reference the percentage of clay (finer than 0.002 mm) contained in the material. The percentage of silt plus very fine sand to be used for Figure 5.1, therefore, is the percentage of material contained between 0.002 mm and 0.1 mm.

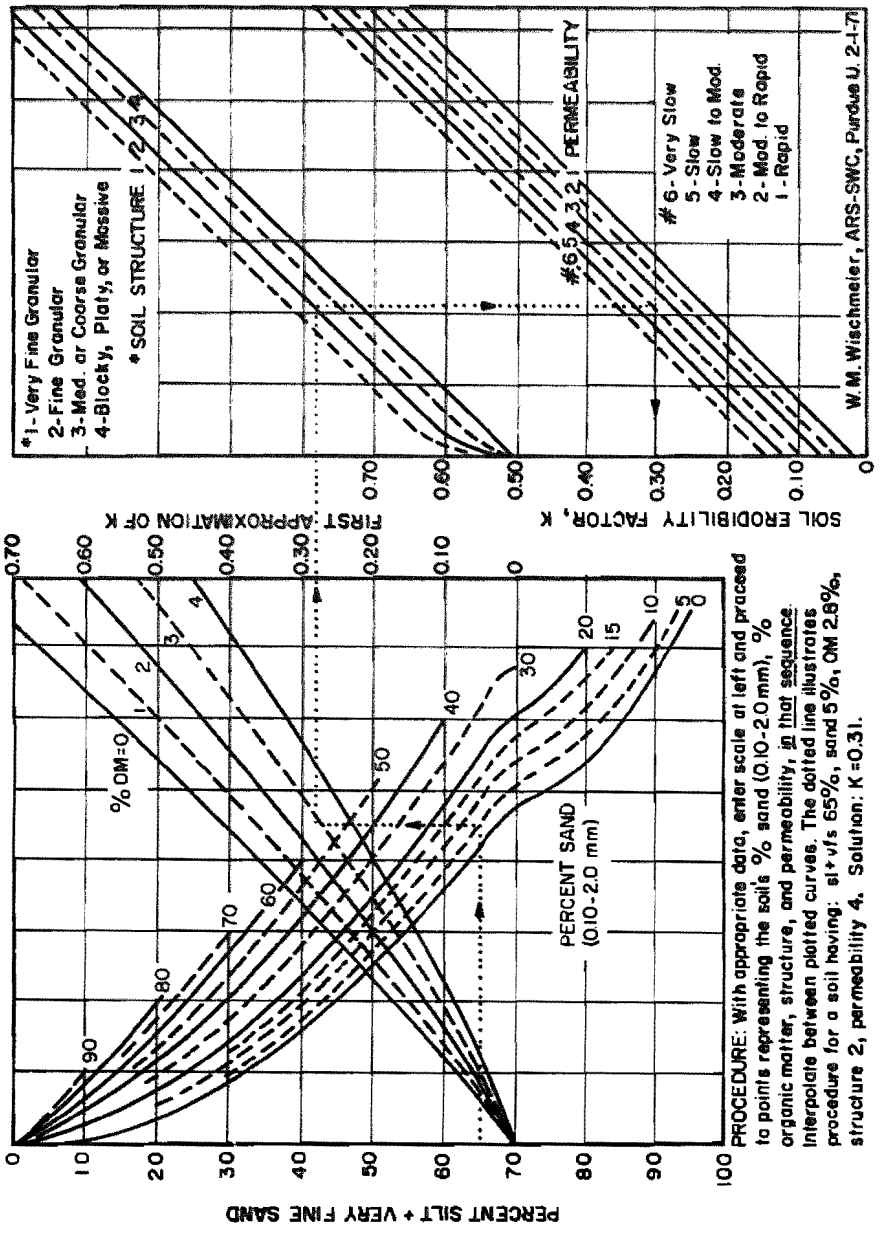

Fig. 5.1. Nomograph for determining soil erodibility factor *K*. *Source:* after Wischmeier et al., 1971.

5.1.2.3 The Topographic Factor (LS)

Although the effects of both length and steepness of slope have been investigated separately in different research efforts, it is more convenient for analytical purposes to combine the two into one topographic factor, LS. Wischmeier and Smith (1978) developed plots correlating the topographic factor for slopes up to 500 meters in length at slope inclinations from 0.5% up to 50%. Note that flat, short slopes will have less erosion than long, steep slopes and it is to the benefit of the design engineer to optimize slope length and gradients to fit the topography.

The equation to determine the LS factor is as follows:

$$LS = \frac{650 + 450s + 6s^2}{10{,}000 + s^2} \quad \frac{L}{72.6}^{m} \qquad (5.2)$$

where LS = topographic factor
L = slope length in feet
s = slope steepness in percent
m = exponent dependent upon slope steepness

The slope dependent exponent m is presented in Table 5.2.

Table 5.2 Slope Dependent Exponent

Slope (percent)	m
$s \leq 1.0$	0.2
$1.0 < s \leq 3.0$	0.3
$3.0 < s \leq 5.0$	0.4
$5.0 < s \leq 10.0$	0.5
$s > 10.0$	0.6

5.1.2.4 The VM Factor

The VM factor is the erosion control factor applied in place of the cover and erosion control factors found in the USLE. The erosion control factor accounts for measures implemented at the construction site to include vegetation, mulching, chemical treatments and sprayed emulsions to impede or reduce erosion due to the overland flow of water. Values of the VM factor relative to site-specific conditions are presented in Table 5.3.

The VM factor is perhaps the most sensitive factor to effect the computed erosion loss for a given site. As shown by the values presented

on Table 5.3, the development of a permanent vegetative cover can have a significant impact in reducing the computed erosion loss. However, the effectiveness of a vegetative cover over long-term periods should be questioned unless other protective schemes, such as armoring of the cover with the proper size material, are also included in the design.

5.1.2.5 Example Problem

An example problem in how to use the MUSLE is provided below.

Assumptions:

Site location:	Western Colorado
Site description:	Uncovered tailings pond
Pond size:	160 acres
Slope:	3%
Length:	2500 ft
Material:	42% sand greater than 0.10 mm; 58% fine sand and silt less than 0.10 mm; 5% clay less than 0.002 mm; 0% organics; (53% silt plus fine sand less than 0.1 mm); Consistency - fine granular; Permeability - slow to moderate.

The following factors have been determined for use in Equation 5.1.

R = 20 from Table 5.1

K = 0.50 from Figure 5.1

LS = 0.747 from Equation 5.2 and Table 5.2

VM = 1.0 (average from Table 5.3 based on an undisturbed surface)

Using Equation 5.1, the annual soil loss (A) from the tailings pond due to sheet erosion caused by flowing water is computed to be 7.47 tons/acre/year, or 1195 tons/year from the facility. Therefore, the cover is estimated to erode at a rate of 0.003 ft per year, or 0.3 ft/century.

5.2 SUMMARY AND FUTURE STUDIES

The main application of the soil loss equation approach in the evaluation of cover integrity is to determine whether it is possible for sheet erosion to penetrate the tailings cover, thereby exposing bare tailings and constituting a failure of the cover. The followup study will concentrate

Table 5.3. Typical VM Factor Values Reported in the Literature.[a]

Condition	VM Factor
1. Bare soil conditions	
freshly disked to 6-8 inches	1.00
after one rain	0.89
loose to 12 inches smooth	0.90
loose to 12 inches rough	0.80
compacted bulldozer scraped up and down	1.30
same except root raked	1.20
compacted bulldozer scraped across slope	1.20
same except root raked across	0.90
rough irregular tracked all directions	0.90
seed and fertilizer, fresh	0.64
same after six months	0.54
seed, fertilizer, and 12 months chemical	0.38
not tilled algae crusted	0.01
tilled algae crusted	0.02
compacted fill	1.24 - 1.71
undisturbed except scraped	0.66 - 1.30
scarified only	0.76 - 1.31
sawdust 2 inches deep, disked in	0.61
2. Asphalt emulsion on bare soil	
1250 gallons/acre	0.02
1210 gallons/acre	0.01 - 0.019
605 gallons/acre	0.14 - 0.57
302 gallons/acre	0.28 - 0.60
151 gallons/acre	0.65 - 0.70
3. Dust binder	
605 gallons/acre	1.05
1210 gallons/acre	0.29 - 0.78
4. Other chemicals	
1000 lb. fiber Glass Roving with 60-150 gallons asphalt emulsion/acre	0.01 - 0.05
Aquatain	0.68
Aerospray 70, 10 percent cover	0.94
Curasol AE	0.30 - 0.48
Petroset SB	0.40 - 0.66
PVA	0.71 - 0.90
Terra-Tack	0.66
Wood fiber slurry, 1000 lb/acre fresh[b]	0.05
Wood fiber slurry, 1400 lb/acre fresh[b]	0.01 - 0.02
Wood fiber slurry, 3500 lb/acre fresh[b]	0.10
5. Seedings	
temporary, 0 to 60 days	0.40
temporary, after 60 days	0.05
permanent, 0 to 60 days	0.40
permanent, 2 to 12 months	0.05
permanent, after 12 months	0.01
6. Brush	
7. Excelsior blanket with plastic net	0.04 - 0.10

[a]Note the variation in values of VM factors reported by different researchers for the same measures. References containing details of research which produced these VM values are included in NCHRP Project 16-3 report, "Erosion Control During Highway Construction. Vol. III. Bibliography of Water and Wind Erosion Control References," Transportation Research Board, 2101 Constitution Avenue, Washington, DC 20418.

[b]This material is commonly referred to as hydromulch.

on using the MUSLE for several alternate cover designs in order to evaluate whether the proposed analytical approach can be successfully used to measure the long-term integrity of protective soil covers for uranium tailings reclamation. Alternative designs will be compared, both from a standpoint of overall integrity and construction difficulty. The covers will also be evaluated using the critical shear stress approach to determine, based on a given PMP, the minimum particle size necessary to protect the cover against long-term degradation.

APPENDIX B

METHOD FOR DETERMINING SACRIFICIAL SLOPE REQUIREMENTS

1 INTRODUCTION

In many cases where tailings extend over a large area, slope lengths may be so long that extremely gentle slopes will be needed to provide long-term stability. Such gentle slopes may necessitate the use of very large amounts of soil, such that some of these slopes (with no tailings directly under them) may extend greatly beyond the edge of the tailings pile.

In such cases, licensees may be able to demonstrate that it is impractical to provide stability for 1,000 years and may choose to show that stability for less than 1,000 years, but for at least 200 years, is a more cost-effective option. Such a design may incorporate tailings embankment "out slopes," where there are no tailings directly under the soil cover. Such slopes, designed for less than the 1,000-year stability period, may be acceptable if properly justified by the licensee.

It should be emphasized that the staff considers that a 200-year sacrificial slope design should be used only in a limited number of cases and only when a design life of 1,000 years cannot be reasonably achieved. However, it should not be assumed that the design period should immediately jump from 1,000 to 200 years. The staff concludes that the selection of a design period should proceed in a stepwise fashion, with consideration given to intermediate design periods from 200-1,000 years. In determining a minimum design, a 200-year sacrificial slope design, as presented below, may be used. However, such a design has a considerable amount of uncertainty associated with its use, due to its development by extrapolation of a relatively limited data base. Therefore, the staff considers that the procedure should be used only after other reclamation designs have been considered. The staff considers that the procedures for justifying a design period of less than 1,000 years, as discussed in Appendix C, should be carefully followed to document that a 200-year sacrificial slope design is the best design that can be reasonably provided.

2 TECHNICAL BASIS

The long-term gully erosion process has the potential to destabilize an earthen embankment or soil cover constructed to prevent waste material release to the environment. Figures B-1 and B-2 present photographs of earthen embankments damaged by gullying. It was apparent to the staff that little criteria were available that assisted the designer in predicting the potential impacts of gullying processes to long-term stability of the waste material. The NRC thereby supported a series of studies to expand the knowledge base on the potential impacts of gullies on reclaimed impoundments and provide guidance for assuring the long-term stability of the waste.

In 1985, Falk et al. conducted a pilot study in an attempt to develop a procedure to predict the maximum depth a gully may incise into a tailing slope as a function of time. Falk characterized 16 reclaimed mine and/or overburden sites in Colorado and Wyoming that demonstrated incision

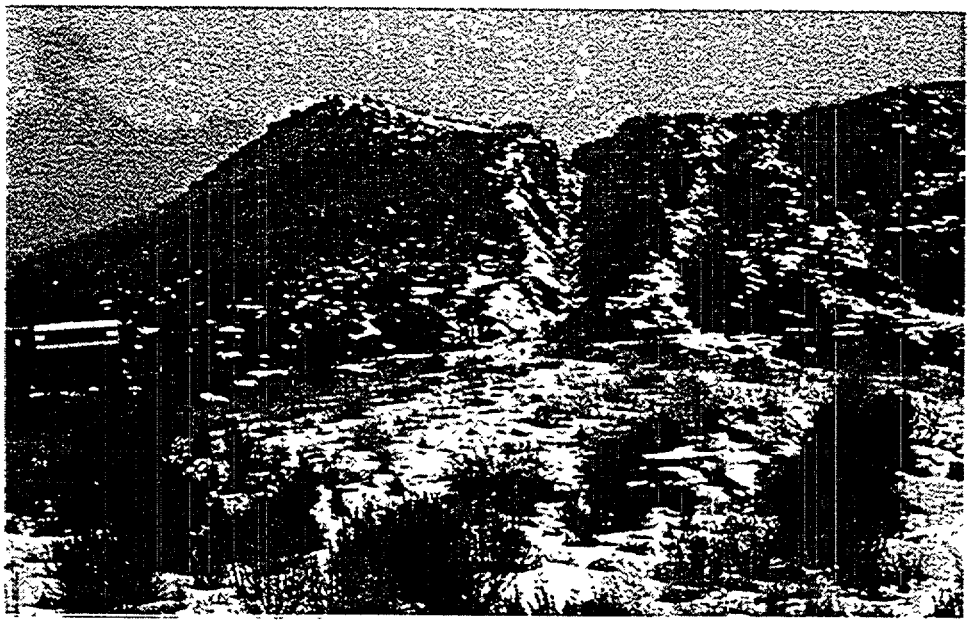

Figure B-1. Damage caused by gullying.

Figure B-2. Damage caused by gullying.

on the side slope and in some cases extended into the top slope areas. Field measurements included gully length, slope length, pile height, pile age, maximum gully depth, and width, tributary drainage area, vegetative cover and soil composition. From these data, Falk et al. attempted to formulate a procedure for estimating the maximum depth of incision, width of gully, and location of the maximum incision from the crest. The estimation procedure had a limited application but indicated that an estimation procedure could potentially be developed.

Pauley (1993) performed a series of flume studies in which near prototype soil embankments were constructed simulating a reclaimed waste impoundment. Figure B-3 presents a photograph of the flume used in the study. A series of rainfall and subsequent runoff events were conducted resulting in gully incision into the embankment. The gullying processes were documented as a function of rainfall duration and volume, soil type, embankment slope and the maximum depth of incision. The results of the study indicated that the gully incision depth was a function of the clay content of the soil, volume of runoff to the gully, and the embankment height (Abt et al. 1994). The gully processes observed by Pauley and later documented by Abt et al. (1995b) in the flume study closely paralleled those observed in the field by Falk (1985) and others.

In an attempt to expand the Falk et al. (1985) data base, Abt et al. (1995a) conducted a study in which 11 field sites that demonstrated gullying on reclaimed impoundments were located, characterized, measured, and sampled in the Colorado and Wyoming region and each gully was characterized (Falk et al. 1985).

The information presented by Falk et al. (1985), Pauley (1993) and Abt et al. (1995a) was consolidated into a composite data base as reported by Abt et al. (1995b). A comprehensive procedure was presented to estimate the maximum depth of gully incision, top width of the gully, and location of the maximum incision from the crest. The procedure allows the designer to determine gully depths and to predict the location of maximum gully incision.

A review of existing waste and tailing reclamation designs in conjunction with extensive site experience indicates that three primary embankment/cover configurations are commonly proposed. The three embankment configurations or types have been proposed or constructed as presented in Figure B-4. It is important to recognize that although each embankment type is similar along the main embankment face, the top slope, and subsequent potential tributary drainage, significantly impact the maximum depth of gully incision, D_{max}, that may intrude into the main slope. Therefore, a different procedure was developed to estimate the potential tributary drainage area and volume of runoff for each embankment type.

An empirical gully incision estimation procedure is presented as a function of the embankment/cover geometry, hydrologic parameters, soil composition, and the design life. It is anticipated that the estimation procedure will provide the user the maximum depth of gully incision, the approximate location of the maximum depth of incision along the embankment slope, and the approximate top width of the gully at the point of maximum incision as schematically presented in Figure B-5. The user will need to insure that the gully incision does not expose the waste/tailings materials.

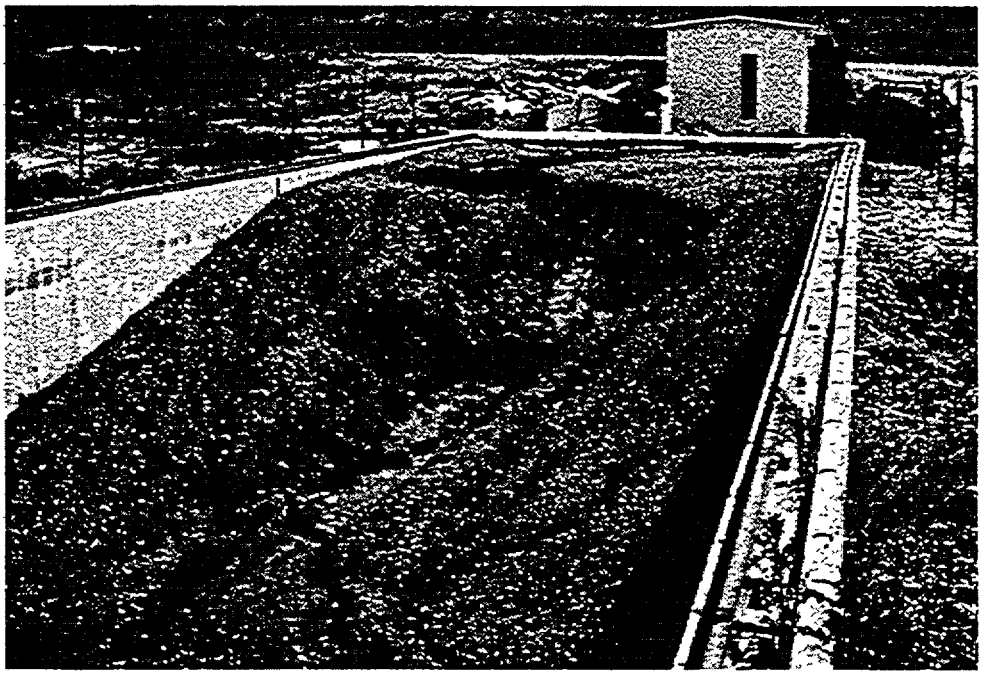

Figure B-3. Flume used by Pauley (1993).

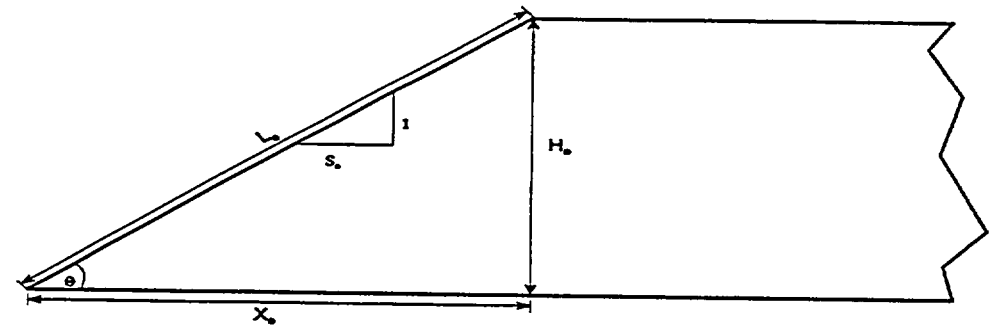

Type 1 Embankment

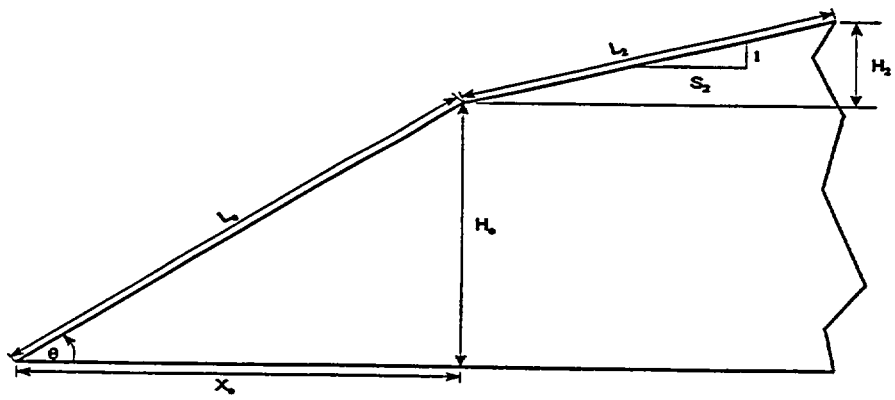

Type 2 Embankment

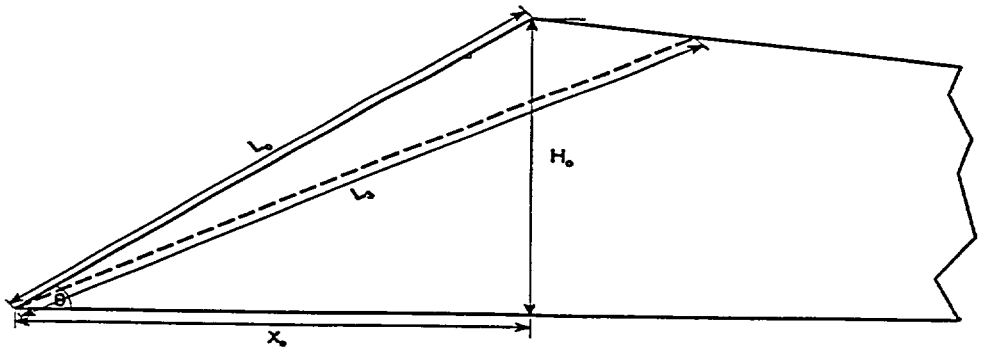

Type 3 Embankment

Figure B-4. Three types of embankment geometry.

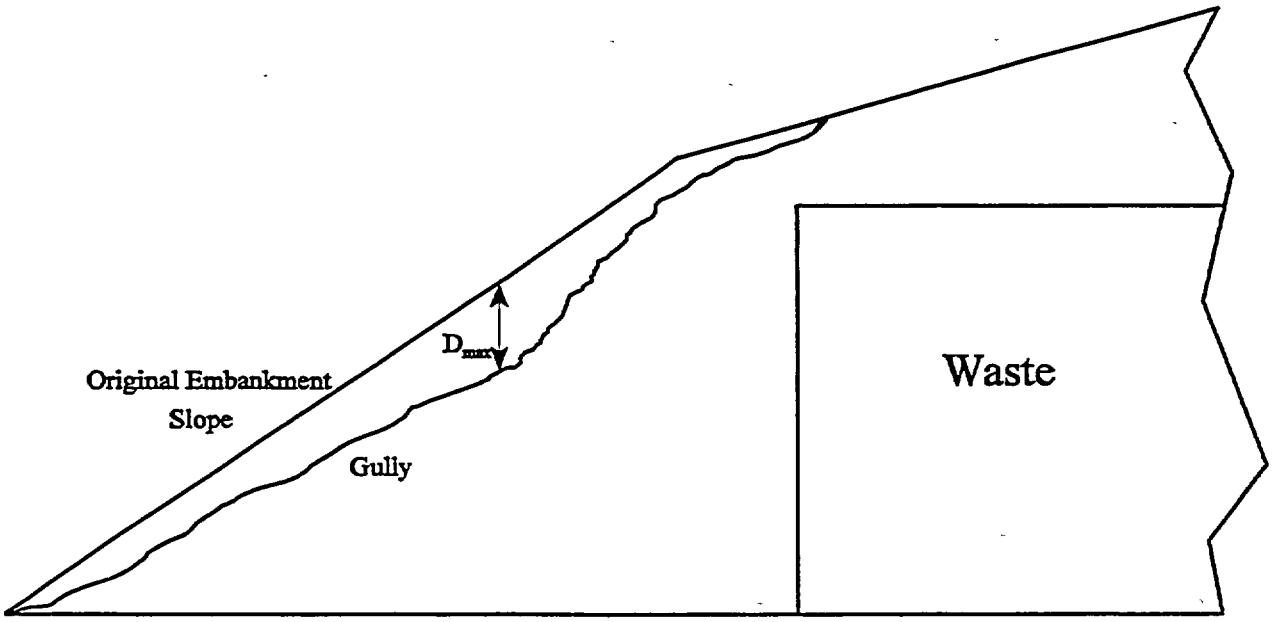

Figure B-5. Schematic of typical waste impoundment.

Staff review indicates that locating the depth of maximum gully incision is the most unpredictable part of the design procedure. The field data and flume data cannot be relied on totally to adequately describe the gully profile along the length of the slope. For example, the procedure may predict that the maximum gully depth will be 20 ft and will occur 500 ft from the embankment crest. However, not reflected in the design procedure is the possibility that the same gully could be 19 ft deep at the crest. The gully profile data available and staff experience suggest that gully depths approaching the maximum gully depth could occur near the crest. Thus, until more data are available, the staff recommends that the location of maximum gullying be assumed to occur near the crest of the slope. In addition, because of the need for significant data extrapolation, the staff suggests that this procedure be used to determine sacrificial slope requirements for a 200-year period.

In situations where increasing the set back distance of waste with respect to the embankment crest is not feasible, the concept of embankment stabilization utilizing launching riprap may be examined. Abt et al. (1997) presents a preliminary approach to the stabilization technique. Figure B-6 presents a photograph of a laboratory simulation of embankment stabilization using launching riprap. Based upon the findings of the pilot test series, a set of preliminary guidelines and a design procedure is outlined by Abt et al. (1997). The procedure presented represents the pilot test series and its application has not been tested and verified under field or near prototype conditions. It is recommended that the procedures outlined by Abt et al. (1997) be applied with a high degree of engineering judgement.

3 PROCEDURES

A procedure has been developed to estimate the effects of gullying over time. The following steps outline the estimation procedure.

Step 1. Determine the embankment design life as outlined in Appendix A. Stability of the embankment must be insured for periods ranging from 200 to 1,000 years.

Step 2. Select the embankment type (Type 1, Type 2, or Type 3) and determine values of the appropriate design variables.

Embankment/cover variables applicable to all three types of embankments include the embankment height (H_o) (m), slope length (L_o) (m), slope angle (θ) (degrees), and horizontal distance from the embankment toe to the crest (X_o) (m) as presented in Figure B-4.

Step 3. Determine the embankment/cover soil composition, expressed as a percentage of the sands, silts, and clays. Discriminating thresholds for gully intrusion potential for embankments are segmented into soils with clay content less than 15 percent, clay content between 15 and 50 percent, and clay content greater than 50 percent.

Step 4. Determine the average annual precipitation (P), expressed in meters, for the embankment site. Estimates of precipitation can be obtained from U.S. Weather Bureau isohyetal maps, local climatological data, or other appropriate means.

Figure B-6. Photograph of launching riprap flume test.

Step 5. Determine the drainage area tributary to the embankment to estimate the volume of runoff to which an embankment will be exposed in its design life. For embankments without external drainage basins, the tributary drainage area that forms on the face of the embankment will determine the total volume of runoff (Abt, Thornton, and Johnson, 1995b). The tributary drainage area that forms on the embankment face is a unique function of the type of embankment being evaluated.

Type 1 Embankment

The tributary drainage area for a Type 1 embankment may be estimated by

$$A = 0.276 * [L_o * \mathrm{Cos}(\theta)]^{1.636} \qquad \text{(B-1)}$$

where: A = tributary drainage area (m^2)
L_o = original embankment length (m)
θ = slope angle in degrees computed as $\mathrm{Tan}^{-1}(S_o)$

Type 2 Embankment

The tributary drainage area for a Type 2 embankment is computed by summing the embankment face length (L_o) and the embankment top length (L_2). The resulting length (L_t) is then entered in Equation B-1 as:

$$A = 0.276 * [L_t * \mathrm{Cos}(\theta)]^{1.636} \qquad \text{(B-2)}$$

where: A = tributary drainage area (m^2)
L_t = total length of embankment
θ = slope angle in degrees computed as $\mathrm{Tan}^{-1}(S_o)$

Type 3 Embankment

The tributary drainage area for a Type 3 embankment can be estimated using Equation B-1; however, an effective embankment length (L_3) must be determined. Flume and field observations indicate that a gully forming on a Type 3 embankment can extend past the crest and into the adverse slope. When this condition occurs, the effective length of the embankment is increased. To provide an estimate of the tributary drainage area at any point in time, the value of the effective embankment length is determined by estimating the final gully bottom slope. Abt et al. (1995b) reported that the gully bottom slope may be estimated as

$$S_b = [1.008 * S_o] - 0.063 \qquad \text{(B-3)}$$

where: S_b = gully bottom slope (rise/run)
S_o = original embankment slope (rise/run)

The effective embankment length can then be computed as:

$$L_3 = 1.175 * L_o \quad \text{(B-4)}$$

where L_o and L_3 are expressed in meters. The tributary drainage area can then be computed using Equation B-1 where L_3 is substituted for L_o.

In situations where the embankment toe is exposed to runoff that develops on a tributary drainage area external to the embankment, the supplemental area (A_x) is added to the drainage area value computed using Equation B-1.

Step 6. The total depth of precipitation to which the site may be exposed to over the design life needs to be determined. In Step 1, the design life of the embankment was estimated. The average annual precipitation for the project site was then estimated based on Step 4. The expected depth of precipitation, in meters, is then calculated as:

$$D_t = \text{Average Precipitation Depth (m)} * \text{Design Life (years)} \quad \text{(B-5)}$$

Step 7. The runoff to rainfall ratio, R_r, is needed to convert the potential depth of precipitation for the embankment design life to potential runoff tributary to the developing gully. The U.S. Geological Survey (USGS) developed a runoff map method (Gebert et al., 1989) to determine the average annual runoff expected from any location in the United States. The USGS map provides the user the annual depth of runoff from a site specific location. The ratio of the runoff to rainfall is computed by dividing the runoff depth derived from Gebert et al. by the average annual precipitation for the appropriate locale. The average runoff-ratio using the USGS Average Annual Runoff Method is 0.127. The runoff-rainfall ratio of 0.127 provides a reasonable estimate for the arid and semi-arid regions of the western United States.

Step 8. The cumulative volume of runoff (V_r) tributary to the embankment toe, in cubic meters, is calculated as:

$$V_r = D_t * R_r * A \quad \text{(B-6)}$$

where A is the tributary drainage area, expressed in square meters, as determined in Step 5. It is acknowledged that a single storm event will significantly impact the development of the gully. Abt et al. (1995a) indicates that the total volume of runoff can serve as a predictor of the ultimate dimensions (i.e., maximum depth, width, etc.)

of the gully. The volume of runoff tributary to the gully for the embankment design life is the primary element reflecting the analysis period.

Step 9. The maximum depth of gully incision (D_{max}) can be estimated as a function of the cumulative volume of runoff, V_r, the embankment height, H_o, the embankment slope length, L_0, L_2, or L_3, the embankment slope, and the clay content of the soil composition. A gully factor, G_f, was developed from the analysis described by Abt et al. (1994) for varying clay content of the proposed construction material. The gully factor is defined as:

$$G_f = \frac{D_{max}}{L_i * S_o} \tag{B-7}$$

where L_i is L_0, L_2, or L_3 as applicable and the embankment slope S_o, is H_0/X_o. The gully factor is computed as:

Clay content < 15%:

$$G_f = \frac{D_{max}}{L_o * S} = \frac{1}{2.25 + \left(0.789 * \frac{V_r}{H_o^3}\right)^{-0.55}} \tag{B-8}$$

Clay content > 15%, < 50%:

$$G_f = \frac{D_{max}}{L_o * S} = \frac{1}{2.80 + \left(0.197 * \frac{V_r}{H_o^3}\right)^{-0.70}} \tag{B-9}$$

Clay content > 50%:

$$G_f = \frac{D_{max}}{L_o * S} = \frac{1}{3.55 + \left(0.76 * \frac{V_r}{H_o^3}\right)^{-0.85}} \tag{B-10}$$

Step 10. The maximum depth of gully incision expected on the embankment slope may then be estimated as:

$$D_{max} = G_f * L_i * S \tag{B-11}$$

where D_{max} is in meters.

Step 11. After the value of D_{max} is determined, the top width of the gully at the deepest incision can be calculated as:

$$W = \left(\frac{D_{max}}{0.61}\right)^{1.149} \tag{B-12}$$

where: W = top width of gully (m)
D_{max} = depth of deepest gully incision (m)

Step 12. In some applications, it is important to estimate the location of the maximum gully incision to evaluate the stability of the embankment or the potential to penetrate into the waste storage area. The location of the maximum depth of incision, measured down slope from the crest, may be determined as:

$$D_\ell = 0.713 * \left(\frac{(V_r * S)}{L_i^3}\right)^{-0.415} \tag{B-13}$$

where: D_l = location of D_{max}
V_r = cumulative volume of runoff (m^3)
S_o = original embankment slope (rise/run)
L_o = original embankment length (m)

Step 13. To provide a conservative estimate of the possible damage caused to an earthen embankment by a migrating gully, it is assumed that the maximum depth of gully intrusion occurs at the crest of the embankment. The embankment material is then assumed to erode, at the angle of repose of the embankment material, up slope of D_{max}. The set back distance of the waste material is determined for each of the three types of embankments by assuming the embankment erodes at the angle of repose.

Step 14. If altering the set back distance is not feasible, protection may be examined utilizing launching riprap. A detailed explanation of the launching riprap application is

presented by Abt et al. (1997). The following preliminary guidelines should be followed in a launching riprap application:

- The minimum riprap size should be determined using accepted riprap sizing criteria for overtopping flow. A minimum median stone size (D_{50}) of 9 cm was found to work well in flume studies.

- The protective riprap layer should have adequate volume to provide slope coverage under maximum expected gully conditions. A layer thickness of approximately 3 D_{50} is recommended, depending on the volume requirements and the length of the riprap layer.

4 RECOMMENDATIONS

The stable slope should be determined using the procedures presented in Appendix A. Appropriately conservative values of input parameters should be used in the computation. Additional refinements can be made after the analysis of the sacrificial slope requirements.

In analyzing Type 2 Embankments, the top slope of the cover should be much flatter (less than or equal to 5%) than the slope of the embankment face. The gully would likely occur far upstream from the crest if the top slope were steep. The following example is presented to outline the stability assessment procedure, not to promote or compare any embankment types.

5 EXAMPLE OF PROCEDURE APPLICATION

The following example is used to outline the procedure of stability analysis of a Type 2 Embankment. Type 2 Embankments, presented in Figure B-4, are identified by an embankment slope that transitions into a flatter top slope. Embankments constructed with Type 2 geometry are evaluated by superimposing the total length of the embankment, L_t, on the slope of the embankment face.

Step 1. Design Life

An embankment design life of 200 years will be evaluated.

Step 2. Embankment Geometry

Once the embankment type is determined, the initial design variables are required. It will be assumed that the embankment has the following physical dimensions:

H_o = embankment height	= 9 meters
L_o = embankment slope length	= 55 meters
S_o = embankment slope	= 0.15 rise/run
L_2 = top embankment length	= 100 meters
S_2 = top embankment slope	= 0.05 rise/run

Step 3. Soil Composition

It is assumed that a soil analysis has been conducted and that the embankment material is composed of 13 percent clay by volume, and has an angle of repose of 34 degrees.

Step 4. Precipitation

Local climatological data indicate an average annual precipitation of 0.20 meters for the site.

Step 5. Potential Tributary Drainage Area

The total potential tributary drainage area for a Type 2 Embankment is determined by computing the total embankment length as shown below

$$L_t = L_o + L_2 \qquad \text{(B-14)}$$

where: L_t = total embankment length (m)
L_o = length of embankment face (m)
L_2 = length of embankment top slope (m)

The value determined for the total embankment length is then combined with the slope of the embankment face and entered into Equation B-2 as shown below

$$A = 0.276 * \{155 \text{ meters} * \cos(8.53)\}^{1.636}$$
$$A = 1038 \text{ meters}^2 \qquad \text{(B-15)}$$

Therefore, the total potential tributary drainage area for the Type 2 Embankment is 1038 square meters. It is assumed that there is no additional drainage area external to the embankment.

Step 6. Potential Depth of Precipitation

The first step in computing the total runoff volume for the site is to determine the potential depth of precipitation, D_t, that the site will be exposed to during the design life. As described in Step 6, the total depth of precipitation is the product of the average annual precipitation and the design life. Therefore,

$$D_t = 0.20 \text{ meters/year} * 200 \text{ years}$$

$$D_t = 40.0 \text{ meters of precipitation} \qquad \text{(B-16)}$$

and a potential depth of precipitation of 40.0 meters is computed.

Step 7. Runoff to Rainfall Ratio

A value of 0.13 is assumed as the average runoff to rainfall ratio, R_r, for the embankment area.

Step 8. The cumulative volume of runoff, V_r, is defined as the product of the potential depth of precipitation, D_t, the runoff to rainfall ratio, R_r, and the potential tributary area, A. Substituting the values of D_t, R_r and A_t obtained above into Equation B-6 yields

$$V_r = 40.0 \text{ meters} * 0.13 * 1038 \text{ meters}^2$$

$$V_r = 5{,}400 \text{ meters}^3 \qquad \text{(B-17)}$$

Therefore, the embankment slope will drain approximately 5,400 cubic meters of runoff during the 200 year design life.

Step 9. Determination of Gully Factor

The gully factor, G_f, for the embankment should be determined as outlined in Step 9. A clay content of 13 percent in the embankment material requires that Equation B-8 be used to calculate the gully factor. Substituting values for H_o and V_r into Equation B-8 gives

$$G_f = \frac{1}{2.25 + \left[0.789 * \left\{\frac{5{,}399.97 \text{ meters}^3}{(9.0 \text{ meters})^3}\right\}\right]^{-0.55}} \qquad \text{(B-18)}$$

$$G_f = 0.380$$

Step 10. Maximum Depth of Gully Incision

A gully factor of 0.380 is entered into Equation B-8 to determine the maximum depth of gully incision as follows

$$D_{max} = 0.380 * 55.0\text{meters} * 0.15$$
$$D_{max} = 3.14 \text{ meters} \qquad \text{(B-19)}$$

Thus, after a 200 year period, a gully incision 3.14 meters deep would be expected on the face of the embankment.

Step 11. Gully Top Width

Equation B-12 presents an empirical relationship that can be used to predict gully top width, W, as a function of maximum gully incision, D_{max}. Substituting the value of 3.14 meters computed for D_{max} into Equation B-12 gives

$$W = \left(\frac{3.14 \text{ meters}}{0.61}\right)^{1.149}$$
$$W = 6.57 \text{ meters} \qquad \text{(B-20)}$$

therefore, 6.33 meters would be the estimated gully width at the point of deepest gully incision.

Step 12. Location of Maximum Depth

Equation B-13 presents an empirical relation predicting the location of D_{max} as a function of the total volume of runoff, embankment length, and embankment slope. Substituting the values determined above into Equation B-13 gives

$$D_l = 0.713 * \left\{\frac{(5{,}399.97 \text{ meters}^3 * 0.15)}{(55 \text{ meters})^3}\right\}^{-0.415}$$
$$D_l = 6.50 \qquad \text{(B-21)}$$

which represents the number of D_{max}'s down slope from the crest the deepest incision is expected to occur. To determine the location in meters, multiply the value determined for D_l by that determined for D_{max}. For this example the deepest incision point will occur approximately 20.4 meters down slope from the embankment crest.

Summarizing the results obtained above yields

D_{max} = 3.14 meters,

W = 6.57 meters

D_1 = 20.4 meters

However, for long-term stability applications, the location of D_{max} should be assumed to be at the crest of the slope.

Step 13. Set Back Distance

For conservatism, the maximum depth of incision is assumed to occur at the crest of the embankment and the material is assumed to erode at the angle of repose (34^0 for this example) upstream of the crest. For the conditions of this example, the set back distance would be 4.66 meters up slope from the crest of the embankment. Therefore, tailings should be located a minimum horizontal distance of 4.66 meters up slope and a vertical distance of 4.71 meters down from the embankment crest.

Step 14. Rock Launching Application

If providing adequate setback distance is not feasible, embankment stabilization with launching rock may be considered. For details and a preliminary application procedure, see Abt et al. (1997). The findings discussed by Abt et al. (1997) should be adapted to each specific site with engineering judgement. In general, a volume of rock should be provided to cover the collapsed slope with a rock layer of 1.5 times the D_{50} size, considering the depth of gully intrusion and the length. It is recommended that the required D_{50} size be specifically determined for a collapsed slope of 1V to 2H. Figure B-7 presents a schematic of the rock launching application concept.

The results of the example outlined above can then be checked with the original design of the soil cover, as described in Appendix A. Engineering judgment then determines if the design is adequate to provide the level of protection necessary throughout the design life.

6 COMPUTER APPLICATION

To aid in the analysis of the stability assessment, a computer program has been developed. The Windows™ application provides an automated method of evaluating the stability procedure described above (Thornton, 1996). The program is available from the U.S. Nuclear Regulatory

in column 6 is given from the sediment rating curve, or Equation 6. For each interval, the water yield in column 5 is calculated from multiplying columns 2 and 6. Likewise, the annual sediment yield in column 7 is calculated from Equation E-5 given Δp, Q and C_s from columns 2, 4 and 6. The interannual total sediment yield is finally obtained from the sum of column 7.

2.5 Trap Efficiency

When sediment-laden water enters reservoirs, lakes, impoundments, and settling basins, the settling of sediment will cause aggradation of the bed. The trap efficiency is used to determine how much sediment is expected to settle in backwater areas. The trap efficiency is defined as the percentage of incoming sediment for a given size fraction (i) that will settle within a given reach. The trap efficiency can be calculated as follows:

$$T_{Ei} = 1 - e^{\frac{-Xw_i}{hV}} \qquad \text{(E-7)}$$

where X is the reach length; w_i is the settling velocity for sediment fraction i from Table E-4; h is the mean flow depth; and V is the mean flow velocity. The exponent is dimensionless and any consistent system of units can be used in this equation.

The sediment load that settles within the reach is given by the product of the incoming sediment load and the trap efficiency. The outgoing sediment load is calculated by subtracting the settling load from the incoming load. The trap efficiency varies with sediment size through the settling velocity. Typically, the trap efficiency is approximately one for coarse sediment, e.g., gravels, and approaches zero for fine sediment, e.g., clays.

2.6 Sediment Transport Capacity of a Channel

Simons, Li, and Fullerton (1981) developed an efficient method of evaluating sediment discharge. The method is based on easy-to-apply power relationships that estimate sediment transport based on the flow depth h and velocity V. These power relationships were developed from a computer solution of the Meyer-Peter and Müller bedload transport equation and Einstein's integration of the suspended bed sediment discharge:

$$q_s = c_{s1} h^{c_{s2}} V^{c_{s3}} \qquad \text{(E-8)}$$

The results of the total bed sediment discharge are presented in Table E-2. The large values of c_{s3} ($3.3 < c_{s3} < 3.9$) show the high level of dependence of sediment transport rates on velocity. Depth has comparatively less influence ($-0.34 < c_{s2} < 0.7$).

Table E-2. Power equations for total bed sediment discharge in sand- and fine-gravel-bed streams.

	$q_s = c_{S1} h^{c_{S2}} V^{c_{S3}}$							
	D_{50} (mm)							
	0.1	**0.25**	**0.5**	**1.0**	**2.0**	**3.0**	**4.0**	**5.0**
Gr = 1.0								
c_{S1}	3.30×10^{-5}	1.42×10^{-5}	7.6×10^{-6}	5.62×10^{-6}	5.64×10^{-6}	6.32×10^{-6}	7.10×10^{-6}	7.78×10^{-6}
c_{S2}	0.715	0.495	0.28	0.06	-0.14	-0.24	-0.30	-0.34
c_{S3}	3.30	3.61	3.82	3.93	3.95	3.92	3.89	3/87
Gr = 2.0								
c_{S1}		1.59×10^{-5}	9.8×10^{-6}	6.94×10^{-6}	6.32×10^{-6}	6.62×10^{-6}	6.94×10^{-6}	
c_{S2}		0.51	0.33	0.12	-0.09	-0.196	-0.27	
c_{S3}		3.55	3.73	3.86	3.91	3.91	3.90	
Gr = 3.0								
c_{S1}			1.21×10^{-5}	9.14×10^{-6}	7.44×10^{-6}			
c_{S2}			0.36	0.18	-0.02			
c_{S3}			3.66	3.76	3.86			
Gr = 4.0								
c_{S1}				1.05×10^{-5}				
c_{S2}				0.21				
c_{S3}				3.71				

Definitions: q_s, unit sediment transport rate in ft^2/s (unbulked); V, velocity in ft/s; h, depth in ft; $G_r = 0.5\ [(D_{84}/D_{50}) + (D_{50}/D_{16})]$ gradation coefficient.

For flow conditions within the range outlined in Table E-3, the regression equations should be accurate within 10%. The equations were obtained for steep sand- and gravel-bed channels under supercritical flow. They do not apply to cohesive material.

The equations assume that all sediment sizes are transported by the flow without armoring. The sediment concentration $c_{mg/l}$ is calculated from

$$c_{mg/l} = 2.65 \times 10^6 \frac{q_s}{q} \qquad \text{(E-9)}$$

where q_s is calculated from Equation E-8 and $q = V_h$ is the unit discharge in ft^2/s.

3 DESIGN AND ANALYSIS PROCEDURES

The following procedures may be used to determine: 1) sheet and rill erosion; 2) gully erosion; 3) calculated sediment yield; 4) measured sediment yield; 5) trap efficiency, and 6) sediment transport capacity of channels.

3.1 Sheet and Rill Erosion Procedure

The following sheet and rill erosion procedure based on the USLE may be used to determine soil erosion losses from upland erosion. If data are available, this approach should be supplemented with field measurements to properly calibrate and ascertain the accuracy of other procedures and/or computer models.

Step A-1. Gather topographic, soil type and land use information. Subdivide the domain into sub-watersheds. For each sub-watershed, determine: drainage area, runoff length, average slope, soil type, percentage of canopy cover and ground cover and any particular method of soil conservation practice.

Step A-2. Determine the mean annual rainfall erodibility factor R for the specific site location.

Step A-3. Determine, for each sub-watershed, the soil erodibility factor K from soil samples.

Step A-4. Determine the slope length-steepness factor LS from the runoff length and average slope.

Step A-5. Determine the cropping-management factor C from the ground and canopy cover data.

Table E-3. Range of parameters for the Simons-Li-Fullerton method.

Parameter	Value range
Froude number	1 - 4
Velocity	6.5 - 26 ft/s
Manning coefficient n	0.015 - 0.025
Bed slope	0.005 - 0.040
Unit discharge	10 - 200 ft/s
Particle size	$D_{50} \geq 0.062$ mm
	$D_{50} \leq 15$ mm

Appendix B

Soil Properties from

Web Soil Survey

Report — RUSLE2 Related Attributes

Grand County, Utah - Central Part

Map symbol and soil name	Pct. of map unit	Hydrologic group	Kf	T factor	Representative value		
					% Sand	% Silt	% Clay
11—Chipeta complex							
Chipeta	40	D	.37	2	20.0	49.0	31.0
Chipeta	30	D	.37	2	20.0	49.0	31.0
18—Hanksville family-Badland complex							
Hanksville family	40	C	.43	3	26.5	53.5	20.0
Badland	35	—	—	—	—	—	—
31—Mesa-Chipeta-Thedalund family complex							
Chipeta	25	D	.37	2	20.0	49.0	31.0
Mesa	25	B	.28	3	66.5	20.0	13.5
Thedalund family	20	C	.37	3	42.1	37.9	20.0

Thedalund family	20	C	.37	3	42.1	37.9	20.0
52—Rizno-Rock outcrop complex							
Rizno	50	D	.28	1	63.1	26.4	10.5
Rock outcrop	25	—	—	—	—	—	—
75—Toddler-Ravola-Glenton families association							
Ravola family	25	B	.43	5	11.6	68.9	19.5
Toddler family	25	B	.43	5	24.8	52.7	22.5
Glenton family	20	B	.28	5	62.5	26.0	11.5

Description — RUSLE2 Related Attributes

RUSLE2 Related Attributes

This report summarizes those soil attributes used by the Revised Universal Soil Loss Equation Version 2 (RUSLE2) for the map units in the selected area. The report includes the map unit symbol, the component name, and the percent of the component in the map unit. Soil property data for each map unit component include the hydrologic soil group, erosion factors Kf for the surface horizon, erosion factor T, and the representative percentage of sand, silt, and clay in the surface horizon.

Ratings – 1 to 40 inches

Summary by Map Unit — Grand County, Utah - Central Part

Map unit symbol	Map unit name	Rating (percent)	Acres in AOI	Percent of AOI
11	Chipeta complex	31.0	9.9	0.8%
18	Hanksville family-Badland complex	41.1	224.6	19.1%
31	Mesa-Chipeta-Thedalund family complex	40.9	24.3	2.1%
52	Rizno-Rock outcrop complex	11.4	12.0	1.0%
75	Toddler-Ravola-Glenton families association	25.2	902.4	76.9%
Totals for Area of Interest (AOI)			**1,173.3**	**100.0%**

Description — Percent Clay

Clay as a soil separate consists of mineral soil particles that are less than 0.002 millimeter in diameter. The estimated clay content of each soil layer is given as a percentage, by weight, of the soil material that is less than 2 millimeters in diameter. The amount and kind of clay affect the fertility and physical condition of the soil and the ability of the soil to adsorb cations and to retain moisture. They influence shrink-swell potential, saturated hydraulic conductivity (Ksat), plasticity, the ease of soil dispersion, and other soil properties. The amount and kind of clay in a soil also affect tillage and earth-moving operations.

Most of the material is in one of three groups of clay minerals or a mixture of these clay minerals. The groups are kaolinite, smectite, and hydrous mica, the best known member of which is illite.

For each soil layer, this attribute is actually recorded as three separate values in the database. A low value and a high value indicate the range of this attribute for the soil component. A "representative" value indicates the expected value of this attribute for the component. For this soil property, only the representative value is used.

Summary by Map Unit — Grand County, Utah - Central Part

Map unit symbol	Map unit name	Rating (percent)	Acres in AOI	Percent of AOI
11	Chipeta complex	20.0	9.9	0.8%
18	Hanksville family-Badland complex	8.5	224.6	19.1%
31	Mesa-Chipeta-Thedalund family complex	48.3	24.3	2.1%
52	Rizno-Rock outcrop complex	62.6	12.0	1.0%
75	Toddler-Ravola-Glenton families association	47.6	902.4	76.9%
Totals for Area of Interest (AOI)			**1,173.3**	**100.0%**

Description — Percent Sand

Sand as a soil separate consists of mineral soil particles that are 0.05 millimeter to 2 millimeters in diameter. In the database, the estimated sand content of each soil layer is given as a percentage, by weight, of the soil material that is less than 2 millimeters in diameter. The content of sand, silt, and clay affects the physical behavior of a soil. Particle size is important for engineering and agronomic interpretations, for determination of soil hydrologic qualities, and for soil classification.

For each soil layer, this attribute is actually recorded as three separate values in the database. A low value and a high value indicate the range of this attribute for the soil component. A "representative" value indicates the expected value of this attribute for the component. For this soil property, only the representative value is used.

Summary by Map Unit — Grand County, Utah - Central Part

Map unit symbol	Map unit name	Rating (percent)	Acres in AOI	Percent of AOI
11	Chipeta complex	20.0	9.9	0.8%
18	Hanksville family-Badland complex	8.5	224.6	19.1%
31	Mesa-Chipeta-Thedalund family complex	48.3	24.3	2.1%
52	Rizno-Rock outcrop complex	62.6	12.0	1.0%
75	Toddler-Ravola-Glenton families association	47.6	902.4	76.9%
Totals for Area of Interest (AOI)			**1,173.3**	**100.0%**

Description — Percent Sand

Sand as a soil separate consists of mineral soil particles that are 0.05 millimeter to 2 millimeters in diameter. In the database, the estimated sand content of each soil layer is given as a percentage, by weight, of the soil material that is less than 2 millimeters in diameter. The content of sand, silt, and clay affects the physical behavior of a soil. Particle size is important for engineering and agronomic interpretations, for determination of soil hydrologic qualities, and for soil classification.

For each soil layer, this attribute is actually recorded as three separate values in the database. A low value and a high value indicate the range of this attribute for the soil component. A "representative" value indicates the expected value of this attribute for the component. For this soil property, only the representative value is used.

Summary by Map Unit — Grand County, Utah - Central Part

Map unit symbol	Map unit name	Rating (percent)	Acres in AOI	Percent of AOI
11	Chipeta complex	15.0	9.9	0.8%
18	Hanksville family-Badland complex	16.8	224.6	19.1%
31	Mesa-Chipeta-Thedalund family complex	18.5	24.3	2.1%
52	Rizno-Rock outcrop complex	5.0	12.0	1.0%
75	Toddler-Ravola-Glenton families association	11.3	902.4	76.9%
Totals for Area of Interest (AOI)			**1,173.3**	**100.0%**

Description — Plasticity Index

Plasticity index (PI) is one of the standard Atterberg limits used to indicate the plasticity characteristics of a soil. It is defined as the numerical difference between the liquid limit and plastic limit of the soil. It is the range of water content in which a soil exhibits the characteristics of a plastic solid.

The plastic limit is the water content that corresponds to an arbitrary limit between the plastic and semisolid states of a soil. The liquid limit is the water content, on a percent by weight basis, of the soil (passing #40 sieve) at which the soil changes from a plastic to a liquid state.

Soils that have a high plasticity index have a wide range of moisture content in which the soil performs as a plastic material. Highly and moderately plastic clays have large PI values. Plasticity index is used in classifying soils in the Unified and AASHTO classification systems.

For each soil layer, this attribute is actually recorded as three separate values in the database. A low value and a high value indicate the range of this attribute for the soil component. A "representative" value indicates the expected value of this attribute for the component. For this soil property, only the representative value is used.

Summary by Map Unit — Grand County, Utah - Central Part

Map unit symbol	Map unit name	Rating (percent)	Acres in AOI	Percent of AOI
11	Chipeta complex	49.0	9.9	0.8%
18	Hanksville family-Badland complex	50.4	224.6	19.1%
31	Mesa-Chipeta-Thedalund family complex	48.2	24.3	2.1%
52	Rizno-Rock outcrop complex	26.0	12.0	1.0%
75	Toddler-Ravola-Glenton families association	64.0	902.4	76.9%
Totals for Area of Interest (AOI)			**1,173.3**	**100.0%**

Description — Percent Silt

Silt as a soil separate consists of mineral soil particles that are 0.002 to 0.05 millimeter in diameter. In the database, the estimated silt content of each soil layer is given as a percentage, by weight, of the soil material that is less than 2 millimeters in diameter.

The content of sand, silt, and clay affects the physical behavior of a soil. Particle size is important for engineering and agronomic interpretations, for determination of soil hydrologic qualities, and for soil classification

For each soil layer, this attribute is actually recorded as three separate values in the database. A low value and a high value indicate the range of this attribute for the soil component. A "representative" value indicates the expected value of this attribute for the component. For this soil property, only the representative value is used.

Summary by Map Unit — Grand County, Utah - Central Part

Map unit symbol	Map unit name	Rating (percent)	Acres in AOI	Percent of AOI
11	Chipeta complex	0.32	9.9	0.8%
18	Hanksville family-Badland complex	0.25	224.6	19.1%
31	Mesa-Chipeta-Thedalund family complex	0.32	24.3	2.1%
52	Rizno-Rock outcrop complex	0.75	12.0	1.0%
75	Toddler-Ravola-Glenton families association	1.20	902.4	76.9%
Totals for Area of Interest (AOI)			**1,173.3**	**100.0%**

Description — Organic Matter

Organic matter is the plant and animal residue in the soil at various stages of decomposition. The estimated content of organic matter is expressed as a percentage, by weight, of the soil material that is less than 2 millimeters in diameter.

The content of organic matter in a soil can be maintained by returning crop residue to the soil. Organic matter has a positive effect on available water capacity, water infiltration, soil organism activity, and tilth. It is a source of nitrogen and other nutrients for crops and soil organisms. An irregular distribution of organic carbon with depth may indicate different episodes of soil deposition or soil formation. Soils that are very high in organic matter have poor engineering properties and subside upon drying.

For each soil layer, this attribute is actually recorded as three separate values in the database. A low value and a high value indicate the range of this attribute for the soil component. A "representative" value indicates the expected value of this attribute for the component. For this soil property, only the representative value is used.

Tables — Hydrologic Soil Group — Summary By Map Unit

Summary by Map Unit — Grand County, Utah - Central Part

Map unit symbol	Map unit name	Rating	Acres in AOI	Percent of AOI
11	Chipeta complex	D	5.5	0.6%
18	Hanksville family-Badland complex	C	142.0	14.5%
31	Mesa-Chipeta-Thedalund family complex	B	26.3	2.7%
75	Toddler-Ravola-Glenton families association	B	803.6	82.2%
Totals for Area of Interest (AOI)			**977.4**	**100.0%**

Grand County, Utah - Central Part

75—Toddler-Ravola-Glenton families association

Map Unit Setting

Elevation: 4,000 to 5,000 feet

Mean annual precipitation: 5 to 8 inches

Mean annual air temperature: 52 to 55 degrees F

Frost-free period: 150 to 180 days

Map Unit Composition

Ravola family and similar soils: 25 percent

Toddler family and similar soils: 25 percent

Glenton family and similar soils: 20 percent

Description of Toddler Family

Setting

Landform: Flood plains, drainageways

Landform position (three-dimensional): Talf

Down-slope shape: Linear

Across-slope shape: Concave

Parent material: Alluvium derived from sandstone and shale

Properties and qualities

Slope: 0 to 3 percent

Depth to restrictive feature: More than 80 inches

Drainage class: Well drained

Capacity of the most limiting layer to transmit water (Ksat): Moderately high (0.20 to 0.60 in/hr)

Depth to water table: More than 80 inches

Frequency of flooding: Rare

Frequency of ponding: None

Calcium carbonate, maximum content: 15 percent

Gypsum, maximum content: 3 percent

Maximum salinity: Nonsaline to slightly saline (2.0 to 8.0 mmhos/cm)

Sodium adsorption ratio, maximum: 10.0

Available water capacity: Moderate (about 8.5 inches)

Grand County, Utah - Central Part

75—Toddler-Ravola-Glenton families association

Map Unit Setting

Elevation: 4,000 to 5,000 feet

Mean annual precipitation: 5 to 8 inches

Mean annual air temperature: 52 to 55 degrees F

Frost-free period: 150 to 180 days

Map Unit Composition

Ravola family and similar soils: 25 percent

Toddler family and similar soils: 25 percent

Glenton family and similar soils: 20 percent

Description of Toddler Family

Setting

Landform: Flood plains, drainageways

Landform position (three-dimensional): Talf

Down-slope shape: Linear

Across-slope shape: Concave

Parent material: Alluvium derived from sandstone and shale

Properties and qualities

Slope: 0 to 3 percent

Depth to restrictive feature: More than 80 inches

Drainage class: Well drained

Capacity of the most limiting layer to transmit water (Ksat): Moderately high (0.20 to 0.60 in/hr)

Depth to water table: More than 80 inches

Frequency of flooding: Rare

Frequency of ponding: None

Calcium carbonate, maximum content: 15 percent

Gypsum, maximum content: 3 percent

Maximum salinity: Nonsaline to slightly saline (2.0 to 8.0 mmhos/cm)

Sodium adsorption ratio, maximum: 10.0

Available water capacity: Moderate (about 8.5 inches)

Interpretive groups

Land capability (nonirrigated): 6e

Ecological site: Alkali Fan (Castlevalley Saltbush) (R034XY003UT)

Typical profile

0 to 7 inches: Silt loam

7 to 12 inches: Silt loam

12 to 36 inches: Sandy clay loam

36 to 60 inches: Fine sandy loam

Description of Ravola Family

Setting

Landform: Flood plains

Landform position (three-dimensional): Talf

Down-slope shape: Linear

Across-slope shape: Concave

Parent material: Alluvium derived from sandstone and shale

Properties and qualities

Slope: 0 to 3 percent

Depth to restrictive feature: More than 80 inches

Drainage class: Well drained

Capacity of the most limiting layer to transmit water (Ksat): Moderately high (0.20 to 0.60 in/hr)

Depth to water table: More than 80 inches

Frequency of flooding: Occasional

Frequency of ponding: None

Calcium carbonate, maximum content: 40 percent

Gypsum, maximum content: 4 percent

Maximum salinity: Very slightly saline to moderately saline (4.0 to 16.0 mmhos/cm)

Sodium adsorption ratio, maximum: 10.0

Available water capacity: Moderate (about 8.5 inches)

Interpretive groups

Land capability (nonirrigated): 7s

Ecological site: Alkali Flat (Black Greasewood) (R034XY006UT)

Other vegetative classification: Alkali Flat (Black Greasewood) (034XY006UT_1)

Typical profile

0 to 3 inches: Silt loam

3 to 7 inches: Silt loam

7 to 10 inches: Fine sandy loam

10 to 29 inches: Silt loam

29 to 60 inches: Silt loam

Description of Glenton Family

Setting

Landform: Drainageways, flood plains

Landform position (three-dimensional): Talf

Down-slope shape: Linear

Across-slope shape: Concave

Parent material: Alluvium derived from sandstone and shale

Interpretive groups

Land capability (nonirrigated): 6e

Ecological site: Alkali Fan (Castlevalley Saltbush) (R034XY003UT)

Typical profile

0 to 7 inches: Silt loam

7 to 12 inches: Silt loam

12 to 36 inches: Sandy clay loam

36 to 60 inches: Fine sandy loam

Description of Ravola Family

Setting

Landform: Flood plains

Landform position (three-dimensional): Talf

Down-slope shape: Linear

Across-slope shape: Concave

Parent material: Alluvium derived from sandstone and shale

Properties and qualities

Slope: 0 to 3 percent

Depth to restrictive feature: More than 80 inches

Drainage class: Well drained

Capacity of the most limiting layer to transmit water (Ksat): Moderately high (0.20 to 0.60 in/hr)

Depth to water table: More than 80 inches

Frequency of flooding: Occasional

Frequency of ponding: None

Calcium carbonate, maximum content: 40 percent

Gypsum, maximum content: 4 percent

Maximum salinity: Very slightly saline to moderately saline (4.0 to 16.0 mmhos/cm)

Sodium adsorption ratio, maximum: 10.0

Available water capacity: Moderate (about 8.5 inches)

Interpretive groups

Land capability (nonirrigated): 7s

Ecological site: Alkali Flat (Black Greasewood) (R034XY006UT)

Other vegetative classification: Alkali Flat (Black Greasewood) (034XY006UT_1)

Typical profile

0 to 3 inches: Silt loam

3 to 7 inches: Silt loam

7 to 10 inches: Fine sandy loam

10 to 29 inches: Silt loam

29 to 60 inches: Silt loam

Description of Glenton Family

Setting

Landform: Drainageways, flood plains

Landform position (three-dimensional): Talf

Down-slope shape: Linear

Across-slope shape: Concave

Parent material: Alluvium derived from sandstone and shale

Properties and qualities

Slope: 0 to 3 percent

Depth to restrictive feature: More than 80 inches

Drainage class: Well drained

Capacity of the most limiting layer to transmit water (Ksat): Moderately high (0.20 to 0.60 in/hr)

Depth to water table: More than 80 inches

Frequency of flooding: Rare

Frequency of ponding: None

Calcium carbonate, maximum content: 40 percent

Gypsum, maximum content: 3 percent

Maximum salinity: Nonsaline to slightly saline (0.0 to 8.0 mmhos/cm)

Sodium adsorption ratio, maximum: 10.0

Available water capacity: Moderate (about 7.2 inches)

18—Hanksville family-Badland complex

Map Unit Setting

- Elevation: 4,200 to 6,100 feet
- Mean annual precipitation: 6 to 8 inches
- Mean annual air temperature: 46 to 54 degrees F

- Frost-free period: 120 to 170 days

Map Unit Composition

- Hanksville family and similar soils: 40 percent
- Badland: 35 percent

Description of Hanksville Family

Setting

- Landform: Cuestas, mesas
- Down-slope shape: Linear
- Across-slope shape: Convex
- Parent material: Colluvium derived from shale and/or residuum weathered from shale

Properties and qualities

- Slope: 30 to 50 percent
- Surface area covered with stones and boulders: 7.0 percent
- Depth to restrictive feature: 20 to 40 inches to paralithic bedrock
- Drainage class: Well drained
- Capacity of the most limiting layer to transmit water (Ksat): Very low to moderately low (0.00 to 0.06 in/hr)
- Depth to water table: More than 80 inches
- Frequency of flooding: None
- Frequency of ponding: None
- Calcium carbonate, maximum content: 15 percent
- Gypsum, maximum content: 10 percent
- Maximum salinity: Nonsaline (0.0 to 2.0 mmhos/cm)
- Sodium adsorption ratio, maximum: 4.0
- Available water capacity: Low (about 5.8 inches)

Interpretive groups

- Land capability (nonirrigated): 7s
- Ecological site: Desert Clay (Castlevalley Saltbush) (R034XY103UT)
- Other vegetative classification: Desert Clay (Castlevalley Saltbush) (034XY103UT_1)

Typical profile

- 0 to 3 inches: Extremely bouldery silt loam
- 3 to 14 inches: Silty clay loam
- 14 to 23 inches: Silty clay
- 23 to 35 inches: Silty clay
- 35 to 39 inches: Weathered bedrock

Description of Badland

Setting

- Landform: Cuestas, mesas
- Down-slope shape: Linear
- Across-slope shape: Convex

Map Unit Legend

Grand County, Utah - Central Part (UT624)

Map Unit Symbol	Map Unit Name	Acres in AOI	Percent of AOI
18	Hanksville family-Badland complex	89.5	45.7%
52	Rizno-Rock outcrop complex	0.0	0.0%
75	Toddler-Ravola-Glenton families association	106.4	54.3%
Totals for Area of Interest (AOI)		**195.9**	**100.0%**

Legend

Soil Map

Scale (not to scale)

Map Unit Legend

Grand County, Utah - Central Part (UT624)

Map Unit Symbol	Map Unit Name	Acres in AOI	Percent of AOI
11	Chipeta complex	9.9	0.8%
18	Hanksville family-Badland complex	224.6	19.1%
31	Mesa-Chipeta-Thedalund family complex	24.3	2.1%
52	Rizno-Rock outcrop complex	12.0	1.0%
75	Toddler-Ravola-Glenton families association	902.4	76.9%
Totals for Area of Interest (AOI)		**1,173.3**	**100.0%**

Legend

Soil Map

Scale (not to scale)

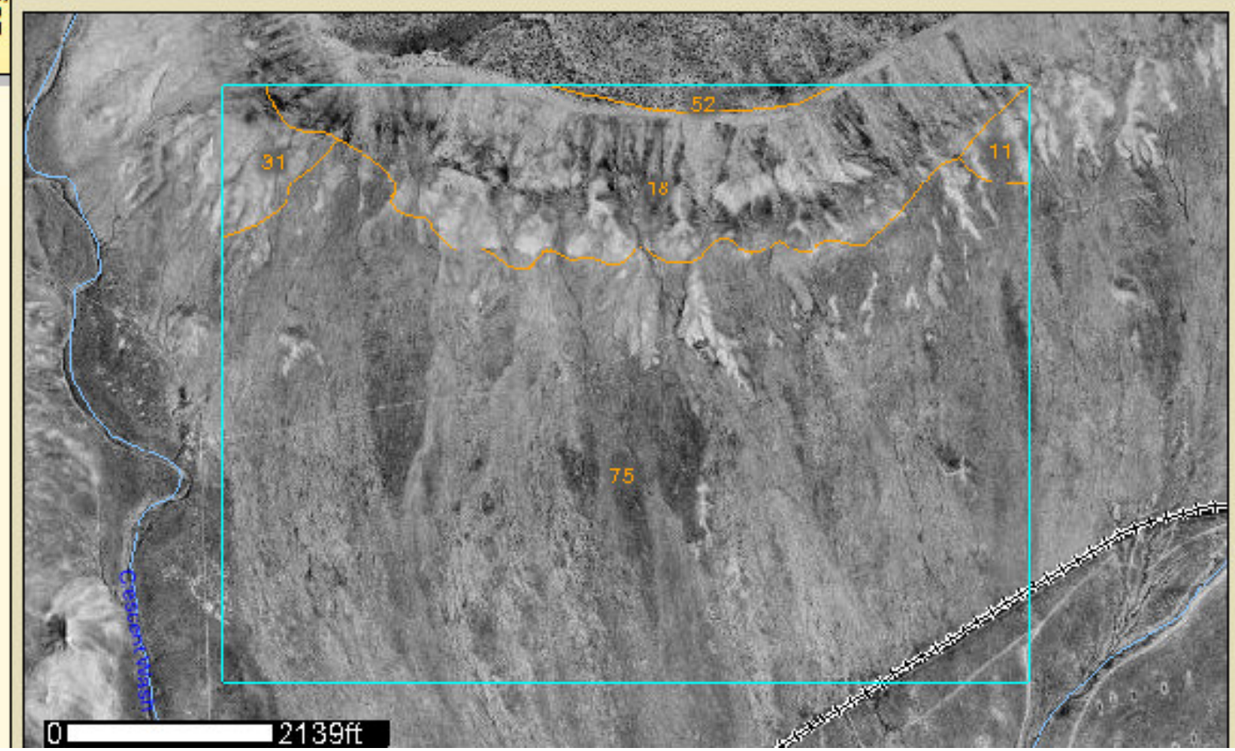

Appendix C

RUSLE2 Results

Worksheet: Crescent Junction Constant Slope

Tract # Book Cliffs
Owner name Bob
Field # West

Info: RUSLE2 simulation of constant slope in the area between the wedge and the Book cliffs.

Compare management alternatives for a single hillslope profile | Compare individual hillslope profiles | Compute avg. soil loss for a field/watershed

Location: Utah\Crescent Junction
Soil: CJ Glenton
Length along slope, ft: 2600
Avg. slope steepness, %: 3.5

Slope Topography

Segment	Steepness, %	Length along slope, ft
1	3.5	1000
2	3.5	800
3	3.5	800

Management alternative table

Temp. scenario	Base management	Residue burial level	General yield level	Contouring	Strips/barriers	Diversion/terrace, sediment ba	Surf. cov. values	Detachment on slope, t/ac/yr	Soil loss erod. portion, t/ac	Soil loss for cons. plan, t/ac/yr	Sediment delivery, t/ac/yr
Profile	...Bare ground, smooth surface	Normal	Normal	...ope	(none)	(none)	.... cover	2.6	2.6	2.6	2.6

Worksheet: Crescent Junction Compund Slope

Tract # Book Cliffs
Owner name Bob
Field # West

Info: RUSLE2 simulation of compound slope of area between the wedge and the Book cliffs.

Compare management alternatives for a single hillslope profile | Compare individual hillslope profiles | Compute avg. soil loss for a field/watershed

Location: Utah\Crescent Junction
Soil: CJ Glenton
Length along slope, ft: 2600
Avg. slope steepness, %: 16

Slope Topography

Segment	Steepness, %	Length along slope, ft
1	40	1000
2	3.5	800
3	2.5	800

Management alternative table

Temp. scenario	Base management	Residue burial level	General yield level	Contouring	Strips/barriers	Diversion/terrace, sediment ba	Surf. cov. values	Detachment on slope, t/ac/yr	Soil loss erod. portion, t/ac	Soil loss for cons. plan, t/ac/yr	Sediment delivery, t/ac/yr
Profile	...Bare ground, smooth surface	Normal	Normal	...ault	(none)	(none)	.... cover	27	28	13	9.1

Soil: CJ Glenton

Graphic
Rock cover, %: 0
Erodibility, US: 0.43
Calculate consol. from precip?: No
Nominal consolid. time, yr: 7.0
Texture: Loam
T value, t/ac/yr:
Hydrologic class: B - mod. low runoff
Hydrologic class with subsurface drai: B - mod. low runoff

Particle sizes | Nomograph Info | Volcanic Info | Detached particles | Info

Sand, %: 45
Silt, %: 30
Clay, %: 25

Climate: Utah\Crescent Junction

R Factor, US	20
10 year EI, US	10.0
Standard EI distribution	US_080
In Req area?	No
Use Req EI dist.?	
R Equiv, US	
EI dist. for Req condition	
Adjust for soil moisture?	
Annual precip, in.	9.9
Vary soil Erod. with climate?	Yes

Monthly | Daily | Info

Monthly Climate

Month	Avg. temp., deg C	Month precip., mm
Jan	-3.1	25
Feb	0.78	14
Mar	5.0	26
Apr	10.0	21
May	15	25
Jun	20	9.0
Jul	25	20
Aug	24	22
Sep	18	26
Oct	12	31
Nov	4.1	17
Dec	-0.31	16

JACOBS	Calculation No: C-04	Page 1 of 27 – Plus Appendices 31 Pgs
Calculation Cover Sheet	Rev. No.: 3	Revision Date: 07/09/08
(Ref. FOWI 116 Design Calculations)	Previous Revision Date: 02/06/08	Current Revision Date:07/09/08
Issuing Department: *Federal Operations Design Engineering*	Supersedes: Previous Revisions	
Client: Energy solutions Project Title: Moab UMTRA Project Number: 35DJ2600 System:	Engineering Discipline: Civil	

Calculation Title: Area between Cell and Wedge

Purpose:

Analyze the area between the wedge and the waste cell to determine.

1. Does the ditch between the south side of the wedge and the access road require erosion protection to prevent runoff from the south side slope of the wedge eroding the berm on which the access road is constructed?

2. The discharge rate of runoff from the north side of the cell and the area between the cell and the access road to determine the need for flow control at the northwest and northeast corners of the cell aprons. The size of rock required for erosion protection north of the berm that diverts this runoff to the spreaders.

3. The size of rock lining required to protect the ditches north of the access road (beyond the end of the road) carrying water to the outlet spreaders on the east and west.

4. The scour depth at the spreader outlets.

5. The size of rock armouring required for the spreaders.

6. The effect of erosion on the south side slope of the wedge on the integrity of the wedge including both sheet and rill erosion and gully formation.

NQA-1 Quality Level: 2

Prepared by: Bob Yager *Jeff Parker for Bob Yager* Date: 07/09/08

Checked by: Bill Barton *Bill Barton* Date: 07/10/08

Engineering Managers Approval: *Bill Barton* Date: 07/10/08

The current applicable version of this publication resides on Jacobs' Intranet. All copies are considered to be uncontrolled.
Copyright© Jacobs Engineering Group Inc., 2007

Revision History:

Pages Affected By Revision	Revised/Added/Deleted	Description of Revision
Revision 1 Modifications		
Page 3	Added	Inserted item 8 in bullet list under "Description of Calculation".
Page 8	Revised	Renumbered items in list under "Description of Calculation"
Page 8	Added	Inserted item 7 in bullet list under "Method of Solution".
Page 11	Added	Added Spreader_Rock_and_Scour.xls under "Calculation Section"
Page 20	Revised	Revised last sentence of first paragraph under "Rock in Channels and on North Side of Berms"
Page 21	Revised	Changed heading from "Scour at Spreader Outlets" to "Rock and Scour at Spreader Outlets"
Page 21	Added	Added two rows to Table 8.
Page 22	Revised	Changed scour depth of 4.47' to 4.46 ft in item 5.
Page 22	Added	Added rock size calculation results to item 5.
Revision 2 Modifications		
Page 3	Revised	Revised first paragraph on page 20 to describe flow in channels instead of along north side of berms.
Page 8	Revised	Revised Table 7 on page 20 to be consistent with flow in channels.
Revision 3 Modifications		
Pages 21 and 22.	Revised	Revised **"Rock in Channels and on North Side of Berms"** on pages 21 and 22 to include the impacts of overflow from the sediment-filled ditches north of the access road to the ditches

The current applicable version of this publication resides on Jacobs' Intranet. All copies are considered to be uncontrolled.
Copyright© Jacobs Engineering Group Inc., 2007

		south of the access road.
Pages 22 and 23	Added	Added **"Protection from Overflow Across Access Road"**
Pages 23 and 24	Revised	Revised **"Rock and Scour at Spreader Outlets."** to include calculations on the rate of spreading of flow and the design of a buried rock blanket for protection against scour at the ends of the spreaders.
Page 25	Revised	Revised **"Summary"** to incorporate the modifications listed above.

The current applicable version of this publication resides on Jacobs' Intranet. All copies are considered to be uncontrolled.
Copyright© Jacobs Engineering Group Inc., 2007

Description of Calculation:

- Determine the runoff from the areas encompassing the south slope of the wedge for design storms with return intervals from 1 year to the PMP.
- Calculate the potential sediment transport in a hypothetical channel that routes the runoff along the south side of the wedge toward the east and toward the west using methods from Johnson, 2002.
- Calculate the sediment loss from the south slope of the wedge using the Modified Universal Soil Loss equation (MUSLE) (Nelson, et. al., 1986)
- Compare the potential sediment loss from the south slope of the wedge with the potential sediment transport in the ditches between the wedge and the access road to determine whether net erosion or sedimentation is expected to occur.
- Calculate the potential depth of gullies formed on the top and side slopes of the wedge using the methodology of Johnson, 2002 to determine whether the wedge may be breached by gullying.
- Calculate the size of rock protection required in the ditch south of the wedge beyond the east and west ends of the access road using the safety factor method.
- Calculate the expected depth of scour at the spreader outlets for the PMP storm using the methods of the Federal Highway Administration.
- Compute the rock size required for erosion protection from the flow in the spreaders.
- Compute the peak runoff from the PMP for the watersheds comprising the areas between the access road berm and the drainage divide on top the cell using SCS methods.
- Compute the rock size required for erosion protection for flow along the north side of the berms from the northwest and northeast corners of the cell using the safety factor method.

The current applicable version of this publication resides on Jacobs' Intranet. All copies are considered to be uncontrolled.
Copyright© Jacobs Engineering Group Inc., 2007

Assumptions:

- The 1-hour PMP event is estimated to be 8.2 inches, ("Site Drainage—Hydrology Parameters" calculation, Draft RAP Attachment 1, Appendix E).
- The rainfall frequency-depth-duration data were developed in the Draft RAP. The 1 year rainfall depth was taken from the NOAA Atlas 14 (http://hdsc.nws.noaa.gov/hdsc/pfds/sa/ut_pfds.html).
- Over a period of 1000 years 12.7% of the total rainfall will become runoff (Johnson, 2002).
- The unit weight of compacted soil in the wedge and the road berm is 103.5 pcf.

The current applicable version of this publication resides on Jacobs' Intranet. All copies are considered to be uncontrolled.
Copyright© Jacobs Engineering Group Inc., 2007

Design Inputs:

See following pages.

Software:

Title	Developer	Versions	Revision Level
EXCEL	Microsoft	2002	
HEC-HMS	USACE	3.1.0	

The current applicable version of this publication resides on Jacobs' Intranet. All copies are considered to be uncontrolled.
Copyright© Jacobs Engineering Group Inc., 2007

Calculation Section:

See following pages.

The current applicable version of this publication resides on Jacobs' Intranet. All copies are considered to be uncontrolled.
Copyright© Jacobs Engineering Group Inc., 2007

Conclusions/Recommendations:

See following pages.

Reference:

See following pages.

The current applicable version of this publication resides on Jacobs' Intranet. All copies are considered to be uncontrolled.
Copyright© Jacobs Engineering Group Inc., 2007

DESCRIPTION OF CALCULATION:

Analyze the area between the wedge and the waste cell to determine.

1. Does the ditch between the south side of the wedge and the access road require erosion protection to prevent runoff from the south side slope of the wedge eroding the berm on which the access road is constructed?

2. The discharge rate of runoff from the north side of the cell and the area between the cell and the access road to determine the need for flow control at the northwest and northeast corners of the cell aprons. The size of rock required for erosion protection north of the berm that diverts this runoff to the spreaders.

3. The size of rock lining required to protect the ditches north of the access road (beyond the end of the road) carrying water to the outlet spreaders on the east and west.

4. The scour depth at the spreader outlets.

5. The effect of erosion on the south side slope of the wedge on the integrity of the wedge including both sheet and rill erosion and gully formation.

METHOD OF SOLUTION:

- Determine the runoff from the areas encompassing the south slope of the wedge for design storms with return intervals from 1 year to the PMP.
- Calculate the potential sediment transport in a hypothetical channel that routes the runoff along the south side of the wedge toward the east and toward the west using methods from Johnson, 2002.
- Calculate the sediment loss from the south slope of the wedge using the Modified Universal Soil Loss equation (MUSLE) (Nelson, et. al., 1986)
- Compare the potential sediment loss from the south slope of the wedge with the potential sediment transport in the ditches between the wedge and the access road to determine whether net erosion or sedimentation is expected to occur.
- Calculate the potential depth of gullies formed on the top and side slopes of the wedge using the methodology of Johnson, 2002 to determine whether the wedge may be breached by gullying.
- Calculate the size of rock protection required in the ditch south of the wedge beyond the east and west ends of the access road using the safety factor method.
- Calculate the size of rock protection required for flow in the spreaders.
- Calculate the expected depth of scour at the spreader outlets for the PMP storm using the methods of the Federal Highway Administration.
- Compute the peak runoff from the PMP for the watersheds comprising the areas between the access road berm and the drainage divide on top of the cell using SCS methods.
- Compute the rock size required for erosion protection for flow along the north side of the berms from the northwest and northeast corners of the cell using the safety factor method.

The current applicable version of this publication resides on Jacobs' Intranet. All copies are considered to be uncontrolled.
Copyright© Jacobs Engineering Group Inc., 2007

ASSUMPTIONS:

- The 1-hour PMP event is estimated to be 8.2 inches, ("Site Drainage—Hydrology Parameters" calculation, Draft RAP Attachment 1, Appendix E).
- The rainfall frequency-depth-duration data were developed in the Draft RAP. The 1 year rainfall depth was taken from the NOAA Atlas 14 (http://hdsc.nws.noaa.gov/hdsc/pfds/sa/ut_pfds.html).
- Over a period of 1000 years 12.7% of the total rainfall will become runoff (Johnson, 2002).
- The unit weight of compacted soil in the wedge and the road berm is 103.5 pcf.

The current applicable version of this publication resides on Jacobs' Intranet. All copies are considered to be uncontrolled.
Copyright© Jacobs Engineering Group Inc., 2007

Figure 1 Configuration of the Wedge and the Waste Cell

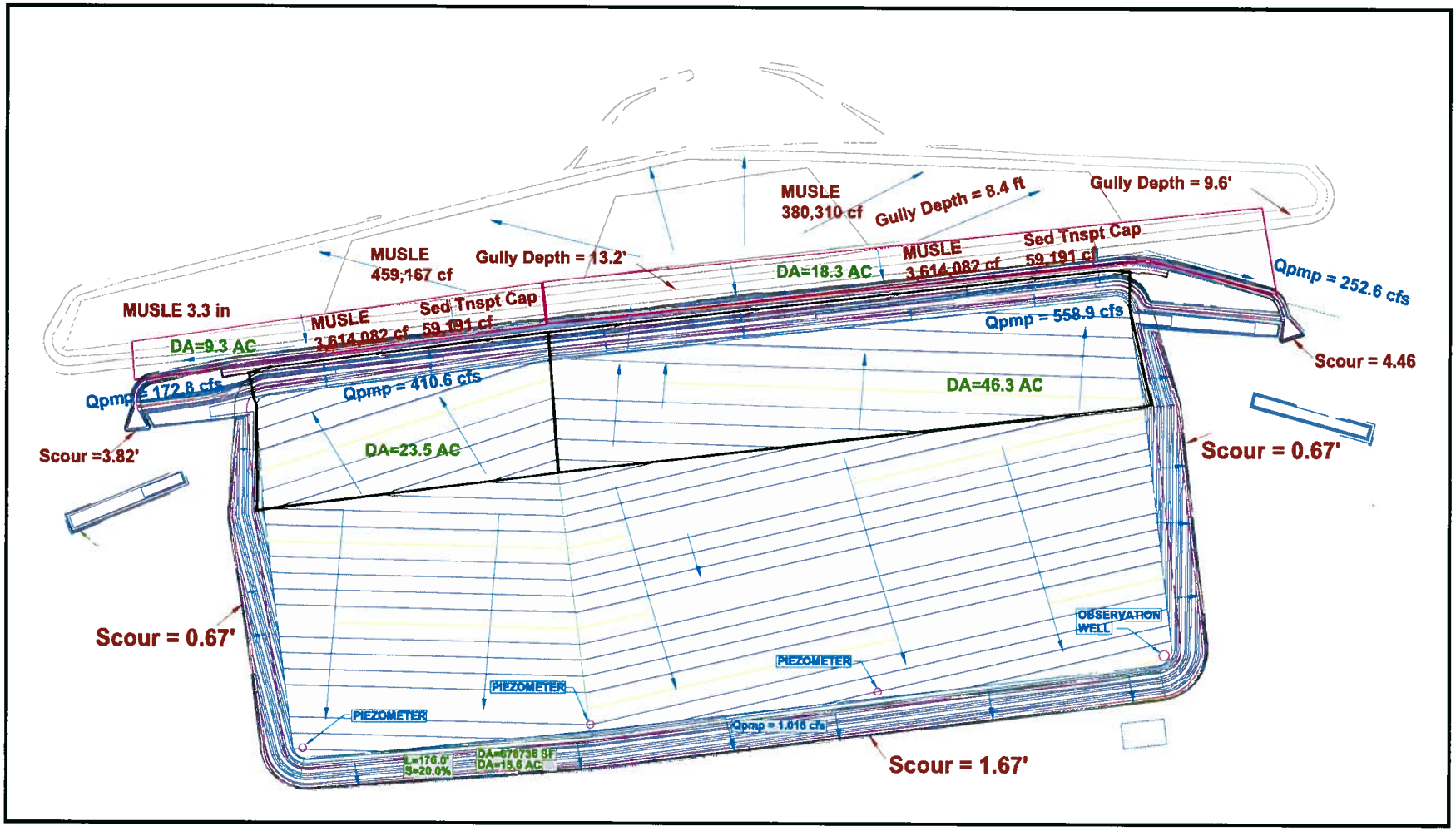

CALCULATION SECTION:

Calculations are performed in the spreadsheets RoadBermNE_Erosion.xls RoadBermNW_Erosion.xls. WatershedParms.xls Channel_Rock_and_Scour.xls Spreader_Rock_and_Scour.xls.

Sediment Transport Capacity

Drainage Area Characteristics

Two drainage areas were delineated between the wedge and the access road draining to the southeast and to the southwest. Two more were delineated between the watershed divide on top the cell and the access road to the northeast and the northwest. These drainage areas are shown in Figure 1. For all storms except the PMP, an initial abstraction of 0.3 inches was estimated for compacted NRCS Type B soil (http://websoilsurvey.nrcs.usda.gov/app/WebSoilSurvey.aspx) with a constant infiltration rate of 0.1inches/hour. For the PMP the initial abstraction was set equal to 0.0 inches. Figure 2 shows a cross section through the south side slope of wedge to the north slope of the waste cell.

Pertinent properties of the four drainage areas are computed in WaterShedParms.xls and listed in Table 1. The flow lengths are used to develop a unit hydrograph using the USBR methodology and the Lag time is used in the SCS unit hydrograph method. The time of concentration was computed as the time along the predominantly east-west flow paths plus the time along the steeper predominantly north-south flow paths.

Table 1. Drainage Area Characteristics

Drainage Area	Area (acres)	Max Flow Length (ft)	Time of Concentration (min)	Lag = 0.6 Tc
Southwest Wedge Side Slope	9.3	2062	23.38	14.0
Southeast Wedge Side Slope	18.3	3470	35.53	21.3
Northwest Portion of Cell	23.5	1471	25.38	15.2
Northeast Portion of Cell	46.3	2891	41.96	25.2

The current applicable version of this publication resides on Jacobs' Intranet. All copies are considered to be uncontrolled. Copyright© Jacobs Engineering Group Inc., 2007

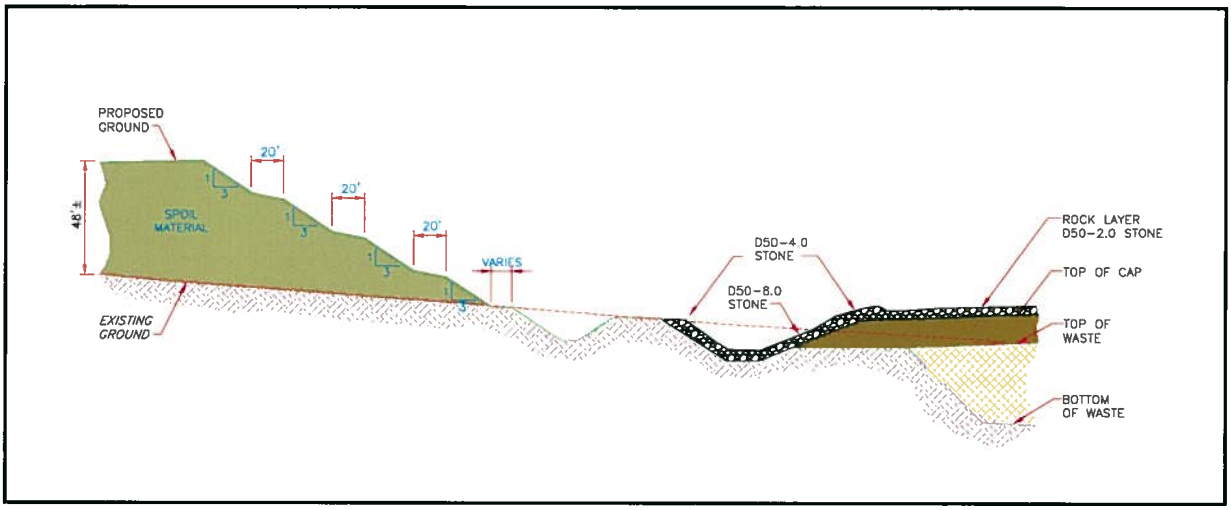

Figure 2 Cross Section of the Area between the Waste Cell and the Wedge.

Runoff Hydrograph Calculations

Since these drainage areas are constructed and not in a natural condition, the SCS unit hydrograph transform was used. The USBR method was developed for natural areas in the west and is not appropriate for the constructed wedge and cell. The runoff hydrographs were computed using the Computer Program HEC-HMS (USACE 2007).

Rainfall Depths Applied

The series of storms for the runoff calculations was developed from the Hydrology data in the draft RAP and NOAA Atlas 14. The number of storms of each depth was chosen conservatively as follows.

- A storm with rainfall depth equal to or greater than the 1000 year storm occurs on the average once every 1000 years. Since the rainfall depth may be any depth between the 1000 year storm and the PMP, the PMP was used for this storm.
- A storm with rainfall depth equal to or greater than the 500 year storm occurs on the average twice every 1000 years. Since the rainfall depth may be any depth between the 500 year storm and the 1000 year storm, the 1000 year rainfall depth was used for this storm. Since the PMP is one of these storms, one 1000 year storm was used.
- A storm with rainfall depth equal to or greater than the 200 year storm occurs on the average five times every 1000 years. Since the rainfall depth may be any depth between the 200 year storm and the 500 year storm, the 500 year rainfall depth was used for this storm. Since two larger storms have already been applied, three 500 year storms were used.

Following this logic through storms of all available return periods resulted in the distribution of rainfall depths and number of storms listed in Table 2. All storms represent 24 hour precipitation depth except for the PMP which is a 6 hour depth.

The current applicable version of this publication resides on Jacobs' Intranet. All copies are considered to be uncontrolled. Copyright© Jacobs Engineering Group Inc., 2007

Table 2 Design Storms used in Sediment Transport Capacity Calculations.

Return Interval Represented (years)	Return Interval Employed (years)	Precipitation Depth (inches)	Number of Storms Equal or Greater than Interval Represented	Number of Storms of Depth Employed
1000	PMP (6 hour)	9.0	1	1
500	1000	3.73	2	1
200	500	3.15	5	3
100	200	2.58	10	5
50	100	2.35	20	10
25	50	2.12	40	20
10	25	1.91	100	60
5	10	1.63	200	100
2	5	1.42	500	300
1	2	1.16	1000	500
< 1	1	0.93	Unknown	1000

The runoff from each area was computed using HEC-HMS with the results from the wedge and from the book cliffs area flowing to the west combined into one hydrograph. A five minute time step was used.

Sediment Transport Capacity

The capacity of the flow to the east and the flow to the west along the north edge of the wedge was estimated using a procedure in NUREG 1823 (Johnson 2002). In this method the sediment transport capacity of a channel can be computed as

$$q_s = c_{s1} h^{c_{s2}} V^{c_{s3}}$$

where
q_s = unit sediment transport rate in ft^2/s (unbulked)
V = velocity in ft/s
h = flow depth in feet

NUREG 1623 gives the coefficient and exponents as a function of grain size distribution. Those that most closely correspond to the grain size distribution of the native soil are

$C_{s1} = 3.3 \times 10^{-5}$
$C_{s2} = 0.715$
$C_{s3} = 3.30$

Trapezoidal channels with a bottom width of 2 feet and a side slope of 3 horizontal to 1 vertical were assumed (See Figure 3). The slope of the channels were 0.007 to the east and 0.005 to the west as determined from the topography of the site and the location of the channels. A table was constructed of sediment transport in cfs as a function of discharge in each channel. The flow in each 5 minute period of a runoff hydrograph was then used to interpolate to find the sediment transport during each 5 minute increment of the hydrograph. The sediment transport of each hydrograph was then computed as the sum of these 5 minute contributions.

For the channel shown below with a discharge Q, a depth h, and a top width T, the volume of sediment transport capacity in a five minute period was calculated as follows. q_s was computed as above. Since this is

The current applicable version of this publication resides on Jacobs' Intranet. All copies are considered to be uncontrolled. Copyright© Jacobs Engineering Group Inc., 2007

the unbulked volume transport rate the unit weight was assumed to be 165 pcf. The value of q_s will vary across the channel as it depends on both the velocity and depth of flow. As a conservative approach, the value q_s computed for the full depth, h, was applied throughout the channel. The total rate of sediment transport in cubic feet/sec (unbulked) was computed as

$$Q_s(unbulked) = q_s T$$

q_s*T and the rate in cf/5 min (bulked) as

$$Qs(5\min_bulked) = Qs(unbulked) * (300\sec) * \frac{165\,pcf}{103.5\,pcf}$$

where the unit weight of compacted soil in the wedge and the road berm is 103.5 pcf.

These 5 minute contributions was summed for each of the 5 minute flow periods of a storm hydrograph to compute the total sediment transport potential in cf of the native soil from a single storm.

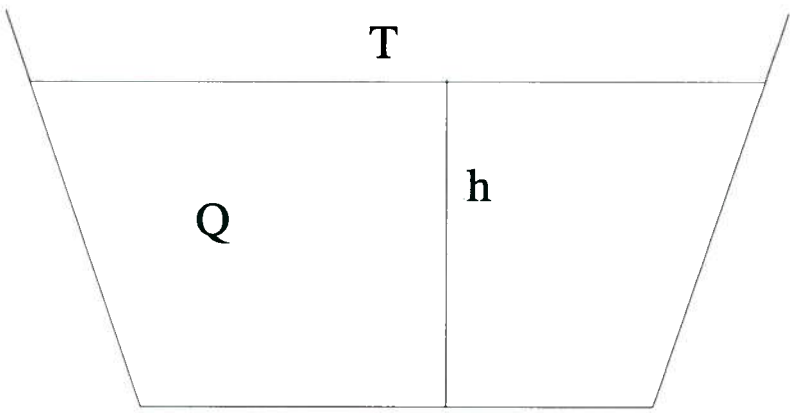

Figure 3 Assumed Cross Section of the Channel Carrying Runoff from the South Side of the Wedge.

This calculation was repeated for all the storms listed in Table 2 and the total potential sediment transport during 1000 years was computed. These calculations are performed in the files RoadBermNE_Erosion.xls and RoadBermNW_Erosion.xls.

Unaccounted for Runoff

The total runoff of water in the listed storms was also computed. Since the annual rainfall at Thompson during the period (1971-2000) was 9.97 inches(reference), and NUREG 1623 states that a reasonable estimate of the ratio of runoff to rainfall in the semi-arid regions of the western United States is 0.127, a volume of total expected runoff during 1000 years was computed. Comparing this volume with that computed from the listed storms indicated that 40% of the runoff had not been accounted for by the listed storms.

Assuming that the sediment concentration in this additional runoff will be equal to the average concentration in the runoff from the one year storm, an additional volume of sediment transport was added by multiplying this average concentration by the volume of additional runoff.

The current applicable version of this publication resides on Jacobs' Intranet. All copies are considered to be uncontrolled. Copyright© Jacobs Engineering Group Inc., 2007

Sediment Supply from the Book Cliffs Area

The runoff from the south side of the wedge will transport sediment toward the ditch between the wedge and the road berm. The total sediment loss over a 1000 year period from the two watersheds on the south slope of the wedge can be estimated with the Modified Universal Soil Loss Equation (MUSLE).

The equation is

$$A = R \times K \times LS \times VM$$

where:

A = soil loss in tons per acre per year,
R = rainfall factor,
K = soil erodibility factor,
LS = topographic factor, and
VM = dimensionless erosion control factor relating to vegetative and mechanical factors.

The rainfall factor is 25, as given in NUREG/CR-4620 (Nelson et al. 1986) for the eastern third of Utah. The soil erodibility factor was estimated using the nomograph given in NUREG/CR-4620 (Nelson et al. 1986).

The topographic factor is calculated by the following equation:

$$LS = \frac{650 + 450 \times s + 65 \times s^2}{10{,}000 + s^2} \times \left(\frac{L}{72.6}\right)^m$$

where:

s = slope steepness in percent,
L = slope length in ft, and
m = exponent dependent upon slope steepness.

The dimensionless erosion control factor used for the undisturbed watersheds was 0.4, from Table 5.3 of NUREG/CR-4620 (Nelson et al. 1986), representing seedings of 0 to 60 days to mimic light vegetation in the area. Over an extended period of time, some vegetation can be expected to develop. Table 3 summarizes the results of the soil loss equation. Since the south side slope of the wedge varies from approximately 118 to 176 feet wide and 30 to 48 feet high, intermediate values of 160 feet wide and 40 feet high were used in this analysis. As the results will indicate, no further refinement was warranted.

The current applicable version of this publication resides on Jacobs' Intranet. All copies are considered to be uncontrolled. Copyright© Jacobs Engineering Group Inc., 2007

Table 3. Results of Soil Loss Equation

Soil Cover	Western End of Side Slope	Eastern End of Side Slope
Rainfall factor, R	25	25
Silt and very fine sand (%)	60	60
Sand (%)	25	25
Organic matter (%)	2	2
Soil structure	Very fine granular	Very fine granular
Relative permeability	Moderate	Moderate
Erodibility factor	0.35	0.35
Topographic factor, LS	7.94	7.94
VM (low density seedings)	0.4	0.4
Soil loss (tons/acre/year)	27.8	27.8
Soil loss (feet)/1,000 years)	12.3	12.3
Area of Side Slope (acres)	6.1	11.9
Total sediment loss in 1000 years (cf)	3,265,142	6,417,082

Sediment Budget

The calculated volumes of potential sediment transport from the ditch and sediment supply from the side slope of the wedge over a 1000 year period are summarized in Table 4.

Table 4 Sediment Budget for the Area between the Road Berm and the Wedge.

Area	Sediment Transport Capacity (cf)	Sediment Yield from MUSLE (cf)
Channel along south side of wedge to the west	22,792	
Channel along south side of the wedge to the east	59,191	
Western portion of the south side of the wedge		3,265,142
Eastern portion of the south side of the wedge		6,417,082
Ratio of sediment supply to transport capacity (west)	143	
Ratio of sediment supply to transport capacity (east)	108	
Volume of Ditch to the West	588,000 cf (18% of potential sediment supply)	
Volume of Ditch to the East	1,156,400 cf (18% of potential sediment supply)	

These results indicate that the water flowing in the ditch along the southern side of the wedge to the west and the east does not have sufficient sediment transport capacity to carry away the supply of sediment from the south side slope of the wedge. These results indicate a sufficient volume of sediment will erode from the south side slope of the wedge to completely fill the ditch in about 180 years. Because of the geometry of the wedge and the ditch, the flow in the ditch will increase from the high point near the east-west center of the wedge and carry increasingly more sediment as the flow proceeds downstream. The nearly uniform sediment supply along the length of the ditch and the increase in sediment transport capacity in a downstream direction will cause the bottom slope of the ditch to increase over time. This will increase the sediment transport capacity of the ditch, but it is not expected to increase enough to carry away the total sediment supply from the side slope of the wedge.

The current applicable version of this publication resides on Jacobs' Intranet. All copies are considered to be uncontrolled. Copyright© Jacobs Engineering Group Inc., 2007

Erosion from Side Slope of the Wedge

The results presented in Table 3 indicate soil to a depth of approximately 12 feet will be lost from the south side slope of the wedge. Since the south side slope of the wedge will be 30 feet high at the east and west ends and 48 feet high in the center, this depth of erosion, while substantial, will not threaten the integrity of the wedge since the top of the wedge is over 230 feet wide at the west end and 150 feet at the east end.

Gully Formation on the Side Slope of the Wedge

In addition to potential erosion of the wedge by sheet and rill erosion from precipitation directly on the south side slope of the wedge, the runoff from precipitation on the south side slope is expected to form gullies on these steep slopes. The potential depth of these gullies can be estimated with an approach detailed in NUREG 1623. The three types of embankment geometries analyzed in this guidance document as shown in Figure 4. Gullies forming on the steep side slope wedge are analyzed as a Type 3 slope. The effective tributary drainage area for a gully is computed as

$$A = 0.276\left[L\cos(\theta)\right]^{1.636}$$

where L = total length of the flow path. A gully factor depending on the soil type, the height of the embankment and the volume of runoff to the toe of the embankment toe is

$$G_f = \frac{1}{2.80 + \left[0.197\frac{V_r}{H_o^{\,3}}\right]^{-0.70}}$$ for a clay content between 15 and 50%.

The current applicable version of this publication resides on Jacobs' Intranet. All copies are considered to be uncontrolled. Copyright© Jacobs Engineering Group Inc., 2007

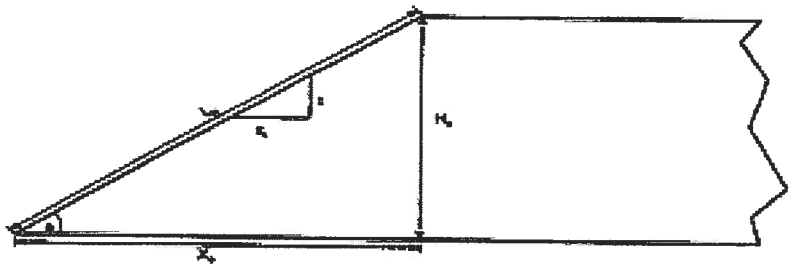

Type 1 Embankment

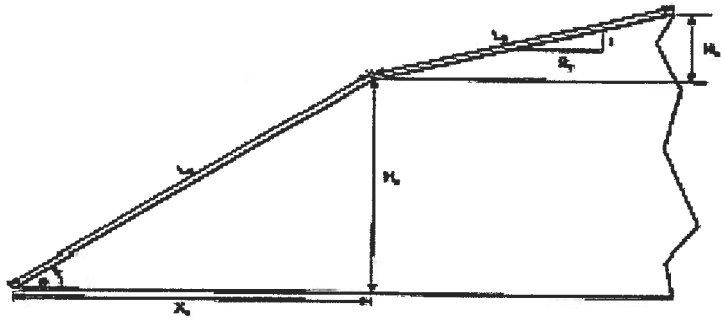

Type 2 Embankment

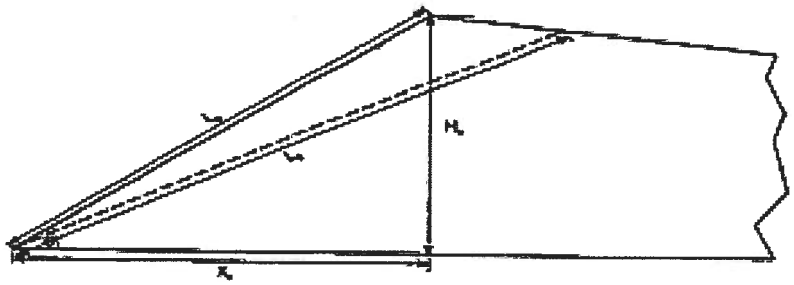

Type 3 Embankment

Figure B-4. Three types of embankment geometry.

NUREG-1623 B-6

Figure 4 The Three Types of Embankment Geometry Analyzed in NUREG 1623 for Gully Formation.

The current applicable version of this publication resides on Jacobs' Intranet. All copies are considered to be uncontrolled. Copyright© Jacobs Engineering Group Inc., 2007

The estimated maximum depth of gully incision is

$$D_{\max} = G_f L_{total} S$$

where S is the original slope of the embankment. The top width of the gully at its deepest point is

$$W = \left[\frac{D_{\max}}{0.61}\right]^{1.149}$$

and the location of the deepest incision measured in units of D_{max} downslope from the crest of the embankment is

$$D_l = 0.713\left[\frac{V_r S}{L_o^{\,3}}\right]^{-0.415}$$

The results of these calculations are summarized in Table 5. The calculations are performed in metric units and the results converted to English units.

Table 5 Data and Results of Calculations of Gully Depths.

Variable	Description	End of South Side Slope	Center of South Side Slope
H_o (ft)	Height of Embankment	30	48
X_o (ft)	Horizontal Length of Embankment	118	176
L_o (ft)	Length of Embankment along Slope	121.8	182.4
θ (radians)	Embankment Slope Angle	0.249	0.266
L_t (ft)	Long Term Embankment Slope Length	143	214
A (sq ft)	Effective Drainage Area	1,358	2,612
V_r (cf)	Rainfall Volume	143,310	275,637
G_f	Gully Factor	0.27	0.22
D_{max} (ft)	Maximum Gully Depth	9.6	13.2
W (ft)	Gully Width at Maximum Depth	20	28.5
D_l (ft)	Distance of D_{max} from Top of Slope	35	58

While the predicted depth of the gullies that will form on the south side slope of the wedge over a period of 1000 years are substantial, the gullies are not expected to threaten the ability of the wedge to route runoff from the Book Cliffs around the waste cell. In each case the height of the wedge is more than three times the calculated gully depth and the minimum north-south dimension of the wedge is 118 feet, much greater than the expected gully depth.

The current applicable version of this publication resides on Jacobs' Intranet. All copies are considered to be uncontrolled. Copyright© Jacobs Engineering Group Inc., 2007

Rock in Channels and on North Side of Berms

The channels carrying runoff from the south side slope of the wedge to the east and to the west will not be armored for most of their lengths because of the excess sediment supply from the south side of the wedge. Beginning approximately 100 feet upstream of each end of the end of the access road, rock will be placed in the channels to protect them against erosion from that point to the spreaders that terminate the channels. If the channels fill with sediments, the flow will leave the channels and flow southward toward the berm shown in Figure 2. Flow from the top of the cell and the area south of the access road and north of the cell will flow to the east and to the west in trapezoidal ditches with 3H to 1V side slopes and a bottom width of 20 feet. The flow in these ditches will continue along the north side of berms that extend from the cell side slopes to the spreaders.

The peak flows resulting from the PMP in each of these areas have been calculated using the SCS unit hydrograph technique with an initial abstraction of 0.0 inches and a constant infiltration rate of 0.1 inches/hour. The results of these calculations are included in Table 6. The time of concentration is calculated as the sum of the times of concentration on each of the slopes in the drainage area. For example, the time of concentration for the flow from the cell toward the west is the sum of T_c(northward flow on the top slope of the cell) + T_c(northward flow on the side slope of the cell) + T_c(westward flow to the point where the channel turns south.) Except for flow on the cell as described in Cell_Rock.doc, the mean of the Kirpich and SCS time of concentration equations was used. Except for the peak flow, these data are copied from Table 1.

Table 6 Peak Flows from the Area between the Wedge and the Waste Cell for the PMP.

Peak flow from PMP	South Side of Wedge (West)	South Side of Wedge (East)	Flow from Cell (West)	Flow from Cell (East)
Drainage Area (acres)	9.3	18.3	23.5	46.3
Time of Concentration(min) (T_c)	23.4	35.5	25.4	42.0
Lag(min) = $0.8T_c$	14.0	21.3	15.2	25.2
Peak Flow (cfs)	172.8	252.6	410.6	558.9

The D50 of stone erosion protection was determined using the safety factor method. The results of these calculations are presented in Table 7. Each of the channels north of the road berm is assumed to have a bottom width of 10 feet and side slopes of 3H to 1V.

Table 7 D50 of the Stone Required for Erosion Protection

D50 for Erosion Protection	South Side of Wedge (West)	South Side of Wedge (East)
Peak Flow (cfs)	172.8	252.6
Channel Slope	.0094	.0076
D50 (inches) on 3:1 Side of Channel	3.3	3.4
D50 (inches) on Bottom of Channel	2.6	2.6
Portion of Channel Draining the South Side of the Wedge after it has Turned Southerly		
Channel Slope	.0175	.0175
D50 (inches) on Side of Channel	5.8	7.2
D50 (inches) on Bottom of Channel	4.5	5.6

After the channels north of the access road have filled with sediment, the flow from that channel will overflow into the channels to the east and west south of the access road. The peak flow in these channels has been estimated as the sum of the peak flows from the south side of the wedge and from the cell presented in Table 7. The channels south of the access road have flat bottoms 15 feet wide, a 3H to 1V side slope on the north

The current applicable version of this publication resides on Jacobs' Intranet. All copies are considered to be uncontrolled. Copyright© Jacobs Engineering Group Inc., 2007

side and 5H to 1V on the south side (the side slope of the cell). Beyond the edges of the cell these channels expand to a 20 foot bottom width with 3H to 1V side slopes on both sides. The D50 of required rock armoring in these channels was computed using the Safety Factors Method. The results are presented in Table 8. Rock armoring with D50 at least as great as presented in Table 8 will extend vertically on the cell side of the ditches to an elevation greater than the predicted maximum water surface elevation.

Table 8 Rock Armoring for Combined Peak Flows in Channels South of the Access Road

	North Side of Cell (West)	North Side of Cell (East)
Peak Flow (cfs)	583.4	811.5
Channel Slope	.0089	.0063
Channel South of Access Road within Cell Boundaries		
Maximum Depth (ft)	2.79	3.46
D50 (inches) on 5:1 Side of Channel	4.2	3.7
D50 (inches) on 3:1 Side of Channel	5.1	4.4
D50 (inches) on Bottom of Channel	3.9	3.4
Channel South of Access Road beyond Cell Boundaries		
Maximum Depth (ft)	2.08	2.6
D50 (inches) on 3:1 Side of Channel	4.7	4.1
D50 (inches) on Bottom of Channel	3.6	3.2

Protection from Overflow Across Access Road

After the ditches north of the access road fill with sediment, the runoff from the south side of the wedge will overflow into the armoured ditch. Since the depth of sediment in the ditches north of the access road can not be accurately predicted as a function of time and location, we have assumed that the overflow will occur uniformly along the length of the ditches within the boundaries of the cell on a slope of 0.01 from north to south. We have also assumed that the flow will concentrate by a factor of 3 in scouring gullies on the access road and also in cascading down the north side slope of the armoured ditches.

With these assumptions the depth of gullies caused by the overflow has been calculated with Federal Highway Administration culvert scour equations as described in Calculation C-02 assuming flow in a V-shaped ditch with 2H to 1V side slopes. The D50 of the required rock armouring for these gullies was computed using the safety factors method.

The D50 of rock armouring needed to protect the armoured ditches as the overflow cascades down the 3H:1V side slope was calculated using the method of Abt and Johnson (1991).

$$D_{50} = 5.23q^{0.56}S^{0.43}$$

The results of these calculations are presented in Table 9.

Table 9 Rock Armor to Protect Against Overflow over Access Road

	West Side	East side
Total Overflow Rate (cfs)	172.8	252.6
Ditch Length (ft)	1470	2891
Overflow (cfs/ft)	0.12	0.09

The current applicable version of this publication resides on Jacobs' Intranet. All copies are considered to be uncontrolled. Copyright© Jacobs Engineering Group Inc., 2007

Concentration Factor	3	3
Design flow (cfs)	0.35	0.26
Gully Scour Depth (ft)	0.64	0.56
D50 to Protect the Gullies (inches)	0.6	0.5
D50 on 3:1 Side Slope of the Ditch (inches)	3.6	2.9
Designed D50 on 3:1 Side Slope (inches)	5.1	4.4

These results indicate that the ditches south of the access road will be protected against potential scour and rock movement caused by overflow from the ditches north of the access road by the existing design. The access road should be protected by rock armoring with a D50 of 1 inch or more to stabilize it against scour in the event of flow concentration greater than 3.

Rock and Scour at Spreader Outlets.

Flow from the channel north of the access road and from the top of the cell will combine at the spreader for discharge onto the natural ground. The peak flows from the PMP have been added to estimate the peak flow from each spreader. To obtain the flow per unit width, the peak flow has been spread over a width of 100 feet. To account for potential channelization in the rock of the spreaders, the unit flow has been multiplied by three for calculation of the required D50 of rock for erosion protection and potential scour depth at the outlet of each spreader. The D50 was calculated using the safety factor method assuming a channel with 3H to 1V side slopes, a 1 ft bottom width and a channel slope of 2.3%. The scour was calculated using the Federal Highway Administration culvert scour equations as described in Calculation C-02 assuming flow in a V-shaped ditch with 2H to 1V side slopes. The results are summarized in Table 10.

Table 10 Calculated Depth of Scour at Spreader Outlets.

	West Spreader	East Spreader
Peak Flow from Channel (cfs)	172.8	252.6
Peak Flow along Berm (cfs)	410.6	558.9
Combined Peak Flow (cfs)	583.4	811.5
Concentration Factor	3	3
Design Flow (cfs/ft)	17.50	24.35
Minimum Rock D50 (in)	4.5	5.2
Estimated Scour Depth (ft)	3.82	4.46

These results assume that the discharge will spread to a width of 100 feet as it flows from the end of the channels to the end of the spreaders. The length of spreaders required to ensure this degree of spreading can be estimated using an equation described in USACE (1994). This equation is the result of research performed by Rouse, et. al.(1951) on the boundary shapes for the expansion of a high-velocity jet on a horizontal floor. Note that the equation presented in the text of USACE (1994) is

$$\frac{Z}{b_1} = \frac{1}{2}\left(\frac{X}{b_1 F1}\right)^{\frac{3}{2}} + \frac{1}{2}$$

where
Z = the half width of the expanded flow (ft)
b1 = flow width before expansion (ft)

The current applicable version of this publication resides on Jacobs' Intranet. All copies are considered to be uncontrolled. Copyright© Jacobs Engineering Group Inc., 2007

X = downstream distance from the beginning of expansion (ft)
F1 = Froude number of the flow before expansion

while Plate B-24 in the same publication which is a reproduction of results from the original paper by Rouse gives the equation as

$$\frac{Z}{b_1} = \frac{1}{8}\left(\frac{X}{b_1 F1}\right)^{\frac{3}{2}} + \frac{1}{2}$$

We have used the equation from the original paper to compute the length of spreaders required to allow complete spreading of flow to the 100 ft width. The results are:

	West	East
Discharge (cfs)	583.4	811.5
Initial Flow Velocity (fps)	8.19	8.4
Initial Flow Cross-Sectional Area (sq ft)	71.24	96.62
Initial Top width (ft)	35.42	39.49
Initial Hydraulic Depth (ft)	2.01	2.45
Initial Froude Number	1.02	0.95
Distance to Expand to 100 feet (ft)	135	125

Design of the Toe of the Spreaders

To protect the toe of the spreaders against head cutting by scour from the discharge of the PMP runoff a 10H to 1V buried rock blanket will be constructed downstream of the toe to protect against erosion down to the expected depth of scour. Figure 5 shows a typical buried rock blanket. The expected scour depths have previously been computed and the D50 of the buried rock was computed using methods described in NUREG 1623. The results for the east and west sides are given below assuming a natural ground slope of 2.3% and a rock blanket slope of 10%. The results of the scour and rock armouring calculations are summarized in Table 11.

Table 11 Rock Size and Scour Depth at Spreader Outlets

	West	East
Scour depth (ft)	3.82	4.46
Discharge (cfs)	583.4	811.5
Spreader Width (ft)	100	100
Discharge/unit width (cfs/ft)	5.83	8.12
Concentration Factor	3	3
Design Unit Discharge (cfs/ft)	17.5	23.3
D50 (inches)	9.7	11.6

The current applicable version of this publication resides on Jacobs' Intranet. All copies are considered to be uncontrolled. Copyright© Jacobs Engineering Group Inc., 2007

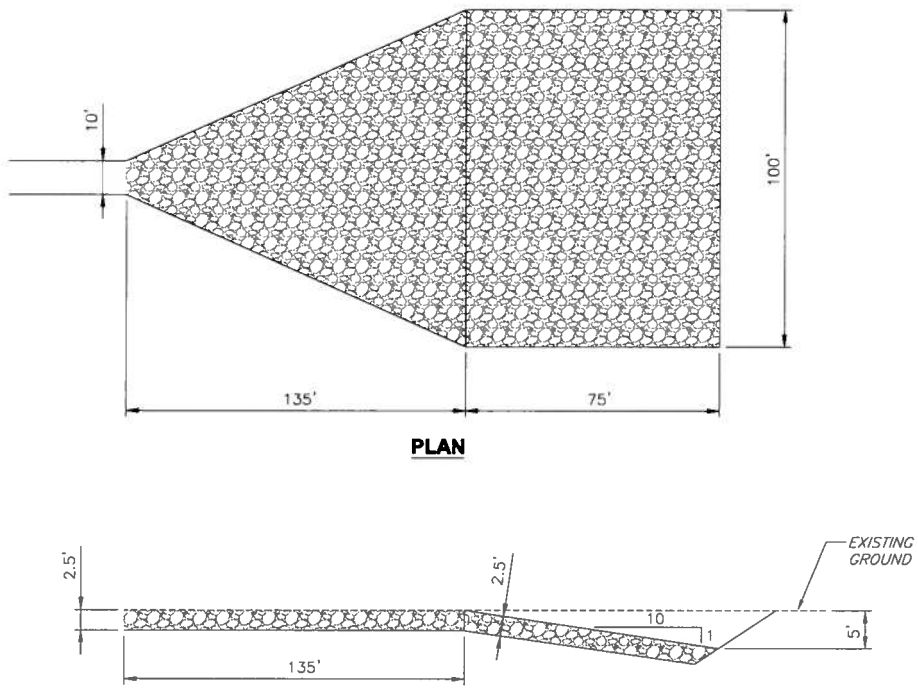

Figure 5 Typical Buried Rock Blanket

Summary

A wedge of spoil material consisting of approximately 3,000,000 cubic yards of soil excavated from the waste cell will be placed between the Book cliffs and the waste cell to divert runoff from the Book Cliffs area around the waste cell. These calculations have been performed to assess whether erosion protection is required for the ditch north of the access road and south of the wedge and to assess the sediment budget in that ditch. The erosion protection requirements of the broad channels that carry flow from the areas between the wedge and the cell to the outlet spreaders on the east and west have also been determined. Specific results/conclusions are summarized here.

1. Runoff from direct precipitation on the south slope of the wedge will be collected and carried to the east and west by ditches between the wedge and the access road. The sediment transport capacity of this runoff during the 1000 year design life has been assessed using equations from NUREG 1623. The supply of sediment by sediment yield from the south side slope of the wedge has been estimated by use of the Modified Universal Soil Loss Equation (MUSLE), as described in NUREG 4620 (Nelson et al. 1986). The results of these calculations indicate that the total sediment carrying capacity of the runoff as it flows to the east and west is approximately 5% of the volume of the access road berm over the 1000 year design life of the cell. The sediment supply to this area estimated from the MUSLE will be many times larger than the sediment transport capacity of the flow in these channels. The net sediment supply to these channel indicates that the channels may fill with sediment in somewhat less than 200 years. The sediment supply will be nearly uniform along the length of the ditch, but the flow will be very small at the high point of the channels and increase nearly uniformly toward the east and west. This will result in a greater sediment transport capacity in a downstream

The current applicable version of this publication resides on Jacobs' Intranet. All copies are considered to be uncontrolled. Copyright© Jacobs Engineering Group Inc., 2007

direction and cause the bottom slope of the ditch to increase over time. This will increase the sediment transport capacity of the ditch, but it is not expected to increase enough to carry away the sediment supply to the channel. This will delay the filling of the ditches with sediment but probably not beyond the 1000 year design life of the waste cell. Some additional flow from the north side of the waste cell may run off over the access road and add to the flow and sediment transport capacity of these channels, but it will not be sufficient to keep them flushed of sediment.

2. Precipitation falling directly on the south side slope of the wedge will run off toward the south. This runoff will erode the side slope of the wedge. Application of the MUSLE to estimate the volume of sediment lost from the wedge through this mechanism indicate that the south side slope will be reduced in average height by approximately 12 feet. With a design height ranging from approximately 30 to 48 feet and a north-south dimension ranging from 150 to 490 feet, this loss of soil will not threaten the integrity of the wedge.

3. Runoff from the south side slope of the wedge will also concentrate and form gullies on the slope. The depth, width, and location of the deepest portions of these gullies has been estimated with techniques described in NUREG 1623 (Johnson 2002). The results are summarized in Table 5. While the predicted depth of the gullies that will form on the south side slope of the wedge over a period of 1000 years are substantial, the gullies are not expected to threaten the ability of the wedge to route runoff from the Book Cliffs around the waste cell. In each case the height of the wedge is more than three times the calculated gully depth and the minimum north-south dimension of the wedge is 118 feet, much greater than the expected gully depth or length. It should be noted that because of the time period over which gullies developed that were used in developing the equations, the NRC staff recommends that this method be used for a design cell life of 200 years. Since the gully depth increases with time, the calculation has been extrapolated to 1000 years as the best available estimate of the extent of potential gully formation over a 1000 design period.

4. Flow from the south side slope of the wedge and from the north portion of the cell top and side slopes will flow to the east and west. The flow from the cell will be carried in a channel south of the access road with the cell apron being the bottom of the channel, one side slope is the cell side slope of 5H to 1V, and the opposite side has a 3H to 1V side slope with rock armoring with a D50 of 4 inches. As this water reaches the east and west edges of the cell apron, the bottom of the channel will widen to 20 feet with side slopes of 3H to 1V. The side slopes will be protected by stone armoring with a D50 of 4 inches. The channels carrying the flow from the side slope of the wedge will not be armored until 100 feet before the end of the access road berm. From that point the channels will be armored with rock with a D50 of 2.0 inches until they turn south. From that point to the spreader the rock D50 will be 4.5 inches on the bottom and 5.8 inches on the side for the channel to the west and 5.6 and 7.2 inches for the channel to east. After the channel north of the access road fills with sediment, the D50 of rock armoring will equal or exceed the sizes presented in Table 8. To protect against scour as water from the ditches north of the access road overflows into the ditches south of the access road, the road will be protected by rock with a D50 of 1 inch or greater.

5. The two channels carrying flow in each direction (east and west) will both discharge into the spreaders and spread to a channel 100 feet wide. The length of the spreaders in the direction of flow has been determined to ensure complete spreading of the flow across th 100 foot width of the spreader. The calculated scour depth for the PMP is 3.82 feet for the spreader on the west and 4.46 feet for the spreader on the east. A concentration factor of three has been assumed for determining the design unit flow. The spreaders will each have rock armoring with a minimum D50 of 4.5 inches on the west and 5.2 inches on the east. A 10H to 1V buried rock blanket will be constructed downstream of the toe to protect against erosion down to the expected depth of scour.

The current applicable version of this publication resides on Jacobs' Intranet. All copies are considered to be uncontrolled. Copyright© Jacobs Engineering Group Inc., 2007

References:

10 CFR 40. U.S. Nuclear Regulatory Commission (NRC), "Domestic Licensing of Source Material," Appendix A, *Code of Federal Regulations*, February 2007.

40 CFR 192. U.S. Environmental Protection Agency (EPA) "Health and Environmental Protection Standards for Uranium and Thorium Mill Tailings," *Code of Federal Regulations*, February 2007.

Abt, S.R., and T.L. Johnson, 1991. "Riprap Design for Overtopping Flow", *Journal of Hydraulic Engineering*, 117(8), pp. 959–972.

Abt, S.R., T.L. Johnson, C.I. Thornton, and S.C. Trabant, 1998. "Riprap Sizing at Toe of Embankment Slopes", *Journal of Hydraulic Engineering*, 124(7), July.

Abt, S.R., J.F. Ruff, and R.J. Wittler, 1991. "Estimating Flow Through Riprap", *Journal of Hydraulic Engineering*, 117(5), pp. 670–675.

Chow, V.T., 1964. *Handbook of Applied Hydrology*, McGraw-Hill Book Company, New York, New York.

DOE (U.S. Department of Energy), 1989. *Technical Approach Document, Revision II*, UMTRA-DOE/AL 050424.0002, December.

DOT (U.S. Department of Transportation), 1983. *Hydraulic Design of Energy Dissipaters for Culverts and Channels*, Hydraulic Engineering Circular No. 14, September.

Geotechnical Engineering Group, Inc. (GEG), 2005. Technical Testing, Crescent Junction, GEG Job No. 2165, December 22.

Johnson, T.L., 2002 *Design of Erosion Protection for Long-Term Stabilization*, Final Report, NUREG-1623, U.S. Nuclear Regulatory Commission, September.

Nelson, J.D., S.R. Abt, R.L. Volpe, D. van Zyl, N.E. Hinkle, W.P. Staub, 1986. *Methodologies for Evaluating Long-Term Stabilization Design of Uranium Mill Tailings Impoundments*, NUREG/CR-4620, U.S. Nuclear Regulatory Commission, June.

Rouse et. al., 1951. Rouse, Hunter, Bhoota, B. V., and Hsu, En-Yun. 1951. "Design of Channel Expansions," Transactions, American Society of Civil Engineers, Vol 116, pp 347-363.

Temple, D.M., K.M. Robinson, R.M. Ahring, and A.G. Davis, 1987. *Stability Design of Grass-Lined Open Channels*, U.S. Department of Agriculture Handbook No. 667, September.

USACE, 1994. "Hydraulic Design of Flood Control Channels", Engineer Manual 1110-2-1601, June, 1994

USDA (U.S. Department of Agriculture), 1994. "Gradation Design of Sand and Gravel Filters", *National Engineering Handbook*, Part 633, Chapter 26, October.

The current applicable version of this publication resides on Jacobs' Intranet. All copies are considered to be uncontrolled. Copyright© Jacobs Engineering Group Inc., 2007

Appendix A

Reference Materials

The current applicable version of this publication resides on Jacobs' Intranet. All copies are considered to be uncontrolled. Copyright© Jacobs Engineering Group Inc., 2007

in column 6 is given from the sediment rating curve, or Equation 6. For each interval, the water yield in column 5 is calculated from multiplying columns 2 and 6. Likewise, the annual sediment yield in column 7 is calculated from Equation E-5 given Δp, Q and C_s from columns 2, 4 and 6. The interannual total sediment yield is finally obtained from the sum of column 7.

2.5 Trap Efficiency

When sediment-laden water enters reservoirs, lakes, impoundments, and settling basins, the settling of sediment will cause aggradation of the bed. The trap efficiency is used to determine how much sediment is expected to settle in backwater areas. The trap efficiency is defined as the percentage of incoming sediment for a given size fraction (i) that will settle within a given reach. The trap efficiency can be calculated as follows:

$$T_{Ei} = 1 - e^{\frac{-Xw_i}{hV}} \qquad \text{(E-7)}$$

where X is the reach length; w_i is the settling velocity for sediment fraction i from Table E-4; h is the mean flow depth; and V is the mean flow velocity. The exponent is dimensionless and any consistent system of units can be used in this equation.

The sediment load that settles within the reach is given by the product of the incoming sediment load and the trap efficiency. The outgoing sediment load is calculated by subtracting the settling load from the incoming load. The trap efficiency varies with sediment size through the settling velocity. Typically, the trap efficiency is approximately one for coarse sediment, e.g., gravels, and approaches zero for fine sediment, e.g., clays.

2.6 Sediment Transport Capacity of a Channel

Simons, Li, and Fullerton (1981) developed an efficient method of evaluating sediment discharge. The method is based on easy-to-apply power relationships that estimate sediment transport based on the flow depth h and velocity V. These power relationships were developed from a computer solution of the Meyer-Peter and Müller bedload transport equation and Einstein's integration of the suspended bed sediment discharge:

$$q_s = c_{s1} h^{c_{s2}} V^{c_{s3}} \qquad \text{(E-8)}$$

The results of the total bed sediment discharge are presented in Table E-2. The large values of c_{s3} ($3.3 < c_{s3} < 3.9$) show the high level of dependence of sediment transport rates on velocity. Depth has comparatively less influence ($-0.34 < c_{s2} < 0.7$).

Table E-2. Power equations for total bed sediment discharge in sand- and fine-gravel-bed streams.

	$q_s = c_{S1} h^{c_{S2}} V^{c_{S3}}$							
	D_{50} (mm)							
	0.1	0.25	0.5	1.0	2.0	3.0	4.0	5.0
Gr = 1.0								
c_{S1}	3.30×10^{-5}	1.42×10^{-5}	7.6×10^{-6}	5.62×10^{-6}	5.64×10^{-6}	6.32×10^{-6}	7.10×10^{-6}	7.78×10^{-6}
c_{S2}	0.715	0.495	0.28	0.06	-0.14	-0.24	-0.30	-0.34
c_{S3}	3.30	3.61	3.82	3.93	3.95	3.92	3.89	3/87
Gr = 2.0								
c_{S1}		1.59×10^{-5}	9.8×10^{-6}	6.94×10^{-6}	6.32×10^{-6}	6.62×10^{-6}	6.94×10^{-6}	
c_{S2}		0.51	0.33	0.12	-0.09	-0.196	-0.27	
c_{S3}		3.55	3.73	3.86	3.91	3.91	3.90	
Gr = 3.0								
c_{S1}			1.21×10^{-5}	9.14×10^{-6}	7.44×10^{-6}			
c_{S2}			0.36	0.18	-0.02			
c_{S3}			3.66	3.76	3.86			
Gr = 4.0								
c_{S1}				1.05×10^{-5}				
c_{S2}				0.21				
c_{S3}				3.71				

Definitions: q_s, unit sediment transport rate in ft^2/s (unbulked); V, velocity in ft/s; h, depth in ft; $G_r = 0.5\ [(D_{84}/D_{50}) + (D_{50}/D_{16})]$ gradation coefficient.

For flow conditions within the range outlined in Table E-3, the regression equations should be accurate within 10%. The equations were obtained for steep sand- and gravel-bed channels under supercritical flow. They do not apply to cohesive material.

The equations assume that all sediment sizes are transported by the flow without armoring. The sediment concentration $c_{mg/l}$ is calculated from

$$c_{mg/l} = 2.65 \times 10^6 \frac{q_s}{q} \qquad \text{(E-9)}$$

where q_s is calculated from Equation E-8 and $q = V_h$ is the unit discharge in ft^2/s.

3 DESIGN AND ANALYSIS PROCEDURES

The following procedures may be used to determine: 1) sheet and rill erosion; 2) gully erosion; 3) calculated sediment yield; 4) measured sediment yield; 5) trap efficiency, and 6) sediment transport capacity of channels.

3.1 Sheet and Rill Erosion Procedure

The following sheet and rill erosion procedure based on the USLE may be used to determine soil erosion losses from upland erosion. If data are available, this approach should be supplemented with field measurements to properly calibrate and ascertain the accuracy of other procedures and/or computer models.

Step A-1. Gather topographic, soil type and land use information. Subdivide the domain into sub-watersheds. For each sub-watershed, determine: drainage area, runoff length, average slope, soil type, percentage of canopy cover and ground cover and any particular method of soil conservation practice.

Step A-2. Determine the mean annual rainfall erodibility factor R for the specific site location.

Step A-3. Determine, for each sub-watershed, the soil erodibility factor K from soil samples.

Step A-4. Determine the slope length-steepness factor LS from the runoff length and average slope.

Step A-5. Determine the cropping-management factor C from the ground and canopy cover data.

Table E-3. Range of parameters for the Simons-Li-Fullerton method.

Parameter	Value range
Froude number	1 - 4
Velocity	6.5 - 26 ft/s
Manning coefficient n	0.015 - 0.025
Bed slope	0.005 - 0.040
Unit discharge	10 - 200 ft/s
Particle size	$D_{50} \geq 0.062$ mm
	$D_{50} \leq 15$ mm

APPENDIX B

METHOD FOR DETERMINING SACRIFICIAL SLOPE REQUIREMENTS

1 INTRODUCTION

In many cases where tailings extend over a large area, slope lengths may be so long that extremely gentle slopes will be needed to provide long-term stability. Such gentle slopes may necessitate the use of very large amounts of soil, such that some of these slopes (with no tailings directly under them) may extend greatly beyond the edge of the tailings pile.

In such cases, licensees may be able to demonstrate that it is impractical to provide stability for 1,000 years and may choose to show that stability for less than 1,000 years, but for at least 200 years, is a more cost-effective option. Such a design may incorporate tailings embankment "out slopes," where there are no tailings directly under the soil cover. Such slopes, designed for less than the 1,000-year stability period, may be acceptable if properly justified by the licensee.

It should be emphasized that the staff considers that a 200-year sacrificial slope design should be used only in a limited number of cases and only when a design life of 1,000 years cannot be reasonably achieved. However, it should not be assumed that the design period should immediately jump from 1,000 to 200 years. The staff concludes that the selection of a design period should proceed in a stepwise fashion, with consideration given to intermediate design periods from 200-1,000 years. In determining a minimum design, a 200-year sacrificial slope design, as presented below, may be used. However, such a design has a considerable amount of uncertainty associated with its use, due to its development by extrapolation of a relatively limited data base. Therefore, the staff considers that the procedure should be used only after other reclamation designs have been considered. The staff considers that the procedures for justifying a design period of less than 1,000 years, as discussed in Appendix C, should be carefully followed to document that a 200-year sacrificial slope design is the best design that can be reasonably provided.

2 TECHNICAL BASIS

The long-term gully erosion process has the potential to destabilize an earthen embankment or soil cover constructed to prevent waste material release to the environment. Figures B-1 and B-2 present photographs of earthen embankments damaged by gullying. It was apparent to the staff that little criteria were available that assisted the designer in predicting the potential impacts of gullying processes to long-term stability of the waste material. The NRC thereby supported a series of studies to expand the knowledge base on the potential impacts of gullies on reclaimed impoundments and provide guidance for assuring the long-term stability of the waste.

In 1985, Falk et al. conducted a pilot study in an attempt to develop a procedure to predict the maximum depth a gully may incise into a tailing slope as a function of time. Falk characterized 16 reclaimed mine and/or overburden sites in Colorado and Wyoming that demonstrated incision

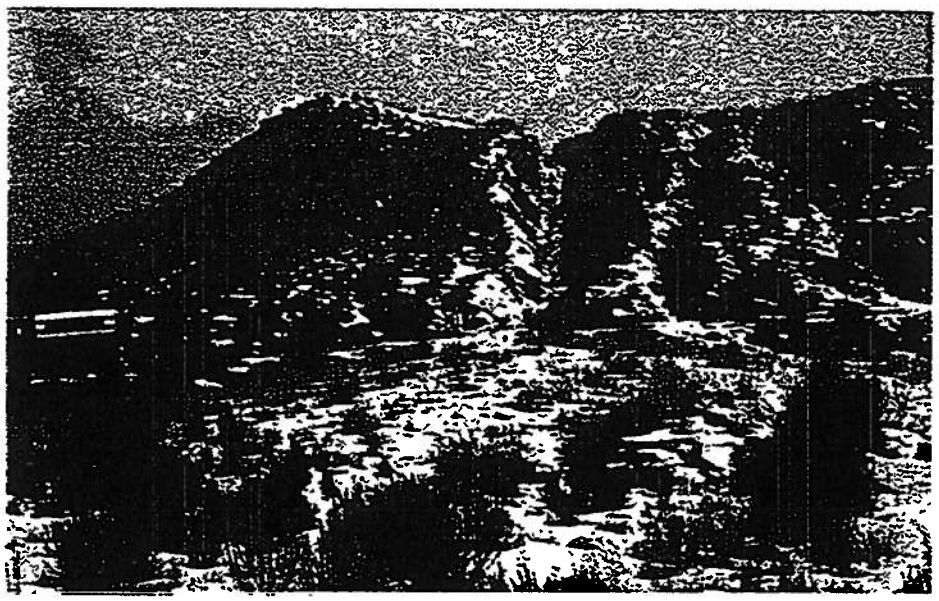

Figure B-1. Damage caused by gullying.

Figure B-2. Damage caused by gullying.

on the side slope and in some cases extended into the top slope areas. Field measurements included gully length, slope length, pile height, pile age, maximum gully depth, and width, tributary drainage area, vegetative cover and soil composition. From these data, Falk et al. attempted to formulate a procedure for estimating the maximum depth of incision, width of gully, and location of the maximum incision from the crest. The estimation procedure had a limited application but indicated that an estimation procedure could potentially be developed.

Pauley (1993) performed a series of flume studies in which near prototype soil embankments were constructed simulating a reclaimed waste impoundment. Figure B-3 presents a photograph of the flume used in the study. A series of rainfall and subsequent runoff events were conducted resulting in gully incision into the embankment. The gullying processes were documented as a function of rainfall duration and volume, soil type, embankment slope and the maximum depth of incision. The results of the study indicated that the gully incision depth was a function of the clay content of the soil, volume of runoff to the gully, and the embankment height (Abt et al. 1994). The gully processes observed by Pauley and later documented by Abt et al. (1995b) in the flume study closely paralleled those observed in the field by Falk (1985) and others.

In an attempt to expand the Falk et al. (1985) data base, Abt et al. (1995a) conducted a study in which 11 field sites that demonstrated gullying on reclaimed impoundments were located, characterized, measured, and sampled in the Colorado and Wyoming region and each gully was characterized (Falk et al. 1985).

The information presented by Falk et al. (1985), Pauley (1993) and Abt et al. (1995a) was consolidated into a composite data base as reported by Abt et al. (1995b). A comprehensive procedure was presented to estimate the maximum depth of gully incision, top width of the gully, and location of the maximum incision from the crest. The procedure allows the designer to determine gully depths and to predict the location of maximum gully incision.

A review of existing waste and tailing reclamation designs in conjunction with extensive site experience indicates that three primary embankment/cover configurations are commonly proposed. The three embankment configurations or types have been proposed or constructed as presented in Figure B-4. It is important to recognize that although each embankment type is similar along the main embankment face, the top slope, and subsequent potential tributary drainage, significantly impact the maximum depth of gully incision, D_{max}, that may intrude into the main slope. Therefore, a different procedure was developed to estimate the potential tributary drainage area and volume of runoff for each embankment type.

An empirical gully incision estimation procedure is presented as a function of the embankment/cover geometry, hydrologic parameters, soil composition, and the design life. It is anticipated that the estimation procedure will provide the user the maximum depth of gully incision, the approximate location of the maximum depth of incision along the embankment slope, and the approximate top width of the gully at the point of maximum incision as schematically presented in Figure B-5. The user will need to insure that the gully incision does not expose the waste/tailings materials.

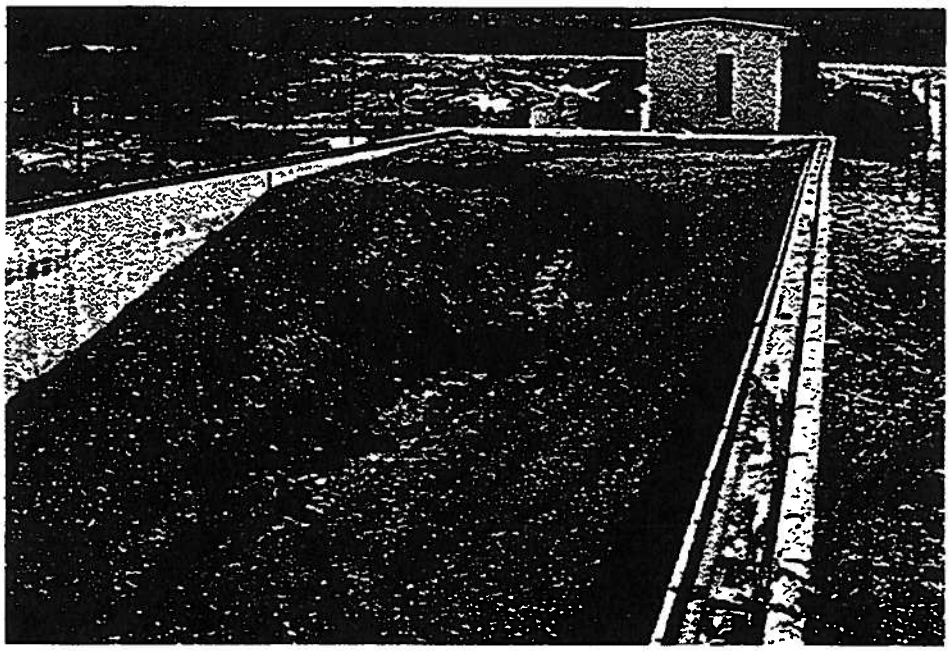

Figure B-3. Flume used by Pauley (1993).

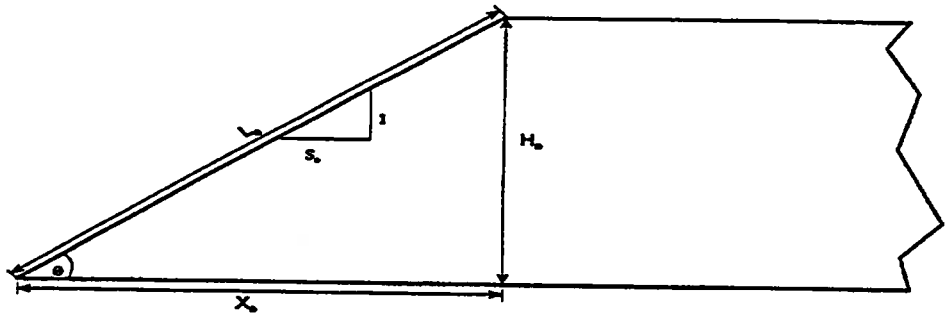

Type 1 Embankment

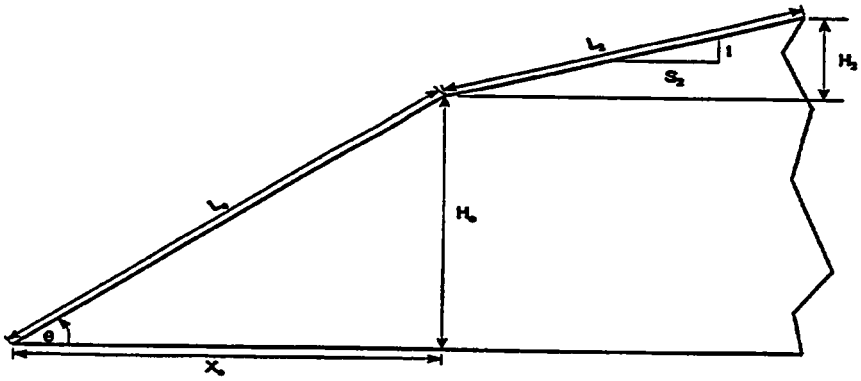

Type 2 Embankment

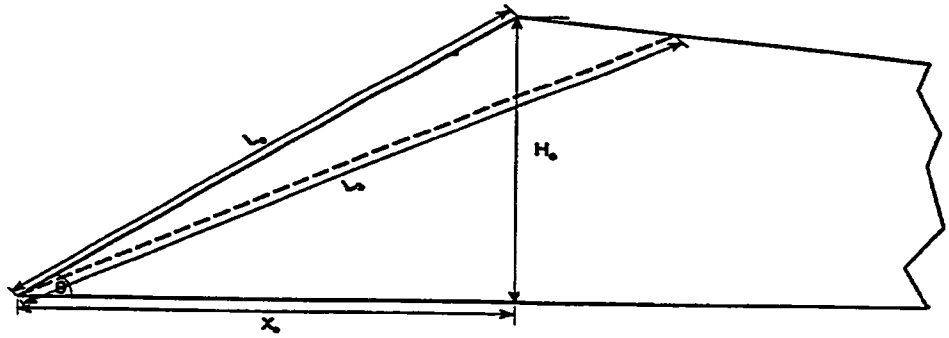

Type 3 Embankment

Figure B-4. Three types of embankment geometry.

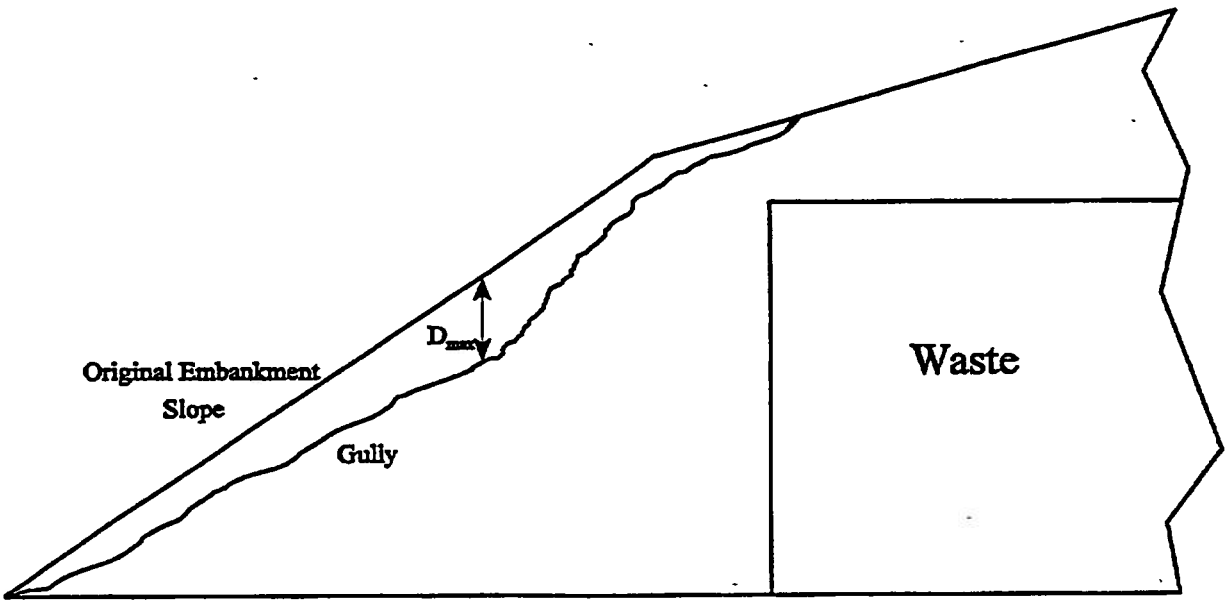

Figure B-5. Schematic of typical waste impoundment.

Staff review indicates that locating the depth of maximum gully incision is the most unpredictable part of the design procedure. The field data and flume data cannot be relied on totally to adequately describe the gully profile along the length of the slope. For example, the procedure may predict that the maximum gully depth will be 20 ft and will occur 500 ft from the embankment crest. However, not reflected in the design procedure is the possibility that the same gully could be 19 ft deep at the crest. The gully profile data available and staff experience suggest that gully depths approaching the maximum gully depth could occur near the crest. Thus, until more data are available, the staff recommends that the location of maximum gullying be assumed to occur near the crest of the slope. In addition, because of the need for significant data extrapolation, the staff suggests that this procedure be used to determine sacrificial slope requirements for a 200-year period.

In situations where increasing the set back distance of waste with respect to the embankment crest is not feasible, the concept of embankment stabilization utilizing launching riprap may be examined. Abt et al. (1997) presents a preliminary approach to the stabilization technique. Figure B-6 presents a photograph of a laboratory simulation of embankment stabilization using launching riprap. Based upon the findings of the pilot test series, a set of preliminary guidelines and a design procedure is outlined by Abt et al. (1997). The procedure presented represents the pilot test series and its application has not been tested and verified under field or near prototype conditions. It is recommended that the procedures outlined by Abt et al. (1997) be applied with a high degree of engineering judgement.

3 PROCEDURES

A procedure has been developed to estimate the effects of gullying over time. The following steps outline the estimation procedure.

Step 1. Determine the embankment design life as outlined in Appendix A. Stability of the embankment must be insured for periods ranging from 200 to 1,000 years.

Step 2. Select the embankment type (Type 1, Type 2, or Type 3) and determine values of the appropriate design variables.

Embankment/cover variables applicable to all three types of embankments include the embankment height (H_o) (m), slope length (L_o) (m), slope angle (θ) (degrees), and horizontal distance from the embankment toe to the crest (X_o) (m) as presented in Figure B-4.

Step 3. Determine the embankment/cover soil composition, expressed as a percentage of the sands, silts, and clays. Discriminating thresholds for gully intrusion potential for embankments are segmented into soils with clay content less than 15 percent, clay content between 15 and 50 percent, and clay content greater than 50 percent.

Step 4. Determine the average annual precipitation (P), expressed in meters, for the embankment site. Estimates of precipitation can be obtained from U.S. Weather Bureau isohyetal maps, local climatological data, or other appropriate means.

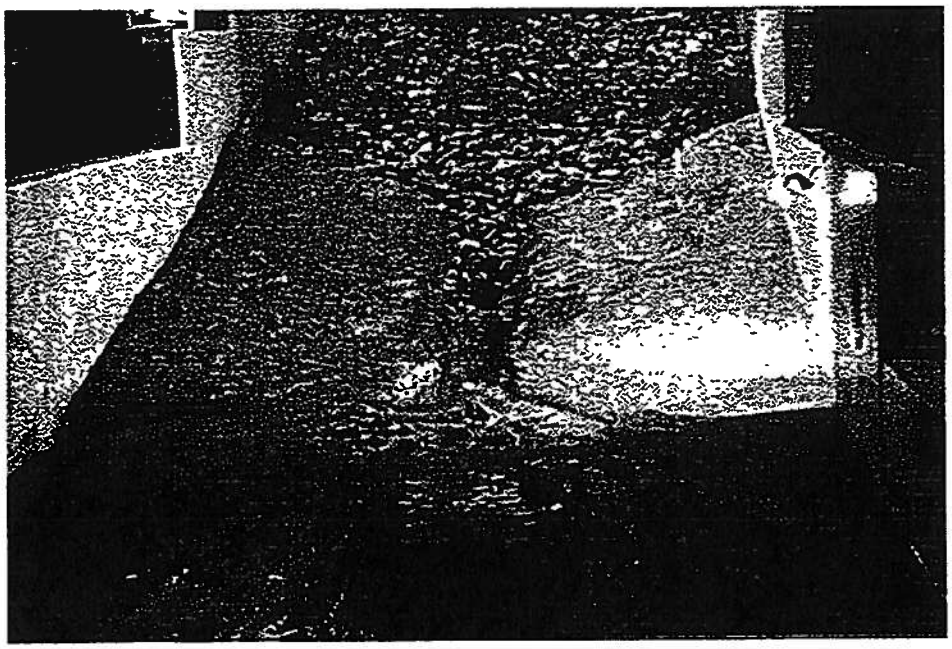

Figure B-6. Photograph of launching riprap flume test.

Step 5. Determine the drainage area tributary to the embankment to estimate the volume of runoff to which an embankment will be exposed in its design life. For embankments without external drainage basins, the tributary drainage area that forms on the face of the embankment will determine the total volume of runoff (Abt, Thornton, and Johnson, 1995b). The tributary drainage area that forms on the embankment face is a unique function of the type of embankment being evaluated.

Type 1 Embankment

The tributary drainage area for a Type 1 embankment may be estimated by

$$A = 0.276 * [L_o * \mathrm{Cos}(\theta)]^{1.636} \qquad \text{(B-1)}$$

where: A = tributary drainage area (m^2)
L_o = original embankment length (m)
θ = slope angle in degrees computed as $\mathrm{Tan}^{-1}(S_o)$

Type 2 Embankment

The tributary drainage area for a Type 2 embankment is computed by summing the embankment face length (L_o) and the embankment top length (L_2). The resulting length (L_t) is then entered in Equation B-1 as:

$$A = 0.276 * [L_t * \mathrm{Cos}(\theta)]^{1.636} \qquad \text{(B-2)}$$

where: A = tributary drainage area (m^2)
L_t = total length of embankment
θ = slope angle in degrees computed as $\mathrm{Tan}^{-1}(S_o)$

Type 3 Embankment

The tributary drainage area for a Type 3 embankment can be estimated using Equation B-1; however, an effective embankment length (L_3) must be determined. Flume and field observations indicate that a gully forming on a Type 3 embankment can extend past the crest and into the adverse slope. When this condition occurs, the effective length of the embankment is increased. To provide an estimate of the tributary drainage area at any point in time, the value of the effective embankment length is determined by estimating the final gully bottom slope. Abt et al. (1995b) reported that the gully bottom slope may be estimated as

$$S_b = [1.008 * S_o] - 0.063 \qquad \text{(B-3)}$$

where: S_b = gully bottom slope (rise/run)
S_o = original embankment slope (rise/run)

The effective embankment length can then be computed as:

$$L_3 = 1.175 * L_o \quad \text{(B-4)}$$

where L_o and L_3 are expressed in meters. The tributary drainage area can then be computed using Equation B-1 where L_3 is substituted for L_o.

In situations where the embankment toe is exposed to runoff that develops on a tributary drainage area external to the embankment, the supplemental area (A_x) is added to the drainage area value computed using Equation B-1.

Step 6. The total depth of precipitation to which the site may be exposed to over the design life needs to be determined. In Step 1, the design life of the embankment was estimated. The average annual precipitation for the project site was then estimated based on Step 4. The expected depth of precipitation, in meters, is then calculated as:

$$D_t = \text{Average Precipitation Depth (m)} * \text{Design Life (years)} \quad \text{(B-5)}$$

Step 7. The runoff to rainfall ratio, R_r, is needed to convert the potential depth of precipitation for the embankment design life to potential runoff tributary to the developing gully. The U.S. Geological Survey (USGS) developed a runoff map method (Gebert et al., 1989) to determine the average annual runoff expected from any location in the United States. The USGS map provides the user the annual depth of runoff from a site specific location. The ratio of the runoff to rainfall is computed by dividing the runoff depth derived from Gebert et al. by the average annual precipitation for the appropriate locale. The average runoff-ratio using the USGS Average Annual Runoff Method is 0.127. The runoff-rainfall ratio of 0.127 provides a reasonable estimate for the arid and semi-arid regions of the western United States.

Step 8. The cumulative volume of runoff (V_r) tributary to the embankment toe, in cubic meters, is calculated as:

$$V_r = D_t * R_r * A \quad \text{(B-6)}$$

where A is the tributary drainage area, expressed in square meters, as determined in Step 5. It is acknowledged that a single storm event will significantly impact the development of the gully. Abt et al. (1995a) indicates that the total volume of runoff can serve as a predictor of the ultimate dimensions (i.e., maximum depth, width, etc.)

of the gully. The volume of runoff tributary to the gully for the embankment design life is the primary element reflecting the analysis period.

Step 9. The maximum depth of gully incision (D_{max}) can be estimated as a function of the cumulative volume of runoff, V_r, the embankment height, H_o, the embankment slope length, L_0, L_2, or L_3, the embankment slope, and the clay content of the soil composition. A gully factor, G_f, was developed from the analysis described by Abt et al. (1994) for varying clay content of the proposed construction material. The gully factor is defined as:

$$G_f = \frac{D_{max}}{L_i * S_o} \tag{B-7}$$

where L_i is L_0, L_2, or L_3 as applicable and the embankment slope S_o, is H_o/X_o. The gully factor is computed as:

Clay content < 15%:

$$G_f = \frac{D_{max}}{L_o * S} = \frac{1}{2.25 + \left(0.789 * \frac{V_r}{H_o^3}\right)^{-0.55}} \tag{B-8}$$

Clay content > 15%, < 50%:

$$G_f = \frac{D_{max}}{L_o * S} = \frac{1}{2.80 + \left(0.197 * \frac{V_r}{H_o^3}\right)^{-0.70}} \tag{B-9}$$

Clay content > 50%:

$$G_f = \frac{D_{max}}{L_o * S} = \frac{1}{3.55 + \left(0.76 * \frac{V_r}{H_o^3}\right)^{-0.85}} \tag{B-10}$$

Step 10. The maximum depth of gully incision expected on the embankment slope may then be estimated as:

$$D_{max} = G_f * L_i * S \qquad \text{(B-11)}$$

where D_{max} is in meters.

Step 11. After the value of D_{max} is determined, the top width of the gully at the deepest incision can be calculated as:

$$W = \left(\frac{D_{max}}{0.61}\right)^{1.149} \qquad \text{(B-12)}$$

where: W = top width of gully (m)
D_{max} = depth of deepest gully incision (m)

Step 12. In some applications, it is important to estimate the location of the maximum gully incision to evaluate the stability of the embankment or the potential to penetrate into the waste storage area. The location of the maximum depth of incision, measured down slope from the crest, may be determined as:

$$D_l = 0.713 * \left(\frac{(V_r * S)}{L_i^3}\right)^{-0.415} \qquad \text{(B-13)}$$

where: D_l = location of D_{max}
V_r = cumulative volume of runoff (m^3)
S_o = original embankment slope (rise/run)
L_o = original embankment length (m)

Step 13. To provide a conservative estimate of the possible damage caused to an earthen embankment by a migrating gully, it is assumed that the maximum depth of gully intrusion occurs at the crest of the embankment. The embankment material is then assumed to erode, at the angle of repose of the embankment material, up slope of D_{max}. The set back distance of the waste material is determined for each of the three types of embankments by assuming the embankment erodes at the angle of repose.

Step 14. If altering the set back distance is not feasible, protection may be examined utilizing launching riprap. A detailed explanation of the launching riprap application is

presented by Abt et al. (1997). The following preliminary guidelines should be followed in a launching riprap application:

- The minimum riprap size should be determined using accepted riprap sizing criteria for overtopping flow. A minimum median stone size (D_{50}) of 9 cm was found to work well in flume studies.

- The protective riprap layer should have adequate volume to provide slope coverage under maximum expected gully conditions. A layer thickness of approximately 3 D_{50} is recommended, depending on the volume requirements and the length of the riprap layer.

4 RECOMMENDATIONS

The stable slope should be determined using the procedures presented in Appendix A. Appropriately conservative values of input parameters should be used in the computation. Additional refinements can be made after the analysis of the sacrificial slope requirements.

In analyzing Type 2 Embankments, the top slope of the cover should be much flatter (less than or equal to 5%) than the slope of the embankment face. The gully would likely occur far upstream from the crest if the top slope were steep. The following example is presented to outline the stability assessment procedure, not to promote or compare any embankment types.

5 EXAMPLE OF PROCEDURE APPLICATION

The following example is used to outline the procedure of stability analysis of a Type 2 Embankment. Type 2 Embankments, presented in Figure B-4, are identified by an embankment slope that transitions into a flatter top slope. Embankments constructed with Type 2 geometry are evaluated by superimposing the total length of the embankment, L_t, on the slope of the embankment face.

Step 1. Design Life

An embankment design life of 200 years will be evaluated.

Step 2. Embankment Geometry

Once the embankment type is determined, the initial design variables are required. It will be assumed that the embankment has the following physical dimensions:

H_o = embankment height	= 9 meters
L_o = embankment slope length	= 55 meters
S_o = embankment slope	= 0.15 rise/run
L_2 = top embankment length	= 100 meters
S_2 = top embankment slope	= 0.05 rise/run

Step 3. Soil Composition

It is assumed that a soil analysis has been conducted and that the embankment material is composed of 13 percent clay by volume, and has an angle of repose of 34 degrees.

Step 4. Precipitation

Local climatological data indicate an average annual precipitation of 0.20 meters for the site.

Step 5. Potential Tributary Drainage Area

The total potential tributary drainage area for a Type 2 Embankment is determined by computing the total embankment length as shown below

$$L_t = L_o + L_2 \qquad \text{(B-14)}$$

where: L_t = total embankment length (m)
L_o = length of embankment face (m)
L_2 = length of embankment top slope (m)

The value determined for the total embankment length is then combined with the slope of the embankment face and entered into Equation B-2 as shown below

$$A = 0.276 * \{155 \text{ meters} * \cos(8.53)\}^{1.636}$$
$$A = 1038 \text{ meters}^2 \qquad \text{(B-15)}$$

Therefore, the total potential tributary drainage area for the Type 2 Embankment is 1038 square meters. It is assumed that there is no additional drainage area external to the embankment.

Step 6. Potential Depth of Precipitation

The first step in computing the total runoff volume for the site is to determine the potential depth of precipitation, D_t, that the site will be exposed to during the design life. As described in Step 6, the total depth of precipitation is the product of the average annual precipitation and the design life. Therefore,

$$D_t = 0.20 \text{ meters/year} * 200 \text{ years}$$

$$D_t = 40.0 \text{ meters of precipitation} \qquad \text{(B-16)}$$

and a potential depth of precipitation of 40.0 meters is computed.

Step 7. Runoff to Rainfall Ratio

A value of 0.13 is assumed as the average runoff to rainfall ratio, R_r, for the embankment area.

Step 8. The cumulative volume of runoff, V_r, is defined as the product of the potential depth of precipitation, D_t, the runoff to rainfall ratio, R_r, and the potential tributary area, A. Substituting the values of D_t, R_r and A_t obtained above into Equation B-6 yields

$$V_r = 40.0 \text{ meters} * 0.13 * 1038 \text{ meters}^2$$

$$V_r = 5{,}400 \text{ meters}^3 \qquad \text{(B-17)}$$

Therefore, the embankment slope will drain approximately 5,400 cubic meters of runoff during the 200 year design life.

Step 9. Determination of Gully Factor

The gully factor, G_f, for the embankment should be determined as outlined in Step 9. A clay content of 13 percent in the embankment material requires that Equation B-8 be used to calculate the gully factor. Substituting values for H_o and V_r into Equation B-8 gives

$$G_f = \frac{1}{2.25 + \left[0.789 * \left\{\frac{5{,}399.97 \text{ meters}^3}{(9.0 \text{ meters})^3}\right\}\right]^{-0.55}} \qquad \text{(B-18)}$$

$$G_f = 0.380$$

Step 10. Maximum Depth of Gully Incision

A gully factor of 0.380 is entered into Equation B-8 to determine the maximum depth of gully incision as follows

$$D_{max} = 0.380 * 55.0\text{meters} * 0.15$$
$$D_{max} = 3.14 \text{ meters} \qquad \text{(B-19)}$$

Thus, after a 200 year period, a gully incision 3.14 meters deep would be expected on the face of the embankment.

Step 11. Gully Top Width

Equation B-12 presents an empirical relationship that can be used to predict gully top width, W, as a function of maximum gully incision, D_{max}. Substituting the value of 3.14 meters computed for D_{max} into Equation B-12 gives

$$W = \left(\frac{3.14 \text{ meters}}{0.61}\right)^{1.149}$$
$$W = 6.57 \text{ meters} \qquad \text{(B-20)}$$

therefore, 6.33 meters would be the estimated gully width at the point of deepest gully incision.

Step 12. Location of Maximum Depth

Equation B-13 presents an empirical relation predicting the location of D_{max} as a function of the total volume of runoff, embankment length, and embankment slope. Substituting the values determined above into Equation B-13 gives

$$D_l = 0.713 * \left\{\frac{(5{,}399.97 \text{ meters}^3 * 0.15)}{(55 \text{ meters})^3}\right\}^{-0.415}$$
$$D_l = 6.50 \qquad \text{(B-21)}$$

which represents the number of D_{max}'s down slope from the crest the deepest incision is expected to occur. To determine the location in meters, multiply the value determined for D_l by that determined for D_{max}. For this example the deepest incision point will occur approximately 20.4 meters down slope from the embankment crest.

Summarizing the results obtained above yields

$$D_{max} = 3.14 \text{ meters,}$$

$$W = 6.57 \text{ meters}$$

$$D_1 = 20.4 \text{ meters}$$

However, for long-term stability applications, the location of D_{max} should be assumed to be at the crest of the slope.

Step 13. Set Back Distance

For conservatism, the maximum depth of incision is assumed to occur at the crest of the embankment and the material is assumed to erode at the angle of repose (34^0 for this example) upstream of the crest. For the conditions of this example, the set back distance would be 4.66 meters up slope from the crest of the embankment. Therefore, tailings should be located a minimum horizontal distance of 4.66 meters up slope and a vertical distance of 4.71 meters down from the embankment crest.

Step 14. Rock Launching Application

If providing adequate setback distance is not feasible, embankment stabilization with launching rock may be considered. For details and a preliminary application procedure, see Abt et al. (1997). The findings discussed by Abt et al. (1997) should be adapted to each specific site with engineering judgement. In general, a volume of rock should be provided to cover the collapsed slope with a rock layer of 1.5 times the D_{50} size, considering the depth of gully intrusion and the length. It is recommended that the required D_{50} size be specifically determined for a collapsed slope of 1V to 2H. Figure B-7 presents a schematic of the rock launching application concept.

The results of the example outlined above can then be checked with the original design of the soil cover, as described in Appendix A. Engineering judgment then determines if the design is adequate to provide the level of protection necessary throughout the design life.

6 COMPUTER APPLICATION

To aid in the analysis of the stability assessment, a computer program has been developed. The Windows™ application provides an automated method of evaluating the stability procedure described above (Thornton, 1996). The program is available from the U.S. Nuclear Regulatory

Two basic approaches exist for the design of suitable erosion-resistant covers for a tailings impoundment surface as originally described by Nelson et al. (1983). The first approach consists of providing a cover material that will resist material transport by flowing water using the concept of critical shear stress. The second approach is based on the Universal Soil Loss Equation, an empirical method originally developed during the 1930's. The methodologies involved with both of these methods are discussed below.

5.1.1 Critical Shear Stress Approach

The critical shear stress approach consists of providing a cover material with a d_{30} grain size (i.e., 70% of the material by weight is coarser than the d_{30}) that will resist movement when subjected to the sheet flow maximum permissible velocity resulting from the application of the PMP over the entire impoundment surface. Minimum d_{30} grain sizes should be determined using the critical shear stress approach similar to the procedures discussed in Simons and Senturk (1977) applicable to overland flow. A numerical solution for selecting an appropriate d_{30} to provide armoring has been developed by Shen and Lu (1983).

The design approach described above, in which the critical grain size is selected to resist the onset of sheet erosion, should evaluate the runoff from PMP storms of different durations, such as 0.5, 1, 2, 4, and 6 hours to select the maximum d_{30} required. Rainfall depths will usually be based on 2.5 to 15 minute durations for small drainage basins as presented in Section 2.1.2. Typically, the minimum construction layer thickness is specified to be at least two times the maximum particle size. If the above approach results in a cover thickness less than about 6 inches, then other considerations - such as nonuniform placement of cover and particle breakdown due to handling, placement and weathering - would suggest that a minimum cover thickness of 10 inches should be considered. If a self-armoring cover can be provided, and there is no major concern for weathering of the cover material, the design is independent of time and the cover should remain intact indefinitely.

5.1.2 Soil Loss Equation Approach

The concept of sheet erosion was recognized by early researchers and the Universal Soil Loss Equation (USLE) was developed in the late 1930's by the Agricultural Research Service to evaluate soil conservation practices for cropland throughout the United States. After its inception, the soil loss procedure was used and modified as field experience and data were obtained incorporating the basic parameters of field slope and length, precipitation, and crop management to estimate soil losses on an annual basis. Application of the USLE to non-cropland areas and specifically for construction sites became feasible when Wischmeier et al. (1971), using basic soil loss characteristics, developed and implemented a soil erodibility factor (K) in the soil loss computation. Subsequent efforts refined the parameters used in the USLE for mining and construction activities in the interior western United States.

The Modified Universal Soil Loss Equation (MUSLE) was developed by the Utah Water Research Laboratory in 1978 for the principal objective of estimating soil losses due to highway construction activities. Alterations were made to the USLE to accomodate unique or special conditions encountered in highway construction, including steep and deep cuts and fill slopes that could cause erosion affecting adjacent or nearby roadways, streams, lakes, or inhabited areas. It is apparent that the modifications made to the USLE extend to many construction and mining sites beyond the scope of highway construction.

The Modified Universal Soil Loss Equation (MUSLE) is a mathematical model based on field determined coefficients and provides the most rational approach to evaluate the long-term erosion potential from an upland area similar to that of the area covering a reclaimed tailings pond. Recent investigations into appropriate methods of modeling major types of sheet erosion (Abt and Ruff, 1978; Nelson et al. 1983; Nyhan and Lane, 1983; and NRC, 1983), indicate that although more rigorous mathematical models are available to simulate erosion as a function of time, the use of the USLE has a strong precedent because it has a 40-year history of runoff and soil loss data.

The MUSLE is used to evaluate average soil losses for certain types of slopes as a function of time. The MUSLE does not consider the potential for gully development or intrusion as discussed in Chapter 4 because the topographic features of the tailings area are assumed to remain constant with time. Also, the MUSLE does not incorporate the concept of the PMP but rather a rainfall factor based on historical rainfall values. The MUSLE is defined by Clyde et al. (1978) as follows:

$$A = R\ K\ (LS)\ (VM) \qquad (5.1)$$

where,

A = the computed loss per unit area in tons per acre per year with the units selected for K and R properly selected;

R = the rainfall factor which is the number for rainfall erosion index units plus a factor for snowmelt, if applicable;

K = the soil erodibility factor, which is the soil loss rate per erosion index unit for a specified soil as measured on a unit plot that is defined as a 72.6-ft length of uniform 9% slope continuously maintained as clean tilled fallow;

LS = the topographic factor, which is the ratio of soil loss from the field slope length to that from a 72.6-ft length under otherwise identical conditions;

VM = the dimensionless erosion control factor relating to vegetative and mechanical factors. This factor replaces the cover management factor (C) and the support factor (P) of the original USLE.

5.1.2.1 The Rainfall and Runoff Factor (R)

As noted by previous research at Los Alamos National Laboratory (Nyhan and Lane, 1983), the R factor as used in the MUSLE is often misinterpreted only as a rainfall factor. In reality, it must quantify both the raindrop impact and provide information on the amount and rate of runoff likely to be associated with the rain. More specifically, the R factor is described in terms of a rainfall storm energy (E) and the maximum 30-minute rainfall intensity (I_{30}). Generalized R factors applicable to the interior western United States are given in Table 5.1. For R factors in specific areas of the United States, it is recommended that erosion index distribution curves be obtained from local SCS offices.

Table 5.1. Generalized Rainfall and Runoff (R) Values.

State	Eastern Third	Central Third	Western Third
N. Dakota	50 - 75	40 - 50	40
S. Dakota	75 - 100	50	40
Montana	30 - 40	20	20 - 50
Wyoming	30 - 50	15 - 30	15 - 25
Colorado	75 - 100	40 - 50	20 - 40
Utah	20 - 30	20 - 50	15 - 40
New Mexico	75 - 100	40 - 50	20 - 40
Arizona	20 - 50	20 - 50	25 - 40

5.1.2.2 The Soil Erodibility Factor (K)

The soil erodibility factor (K) recognized the fact that the erodibility potential of a given soil is dependent on its compositional makeup, which in turn reflects the grain size distribution of the soil. To predict soil erodibility, five soil characteristics that include the percent silt and fine sand, percent sand greater than 0.1 mm, percent organic material, general soil structure and general permeability are determined. The K factor is then found by using the Wischmeier nomograph presented in Figure 5.1.

The makeup of the various soil fractions presented in Figure 5.1 is based on separating sand and silt at the 0.1 mm size. This differs from the Unified Soil Classification System which uses the No. 200 sieve size (0.075 mm) for the separation between sand and silt. The value to enter Figure 5.1 with should be the percentage of material finer than 0.1 mm in size, not the percentage passing the No. 200 sieve. Also, the determination of the Soil Erodibility Factor (K) as shown on Figure 5.1 does not specifically reference the percentage of clay (finer than 0.002 mm) contained in the material. The percentage of silt plus very fine sand to be used for Figure 5.1, therefore, is the percentage of material contained between 0.002 mm and 0.1 mm.

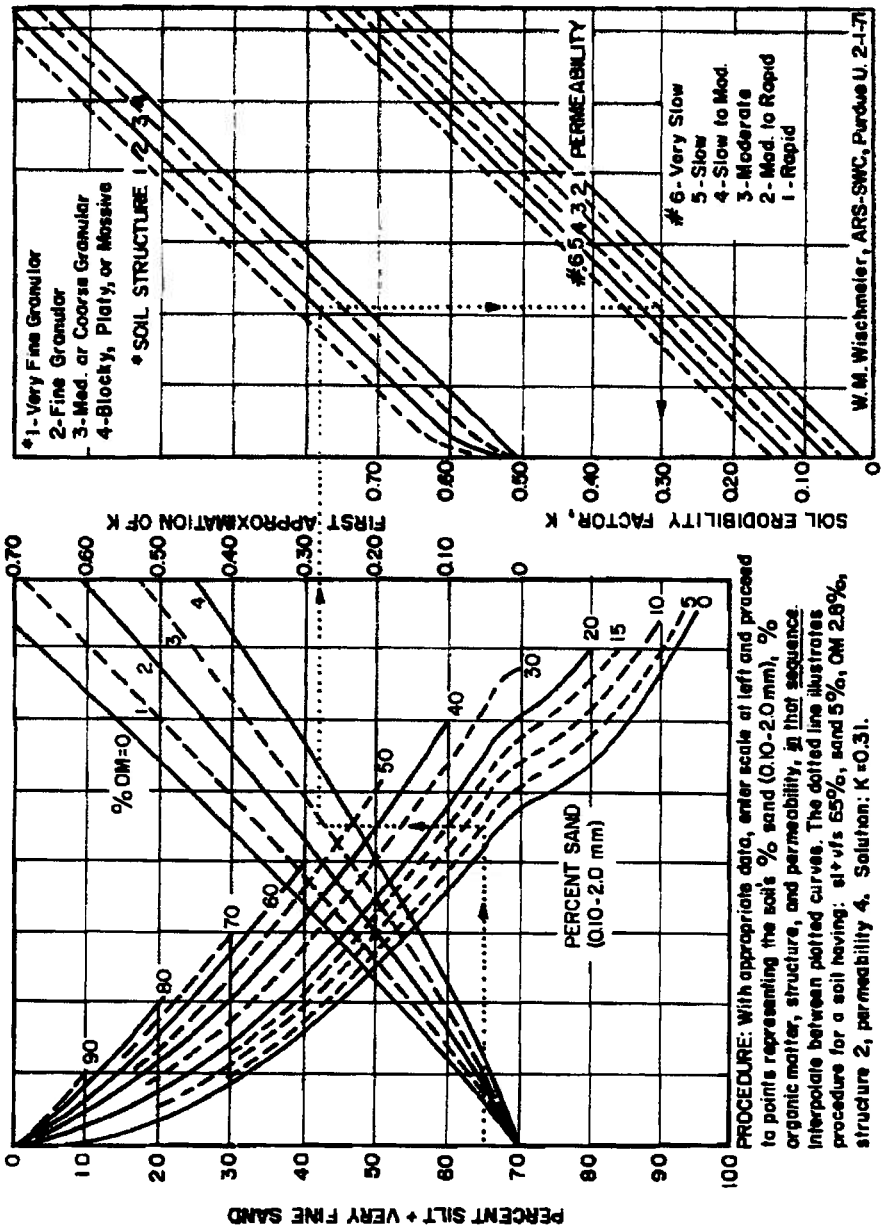

Fig. 5.1. Nomograph for determining soil erodibility factor *K*. *Source:* after Wischmeier et al., 1971.

5.1.2.3 The Topographic Factor (LS)

Although the effects of both length and steepness of slope have been investigated separately in different research efforts, it is more convenient for analytical purposes to combine the two into one topographic factor, LS. Wischmeier and Smith (1978) developed plots correlating the topographic factor for slopes up to 500 meters in length at slope inclinations from 0.5% up to 50%. Note that flat, short slopes will have less erosion than long, steep slopes and it is to the benefit of the design engineer to optimize slope length and gradients to fit the topography.

The equation to determine the LS factor is as follows:

$$LS = \frac{650 + 450s + 6s^2}{10{,}000 + s^2} \quad \frac{L}{72.6}^{m} \qquad (5.2)$$

where LS = topographic factor
L = slope length in feet
s = slope steepness in percent
m = exponent dependent upon slope steepness

The slope dependent exponent m is presented in Table 5.2.

Table 5.2 Slope Dependent Exponent

Slope (percent)	m
$s \leq 1.0$	0.2
$1.0 < s \leq 3.0$	0.3
$3.0 < s \leq 5.0$	0.4
$5.0 < s \leq 10.0$	0.5
$s > 10.0$	0.6

5.1.2.4 The VM Factor

The VM factor is the erosion control factor applied in place of the cover and erosion control factors found in the USLE. The erosion control factor accounts for measures implemented at the construction site to include vegetation, mulching, chemical treatments and sprayed emulsions to impede or reduce erosion due to the overland flow of water. Values of the VM factor relative to site-specific conditions are presented in Table 5.3.

The VM factor is perhaps the most sensitive factor to effect the computed erosion loss for a given site. As shown by the values presented

on Table 5.3, the development of a permanent vegetative cover can have a significant impact in reducing the computed erosion loss. However, the effectiveness of a vegetative cover over long-term periods should be questioned unless other protective schemes, such as armoring of the cover with the proper size material, are also included in the design.

5.1.2.5 Example Problem

An example problem in how to use the MUSLE is provided below.

Assumptions:

Site location:	Western Colorado
Site description:	Uncovered tailings pond
Pond size:	160 acres
Slope:	3%
Length:	2500 ft
Material:	42% sand greater than 0.10 mm; 58% fine sand and silt less than 0.10 mm; 5% clay less than 0.002 mm; 0% organics; (53% silt plus fine sand less than 0.1 mm); Consistency - fine granular; Permeability - slow to moderate.

The following factors have been determined for use in Equation 5.1.

R = 20 from Table 5.1

K = 0.50 from Figure 5.1

LS = 0.747 from Equation 5.2 and Table 5.2

VM = 1.0 (average from Table 5.3 based on an undisturbed surface)

Using Equation 5.1, the annual soil loss (A) from the tailings pond due to sheet erosion caused by flowing water is computed to be 7.47 tons/acre/year, or 1195 tons/year from the facility. Therefore, the cover is estimated to erode at a rate of 0.003 ft per year, or 0.3 ft/century.

5.2 SUMMARY AND FUTURE STUDIES

The main application of the soil loss equation approach in the evaluation of cover integrity is to determine whether it is possible for sheet erosion to penetrate the tailings cover, thereby exposing bare tailings and constituting a failure of the cover. The followup study will concentrate

Table 5.3. Typical VM Factor Values Reported in the Literature.[a]

Condition	VM Factor
1. Bare soil conditions	
freshly disked to 6-8 inches	1.00
after one rain	0.89
loose to 12 inches smooth	0.90
loose to 12 inches rough	0.80
compacted bulldozer scraped up and down	1.30
same except root raked	1.20
compacted bulldozer scraped across slope	1.20
same except root raked across	0.90
rough irregular tracked all directions	0.90
seed and fertilizer, fresh	0.64
same after six months	0.54
seed, fertilizer, and 12 months chemical	0.38
not tilled algae crusted	0.01
tilled algae crusted	0.02
compacted fill	1.24 - 1.71
undisturbed except scraped	0.66 - 1.30
scarified only	0.76 - 1.31
sawdust 2 inches deep, disked in	0.61
2. Asphalt emulsion on bare soil	
1250 gallons/acre	0.02
1210 gallons/acre	0.01 - 0.019
605 gallons/acre	0.14 - 0.57
302 gallons/acre	0.28 - 0.60
151 gallons/acre	0.65 - 0.70
3. Dust binder	
605 gallons/acre	1.05
1210 gallons/acre	0.29 - 0.78
4. Other chemicals	
1000 lb. fiber Glass Roving with 60-150 gallons asphalt emulsion/acre	0.01 - 0.05
Aquatain	0.68
Aerospray 70, 10 percent cover	0.94
Curasol AE	0.30 - 0.48
Petroset SB	0.40 - 0.66
PVA	0.71 - 0.90
Terra-Tack	0.66
Wood fiber slurry, 1000 lb/acre fresh[b]	0.05
Wood fiber slurry, 1400 lb/acre fresh[b]	0.01 - 0.02
Wood fiber slurry, 3500 lb/acre fresh[b]	0.10
5. Seedings	
temporary, 0 to 60 days	0.40
temporary, after 60 days	0.05
permanent, 0 to 60 days	0.40
permanent, 2 to 12 months	0.05
permanent, after 12 months	0.01
6. Brush	
7. Excelsior blanket with plastic net	0.04 - 0.10

[a]Note the variation in values of VM factors reported by different researchers for the same measures. References containing details of research which produced these VM values are included in NCHRP Project 16-3 report, "Erosion Control During Highway Construction. Vol. III. Bibliography of Water and Wind Erosion Control References," Transportation Research Board, 2101 Constitution Avenue, Washington, DC 20418.

[b]This material is commonly referred to as hydromulch.

on using the MUSLE for several alternate cover designs in order to evaluate whether the proposed analytical approach can be successfully used to measure the long-term integrity of protective soil covers for uranium tailings reclamation. Alternative designs will be compared, both from a standpoint of overall integrity and construction difficulty. The covers will also be evaluated using the critical shear stress approach to determine, based on a given PMP, the minimum particle size necessary to protect the cover against long-term degradation.

JACOBS	Calculation No: C-05	Page 1 of 35
Calculation Cover Sheet	Rev. No.:0	Revision Date: 01/09/08
(Ref. FOWI 116 Design Calculations)	Previous Revision Date:	Current Revision Date:
Issuing Department: *Federal Operations Design Engineering*	Supersedes:	
Client: Energy Solutions Project Title: Moab UMTRA Project Number: 35DJ2600 System:	Engineering Discipline: Civil	
Calculation Title: Radon Barrier Evaluation		

Purpose:

- Part 40 of the United States *Code of Federal Regulations*, section 192.02 (40 CFR 192.02) requires that control of radioactive materials and their listed constituents shall be designed to provide reasonable assurance that release of radon-222 from residual radioactive material (RRM) to the atmosphere will not exceed an average of 20 picocuries per square meter per second (pCi/m^2/sec), averaged over the entire cover top slope.
- The cover of the Crescent Junction Disposal Cell must be sufficient to provide isolation of tailings and control of radon emanation for the period of up to one thousand years, to the extent reasonably achievable, and, in any case, for at least 200 years.
- This calculation establishes the dimensions and input parameters for design of the Crescent Junction Disposal Cell radon barrier that will provide the requisite reasonable assurance of performance.

NQA-1 QUALITY LEVEL: 2

Prepared by: Bob Yager Robert E. Yager Date: 01/09/08

Checked by: Bill Barton Bill Barton Date: 1/25/08

Engineering Managers Approval: Bill Barton Date: 1/25/08

The current applicable version of this publication resides on Jacobs' Intranet. All copies are considered to be uncontrolled.
Copyright© Jacobs Engineering Group Inc., 2007

Revision History:

Pages Affected By Revision	Revised/Added/Deleted	Description of Revision
All		

The current applicable version of this publication resides on Jacobs' Intranet. All copies are considered to be uncontrolled.
Copyright© Jacobs Engineering Group Inc., 2007

Description of Calculation:

- Site-specific data for the RRM, which includes tailings, contaminated soils, mill debris, and other contaminated materials, and for the native cover materials were developed through thorough field investigations and laboratory testing programs (Golder 2006a, Remedial Action Plan calculations referenced herein). These site-specific data are presented in summary tables in Appendix B.
- The Uranium Mill Tailings Remedial Action (UMTRA) checklist cover was evaluated. This consists of an interim cover and a compacted-clay radon barrier.
- The Nuclear Regulatory Commission (NRC) computer code RADON (NRC 1989a) was used to calculate the optimum radon-barrier thickness, given the specific input parameters for two model runs with different radium activities in the waste. The estimated radon release rate was also calculated for the barrier thickness selected in the preferred design assuming that the radium activity would be monitored as it is placed to ensure a radium activity of 707 pCi/g or less in the upper 7 feet of the waste.

Assumptions:

- Tailings activity will be monitored as they are placed to ensure that no high activity material is placed in the upper layers of the waste cell. The upper layer is assumed to have an activity of 707 pCi/g (the mean of all the samples collected from the tailings pile) and the lower layer is assumed to have an activity of 1,349 pCi/g (the mean of the samples collected from the slimes). It is anticipated that the cover design will be re-evaluated during construction using actual as-placed source material activities and properties to ensure the cover is optimized for as-built conditions.
- The maximum tailings thickness will be 43 feet.
- Bottom-boundary radon flux is equal to zero, as per the Technical Approach Document (TAD) (DOE 1989).
- Ambient air radon concentrations were assumed to equal the conservative default value of zero, no local ambient air radon concentration data were available. Should these data become available prior to construction, these measured values should be considered in evaluation of the final cover design.
- The cell side slopes will be constructed of dikes made from clean fill to thicknesses far in excess of the cover and with properties comparable to the cover material; therefore, radon flux through the side slopes was not modelled.
- Following UMTRA precedence, materials above the radon barrier (e.g., frost protection layers, riprap, or rock mulch erosion-protection layers) were not modelled. These overlying materials provide additional radon attenuation. This conservative assumption enhances the reasonable assurance that the barrier as designed will provide the requisite protection and long-term performance.
- A clean-fill interim cover with a minimum thickness of 1 foot (ft) will be placed over the tailings as a best management practice.

The current applicable version of this publication resides on Jacobs' Intranet. All copies are considered to be uncontrolled.
Copyright© Jacobs Engineering Group Inc., 2007

- Physical properties of the cover materials are adequately represented by the characterization data.
- RADON model (NRC 1989a) default values for radon-emanation coefficient (0.35) are assumed conservative and appropriate.
- Capillary breaks, drainage layers/biointrusion layers were assumed to have insignificant impact on radon attenuation, given their large pore size and low long-term moisture content. Therefore, these layers have conservatively been omitted from the RADON model runs.

The current applicable version of this publication resides on Jacobs' Intranet. All copies are considered to be uncontrolled.
Copyright© Jacobs Engineering Group Inc., 2007

Design Inputs:

See following pages.

Software:

Title	Developer	Versions	Revision Level
RADONC	NRC	1.2	

The current applicable version of this publication resides on Jacobs' Intranet. All copies are considered to be uncontrolled.
Copyright© Jacobs Engineering Group Inc., 2007

Calculation Section:

See following pages.

The current applicable version of this publication resides on Jacobs' Intranet. All copies are considered to be uncontrolled.
Copyright© Jacobs Engineering Group Inc., 2007

Conclusions/Recommendations:

See following pages.

Reference:

See following pages.

The current applicable version of this publication resides on Jacobs' Intranet. All copies are considered to be uncontrolled.
Copyright© Jacobs Engineering Group Inc., 2007

Problem Statement:

- Part 40 of the United States *Code of Federal Regulations*, section 192.02 (40 CFR 192.02) requires that control of radioactive materials and their listed constituents shall be designed to provide reasonable assurance that release of radon-222 from residual radioactive material (RRM) to the atmosphere will not exceed an average of 20 picocuries per square meter per second (pCi/m^2/sec), averaged over the entire cover top slope.
- The cover of the Crescent Junction Disposal Cell must be sufficient to provide isolation of tailings and control of radon emanation for the period of up to one thousand years, to the extent reasonably achievable, and, in any case, for at least 200 years.
- This calculation establishes the dimensions and input parameters for design of the Crescent Junction Disposal Cell radon barrier that will provide the requisite reasonable assurance of performance.

Method of Solution:

- Site-specific data for the RRM, which includes tailings, contaminated soils, mill debris, and other contaminated materials, and for the native cover materials were developed through thorough field investigations and laboratory testing programs (Golder 2006a, Remedial Action Plan calculations referenced herein). These site-specific data are presented in summary tables in Appendix B.
- The Uranium Mill Tailings Remedial Action (UMTRA) checklist cover was evaluated. This consists of an interim cover and a compacted-clay radon barrier.
- The Nuclear Regulatory Commission (NRC) computer code RADON (NRC 1989a) was used to calculate the optimum radon-barrier thickness, given the specific input parameters for two model runs with different radium activities in the waste. The estimated radon release rate was also calculated for the barrier thickness selected in the preferred design assuming that the radium activity would be monitored as it is placed to ensure a radium activity of 707 pCi/g or less in the upper 7 feet of the waste.

Assumptions:

- Tailings activity will be monitored as they are placed to ensure that no high activity material is placed in the upper layers of the waste cell. The upper layer is assumed to have an activity of 707 pCi/g (the mean of all the samples collected from the tailings pile) and the lower layer is assumed to have an activity of 1,349 pCi/g (the mean of the samples collected from the slimes). It is anticipated that the cover design will be re-evaluated during construction using actual as-placed source material activities and properties to ensure the cover is optimized for as-built conditions.
- The maximum tailings thickness will be 43 feet.
- Bottom-boundary radon flux is equal to zero, as per the Technical Approach Document (TAD) (DOE 1989).
- Ambient air radon concentrations were assumed to equal the conservative default value of zero, no local ambient air radon concentration data were available. Should these data become available prior to construction, these measured values should be considered in evaluation of the final cover design.
- The cell side slopes will be constructed of dikes made from clean fill to thicknesses far in excess of the cover and with properties comparable to the cover material; therefore, radon flux through the side slopes was not modeled.

The current applicable version of this publication resides on Jacobs' Intranet. All copies are considered to be uncontrolled.
Copyright© Jacobs Engineering Group Inc., 2007

- Following UMTRA precedence, materials above the radon barrier (e.g., frost protection layers, riprap, or rock mulch erosion-protection layers) were not modeled. These overlying materials provide additional radon attenuation. This conservative assumption enhances the reasonable assurance that the barrier as designed will provide the requisite protection and long-term performance.
- A clean-fill interim cover with a minimum thickness of 1 foot (ft) will be placed over the tailings as a best management practice.
- Physical properties of the cover materials are adequately represented by the characterization data.
- RADON model (NRC 1989a) default values for radon-emanation coefficient (0.35) are assumed conservative and appropriate.
- Capillary breaks, drainage layers/ biointrusion layers were assumed to have insignificant impact on radon attenuation, given their large pore size and low long-term moisture content. Therefore, these layers have conservatively been omitted from the RADON model runs.

Calculation:

- The mean value (x_{mean}) of any parameter is calculated by the equation:

$$x_{mean} = \sum \frac{x_i}{n}$$

where: x_i = the ith value, and
n = the total number of values.

- The standard deviation (s) of a set of values is calculated by the equation:

$$s = \sqrt{\sum \frac{(x_i - x_{mean})^2}{n-1}}$$

- Porosity (η) of a sample is calculated from the equation:

$$\eta = 1 - \frac{(dry_bulk_unit_weight)}{(specific_gravity) * (unit_weight_of_water)}$$

where the unit weight of water is 62.4 pounds per cubic foot (pcf) (l g/cc)

- Radon (^{222}Rn) Diffusion coefficients were calculated using equation 9 from Rogers and Nielson (1991) as follows:

$$D = D_a \eta \exp(-6m\eta - 6m^{14\eta})$$

where: D = the calculated ^{222}Rn diffusion coefficient
D_a = the ^{222}Rn diffusion coefficient in air (1.10×10^{-5} m^2/s)
η = the porosity of the individual material

The current applicable version of this publication resides on Jacobs' Intranet. All copies are considered to be uncontrolled.
Copyright© Jacobs Engineering Group Inc., 2007

m = moisture saturation fraction of the material

$$m = 10^{-2} \frac{\rho w}{\eta \rho_w}$$

where: ρ = dry bulk density of the material
w = average term average moisture content of the material (dry weight %)
ρ_w = 1 (density of water)

- The density of a sample in g/cc is converted to pcf by multiplying the unit weight of water (62.4 pcf).
- The Rawls & Brakensiek equation referenced in the NRC Regulatory Guide 3.64 (NRC 1989b) can be used to estimate the 15 bar moisture content (θ) as a reasonable lower bound of long-term moisture content. The equation is:

$$\theta = 0.026 + 0.005z + 0.0158y$$

where: z = percent clay in the soil
y = percent organic matter in the soil

For example, the calculated 15 bar moisture content of the alluvial site materials, which have a mean clay content of 18.63 percent and a mean organic matter content of 0.28 percent is:

$$\theta = 0.026 + 0.005 * 18.23 + 0.0158 * 0.28) = 0.075$$

The individual RADON model (NRC 1989a) output files, which include the input parameter values for each model layer, are included in Appendix A. Appendix B provides additional calculations and data supporting development of the input parameters.

Discussion:

The typical UMTRA-style cover consists of a compacted, native-clay radon barrier as shown in Figure 1. It has been assumed as a best management practice that a 1-ft-thick interim cover of clean native materials will be placed on the RRM to control wind transport of fine material and to provide for a relatively clean and uniform work surface on which the radon barrier will be constructed.

The radon barrier layer has been fixed at four feet and the thickness of the top, lower activity, layer of tailings has been determined to by the RADON model to limit the radon flux to 20 pCi/m^2/sec under long-term moisture content conditions. As with previous UMTRA Title I cover designs, the attenuation of radon by the drainage layer or frost protection layers are not considered in these analyses, though these layers will further reduce the radon flux rate at the Disposal Cell surface.

Clean fill embankments made of native materials will be used around the perimeter of the new disposal cell constructed with 5H:1V exterior side slopes and a minimum 30-ft-wide crest. Consequently, the tailings side slope thicknesses will be far in excess of the cover requirements.

The current applicable version of this publication resides on Jacobs' Intranet. All copies are considered to be uncontrolled.
Copyright© Jacobs Engineering Group Inc., 2007

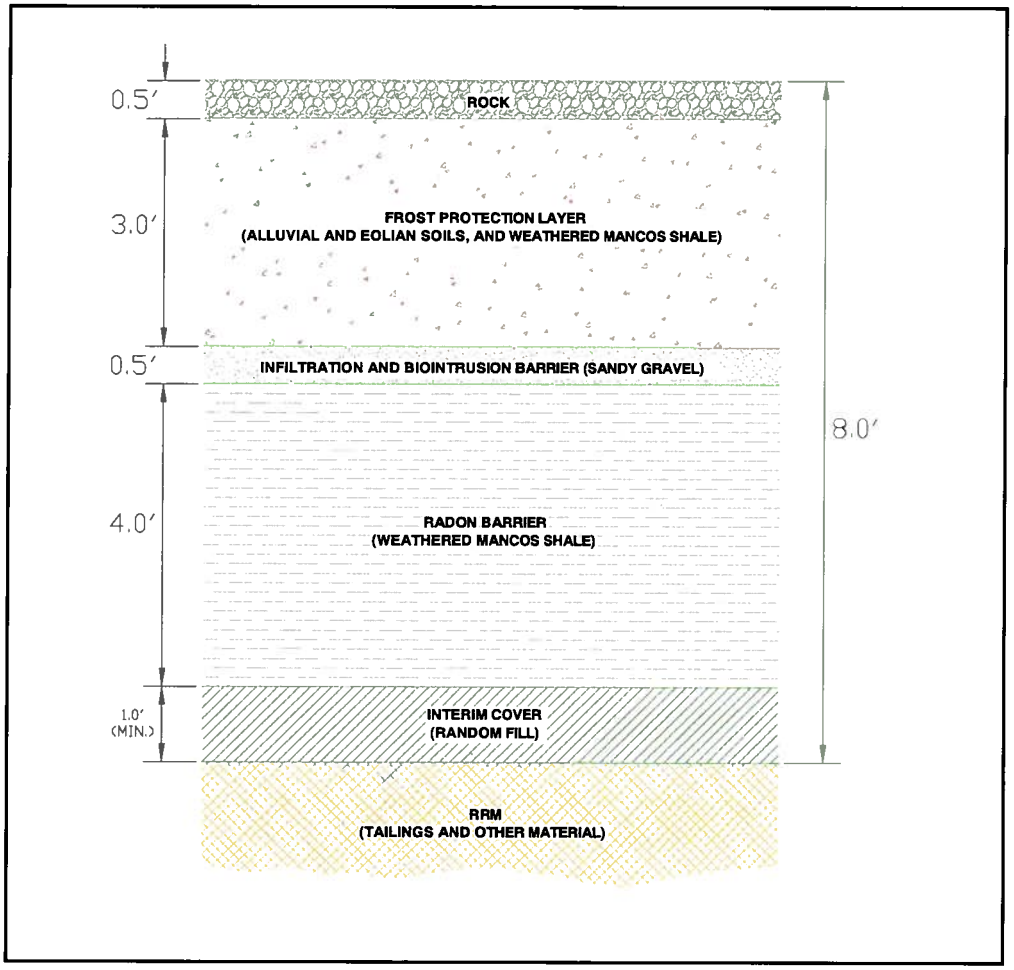

Figure 1. Proposed Waste Cell Cover

Model Runs

The current conceptual design of the UMTRA cover system consists of 1 ft of interim cover on the tailings surface below the compacted-clay radon barrier consisting of clean, native materials placed as a best management practice to control wind transport of fine material and to provide for a relatively clean, uniform work surface upon which to construct the radon barrier. The model is used to optimize the layer thickness of the compacted-clay radon barrier and to compute the release rate of radon through the barrier layer for a specified design. Several model runs were performed to assess model sensitivity to certain variables as described below.

- Model run UMTRA 1a uses the mean radium activity of all samples collected from the tailings (707 pCi/g) for the activity of the waste and optimizes the barrier layer thickness.

- Model run UMTRA 1b uses the volume weighted mean value of the radium activity of the four material types (565 pCi/g) for the activity of the waste and optimizes the barrier layer thickness.

- Model run UMTRA 1c uses the mean radium activity of all samples (707 pCi/g) for the radium activity of the top 7 feet of the tailings and the mean activity of the slimes (1349.3 pCi/g) for the radium activity of the 36 feet of tailings below the upper layer. The barrier layer thickness is specified as 4 feet and the release rate

The current applicable version of this publication resides on Jacobs' Intranet. All copies are considered to be uncontrolled.
Copyright© Jacobs Engineering Group Inc., 2007

of radon through the barrier layer is computed. This configuration assumes that the radium activity of the waste will be monitored as it is placed and no waste with an activity more than 707 pCi/g will be placed in the upper 7 feet.

Description of Model and Input Values

Radon emanation calculations from a multilayered cover system were made with the RADON model, a one-dimensional model that calculates radon flux from decay of a radium-226 (Ra-226) source (such as the tailings). The key input parameters to the model include:

- Layer thickness.
- Porosity.
- Mass density.
- Ra-226 activity concentration.
- Emanation coefficient.
- Weight percent moisture.
- Coefficient of radon diffusion.

Only those material layers including the radon barrier and below are modeled. This ensures that the radon barrier alone can meet the long-term average radon flux requirement of 20 pCi/m^2/s, without the additional attenuation provided by overlying layers such as freeze/thaw protection layers or rock mulch layers. The input parameters and values used in the model are outlined below. Table 1 summarizes the individual input parameters used for all of the models run and their bases and the results of the model runs. Appendix A presents the RADON model output files. Appendix B presents all raw data used in developing the model input parameters.

Layer Thickness

The layers and material sequences for the UMTRA cover are illustrated in
Figure 1. Therefore, radon flux through the side slopes was not modeled. For all model runs, a total tailings thickness of 43 feet (1310.6 cm) is used. This is the maximum anticipated tailings thickness in the waste cell.

The UMTRA cover design evaluated for radon flux consists of an a 1-ft-thick interim cover constructed of clean native alluvium and a compacted clay radon barrier constructed from conditioned on-site weathered Mancos Shale. The overlying sand drainage/biointrusion layer, frost protection layer and rock mulch erosion protection layer are not considered in the base-line modeling consistent with the historic UMTRA design approach.

The current applicable version of this publication resides on Jacobs' Intranet. All copies are considered to be uncontrolled.
Copyright© Jacobs Engineering Group Inc., 2007

Table 1. Crescent Junction Disposal Cell Radon Barrier Design, RADON Model Runs Summary

Model Run	Layer Type	Layer Thickness (cm)	Layer Thickness (ft)	Porosity	Density (g/cc)	Ra-226 Activity (pCi/g)	Gravimetric Moisture Content (%)	Moisture Saturation Fraction	Calculated Diffusion Coefficient (m^2/s)	Notes
(Appendix B data reference)				Table 2	Table 2	Table 3	Table 4	Table 5	Table 5	
UMTRA 1A	Tailings	1310.6	43	0.44	1.57	707	15	0.535	0.010370	UMTRA Cover baseline model run, Mean Tailings Radium Concentration = 707
	Interim Cover	30.48	1	0.38	1.66	1.9	9	0.393	0.016358	
	Radon Barrier	**119.7**	**3.9**	0.33	1.77	2.3	12	0.644	0.004636	
UMTRA 1B	Tailings	1310.6	43	0.44	1.57	565	15	0.535	0.010370	UMTRA Cover, Vol Weighted Mean Radium Concentration = 565
	Interim Cover	30.48	1	0.38	1.66	1.9	9	0.393	0.016358	
	Radon Barrier	**109.2**	**3.6**	0.33	1.77	2.3	12	0.644	0.004636	
UMTRA 1C	Lower Tailings	1097.3	36	0.44	1.57	1349.3	15	0.535	0.010370	Two Tailings Layers with Concentration 1349.3 and 707
	Upper Tailings	**213.4**	**7**	0.44	1.57	707	15	0.535	0.010370	
	Interim Cover	30.48	**1**	0.38	1.66	1.9	9	0.393	0.016358	
	Radon Barrier	**121.9**	**4**	0.33	1.77	2.3	12	0.644	0.004636	

UMTRA 1A and UMTRA 1D optimized the barrier layer thickness for a surface radon flux of 20 pCi/m^2/sec.

UMTRA 1C specified the barrier layer thickness as 4 feet and a 2 layer waste configuration resulting in a predicted surface radon flux of 19.9 pCi/m^2/sec.

The current applicable version of this publication resides on Jacobs' Intranet. All copies are considered to be uncontrolled. Copyright© Jacobs Engineering Group Inc., 2007

Porosity (n)

The porosity of the layer materials have been calculated based on the dry density and the specific gravity of the specific materials according to the equation identified in the previous section.

The porosity of the tailings was modeled as 0.44, given a mean specific gravity of 2.8 for the tailings based on the data in the "Geotechnical Laboratory Testing Results for the Moab Processing Site" calculation (RAP Attachment 5, Vol. I, Appendix J), and a designed placement density of 1.57 g/cc (98 pcf).

The porosity of the interim cover and the monolithic layer of the alternative cover, to be developed from the alluvial silty sands and sheetwash deposits overlying the in-situ weathered Mancos Shale, was modeled as 0.38, given a mean specific gravity of 2.65—based on nine samples presented in the "Geotechnical Properties of Native Materials" calculation (RAP Attachment 5, Vol. I, Appendix E) and Appendix B—and a designed placement density of 1.66 g/cc (103 pcf). These two layers will be constructed of the same on-site materials from the Crescent Junction Site and will be placed in the same conditions. The porosity of the frost protection layer was modeled assuming the same conditions as the interim cover material.

The porosity of the compacted Mancos Shale was modeled as 0.33, given a mean specific gravity for the Mancos Shale of 2.65—based on the data in the "Geotechnical Properties of Native Materials" calculation (RAP Attachment 5, Vol. I, Appendix E) and Appendix B—and a designed placement density of 1.77 g/cc (111 pcf).

Mass Density

The dry density of the tailings as placed has been modeled as 1.57 g/cc (98 pcf), which is 90 percent of the mean standard Proctor maximum dry density of transition tailings materials as reported in the Draft Tech Memo by Golder Associates (2006b).

The density of the interim cover materials and the alternative cover monolithic layer, as placed, has been modeled as 1.66 g/cc (103 pcf), which is 85 percent of the mean modified Proctor dry density value (121.8 pcf) for these materials as developed in the "Geotechnical Properties of Native Materials" calculation (RAP Attachment 5, Vol. I, Appendix E). The density of the frost protection layer has been modeled as the same as the interim cover materials. Because these materials will be installed using more energy and in a different manner than the native in-situ alluvial materials, it is anticipated that the frost protection layer will have long-term density more representative of the as-placed conditions than the native in-situ material conditions.

The density of the compacted clay materials and the UMTRA-style cover, as placed, has been modeled as 1.77 g/cc (111 pcf), which is 90 percent of the mean modified Proctor dry density value (123 pcf) for these materials, as developed in the "Geotechnical Properties of Native Materials" calculation (RAP Attachment 5, Vol. I, Appendix E).

Radium Activity Concentration

The Ra-226 activity concentration values used in the model for each specific material are outlined below.

Tailings

Radium-226 concentrations for the tailings pile materials were assessed based on 94 samples of tailings sands, slimes, transitional tailings and other contaminated materials. Radium-226 analyses were performed by gamma spectroscopy from these locations. The estimated volumes of tailings material are provided in the "Volume Calculation for the Moab Tailings Pile," calculation (RAP Attachment 1, Appendix I). The mean value of all the Ra-226 activity data for the contaminated materials is 707 picocuries per gram (pCi/g), with

The current applicable version of this publication resides on Jacobs' Intranet. All copies are considered to be uncontrolled.
Copyright© Jacobs Engineering Group Inc., 2007

values ranging from 2 to 2,195 pCi/g, as developed in the "Average Radium-226 Concentrations for the Moab Tailings Pile," calculation (RAP Attachment 1, Appendix K) (see also Appendix B of this calculation).

The current conceptual plan for tailings removal and placement would entail a significant amount of blending of the four materials from which samples were collected. Since the volumes of the four types of materials are not equal and the number of samples from each material is not proportional to its volume a volume weighted mean radium activity of 565 pCi/g has been computed to represent the activity of the blended materials.

It is highly likely that lower-activity contaminated sub-pile soils and contaminated soils from the mill site and cleanup of peripheral and vicinity properties will be placed above the higher activity tailings, which will serve to further reduce Ra-226 activity at the base of the cover. To test the effect of this approach a simulation was performed using two layers for the tailings in the disposal cell. The upper layer is assumed to have an activity of 707 pCi/g (the mean of all the samples collected from the tailings pile) and the lower layer is assumed to have an activity of 1,349 pCi/g (the mean of the samples collected from the slimes). The thickness of the upper layer necessary to achieve a release of 20 pCi/m^2/sec or less from the top of the radon barrier will be determined. The tailings source term activity, as well as the actual cover materials properties site, should be reevaluated once delivered to ensure that the cover design is optimized for the actual as-built conditions of the cell contents.

Interim Cover

The Ra-226 activity of the alluvial materials to be used for the interim cover, alternative cover, and the clean-fill perimeter dikes is based on five samples of native materials collected from the Crescent Junction Site as developed in the "Geotechnical Properties of Native Materials" calculation (RAP Attachment 5, Vol. I, Appendix E) (see also Appendix B of this calculation). Samples were collected from alluvial materials and weathered Mancos Shale with depths ranging from 4 to 22 ft below the surface. The Ra-226 activity of the alluvial material ranged from 1.4 to 2.3 pCi/g, with a mean value of 1.9 pCi/g.

Compacted Clay Layer

The Ra-226 activity value for the compacted clay layer is based on two samples of Mancos Shale collected from the Crescent Junction Site that will be used to construct the compacted-clay radon barrier and clean-fill perimeter dikes (see Appendix B). Samples were collected from weathered Mancos Shale samples with depths of approximately 20 to 22 ft below the surface. The Ra-226 activity of the weathered Mancos Shale ranged from 1.6 to 3.0 pCi/g, with a mean value of 2.3 pCi/g.

Radon Emanation Coefficient

A radon-emanation coefficient of 0.35 was used for all of the tailings, random fill, and cover materials. This is the conservative default value used in the RADON model.

Long-Term Weight Percent Moisture

The mean weight percent moisture of the tailings has been modeled as 15 percent, which is in the typical range for tailings and is below that value used for the modeling of the Grand Junction UMTRA Site (18 percent). Sensitivity analyses for the influence of long-term tailings moisture content were used to evaluate the influence of this parameter on predicted radon barrier thicknesses. Values of 10 percent moisture content and 20 percent moisture content were modeled. The results of the sensitivity analyses are discussed in the "Conclusion and Recommendations" section.

The mean long-term gravimetric moisture content of the interim cover is modeled as 9 percent. This value is based on the mean of 20 measured 15 bar tests as determined by ASTM Method D3152 and presented in the "Supplemental Geotechnical Properties of Native Materials" calculation (Attachment 5, Vol. I, Appendix K). This mean measured value was evaluated for reasonableness using the Rawls and

The current applicable version of this publication resides on Jacobs' Intranet. All copies are considered to be uncontrolled.
Copyright© Jacobs Engineering Group Inc., 2007

Brakensiek equation as presented in the NRC Regulatory Guide 3.64 (NRC 1989b). The Rawls and Brakensiek equation is a simplified empirical relationship based on the correlation of measured 15-bar moisture contents to the percent clay and organic matter in a range of soils. However, this relationship is not considered as reliable as the site-specific test data, and is considered as confirmatory information only. The calculated value, using the mean percent clay of eight alluvial samples and the percent organic matter of six alluvial samples, is 7.5 percent, which agrees well with the measured value of site-specific soils, or 9 percent. These data and calculations are summarized in Appendix B.

The mean long-term moisture content of the compacted clay derived from the on-site weathered Mancos Shale is modeled as 12 percent. This value is based on the mean of 12 measured 15 bar moisture content (12.1 percent) as determined by ASTM Method D3152 and presented in "Supplemental Geotechnical Properties of Native Materials" calculation (Attachment 5, Vol. I, Appendix K). This mean measured value was also evaluated for reasonableness using the Rawls and Brakensiek equation as presented in the NRC Regulatory Guide 3.64 (NRC 1989b). The calculated value is 12.4 percent, which agrees well with the measured value of site-specific soils, or 9 percent. These data and calculations are summarized in Appendix B.

In-situ moisture content for weathered Mancos was not included in the calculation of the mean, as in-situ moisture contents are not representative of remolded weathered Mancos. Long-term moisture content of the remolded weathered Mancos are better represented by the calculated and measured 15 bar moisture content test values due to the significantly different fabric the material will have as placed in the cell cover.

Radon-Diffusion Coefficient

The radon-diffusion coefficient used in the RADON model can either be calculated within the model (based on an empirical relationship with degree of saturation and porosity) or input directly into the model using values measured from laboratory testing. However, the radon diffusion equations in the 1989 version of RADON are not consistent with the later equations based on a much larger set of data correlating radon diffusion with soil cover materials. Therefore, the model was modified to compute coefficients based on equation 9 from Rogers and Nielson (1991. The diffusion coefficients are presented in Table 1.

Radon in Ambient Air

The ambient air radon concentrations above the radon-barrier layer are assumed to be zero (0) in absence of site-specific data.

Conclusions

- Based on the model runs developed in this evaluation, the UMTRA checklist cover is capable of meeting the requisite reasonable assurance of providing long-term control of radon flux to the specific average of 20 pCi/m^2/sec.
- As shown in Table 1, the compacted-clay radon barrier of the UMTRA checklist-type cover under the modeled conditions may be a minimum of 3.9 ft for a radium activity of 707 pCi/m^2/sec and 3.6 ft for a radium activity of 565 pCi/m^2/sec.
- The predicted Radon flux through a 4 ft thick Radon barrier with a two layer waste configuration is 19.9 pCi/m^2/sec. This simulation assumes a lower tailings layer 36 feet thick with a radium activity of 1349.3 pCi/m^2/sec and an upper layer 7 feet thick with a radium activity of 707 pCi/m^2/sec. This result implies that waste of higher radium activity may be placed in the lower portion of the waste cell providing that the waste is monitored as it is placed to ensure that the top seven feet of waste has a radium activity of 707 pCi/g or less. This is a very conservative approach as, with a total maximum thickness of waste of 43 feet and an upper layer thickness of 7 feet, the average radium activity modeled is 1245 pCi/g.

The current applicable version of this publication resides on Jacobs' Intranet. All copies are considered to be uncontrolled.
Copyright© Jacobs Engineering Group Inc., 2007

Computer Source:

See NRC 1989a, below.

References:

DOE (U.S. Department of Energy), 1989. *Technical Approach Document, Revision II*, UMTRA-DOE/AL 050425.0002, U.S. Department of Energy, Uranium Mill Tailings Remedial Action Project, December.

Golder Associates, 2006a. Bench Scale Testing Program on Uranium Mill Tailings, April.

Golder Associates, 2006b. Draft Tech Memo, April 3.

NRC (Nuclear Regulatory Commission), 1989a. *Staff Technical Position, Standard Format and Content for Documentation of Remedial Action Selection at Title I Uranium Mill Tailings Sites*, February 24.

NRC (Nuclear Regulatory Commission), 1989b. *Calculation of Radon Flux Attenuation by Earthen Uranium Mill Tailings Covers,* Regulatory Guide 3.64.

Rogers, V.C., and K.K. Nielson, 1991. "Correlations for Predicting Air Permeabilities and ^{222}Rn Diffusion Coefficients of Soils," *Health Physics*, 61(2), pp. 235–230.

Rogers, V.C., K.K. Nielson, and D.R. Kalkwarf, 1984. *Radon Attenuation Handbook for Uranium Mill Tailings Cover Design,* NUREG/CR-3533, prepared for U.S. Nuclear Regulatory Commission (NRC), April.

The current applicable version of this publication resides on Jacobs' Intranet. All copies are considered to be uncontrolled.
Copyright© Jacobs Engineering Group Inc., 2007

Appendix A

RADON Model Output Files

The current applicable version of this publication resides on Jacobs' Intranet. All copies are considered to be uncontrolled.
Copyright© Jacobs Engineering Group Inc., 2007

P:\UMTRA_1A.out

-----*****! RADON !*****-----

Version 1.2 - Feb. 2, 1989 - G.F. Birchard tel.# (301)492-7000
U.S. Nuclear Regulatory Commission Office of Research

RADON FLUX, CONCENTRATION AND TAILINGS COVER THICKNESS
ARE CALCULATED FOR MULTIPLE LAYERS

Mean Radium Activity: 707

CONSTANTS

RADON DECAY CONSTANT	.0000021	s^-1
RADON WATER/AIR PARTITION COEFFICIENT	.26	
SPECIFIC GRAVITY OF COVER & TAILINGS	2.65	

GENERAL INPUT PARAMETERS

LAYERS OF COVER AND TAILINGS	3	
DESIRED RADON FLUX LIMIT	20	pCi m^-2 s^-1
NO. OF THE LAYER TO BE OPTIMIZED	3	
DEFAULT SURFACE RADON CONCENTRATION	0	pCi l^-1
RADON FLUX INTO LAYER 1	0	pCi m^-2 s^-1
SURFACE FLUX PRECISION	.001	pCi m^-2 s^-1

LAYER INPUT PARAMETERS

LAYER 1

THICKNESS	1310.6	cm
POROSITY	.44	
MEASURED MASS DENSITY	1.57	g cm^-3
MEASURED RADIUM ACTIVITY	707	pCi/g^-1
MEASURED EMANATION COEFFICIENT	.35	
CALCULATED SOURCE TERM CONCENTRATION	1.854D-03	pCi cm^-3 s^-1
WEIGHT % MOISTURE	15	%
MOISTURE SATURATION FRACTION	.535	
MEASURED DIFFUSION COEFFICIENT	.01037	cm^2 s^-1

LAYER 2

THICKNESS	30.48	cm
POROSITY	.38	
MEASURED MASS DENSITY	1.66	g cm^-3
MEASURED RADIUM ACTIVITY	1.9	pCi/g^-1
MEASURED EMANATION COEFFICIENT	.35	
CALCULATED SOURCE TERM CONCENTRATION	6.100D-06	pCi cm^-3 s^-1
WEIGHT % MOISTURE	9	%
MOISTURE SATURATION FRACTION	.393	
MEASURED DIFFUSION COEFFICIENT	.016358	cm^2 s^-1

The current applicable version of this publication resides on Jacobs' Intranet. All copies are considered to be uncontrolled.
Copyright© Jacobs Engineering Group Inc., 2007

LAYER 3

THICKNESS	10	cm
POROSITY	.33	
MEASURED MASS DENSITY	1.77	g cm^-3
MEASURED RADIUM ACTIVITY	2.3	pCi/g^-1
MEASURED EMANATION COEFFICIENT	.35	
CALCULATED SOURCE TERM CONCENTRATION	9.067D-06	pCi cm^-3 s^-1
WEIGHT % MOISTURE	12	%
MOISTURE SATURATION FRACTION	.644	
MEASURED DIFFUSION COEFFICIENT	.004636	cm^2 s^-1

DATA SENT TO THE FILE `RNDATA'

N	F01	CN1	ICOST	CRITJ	ACC
3	0.000D+00	0.000D+00	3	2.000D+01	1.000D-03

LAYER	DX	D	P	Q	XMS	RHO
1	1.311D+03	1.037D-02	4.400D-01	1.854D-03	5.352D-01	1.570
2	3.048D+01	1.636D-02	3.800D-01	6.100D-06	3.932D-01	1.660
3	1.000D+01	4.636D-03	3.300D-01	9.067D-06	6.436D-01	1.770

BARE SOURCE FLUX FROM LAYER 1: 5.733D+02 pCi m^-2 s^-1

RESULTS OF THE RADON DIFFUSION CALCULATIONS

LAYER	THICKNESS (cm)	EXIT FLUX (pCi m^-2 s^-1)	EXIT CONC. (pCi l^-1)
1	1.311D+03	2.492D+02	4.990D+05
2	3.048D+01	1.196D+02	4.963D+05
3	1.197D+02	1.999D+01	0.000D+00

The current applicable version of this publication resides on Jacobs' Intranet. All copies are considered to be uncontrolled.
Copyright© Jacobs Engineering Group Inc., 2007

P:\UMTRA_1B.out

-----*****! RADON !*****-----

Version 1.2 - Feb. 2, 1989 - G.F. Birchard tel.# (301)492-7000
U.S. Nuclear Regulatory Commission Office of Research

RADON FLUX, CONCENTRATION AND TAILINGS COVER THICKNESS
ARE CALCULATED FOR MULTIPLE LAYERS

Weighted mean activity: 565

CONSTANTS

RADON DECAY CONSTANT	.0000021	s^-1
RADON WATER/AIR PARTITION COEFFICIENT	.26	
SPECIFIC GRAVITY OF COVER & TAILINGS	2.65	

GENERAL INPUT PARAMETERS

LAYERS OF COVER AND TAILINGS	3	
DESIRED RADON FLUX LIMIT	20	pCi m^-2 s^-1
NO. OF THE LAYER TO BE OPTIMIZED	3	
DEFAULT SURFACE RADON CONCENTRATION	0	pCi l^-1
RADON FLUX INTO LAYER 1	0	pCi m^-2 s^-1
SURFACE FLUX PRECISION	.001	pCi m^-2 s^-1

LAYER INPUT PARAMETERS

LAYER 1

THICKNESS	1310.6	cm
POROSITY	.44	
MEASURED MASS DENSITY	1.57	g cm^-3
MEASURED RADIUM ACTIVITY	565	pCi/g^-1
MEASURED EMANATION COEFFICIENT	.35	
CALCULATED SOURCE TERM CONCENTRATION	1.482D-03	pCi cm^-3 s^-1
WEIGHT % MOISTURE	15	%
MOISTURE SATURATION FRACTION	.535	
MEASURED DIFFUSION COEFFICIENT	.01037	cm^2 s^-1

LAYER 2

THICKNESS	30.48	cm
POROSITY	.38	
MEASURED MASS DENSITY	1.66	g cm^-3
MEASURED RADIUM ACTIVITY	1.9	pCi/g^-1
MEASURED EMANATION COEFFICIENT	.35	
CALCULATED SOURCE TERM CONCENTRATION	6.100D-06	pCi cm^-3 s^-1
WEIGHT % MOISTURE	9	%
MOISTURE SATURATION FRACTION	.393	
MEASURED DIFFUSION COEFFICIENT	.016358	cm^2 s^-1

The current applicable version of this publication resides on Jacobs' Intranet. All copies are considered to be uncontrolled.
Copyright© Jacobs Engineering Group Inc., 2007

LAYER 3

THICKNESS	10	cm
POROSITY	.33	
MEASURED MASS DENSITY	1.77	g cm^-3
MEASURED RADIUM ACTIVITY	2.3	pCi/g^-1
MEASURED EMANATION COEFFICIENT	.35	
CALCULATED SOURCE TERM CONCENTRATION	9.067D-06	pCi cm^-3 s^-1
WEIGHT % MOISTURE	12	%
MOISTURE SATURATION FRACTION	.644	
MEASURED DIFFUSION COEFFICIENT	.004636	cm^2 s^-1

DATA SENT TO THE FILE `RNDATA'

N	F01	CN1	ICOST	CRITJ	ACC
3	0.000D+00	0.000D+00	3	2.000D+01	1.000D-03

LAYER	DX	D	P	Q	XMS	RHO
1	1.311D+03	1.037D-02	4.400D-01	1.482D-03	5.352D-01	1.570
2	3.048D+01	1.636D-02	3.800D-01	6.100D-06	3.932D-01	1.660
3	1.000D+01	4.636D-03	3.300D-01	9.067D-06	6.436D-01	1.770

BARE SOURCE FLUX FROM LAYER 1: 4.582D+02 pCi m^-2 s^-1

RESULTS OF THE RADON DIFFUSION CALCULATIONS

LAYER	THICKNESS (cm)	EXIT FLUX (pCi m^-2 s^-1)	EXIT CONC. (pCi l^-1)
1	1.311D+03	1.993D+02	3.985D+05
2	3.048D+01	9.598D+01	3.962D+05
3	1.092D+02	1.998D+01	0.000D+00

The current applicable version of this publication resides on Jacobs' Intranet. All copies are considered to be uncontrolled.
Copyright© Jacobs Engineering Group Inc., 2007

P:\UMTRA_1C.out

```
-----*****! RADON !*****-----

Version 1.2 - Feb. 2, 1989 - G.F. Birchard tel.# (301)492-7000
U.S. Nuclear Regulatory Commission Office of Research

RADON FLUX, CONCENTRATION AND TAILINGS COVER THICKNESS
ARE CALCULATED FOR MULTIPLE LAYERS


Two layer tailings with activities of 1349.3 and 707


              CONSTANTS

RADON DECAY CONSTANT                        .0000021     s^-1
RADON WATER/AIR PARTITION COEFFICIENT       .26
SPECIFIC GRAVITY OF COVER & TAILINGS        2.65


              GENERAL INPUT PARAMETERS

LAYERS OF COVER AND TAILINGS                4
NO LIMIT ON RADON FLUX
LAYER THICKNESS NOT OPTIMIZED
DEFAULT SURFACE RADON CONCENTRATION         0            pCi l^-1
RADON FLUX INTO LAYER 1                     0            pCi m^-2 s^-1
SURFACE FLUX PRECISION                      .001         pCi m^-2 s^-1


              LAYER INPUT PARAMETERS

LAYER 1


THICKNESS                                   1097.3       cm
POROSITY                                    .44
MEASURED MASS DENSITY                       1.57         g cm^-3
MEASURED RADIUM ACTIVITY                    1349.3       pCi/g^-1
MEASURED EMANATION COEFFICIENT              .35
CALCULATED SOURCE TERM CONCENTRATION        3.539D-03    pCi cm^-3 s^-1
WEIGHT % MOISTURE                           15           %
MOISTURE SATURATION FRACTION                .535
MEASURED DIFFUSION COEFFICIENT              .01037       cm^2 s^-1


LAYER 2


THICKNESS                                   213.4        cm
POROSITY                                    .44
MEASURED MASS DENSITY                       1.57         g cm^-3
MEASURED RADIUM ACTIVITY                    707          pCi/g^-1
MEASURED EMANATION COEFFICIENT              .35
CALCULATED SOURCE TERM CONCENTRATION        1.854D-03    pCi cm^-3 s^-1
WEIGHT % MOISTURE                           15           %
MOISTURE SATURATION FRACTION                .535
MEASURED DIFFUSION COEFFICIENT              .01037       cm^2 s^-1
```


The current applicable version of this publication resides on Jacobs' Intranet. All copies are considered to be uncontrolled.
Copyright© Jacobs Engineering Group Inc., 2007

LAYER 3

THICKNESS	30.48	cm
POROSITY	.38	
MEASURED MASS DENSITY	1.66	g cm^-3
MEASURED RADIUM ACTIVITY	1.9	pCi/g^-1
MEASURED EMANATION COEFFICIENT	.35	
CALCULATED SOURCE TERM CONCENTRATION	6.100D-06	pCi cm^-3 s^-1
WEIGHT % MOISTURE	9	%
MOISTURE SATURATION FRACTION	.393	
MEASURED DIFFUSION COEFFICIENT	.016358	cm^2 s^-1

LAYER 4

THICKNESS	121.9	cm
POROSITY	.33	
MEASURED MASS DENSITY	1.77	g cm^-3
MEASURED RADIUM ACTIVITY	2.3	pCi/g^-1
MEASURED EMANATION COEFFICIENT	.35	
CALCULATED SOURCE TERM CONCENTRATION	9.067D-06	pCi cm^-3 s^-1
WEIGHT % MOISTURE	12	%
MOISTURE SATURATION FRACTION	.644	
MEASURED DIFFUSION COEFFICIENT	.004636	cm^2 s^-1

DATA SENT TO THE FILE `RNDATA'

N	F01	CN1	ICOST	CRITJ	ACC
4	0.000D+00	0.000D+00	0	0.000D+00	1.000D-03

LAYER	DX	D	P	Q	XMS	RHO
1	1.097D+03	1.037D-02	4.400D-01	3.539D-03	5.352D-01	1.570
2	2.134D+02	1.037D-02	4.400D-01	1.854D-03	5.352D-01	1.570
3	3.048D+01	1.636D-02	3.800D-01	6.100D-06	3.932D-01	1.660
4	1.219D+02	4.636D-03	3.300D-01	9.067D-06	6.436D-01	1.770

BARE SOURCE FLUX FROM LAYER 1: 1.094D+03 pCi m^-2 s^-1

RESULTS OF THE RADON DIFFUSION CALCULATIONS

LAYER	THICKNESS (cm)	EXIT FLUX (pCi m^-2 s^-1)	EXIT CONC. (pCi l^-1)
1	1.097D+03	2.723D+02	1.266D+06
2	2.134D+02	2.601D+02	5.208D+05
3	3.048D+01	1.248D+02	5.181D+05
4	1.219D+02	1.993D+01	0.000D+00

The current applicable version of this publication resides on Jacobs' Intranet. All copies are considered to be uncontrolled.
Copyright© Jacobs Engineering Group Inc., 2007

Appendix B

SUPPORTING CALCULATIONS AND DATA

The current applicable version of this publication resides on Jacobs' Intranet. All copies are considered to be uncontrolled.
Copyright© Jacobs Engineering Group Inc., 2007

Table B–1. Moab Project, Crescent Junction Native Materials Index Test Results Summary

Geotechnical Testing Data from the "Geotechnical Properties of Native Materials" Calculation (RAP Attachment 5, Vol. I, Appendix E)

Sample	No.	Field Description	Test Depth (ft)	Natural Moisture (%)	Dry Density (pcf)	Liquid Limit (%)	Plasticity Index (%)	Passing No. 200 (%)	Specific Gravity	□max (Modified Proctor) (pcf)	□max (Modified Proctor) (g/cc)	w_{opt} (Modified Proctor) (%)	Sieve			Hydrometer		% Organic Matter	Double Hydro-meter	Ra-226 (pCi/g)
													% Gravel	% Sand	% Fines	% silt	% clay			
BH	031	Clay, sandy, silty L/SC)	12	8.2	96.0	24	4	50												
BH	007	Clay, silty sandy (CL)	7	4.9		23	8	94												
BH	007	Clay, silty sandy (CL)	10.5	4.5	100.0	21	9	62												
BH	045	Clay, silty sandy (CL)	1.5	4.6	84.0	19	7	57												
BH	005	Clay, silty sandy (CL)	2	4.2	91.0	21	4	69												
BH	011	Clay, silty sandy (CL)	2	6.1	83.0	22	9	78												
BH	064	Clay, silty, sandy (CL)	2	12.4	95.0	34	5	74												
BH	068	Clay, silty, sandy (CL)	2	4.2	94.0	21	6	36												
BH	092	Clay, silty, sandy (CL)	2	5.7	87.0	22	9	63												
BH	013	Clay, silty sandy (CL)	2.5	5.8	89.0	24	9	70												
BH	080	Clay, silty, sandy (CL)	3	2.8	95.0	19	5	53												
BH	023	Clay, silty sandy (CL)	3.5	6.0		25	8	72												
BH	043	Clay, silty, sandy (CL)	3.5	6.1	90.0	25	8	53												
BH	051	Clay, silty, sandy (CL)	3.5	3.8	85.0	20	6	57												
BH	066	Clay, silty, sandy (CL)	3.5	4.7	90.0	21	5	53												
BH	100	Clay, silty sandy (CL)	4	8.0		25	5	69												
BH	009	Clay, silty sandy (CL)	4	6.6	83.0	24	9	74												
BH	062	Clay, silty, sandy (CL)	4	7.6	103.0	29	10	69												
BH	094	Clay, silty, sandy (CL)	4	12.2	89.0	31	10	61												
BH	031	Clay, silty, sandy (CL)	5.5	7.0	87.0	25	9	85												
BH	025	Clay, silty, sandy (CL)	6	4.9	89.0	24	9	59												
BH	007	Clay, silty sandy (CL)	6.5	6.5		23	5													
BH	045	Clay, silty, sandy (CL)	6.5	8.6	98.0	32	9	78												
BH	049	Clay, silty, sandy (CL)	6.5	6.0	83.0	20	6	62												
BH	029	Clay, silty, sandy (CL)	7	13.4	77.0	23	6	77												
BH	078	Clay, silty, sandy (CL)	7	5.7	85.0	23	7	70												
BH	080	Clay, silty, sandy (CL)	7	6.0	89.0	24	7	65												
BH	095	Clay, silty, sandy (CL)	7	6.5	85.0	23	7	46												
BH	049	Clay, silty, sandy (CL)	12	5.4	102.0	19	5	80												
BH	082	Clay, silty, sandy (CL)	12	4.7	91.0	21	8	79												
BH	025	Clay, silty sandy (CL)	16.5	7.3	106.0	21	6	66												
BH	027	Clay, silty, sandy (CL)	16.5	8.4	108.0	24	11	87												
BH	094	Clay, silty, sandy (CL)	17	7.1	102.0	20	5	37												
TP	153	Clay, silty, sandy (CL)	3.5	5.7		23	5	72	2.68	120.5	1.93	12.5	0	27	73	60	13			
TP	154	Clay, silty, sandy (CL)	4	7.6		22	4	83		123.0	1.97	12.0	0	16	84	62	22	0.5	79	2.3
TP	151	Clay, silty, sandy (CL)	4.5	5.6		24	5	66		118.5	1.90	13.0	4	30	66					
TP	152	Clay, silty, sandy (CL)	7.5	4.3		26	9	74	2.64	121.0	1.94	13.5	0	25	75	59	16			1.9

The current applicable version of this publication resides on Jacobs' Intranet. All copies are considered to be uncontrolled. Copyright© Jacobs Engineering Group Inc., 2007

Sample	No.	Field Description	Test Depth (ft)	Natural Moisture (%)	Dry Density (pcf)	Liquid Limit (%)	Plasticity Index (%)	Passing No. 200 (%)	Specific Gravity	□max (Modified Proctor) (pcf)	□max (Modified Proctor) (g/cc)	Wopt (Modified Proctor) (%)	Sieve			Hydrometer		% Organic Matter	Double Hydro-meter	Ra-226 (pCi/g)
													% Gravel	% Sand	% Fines	% silt	% clay			
TP	154	Clay, silty, sandy (CL)	12	2.7		20	3	63	2.65	122.5	1.96	12.0	0	33	67	40	27	0.2	62	1.6
TP	156	Clay, silty, sandy (CL)	12	2.7		19	2	64	2.64	124.5	1.99	11.0	0	35	65	39	26	0.1	83	2.1
TP	152	Clay, silty, sandy (CL)	15	2.9		21	3	84	2.63	128.0	2.05	10.5	49	22	29	15	14	0.2		1.4
TP	156	Clay, silty, sandy (CL)	4-5	7.2			7	69	2.82	120.0	1.92	11.5	1	29	70	54	16		61	
TP liner	156	Eolian	12.25	7.9	88.0	0	0	50												
TP liner	154	Eolian	13	5.7	82.0	20	2	69												
TP	156	Fluvial/eolian	15															0.2		
BH	027	Sand, clayey, silty (SC)	4	5.9		24	3	44												
BH	099	Sand, clayey, silty (C/SM)	2.5	4.8	87.0	18	3	47												
BH	011	Sand, silty gravelly	11.5	2.6		21	4	19												
BH	013	Sandy silt	7	8.3	113.4	0	0	43												
TP	155	Sheetwash	4															0.4		
TP liner	156	Sheetwash	3.5	9.5	89.0	0	0	79												
TP liner	154	Sheetwash	4	9.5	81.0	22	5	81												
TP liner	156	Sheetwash	7.25	6.0	91.0			63										0.3		
TP	153	Silt, sandy, clayey (ML)	8.5	4.4		0	0	67	2.65	118.0	1.89	11.0	1	32	67	52	15			
BH	064	Weathered shale	3.5	10.0	109.0	31	19	86												
BH	043	Weathered shale	6	5.0	93.0	24	16	47												
BH	009	Weathered shale	6.5	6.6	107.2	28	9	84												
BH	066	Weathered shale	7	12.3	112.0	31	10	90												
BH	079	Weathered shale	10.5	4.4		25	10	78												
BH	033	Weathered shale	10.75	6.7	117.0	34	18	82												
BH	005	Weathered shale	11	6.0	118.0	25	10	79												
BH	090	Weathered shale	12	8.2	99.0	22	5	55												
BH	092	Weathered shale	12	7.7	71.0	26	6	71												
BH	026	Weathered shale	15.5	5.7		24	10	71												
BH	011	Weathered shale	16	7.9	119.4	37	20	96												
BH	082	Weathered shale	17	7.1	118.0	34	14	93												
BH	094	Weathered shale	21.5	6.8	112.0	21	4	33												
BH	029	weathered shale	27	6.4	81.0	29	10	81												
TP	154	weathered shale	20	5.5		38	20	95	2.73	120.5	1.93	13.0	0	5	95	55	40		62	1.6
TP	156	Weathered shale	22			25	7	84	2.56	127.5	2.04	11.0	2	14	84	53	31	0.4	86	3.0
TP	152	Weathered shale	23	5.5		33	12	97		121.0	1.94	12.0	0	3	97	55	42			
		Weathered Mancos Shale	**Max**	12.3	119.4	38.0	20.0	97.0	2.73	127.5	2.04	13.0	2.0	14.0	97.0	55.0	42.0	0.4	86.0	3.0
			Min	4.4	71.0	21.0	4.0	33.0	2.56	120.5	1.93	11.0	0.0	3.0	84.0	53.0	31.0	0.4	62.0	1.6
			Mean	**7.0**	**104.7**	**28.6**	**11.8**	**77.8**	**2.65**	**123.0**	**1.97**	**12.0**	**0.7**	**7.3**	**92.0**	**54.3**	**37.7**	**0.4**	**74.0**	**2.3**
			Median	6.7	110.5	28.0	10.0	82.0	2.65	121.0	1.94	12.0	0.0	5.0	95.0	55.0	40.0	0.4	74.0	2.3
			count	16	12	17	17	17	2	3	3	3	3	3	3	3	3	1	2	2
		Alluvium	**Max**	13.4	113.4	34.0	11.0	94.0	2.82	128.0	2.05	13.5	49.0	35.0	84.0	62.0	27.0	0.5	83.0	2.3

The current applicable version of this publication resides on Jacobs' Intranet. All copies are considered to be uncontrolled. Copyright© Jacobs Engineering Group Inc., 2007

Sample	No.	Field Description	Test Depth (ft)	Natural Moisture (%)	Dry Density (pcf)	Liquid Limit (%)	Plasticity Index (%)	Passing No. 200 (%)	Specific Gravity	□max (Modified Proctor) (pcf)	□max (Modified Proctor) (g/cc)	Wopt (Modified Proctor) (%)	Sieve			Hydrometer		% Organic Matter	Double Hydro-meter	Ra-226 (pCi/g)
													% Gravel	% Sand	% Fines	% silt	% clay			
		(All Data w/out Weath. Mancos Shale)	Min	2.6	77.0	0.0	0.0	19.0	2.63	118.0	1.89	10.5	0.0	16.0	29.0	15.0	13.0	0.1	61.0	1.4
			Mean	**6.3**	**91.3**	**21.1**	**5.8**	**64.8**	**2.67**	**121.8**	**1.95**	**11.9**	**6.1**	**27.7**	**66.2**	**47.6**	**18.6**	**0.3**	**71.3**	**1.9**
			Median	6.0	89.0	22.0	6.0	66.5	2.65	121.0	1.94	12.0	0.0	29.0	67.0	53.0	16.0	0.2	70.5	1.9
			Count	51	36	49	50	50	7	9	9	9	9	9	9	8	8	7	4	5

liner = Brass Liner samples collected in pit side walls

The current applicable version of this publication resides on Jacobs' Intranet. All copies are considered to be uncontrolled. Copyright© Jacobs Engineering Group Inc., 2007

Table B–2. Radon Barrier Design, RAECOM Model Runs, Summary of Key Parameters

Porosity f (G_s)	No. of Samples	Mean Specific Gravity (G_s)	No. of Samples	Mean Dry Density (g/cc)	Porosity
Alluvium	7	2.67	9	1.66	0.38
Alluvium (in-situ)	7	2.67	36	1.46	0.45
Weathered Mancos	2	2.65	3	1.77	0.33
Tailings	5	2.8	5	1.57	0.44

Long-term Gravimetric Moisture Content (%)	No. of Samples	In Situ	Rawls & Brakensiek [3]	No. of Samples	ASTM D3151 15 bar tests	Used
			Avg		Avg	
Alluvium	51	6.3	7.5	20	9.0	91
Weathered Mancos	16	7.0	12.4	12	12.1	12
Tailings	NA	NA	Not Available	Not Available	Not Available	15

Ra-226 Activity (pCi/g)	No. of Samples	Volume Weighted Mean
Alluvium	5	1.9
Weathered Mancos	2	2.3
Tailings & Contaminated Materials	94	565 (UCL = 655.5)

Cover Layer	Calculated Diffusion Coefficient (cm^2/s)
Tailings (both cover designs)	0.010370
Interim Cover (both cover designs)	0.016358
UMTRA Cover Radon Barrier	0.004636

Note:
NA = Not applicable
Mean Dry density as placed for alluvium = 85% of Maximum Dry Density from Modified Proctor Density Tests
Mean Dry density as placed for weathered Mancos = 90% of Maximum Dry Density from Modified Proctor Density Tests
Mean Dry density as placed for tailings = 90% of Maximum Dry Density from Standard Proctor Density Tests
Porosity (n) is calculated form Gs and Dry density by n = 1 - Dry density/(Gs x Unit weight of water)
Unit weight of water is = 1 g/cc
Mean values developed from raw data presented in Table 1

[1] Long-term moisture content of Alluvium based on 20 ASTM D5131 15 Bar moisture tests, calculated value using Rawls & Brakensiek Equation (in NRC 1989b) is approximately 1 standard deviation from the mean test value ands is considered confirmatory of the mean value.
[2] In-situ moisture content for weathered Mancos is not included in the calculation of the mean long-term moisture as in-situ moisture contents are not representative of remolded weathered Mancos. Remolded weathered Mancos long-term moisture contents are better represented by the calculated and 15 bar test values due to the significantly different fabric of the material as placed in the cell cover.
[3] Rawls & Brakensiek equation (in NRC 1989b) based on mean values for each material type

The current applicable version of this publication resides on Jacobs' Intranet. All copies are considered to be uncontrolled.
Copyright© Jacobs Engineering Group Inc., 2007

Table B–3. Moab Project, Crescent Junction Disposal Cell Tailings and Other Contaminated Materials Ra-226

No. of Samples	Sample	Depth	Ra-226 Activity (pCi/g)	Material Type	No. of Samples	Sample	Depth	Ra-226 Activity (pCi/g)	Material Type
Transitional Tailings					**Slimes**				
1	BH-701	0-20	400.9	trans	1	PB-2	34-36	782	slime
2	BH-701	20-40	480.8	trans	2	PB-2	54-56	2070	slime
3	BH-703	0-20	457.6	trans	3	437	40.75-41	2194.9	slime
4	BH-703	20-40	610.1	trans	4	438	72.75-73	1891.7	slime
5	BH-705	20-40	616.9	trans	5	439	82-82.25	2157.5	slime
6	BH-709	20-40	546.6	trans	6	AR-10	75-86	588.8	slime
7	BH-713	20-36.5	631.1	trans	7	BH-700	30-60	466.5	slime
8	BH-715	20-40	278.9	trans	8	BH-701	40-60	758.9	slime
9	BH-718	0-20	717.8	trans	9	BH-701	60-80	1215.8	slime
10	BH-718	20-40	917.3	trans	10	BH-703	40-60	1396.3	slime
11	BH-719	0-20	357.4	trans	11	BH-703	65-73	1333	slime
12	PB-1	39-41	335	trans	12	BH-705	40-60	1232.8	slime
13	PB-1	44-46	464	trans	13	BH-709	40-60	1195.3	slime
14	PB-1	49-51	566	trans	14	BH-709	60-65	1205.8	slime
15	PB-1	64-66	418	trans	15	BH-715	0-20	1000.5	slime
16	PB-1	74-76	605	trans	16	BH-715	40-60	1225.9	slime
17	PB-1	76-81	220	trans	17	BH-715	60+	1518.6	slime
18	PB-1	81-83	201	trans	18	BH-718	40-43	1601.7	slime
19	PB-2	9-11	803	trans	19	BH-719	20-40	1117.7	slime
20	PB-2	29-31	192	trans	20	BH-719	40-51.5	1669.7	slime
21	PB-2	39-41	325	trans	21	PB-1	59-61	236	slime
22	PB-2	49-51	816	trans	22	PB-1	69-71	748	slime
23	PB-2	59-61	781	trans	23	PB-1	83-85	1600	slime
24	PB-2	61-66	711	trans	24	PB-1	85-87	2040	slime
25	PB-2	69-71	614	trans	25	PB-1	87-89	1640	slime
26	AR-4S	20-21	530.6	unconsol	26	PB-1	89-91	1690	slime
27	AR-8	21-22	594.8	unconsol	27	PB-2	44-46	1740	slime
28	AR-8	25-35	639.9	unconsol	28	PB-2	71-73	1390	slime
					29	PB-2	73-75	1280	slime
Sands					30	PB-2	75-77	1130	slime
1	Impound 2	imp	12.7	imp	31	PB-2	77-79	1240	slime
2	Impound 3	imp	87.4	imp	32	PB-2	79-81	1550	slime
3	AR-10	3-4	311.8	sand	33	PB-2	84-86	1620	slime
4	AR-10	20-25	98	sand					
5	AR-6	35-40	100.4	sand	**Alluvium**				
6	AR-9	10-11	320.2	sand	1	437	44-44.25	135.5	alluvium
7	AR-9	30-32	87.2	sand	2	438	74-74.25	134.3	alluvium
8	BH-705	0-20	186.2	sand	3	438	75-75.25	92.8	alluvium
9	BH-709	0-20	289.9	sand	4	438	76-76.25	31.3	alluvium

The current applicable version of this publication resides on Jacobs' Intranet. All copies are considered to be uncontrolled.
Copyright© Jacobs Engineering Group Inc., 2007

No. of Samples	Sample	Depth	Ra-226 Activity (pCi/g)	Material Type	No. of Samples	Sample	Depth	Ra-226 Activity (pCi/g)	Material Type
10	PB-1	9-11	215	sand	5	438	78-78.25	118.4	alluvium
11	PB-1	14-16	99.7	sand	6	439	87-87.25	23.9	alluvium
12	PB-1	19-21	202	sand	7	AR-5	0-1	84.3	alluvium
13	PB-1	24-26	148	sand	8	AR-6	0-1	17.3	alluvium
14	PB-1	29-31	153	sand	9	PB-1	94-96	208	alluvium
15	PB-1	34-36	447	sand	10	PB-2	89-91	1.83	alluvium

Table B–3 (continued). Moab Project, Crescent Junction Disposal Cell Tailings and Other Contaminated Materials Ra-226

No. of Samples	Sample	Depth	Ra-226 Activity (pCi/g)	Material Type
16	PB-1	54-56	849	sand
17	PB-2	14-16	269	sand
18	PB-2	19-21	150	sand
19	PB-2	24-26	100	sand
20	AR-2	5.5-10	786.5	silt
21	AR-7	20-25	562.2	silt
22	AR-9	50-55	543.6	silt
23	AR-9	60-62	239.1	silt

	All Data	Sands	Transitional Tailings	Slimes	Off Pile & Sub Pile & Interim Cover Materials (Alluvium)
Max:	2,195	849	917	2,195	208
Min:	2	13	192	236	2
Mean:	707	**272**	**530**	**1,349**	**85**
Median:	564	202	556	1,333	89
Std Dev.:	589	224	195	479	66
Count:	94	23	28	33	10
Material Volume (cy)	14,546,054	3,743,474	4,864,651	3,258,910	2,679,019
Volume %:	100%	26%	33%	22%	18%
Weighted Mean Activity (pCi/g)	**565**	70	177	302	16
95 % UCL of Mean		371	592.4	1491	123.1
Weighted 95% UCL of Means	**655.5**	100.6	198.1	334.0	22.7

The current applicable version of this publication resides on Jacobs' Intranet. All copies are considered to be uncontrolled.
Copyright© Jacobs Engineering Group Inc., 2007

Table B–4. Moab Project, Crescent Junction Disposal Cell 15 Bar Moisture Content

Sample Description	Soil Type	% Moisture (15 Bar)		
TP-153, 8.5, A	Fluvial/Eolian	6.74	**All Data**	
TP-153, 8.5, A-R	Fluvial/Eolian	6.75	Maximum	14.0
TP-153, 8.5 B	Fluvial/Eolian	6.56	Minimum	6.4
TP-153, 8.5 B-R	Fluvial/Eolian	6.43	Mean	10.1
TP-152, 15, A	Fluvial/Eolian	8.53	Median	10.1
TP-152, 15, A-R	Fluvial/Eolian	8.52	St. Deviation	2.1
TP-152, 15, B	Fluvial/Eolian	8.61	Count	32
TP-152, 15, B-R	Fluvial/Eolian	8.62		
TP-153, 3.5, A	Sheetwash	10.86		
TP-153, 3.5, A-R	Sheetwash	10.6		
TP-153, 3.5 B	Sheetwash	10.49	**Sheetwash/Fluvial/Eolian**	
TP-153, 3.5 B-R	Sheetwash	10.52	Maximum	10.9
TP-152, 7.5 A	Sheetwash	10.08	Minimum	6.4
TP-152, 7.5 A-R	Sheetwash	10.19	Mean	9.0
TP-152, 7.5, B	Sheetwash	9.99	Median	9.0
TP-152, 7.5, B-R	Sheetwash	10.03	St. Deviation	1.4
TP-155, 5, A	Sheetwash	9.56	Count	20
TP-155, 5, A-R	Sheetwash	9.28		
TP-155, 5, B	Sheetwash	8.75		
TP-155, 5, B-R	Sheetwash	8.72		
TP-154, 20, A	Weathered Shale	12.1	**Weathered Shale**	
TP-154, 20, A-R	Weathered Shale	12.33	Maximum	14.0
TP-154, 20, B	Weathered Shale	12.19	Minimum	9.3
TP-154, 20, B-R	Weathered Shale	12.22	Mean	12.1
TP-152, 23, A	Weathered Shale	13.99	Median	12.2
TP-152, 23, A-R	Weathered Shale	13.73	St. Deviation	1.6
TP-152, 23, B	Weathered Shale	13.47	Count	12
TP-152, 23, B-R	Weathered Shale	13.56		
TP-156, 22, A	Weathered Shale	11.16		
TP-156, 22, A-R	Weathered Shale	11.16		
TP-156, 22, B	Weathered Shale	9.28		
TP-156, 22, B-R	Weathered Shale	9.52		

Note: values are gravimetric moisture content on a dry unit weight basis

The current applicable version of this publication resides on Jacobs' Intranet. All copies are considered to be uncontrolled.
Copyright© Jacobs Engineering Group Inc., 2007

Table B–5. Moab Project, Crescent Junction Disposal Cell Calculation of Radon Diffusion Coefficients Using Updated Equation (Rogers and Nielson, 1991)

Cover Layer	Mass Density (g/cm3)	Dry Density (pcf)	Long-Term Water Content (w)	Specific Gravity (G_s)	Porosity[1] (p)	Calculated Saturation[2] (S)	Calculated Diffusion Coefficient[3] (cm^2/s)
Tailings (both cover designs)	1.57	97.8	0.15	2.8	0.44	53.4%	1.044E-02
(moisture content = 10%)	1.57	97.8	0.10	2.8	0.44	35.6%	1.873E-02
(moisture content = 20%)	1.57	97.8	0.20	2.8	0.44	71.2%	3.541E-03
Interim Cover (both cover designs)	1.66	103.5	0.09	2.67	0.38	39.4%	1.629E-02
Alternative Cover Radon Barrier	1.66	103.5	0.09	2.67	0.38	39.4%	1.629E-02
UMTRA Cover Radon Barrier	1.77	110.7	0.12	2.65	0.33	64.4%	4.636E-03

[1]Porosity (p) = 1 - dry density/(specific gravity x unit weight of water)
[2]Saturation (S) = Long-term water content/((unit weight of water/dry density) - (1 - specific gravity))
[3]D=Da*p*exp(-6Sp-6S14p) Source: Rogers and Nielson, 1991, equation 9

unit weight of water	62.4	pcf
^{222}Rn diffusion coefficient in air (Da)	1.10E-05	m^2/s

Rogers and Nielson, 1991. Correlations for Predicting Air Permeabilities and ^{222}Rn Diffusion Coefficients of Soils, Health Physics, Vol. 61, No. 2, pp. 225-230, August.

The current applicable version of this publication resides on Jacobs' Intranet. All copies are considered to be uncontrolled.
Copyright© Jacobs Engineering Group Inc., 2007

Table B–6. Moab Project, Crescent Junction Disposal Cell Calculation of 15 bar Moisture Content Using Empirical Relationship Rawls & Brakensiek (in NRC 1989b): 15 bar Vol. moisture content = 0.026 + 0.005z + 0.0158y (where z = % of Clay in the soil and y = % of organic matter in the soil)

Alluvium			
Mean Max. Dry Density as placed =	103.4	lbs/cu. ft.	(1.66 g/cc; 85% of Max Dry Density from Modified Proctor Tests)
Mean % Clay =	18.6		
Mean % Organic Matter =	0.3		
15 bar vol. moisture content = 0.026 + 0.005(18.63) + 0.0158(0.3)			
	Volumetric (%)	**Gravimetric (%)**	
15 bar Vol. Moisture Content =	12.3	7.5	Using mean values
Weathered Mancos			
Mean Max. Dry Density as placed =	110.7	lbs/cu. ft.	(1.77 g/cc; 90% of Max. Dry Density from Modified Proctor Tests)
Mean % Clay =	37.7		
Mean % Organic Matter =	0.4		
15 bar vol. moisture content = 0.026 + 0.005(37.67) + 0.0158(0.4)			
	Volumetric (%)	**Gravimetric (%)**	
15 bar Vol. Moisture Content =	22.1	12.4	Using mean values

The current applicable version of this publication resides on Jacobs' Intranet. All copies are considered to be uncontrolled.
Copyright© Jacobs Engineering Group Inc., 2007

Table B–7. Tailings Density

Tailings Maximum Dry Density				
Source: Golder Associates 4/3/06 Draft Tech Memo				
Standard Proctor Maximum Dry Density of Transition Tailings				
Sample Number	**Max Dry Density (pcf)**			
GABT-05	113.3			
GABT-07	107.3			
GABT-08	112.8			
GABT-09	102			
GABT-10	107.8		**90% of Mean**	
	108.6	**Mean**	98	pcf
	5	**Count**	1.57	g/cc

The current applicable version of this publication resides on Jacobs' Intranet. All copies are considered to be uncontrolled.
Copyright© Jacobs Engineering Group Inc., 2007

JACOBS	Calculation No: C-06	Page 1 of 12
Calculation Cover Sheet	Rev. No.: 0	Revision Date:
(Ref. FOWI 116 Design Calculations)	Previous Revision Date:	Current Revision Date:1/09/08
Issuing Department: *Federal Operations Design Engineering*	Supersedes:	
Client: Energy solutions Project Title: Moab UMTRA Project Number: 35DJ2600 System:	Engineering Discipline: Civil	
Calculation Title: Drainage During First Phase of Construction		

Purpose:

To develop flows for sizing sediment ponds and culverts for the first phase of construction.

Prepared by: Bob Yager Robert E. Yager Date: 1/09/08

Checked by: Bill Barton Bill Barton Date: 1/25/08

Engineering Managers Approval: Bill Barton Date: 1/25/08

The current applicable version of this publication resides on Jacobs' Intranet. All copies are considered to be uncontrolled.
Copyright© Jacobs Engineering Group Inc., 2007

Revision History:

Pages Affected By Revision	Revised/Added/Deleted	Description of Revision
All		

The current applicable version of this publication resides on Jacobs' Intranet. All copies are considered to be uncontrolled.
Copyright© Jacobs Engineering Group Inc., 2007

Description of Calculation:

Compute the peak discharges and the volumes of runoff from the 10yr 24 hour design storm to size culverts and sediment ponds for use during the construction of the waste cell at Crescent Junction. There are three sediment ponds and 5 culverts as shown in Figure 1. Culvert Culv_5 is used only for bleeding off some of the flow from near the active working area and is not sized as the other culverts are capable of carrying the computed discharges.

- Divide the areas into subwatersheds and assign initial abstraction, constant long-term infiltration rate, an SCS unit hydrograph lag time, or a USBR unit hydrograph to each subwatershed. A USBR unit hydrograph was developed only for the larger, principally undisturbed watersheds designated, S, X, and EMPUL.
- Apply a 10, 25, and 100 year 24 hour frequency storm to the system using HEC-HMS version 3.1.0 and extract the peak discharges and volumes of runoff.
- By trial and error using HEC-HMS, determine the configuration of culverts that will carry the 10 year 24 hour flow without overtopping the roads.
- Check culvert sizes using the Federal Highway Administration's culvert software HY8, version 7.0.

Assumptions:

- The 10, 25, and 100 year storms were developed in the Draft RAP. ("Site Drainage—Hydrology Parameters" calculation, Draft RAP Attachment 1, Appendix E).
- For the larger, relatively undisturbed subwatersheds, S, X, and EMPUL, a USBR unit hydrograph is appropriate. For smaller watersheds and/or more disturbed subwatersheds, the SCS unit hydrograph is appropriate.
- It is assumed that rainfall falling directly on the open excavation will be contained and pumped out at a later time. This rainfall is not included in this calculation.
- The volume of the ponds is required to contain the runoff from the 10-yr 24-hr storm plus 67 cubic yards of sediment/acre of drainage area.
- Each pond will be cleaned out at least once per year.

The current applicable version of this publication resides on Jacobs' Intranet. All copies are considered to be uncontrolled.
Copyright© Jacobs Engineering Group Inc., 2007

Design Inputs:

See following pages.

Software:

Title	Developer	Versions	Revision Level
HEC-HMS	USACE	3.1.0	
EXCEL	Microsoft	2002	
HY-8	FHWA	7.0	

The current applicable version of this publication resides on Jacobs' Intranet. All copies are considered to be uncontrolled.
Copyright© Jacobs Engineering Group Inc., 2007

Calculation Section:

See following pages.

The current applicable version of this publication resides on Jacobs' Intranet. All copies are considered to be uncontrolled.
Copyright© Jacobs Engineering Group Inc., 2007

Conclusions/Recommendations:

See following pages.

Reference:

See following pages.

The current applicable version of this publication resides on Jacobs' Intranet. All copies are considered to be uncontrolled.
Copyright© Jacobs Engineering Group Inc., 2007

DESCRIPTION OF CALCULATION:

Compute the peak discharges and the volumes of runoff from the 10yr 24 hour design storm to size culverts and sediment ponds for use during the construction of the waste cell at Crescent Junction (Stoller 2006). There are three sediment ponds and 5 culverts as shown in Figure 1. Culvert Culv_5 is used only for bleeding off some of the flow from near the active working area and is not sized as the other culverts are capable of carrying the computed discharges.

METHOD OF SOLUTION:

- Divide the areas into subwatersheds and assign initial abstraction, constant long-term infiltration rate, an SCS unit hydrograph lag time, or a USBR unit hydrograph to each subwatershed. A USBR unit hydrograph was developed only for the larger, principally undisturbed watersheds designated, S, X, and EMPUL.
- Apply a 10, 25, and 100 year 24 hour frequency storm to the system using HEC-HMS version 3.1.0 and extract the peak discharges and volumes of runoff.
- By trial and error using HEC-HMS, determine the configuration of culverts that will carry the 10 year 24 hour flow without overtopping the roads.
- Check culvert sizes using the Federal Highway Administration's culvert software HY8, version 7.0.

ASSUMPTIONS:

- The 10, 25, and 100 year storms were developed in the Draft RAP. ("Site Drainage—Hydrology Parameters" calculation, Draft RAP Attachment 1, Appendix E).
- For the larger, relatively undisturbed subwatersheds, S, X, and EMPUL, a USBR unit hydrograph is appropriate. For smaller watersheds and/or more disturbed subwatersheds, the SCS unit hydrograph is appropriate.
- It is assumed that rainfall falling directly on the open excavation will be contained and pumped out at a later time. This rainfall is not included in this calculation.

The current applicable version of this publication resides on Jacobs' Intranet. All copies are considered to be uncontrolled.
Copyright© Jacobs Engineering Group Inc., 2007

JACOBS (Ref. FOWI 116 Design Calculations)	Calculation Sheet Project: 35DJ2600 Calculation Number: C-06 Page 8 of 12

Figure 1. Layout of cell drainage during the first phase of construction.

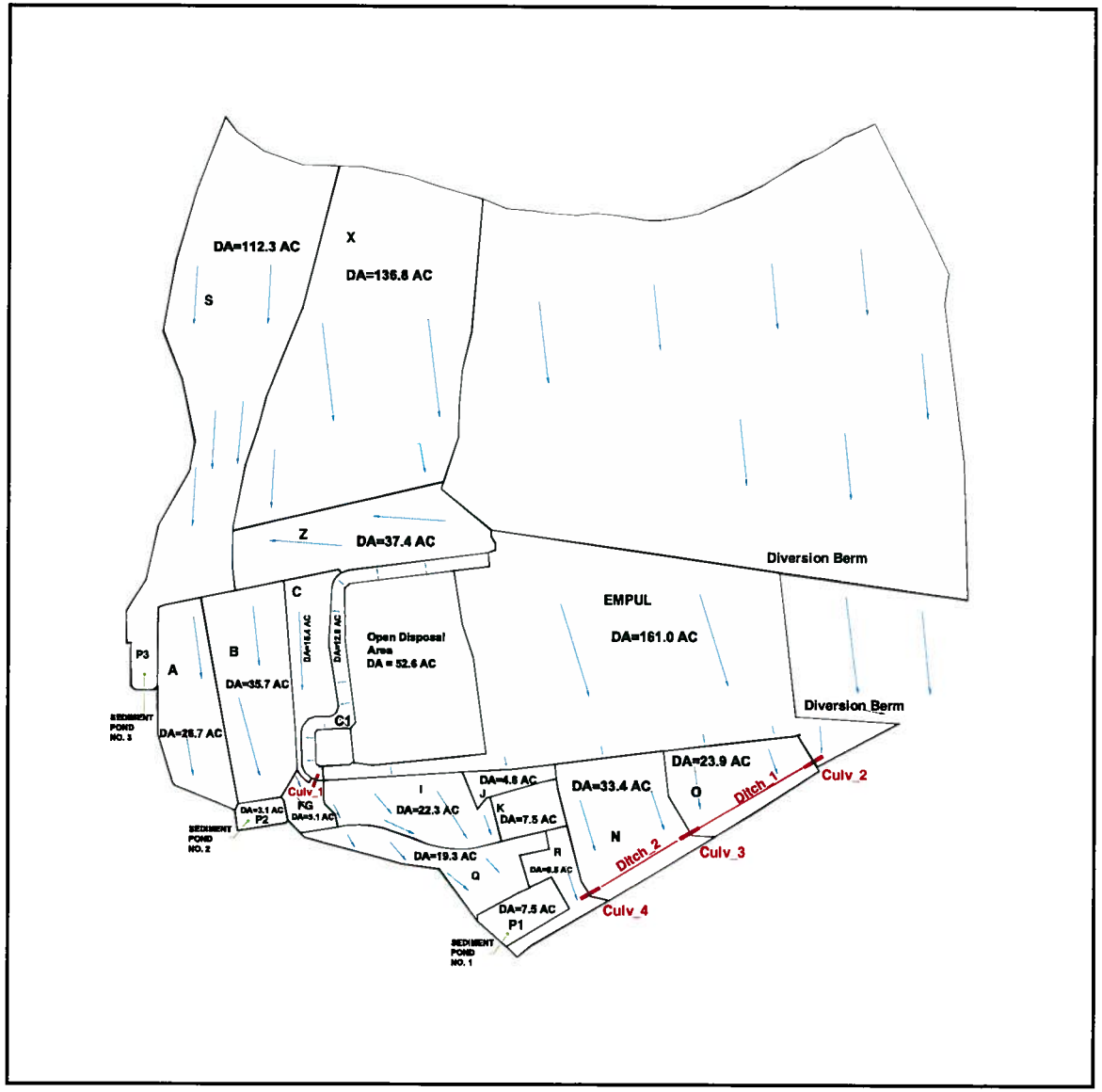

CALCULATION SECTION

Drainage Area Characteristics WatershedParms.xls

The drainage areas used in this analysis are shown in Figure 1.

For the undisturbed watersheds S and X composite curve numbers were developed. The western drainage is approximately 70% Toddler-Ravola-Glenton families association with an HSG of B and a constant infiltration rate of 0.2 – 0.6 inches/hr. The remainder is Hanksville family-Badland complex with an HSG of C and an infiltration rate of 0.0 – 0.06 inches/hr (WEB Soil Survey, http://websoilsurvey.nrcs.usda.gov/app/WebSoilSurvey.aspx, and Appendix B). For drainage X the Toddler-Ravola-Glenton families association comprises approximately 63% of the area with the remainder being Hanksville family-Badland complex. Assigning a runoff curve number of 75 to the type B soils for semiarid rangelands with herbaceous cover in fair to poor condition and 87 to the type C soils for the same use in poor condition (TR-55,), resulted in composite curve numbers of 78.6 for the S drainage and 79.4 for the X drainage. Computing initial abstraction using the NRCS curve number approach yields 0.54 inches for S and 0.52 for X. The NRCS initial abstraction is

$$I_a = 0.2\left[\frac{1000}{CN} - 10\right]$$

For largely natural areas consisting of the Toddler-Ravola-Glenton families association with an HSG of B and an infiltration rate of 0.2 – 0.6 inches/hr an NRCS curve number of 75 was used with an initial abstraction of 0.67 inches and a constant infiltration rate of 0.3 inches/hr. In areas that will be incidentally compacted by construction activities, the initial abstraction was assigned as 0.5 inches and the constant infiltration rate was 0.2 inches/hr.

Pertinent properties of the four drainage areas are computed in WatershedParms.xls and listed in Table 1. The flow lengths are used to develop a unit hydrograph using the USBR methodology and the Lag time is used in the SCS unit hydrograph method. The mean of the Kirpich and SCS time of concentration formulas is used for the time of concentration.

The Kirpich equation is $T_c = 0.0078\frac{L^{0.77}}{S^{0.385}}$ where

T_c = time of concentration (minutes)
L = slope length (feet [ft])
S = slope (ft/ft).

and the SCS equation is $T_c = \left(\frac{11.9L^3}{H}\right)^{0.385}$ where

T_c = time of concentration (hours)
L = slope length (miles)
H = slope height (ft).

The current applicable version of this publication resides on Jacobs' Intranet. All copies are considered to be uncontrolled.
Copyright© Jacobs Engineering Group Inc., 2007

Table 1. Drainage Area Characteristics

Drainage Area	Unit Hydrograph Approach	Area (acres)	Max Flow Length (ft)	Flow Length from Centroid	Elevation Difference (ft)	Lag (min)
A	SCS	26.7	2132		32	8.63
B	SCS	35.7	2173		34	8.61
C	SCS	15.4	2293		38	8.78
C1	SCS	12.8	3841		44	15.06
EMPUL	USBR	161	4934	3038	68	
FG	SCS	5.1	632		8	3.61
HI	SCS	22.3	1834		14	9.96
J	SCS	4.6	721		4	5.49
K	SCS	7.5	783		7	4.87
N	SCS	33.4	1598		24	6.91
O	SCS	23.9	1268		14	6.51
Q	SCS	19.3	2174		16	11.52
R	SCS	9.5	715		14	3.36
S	USBR	112.3	5580	3383	680	
X	USBR	136.8	4270	2424	756	
Z	SCS	37.4	2392		30	10.10
P1 (Pond)	SCS	7.5	500		2	4.7
P2 (Pond)	SCS	3.1	500		2	4.7

The data for ponds is included simply to add the volume of precipitation on the surface.

Runoff Hydrograph Calculations ConstructionRunoff.hms

For drainage areas that are large and in a largely natural condition, the USBR (Design of small dams, 1978) unit hydrograph transform was used. The USBR method was developed for natural areas in the west and is not appropriate for the constructed wedge and cell. For drainage areas that are constructed, disturbed, or small, the SCS unit hydrograph transform was used. The runoff hydrographs were computed using the Computer Program HEC-HMS (USACE 2007). The rainfall distribution was the built-in frequency storm distribution.

Design Storms

The sediment ponds, drainage ditches, and culverts are designed for the 10 year 24 hour storm as specified in Table 2. Runoff from the 25 year and 100 years storms was also computed.

The current applicable version of this publication resides on Jacobs' Intranet. All copies are considered to be uncontrolled.
Copyright© Jacobs Engineering Group Inc., 2007

Table 2 Rainfall Depths for Design Storms.

Precipitation Duration	Precipitation Depth (inches)		
	10 Year	25 Year	100 Year
5 Minutes	0.25	0.34	0.53
15 Minutes	0.48	0.64	0.99
1 Hour	0.80	1.07	1.65
2 Hours	0.91	1.21	1.82
3 Hours	0.97	1.26	1.84
6 Hours	1.13	1.42	1.95
12 Hours	1.36	1.65	2.16
24 Hours	1.63	1.91	2.35

Hydrograph Routing

The runoff from sub-basin C1 is conveyed to pond P2 through culvert Culv_1. This was simulated in the HEC-HMS model by a reservoir with minimal storage; less than 5 cubic feet maximum for the 10 year storm. The flow from sub-basins N, O and EMPUL is routed through culverts Culv_2, Culv_3, and Culv_4 using the reservoir option with culvert outlets and through ditches Ditch_1 and Ditch_2 using the kinematic wave option in trapezoidal ditches with a 10 foot bottom width and 3/1 side slopes. The flow in the ditches is less than 2 feet deep for the peak flow of the 10 year storm. Culverts Culv_2, Culv_3, and Culv_4 are also modeled as reservoirs with culvert outlets. In each case the maximum reservoir storage is less than 7 cubic feet for the 10 year storm. Culvert Culv_5 is not simulated in the HEC-HMS model. It is included in the plans to allow some of the drainage from near the open excavation to bypass the culverts and ditches draining to Pond P1.

The pertinent parameters of the culverts and ditches are presented in Table 3.

Table 3 Culvert Data and Predicted Maximum Water Surface Elevation

Culvert	Configuration	Inlet Invert	Outlet Invert	Length	Road Crest Elevation	Peak Flow (cfs)	Maximum WS Elevation in 10 Year Storm
Culv_1	Single 30" RCP	4950.48	4949.33	65	4955.43	15.8	4952.47
Culv_2	Double 36" RCP	4931.95	4930.68	148	4936.91	105.0	4935.76
Culv_3	Double 36" RCP	4922.70	4921.16	232	4931.04	105.0	4926.51
Culv_4	Double 36" RCP	4916.20	4915.26	193	4926.19	106.3	4920.06
Culv_5	Single 30" RCP	NA					
Check Culverts with HY8							
Culv_1	Single 30" RCP	4950.48	4949.33	65	4955.43	15.8	4952.39
Culv_2	Double 36" RCP	4931.95	4930.68	148	4936.91	105.0	4935.76
Culv_3	Double 36" RCP	4922.70	4921.16	232	4931.04	105.0	4926.51
Culv_4	Double 36" RCP	4916.20	4915.26	193	4926.19	106.3	4920.06
Ditch	Length	Bottom Width (ft)	Side Slope	Channel Slope	Peak Flow (cfs)	Manning n	Depth at Peak Flow (ft)
Ditch_1	1206	10	3	0.0066	98.7	.025	1.39
Ditch_2	962	10	3	0.0057	98.8	.025	1.45

The current applicable version of this publication resides on Jacobs' Intranet. All copies are considered to be uncontrolled.
Copyright© Jacobs Engineering Group Inc., 2007

Volume of Flow to Sediment Ponds

The required volume of sediment ponds is equal to 67-cy of sediment volume per acre of drainage area plus the runoff volume from the 10 year 24 hour storm. The three sediment ponds listed in Table 4. are sized according to these criteria.

Table 4 Required Volumes of Sediment Ponds.

Pond	Drainage Area (acres)	Volume Required for Sediment (ac-ft)	Volume of Runoff (ac-ft) from 10 yr storm (HMS)	Total Required Volume (ac-ft)
P1	306.9	12.7	10.8	23.5
P2	80.9	3.4	5.3	8.7
P3	286.5	11.9	12.6	24.5

Summary

Ditches, culverts, and sediment ponds have been sized to handle the runoff from the 10 year 24 hour storm. Their specifications are presented in Tables 3, and 4. Pond P3 is slightly smaller than the volume specified in Table 4 and, therefore, must be cleaned out approximately once every 10 months.

References:

HEC-HMS Users Guide, USACE, 2006

HEC-HMS Applications Guide, USACE, 2002

HEC-HMS Technical Reference Manual, 2000

Stoller, 2006 - Moab UMTRA Project, Crescent Junction Disposal Site, Storm Water Pollution Prevention Plan, DOE-EM/GJ1238-2006, July 2006

The current applicable version of this publication resides on Jacobs' Intranet. All copies are considered to be uncontrolled.
Copyright© Jacobs Engineering Group Inc., 2007

JACOBS *Calculation Cover Sheet*	Calculation No: C-09	Page 1 of 8
	Rev. No.: A	Revision Date: 1/23/08
	Previous Revision Date:	Current Revision Date:
Issuing Department: *Federal Operations Design Engineering*	Supersedes:	
Client: Project Title: Moab Project Number: 35DJ2600 System:	Engineering Discipline: Civil	
Calculation Title: Verification of Actual Pond Size to Pond Size Required		
Purpose: To determine the size of the sediment ponds at the Crescent Junction Site		

Prepared by: Frank Parton *Frank Parton* Date: 1/10/08

Checked by: Bill Barton *Bill Barton* Date: 1/11/08

Engineering Managers Approval: *Bill Barton* Date: 1/28/09

C09_Verification_Pond_Size_012308.doc

The current applicable version of this publication resides on Jacobs' Intranet. All copies are considered to be uncontrolled.
Copyright© Jacobs Engineering Group Inc., 2007

Revision History:

Pages Affected By Revision	Revised/Added/Deleted	Description of Revision

The current applicable version of this publication resides on Jacobs' Intranet. All copies are considered to be uncontrolled.
Copyright© Jacobs Engineering Group Inc., 2007

Description of Calculation:
This calculation will size the ponds at the Crescent Juction site to hold a 10-year, 24-hour run-off event plus 67 CY/acre/year of sediment accumulation.

Assumptions:

It is assumed that each sediment basin will be cleaned out at least one time per year.

Design Inputs:
Area of each contour from within the ponds were taken from the Autocad drawing.

Software: None.

Title	Developer	Versions	Revision Level

The current applicable version of this publication resides on Jacobs' Intranet. All copies are considered to be uncontrolled.
Copyright© Jacobs Engineering Group Inc., 2007

Calculation Section:

Sediment Pond No. 1

Elevation	Area	Volume
4907	0	
		37437
4908	74874.6	
		317972
4910	243097	
		507522
4912	264425	
		70139
4914	280556.5	
4914.5	0	
Total		1478052 CF = 54743 CY
	Total Storage Available	= 33.9 AC-FT

Storage Required:

Sediment storage = 67 Cy/Ac disturbed (assumed)

Disturbed Area = 307 Ac

Sediment storage = 67 Cy/Ac X 307 Ac = 20569 Cy = 555363 Cf = 12.7 AC-FT

10 yr – 24 hr Storage Required = 10.8 AC-FT (from calculation C-06)

Total Storage Required = 23.5 AC-FT

Total Storage Available is larger than Total Storage Required

The current applicable version of this publication resides on Jacobs' Intranet. All copies are considered to be uncontrolled.
Copyright© Jacobs Engineering Group Inc., 2007

Sediment Pond No. 2

Elevation	Area	Volume
4942.3	0	
		29194
4944	34345.5	
		122391
4946	88045.5	
		203844
4948	115798.6	
		28950
4948.5	0	
Total		384378 CF = 14236 CY
	Total Storage Available	= 8.8 AC-FT

Storage Required:

Sediment storage = 67 Cy/Ac disturbed (assumed)

Disturbed Area = 81 Ac

Sediment storage = 67 Cy/Ac X 81 Ac = 5427 Cy = 146529 Cf = 3.4 AC-FT

10 yr – 24 hr Storage Required = 5.3 AC-FT (from calculation C-06)

Total Storage Required = 8.7 AC-FT

Total Storage Available is larger than Total Storage Required

Sediment Pond No. 3

Elevation	Area	Volume
4967.5	0	
		10089
4968	40356	
		85642
4970	45286	
		162914
4972	117628	
		243827
4974	126199	
		274069
4976	147870	
		147870
4978	0	

The current applicable version of this publication resides on Jacobs' Intranet. All copies are considered to be uncontrolled.
Copyright© Jacobs Engineering Group Inc., 2007

Total		924411 CF = 34237 CY
	Total Storage Available	= 21.2 AC-FT

Storage Required:

Sediment storage = 67 Cy/Ac

Disturbed Area = 286.5 Ac

Sediment storage = 67 Cy/Ac X 286.5 Ac = 19196 Cy = 518279 Cf = 11.9 AC-FT

10 yr – 24 hr Storage Required = 12.6 AC-FT (from calculation C-06)

Total Storage Required = 24.5AC-FT

Total Storage Available is smaller than Total Storage Required, therefore the pond must be cleaned out more than once a year to maintain the water volume and sediment storage required.

Sediment Pond No. 4

Elevation	Area	Volume
4959	0	
		12982
4960	25964	
		55702
4962	29738	
		129150
4964	99412	
		209719
4966	110307	
		231311
4968	121004	
		252504
4970	131500	
		32875
4970.5	0	
Total		924243 CF = 34231 CY
	Total Storage Available	= 21.2 AC-FT

Storage Required:

Sediment storage = 67 Cy/Ac

Disturbed Area = 32.7 Ac

Sediment storage = 67 Cy/Ac X 32.7 Ac = 2188.2 Cy = 59081.9 Cf = 1.4 AC-FT

The current applicable version of this publication resides on Jacobs' Intranet. All copies are considered to be uncontrolled.
Copyright© Jacobs Engineering Group Inc., 2007

10 yr – 24 hr Storage Required = 14.3 AC-FT (from calculation C-06)

Total Storage Required = 15.7 AC-FT

Total Storage Available is larger than Total Storage Required

The current applicable version of this publication resides on Jacobs' Intranet. All copies are considered to be uncontrolled.
Copyright© Jacobs Engineering Group Inc., 2007

Conclusions/Recommendations:

The ponds are adequately sized to hold the 10 – year, 24 – hour storm and the sediment from the disturbed areas upstream for one year.

Reference:

The current applicable version of this publication resides on Jacobs' Intranet. All copies are considered to be uncontrolled.
Copyright© Jacobs Engineering Group Inc., 2007

JACOBS	Calculation No: C-10	Page: 1 of 13
Calculation Cover Sheet	Rev. No.: 2	Revision Date: 4/17/08
(Ref. FOWI 116 Design Calculations)	Previous Revision Date: 2/15/08	Current Revision Date: 4/17/08
Issuing Department: *Federal Operations Design Engineering*	Supersedes: Revision 1 (dated 2/15/08)	
Client: Project Title: Moab UMTRA Project Project Number: System:	Engineering Discipline: Geotechnical	

Calculation Title:
Slope Stability of Crescent Junction Disposal Cell

Purpose:

Uranium containment dike must be stable at the end of construction and for long term once the cover material is placed above it. For this purpose, slope stability runs were made to calculate factor of safety for various static and seismic conditions for both End of Construction and Long Term cases.

NQA-1 QUALITY LEVEL: 2

Prepared by: Omar Ibarra Date: 4-17-2008

Checked by: K.K. Chelkowski Date: 4-17-2008

Engineering Managers Approval: William D. Bartlett Date: 5/5/2008

The current applicable version of this publication resides on Jacobs' Intranet. All copies are considered to be uncontrolled.
Copyright© Jacobs Engineering Group Inc., 2007

Revision History:

Pages Affected By Revision	Revised/Added/Deleted	Description of Revision
Rev. 2	Revision Page 4 of 13 Design Input	Changes to the tailings geometry obtained from the 90% drawings resulted in the following changes: Top of Dike: El. 4967' (instead of 4964') Cover thickness: 9 ft (instead of 10 ft) Cover top elevation: El. 4978 – 4982' at analysis location (instead of El. 4972')
	Addition Page 6 of 13 Calculation Section	Summary of results and analysis.
	Addition / Revision Pages 7 and 8 of 13 Drawings	Inserted new contour plan of tailings pile. Inserted new detail of tailings embankment geometry.
	Revision Pages 10 and 11 of 13 Slope Stability Analyses	New FS results – End of Construction (static). New FS results – End of Construction (seismic)
	Revision Page 12 and 13 of 13 Slope Stability Analyses	New results – Long Term (static) New results – Long Term (seismic)

The current applicable version of this publication resides on Jacobs' Intranet. All copies are considered to be uncontrolled. Copyright© Jacobs Engineering Group Inc., 2007

Description of Calculation:

The calculations presented here are for determining and verifying stability of the disposal cell at the Crescent Junction disposal site in order to assess long term stability of the tailings.

A disposal cell section at southwest corner of the cell was analysed for End of Construction (short term) and Long Term cases. Stability of the cell dike was also assessed for the design seismic event for both short term and long term cases.

The subsurface conditions were determined from borings taken near the section. Geotechnical design parameters were developed/obtained from project reports and previous analyses.

The analyses were performed with an established commercial program SLIDE, V 5.0 by Rocscience. The SLIDE program analyzes the slope with various methods to determine factor of safety including Bishop Simplified, Janbu Simplified, Janbu Corrected, Spencer, Morgenstern-Price and Corps of Engineer Methods. Bishop and Janbu methods employ limit equilibrium analysis method while Spencer and Morgenstern-Price methods use both force equilibrium and moment equilibrium to calculate safety factors. In this analysis, Spencer results were reviewed for the lowest factor of safety.

Assumptions:

The plan location and cross section selected for analyses are shown in Figure 1 and 2. The location is within first phase of construction near southwest section of the disposal cell and represents critical height and geometry.

No groundwater table was assumed. All borings were dry, and the review of historical data indicated that water table at depth exceeding 100 feet below ground surface. It is assumed that the tailings will be deposited by compacting it to 90 percent of the maximum density as determined by ASTM D1557 at slightly above (2%) optimum moisture content. From the review of test results and previous analyses, it is determined that excess pore pressure will not be a factor in the stability analysis.

The current applicable version of this publication resides on Jacobs' Intranet. All copies are considered to be uncontrolled. Copyright© Jacobs Engineering Group Inc., 2007

Design Inputs:

For SLIDE computer program, the design inputs were:

Material Properties

The material properties were obtained from borings, laboratory test results and from previous analyses performed by others.

MATERIAL	Unit Weight			Shear Strength			
				Total		Effective	
	Dry (pcf)	Moisture Content (%)	Moist (pcf)	Friction Angle (Degree)	Cohesion (psf)	Friction Angle (Degree)	Cohesion (psf)
UMTRA Cover	111	11.7	124	26	0	26	0
Tailings	98	17.4	115	0	615	32	0
Dike Fill	111	11.7	124	19	0	26	0
In-situ Overburden Material - ML	92	6.7	98	26	0	26	0
Weathered Mancos Shale	104	7.3	112	25	0	25	0

Note:
Physical properties of in-situ overburden soils and weathered Mancos Shale were determined from the earlier design phase calculations – 'Geotechnical Properties of Native Soils', Attachment 5, Vol. 1, Appendix E. Physical properties of UMTRA cover, tailings and dike fill, and strength properties of all materials were obtained from Attachment 5, Vol. 1, Appendix C.

Slope Geometry

The slope cross section was selected from 90% plans and shown in Figure 2.
Ground surface elevation at this section varied from 4954' to 4944' dipping towards the south.
Top of dike was estimated at Elevation 4967'.
Cover material will be 9-foot thick with top Elevation at 4978' – 4982' at the analysis location.
For site characterization and to determine geotechnical design parameters for the in-situ materials, Borings CRJ01 – 0205 and CRJ01 – 0212 were used.
Water surface was not used.
Dike exterior slope was configured at 5 horizontal to 1 vertical.

Analysis Conditions

End of Construction (short term) using shear strength derived from total stresses.
Long Term case was analysed using effective stresses.

The current applicable version of this publication resides on Jacobs' Intranet. All copies are considered to be uncontrolled. Copyright© Jacobs Engineering Group Inc., 2007

Earthquake Effects

Seismic conditions were analyzed using guidance provided in the Technical Approach Document (TAD), 1989. TAD requires the use of pseudo-static approach where Peak Horizontal Acceleration (PHA) value of 0.22 g (previously determined) is taken as half of PHA or 0.11 g for End of Construction case, and 2/3rd of PHA or 0.15 g for Long Term case.

Required Minimum Factor of Safety

Guidelines provided in TAD for minimum acceptable safety factors are as under:

End of Construction – Static 1.3
End of Construction – Seismic 1.0

Long Term - Static 1.5
Long Term - Seismic 1.0

Software:

Title	Developer	Versions	Revision Level
SLIDE	Rocscience, Inc	5.0	

The current applicable version of this publication resides on Jacobs' Intranet. All copies are considered to be uncontrolled. Copyright© Jacobs Engineering Group Inc., 2007

Calculation Section:

See attached

As seen in the attached stability runs, the following factor of safety were obtained for the containment dike:

End of Construction – Static		2.15
End of Construction – Seismic		1.31
Long Term	- Static	2.78
Long Term	- Seismic	1.51

The current applicable version of this publication resides on Jacobs' Intranet. All copies are considered to be uncontrolled. Copyright© Jacobs Engineering Group Inc., 2007

Conclusions/Recommendations:

Based on the stability analyses, the disposal cell with its containment dike and cover material meets the factor of safety standards established for this structure. The stability results obtained by these analyses verify the results obtained and presented in the Revised Remedial Action Plan.

Reference:

DOE (U.S. Department of Energy), Revised Remedial Action Plan and Site Design for Stabilization of Moab Title I Uranium Mill Tailings at the Crescent Junction, Utah, Disposal Site, Attachment 1 and Attachment 5, June 2007

U.S. Department of Energy, Technical Approach Document, 1989, DOE/UMTRA

SLIDE Computer program, prepared by Rocscience Inc. 31 Balsam Avenue, Toronto, Ontario

The current applicable version of this publication resides on Jacobs' Intranet. All copies are considered to be uncontrolled. Copyright© Jacobs Engineering Group Inc., 2007

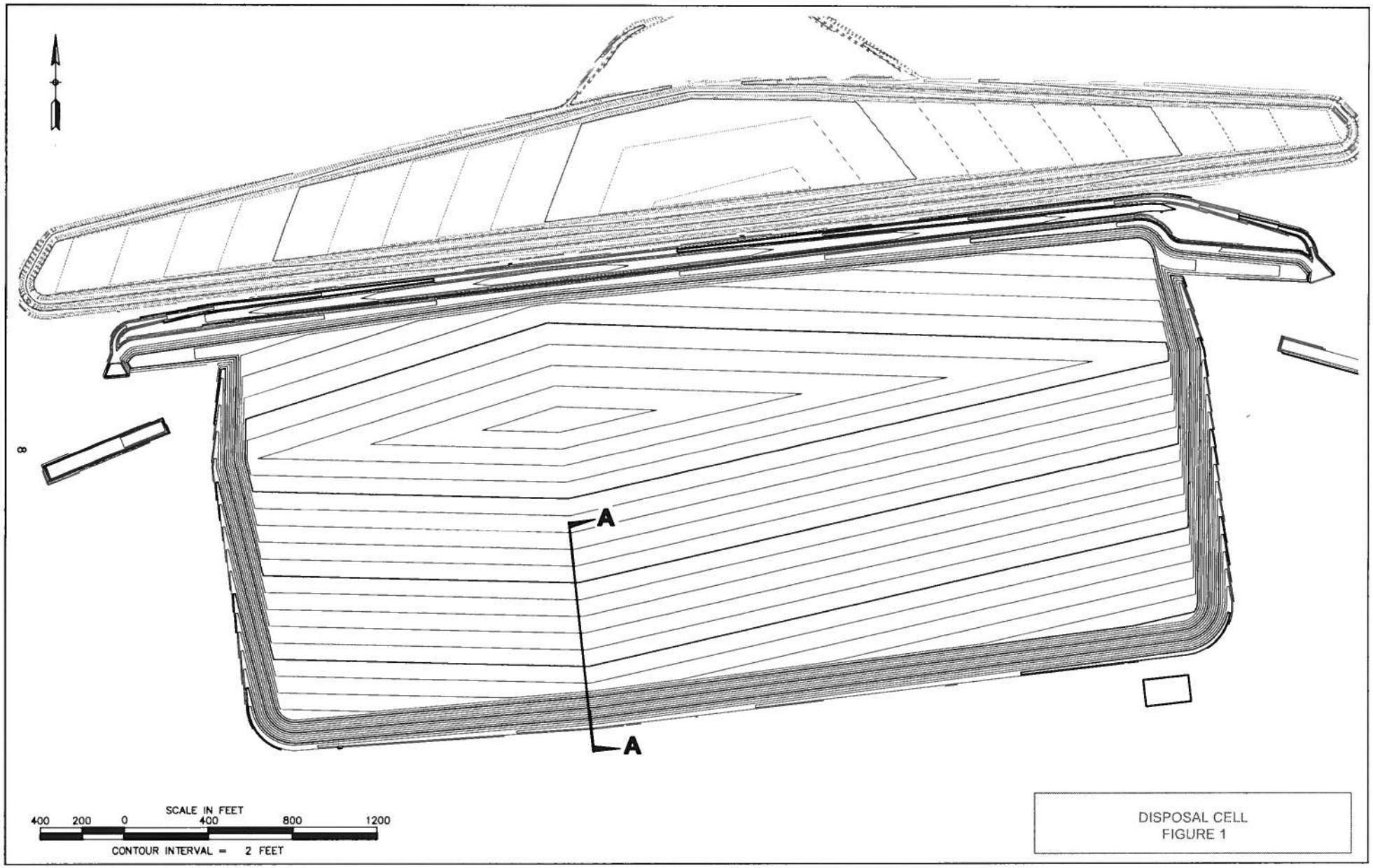

DISPOSAL CELL
FIGURE 1

L:\eng\CMR\Documents\FIG-FULL-SL-STABILITY-PLAN.dwg, Layout1, 4/7/2009 9:04:42 AM, DWG To PDF.pc3, ANSI expand B (11.00 x 17.00 Inches), 1:1.00000

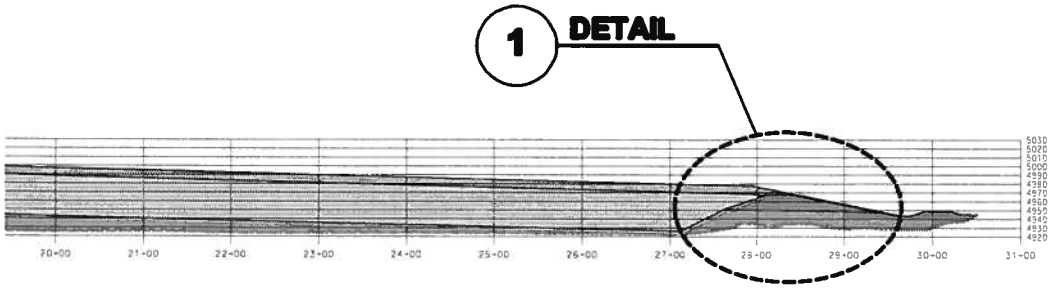

CAP CROSS-SECTION A-A - NORTH-SOUTH

SCALE: HORIZONTAL 1"=200'
VERTICAL 1"=200'

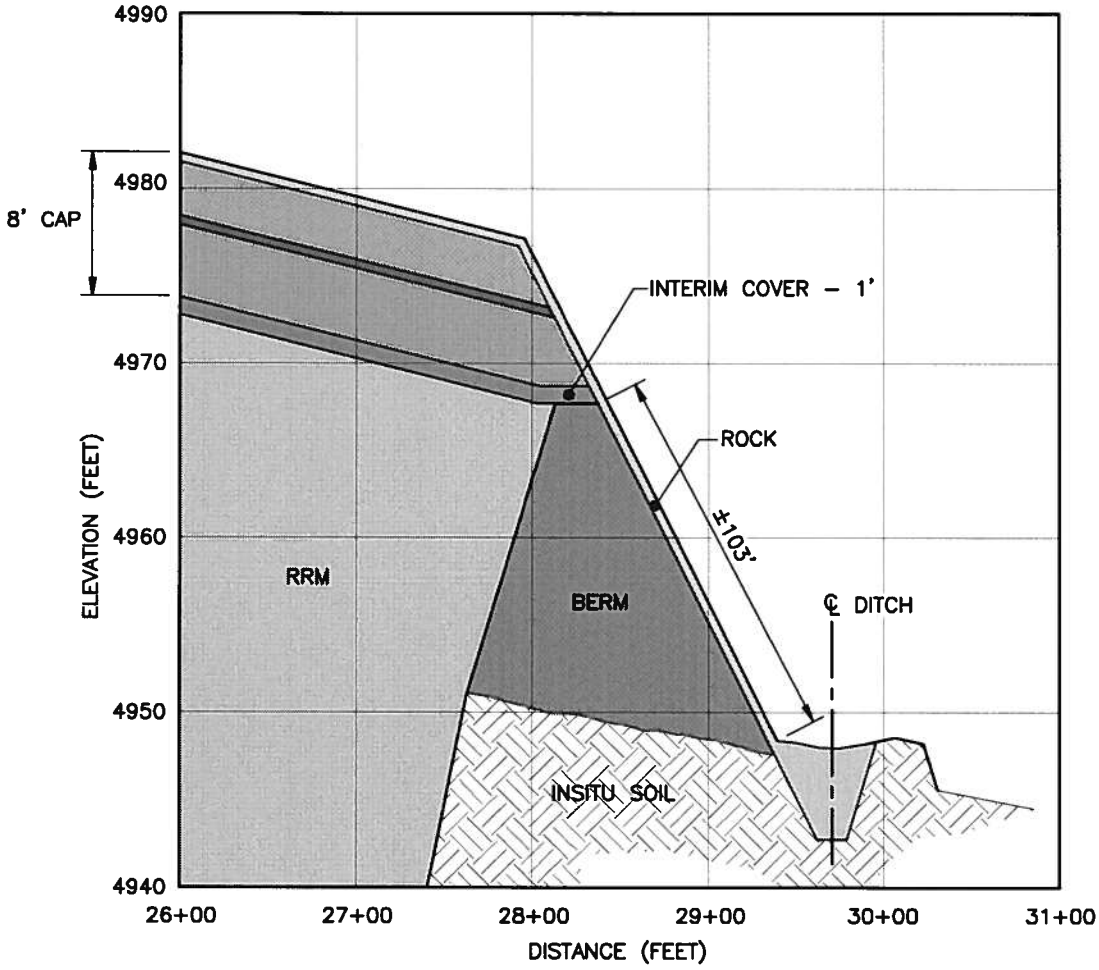

1 **DETAIL**

SCALE: HORIZONTAL 1"=100'
VERTICAL 1"=10'

DISPOSAL CELL DIKE
FIGURE 2

I:\eng\Civil\Documents\FIG-01-STABILITY-SECTIONS.dwg, Layout1, 4/7/2006 8:55:19 AM, DWG To PDF.pc3, ANSI expand A (8.50 x 11.00 Inches), 1:1.03446

Crescent Junction Disposal Cell

Material Properties

Material: UMTRA Cover
Unit Weight: 124 lb/ft3, Cohesion: 0 psf, Friction Angle: 26 degrees

Material: Tailings
Unit Weight: 115 lb/ft3, Cohesion: 615 psf, Friction Angle: 0 degrees

Material: Dike Fill
Unit Weight: 124 lb/ft3, Cohesion: 0 psf, Friction Angle: 19 degrees

Material: Overburden
Unit Weight: 98 lb/ft3, Cohesion: 0 psf, Friction Angle: 26 degrees

Material: Weathered Mancos shale
Unit Weight: 112 lb/ft3, Cohesion: 0 psf, Friction Angle: 25 degrees

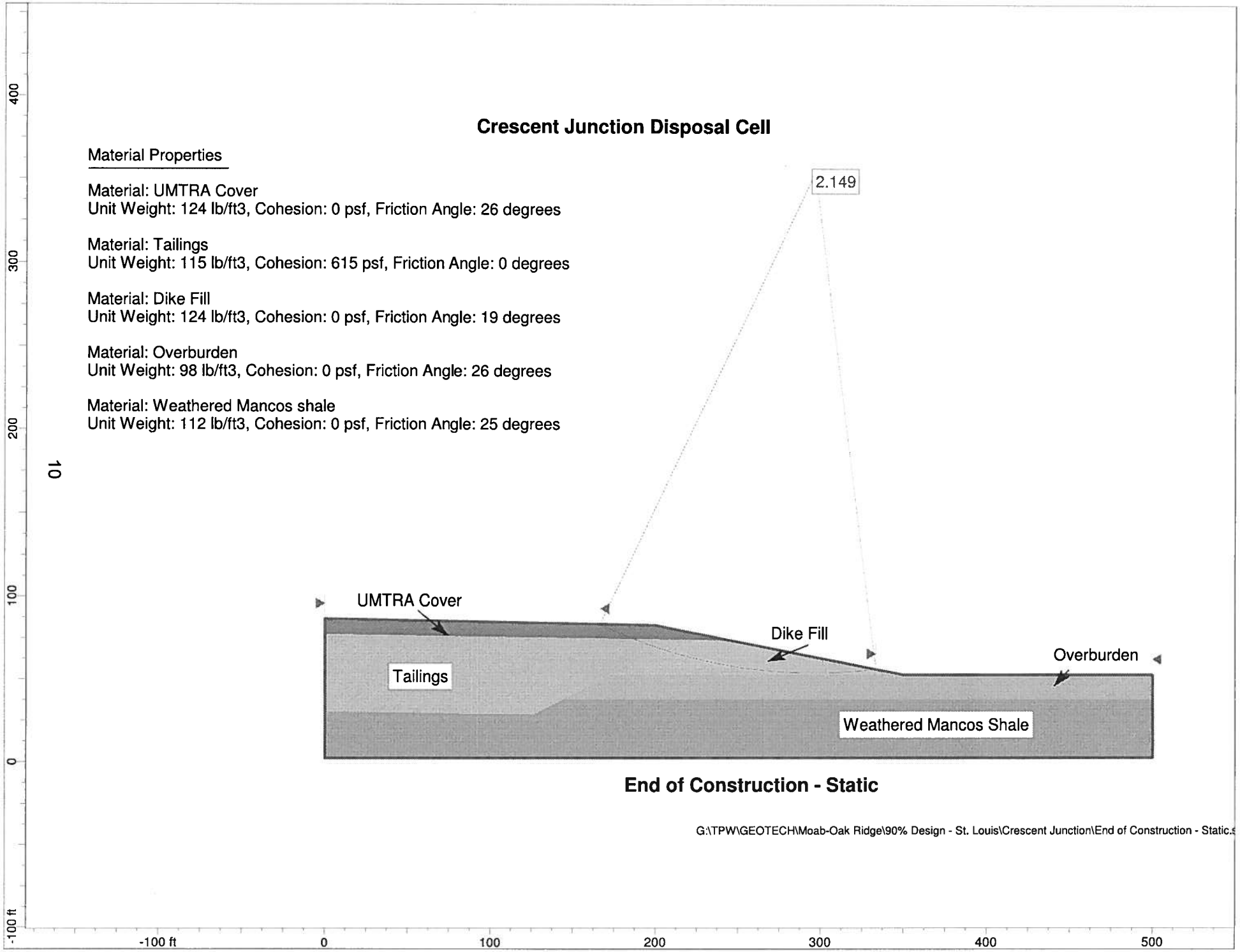

End of Construction - Static

G:\TPW\GEOTECH\Moab-Oak Ridge\90% Design - St. Louis\Crescent Junction\End of Construction - Static.s

Crecsent Junction Disposal Cell

Material Properties

UMTRA Cover
Unit Weight: 124 lb/ft3, Cohesion: 0 psf, Friction Angle: 26 degrees

Tailings
Unit Weight: 115 lb/ft3, Cohesion: 615 psf, Friction Angle: 0 degrees

Dike Fill
Unit Weight: 124 lb/ft3, Cohesion: 0 psf, Friction Angle: 19 degrees

Overburden
Unit Weight: 98 lb/ft3, Cohesion: 0 psf, Friction Angle: 26 degrees

Weathered Mancos shale
Unit Weight: 112 lb/ft3, Cohesion: 0 psf, Friction Angle: 25 degrees

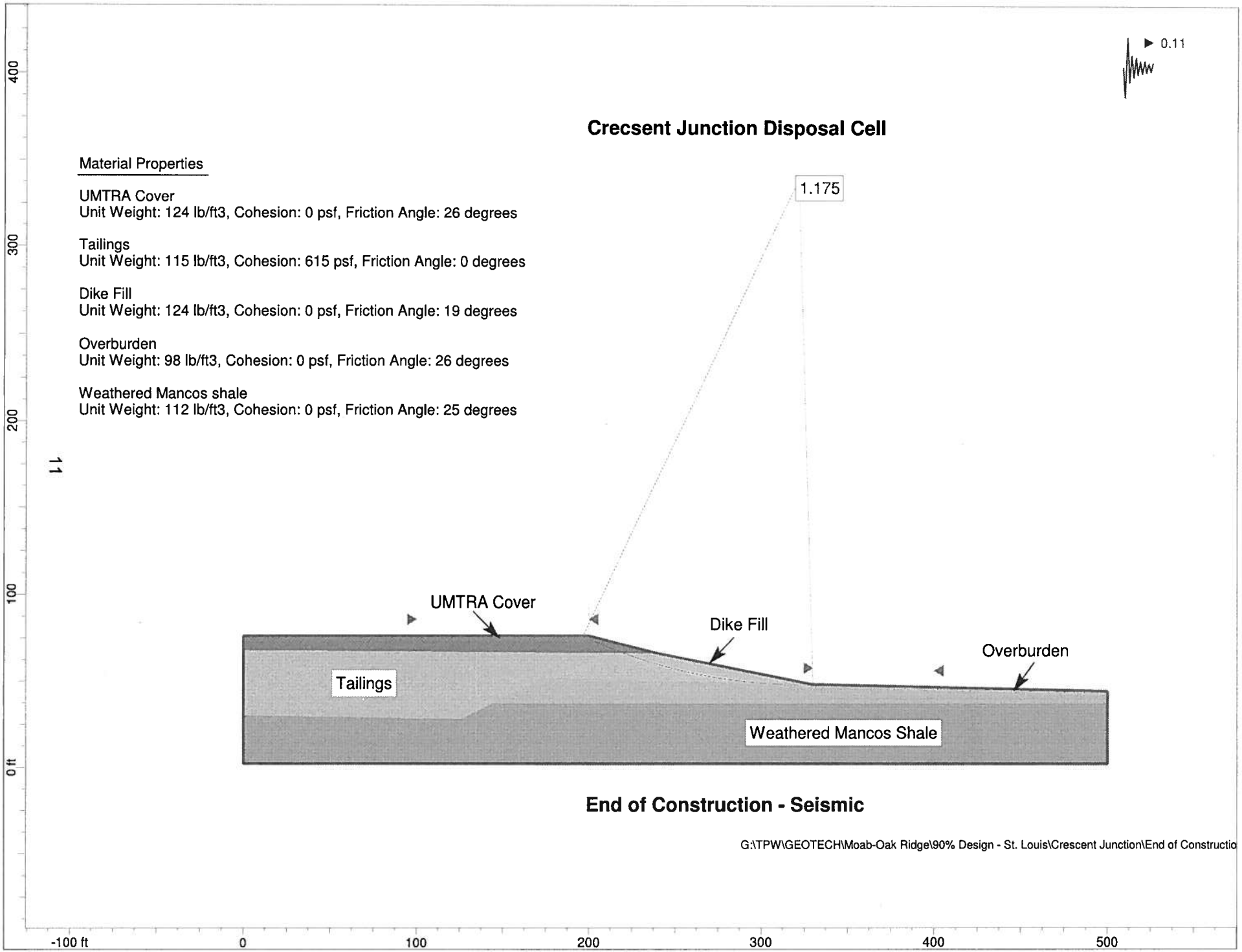

End of Construction - Seismic

G:\TPW\GEOTECH\Moab-Oak Ridge\90% Design - St. Louis\Crescent Junction\End of Constructio

Crescent Junction Disposal Cell

Material Properties

Material: UMTRA Cover
Unit Weight: 124 lb/ft3, Cohesion: 0 psf, Friction Angle: 26 degrees

Material: Tailings
Unit Weight: 115 lb/ft3, Cohesion: 0 psf, Friction Angle: 32 degrees

Material: Dike Fill
Unit Weight: 124 lb/ft3, Cohesion: 0 psf, Friction Angle: 26 degrees

Material: Overburden
Unit Weight: 98 lb/ft3, Cohesion: 0 psf, Friction Angle: 26 degrees

Material: Weathered Mancos shale
Unit Weight: 112 lb/ft3, Cohesion: 0 psf, Friction Angle: 25 degrees

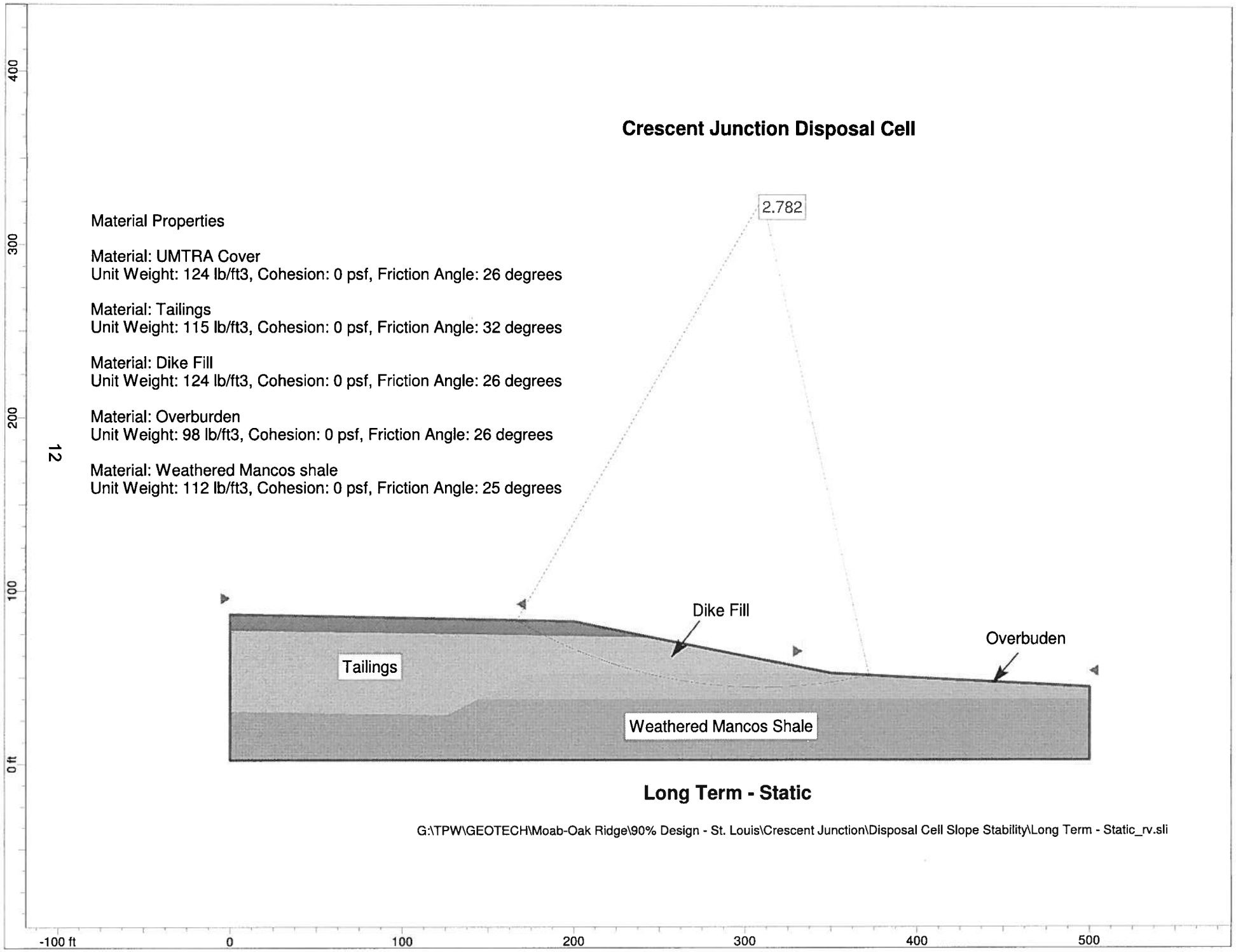

Long Term - Static

G:\TPW\GEOTECH\Moab-Oak Ridge\90% Design - St. Louis\Crescent Junction\Disposal Cell Slope Stability\Long Term - Static_rv.sli

Crescent Junction Disposal Cell

Material Properties

Material: UMTRA Cover
Unit Weight: 124 lb/ft3, Cohesion: 0 psf, Friction Angle: 26 degrees

Material: Tailings
Unit Weight: 115 lb/ft3, Cohesion: 0 psf, Friction Angle: 32 degrees

Material: Dike Fill
Unit Weight: 124 lb/ft3, Cohesion: 0 psf, Friction Angle: 26 degrees

Material: Overburden
Unit Weight: 98 lb/ft3, Cohesion: 0 psf, Friction Angle: 26 degrees

Material: Weathered Mancos shale
Unit Weight: 112 lb/ft3, Cohesion: 0 psf, Friction Angle: 25 degrees

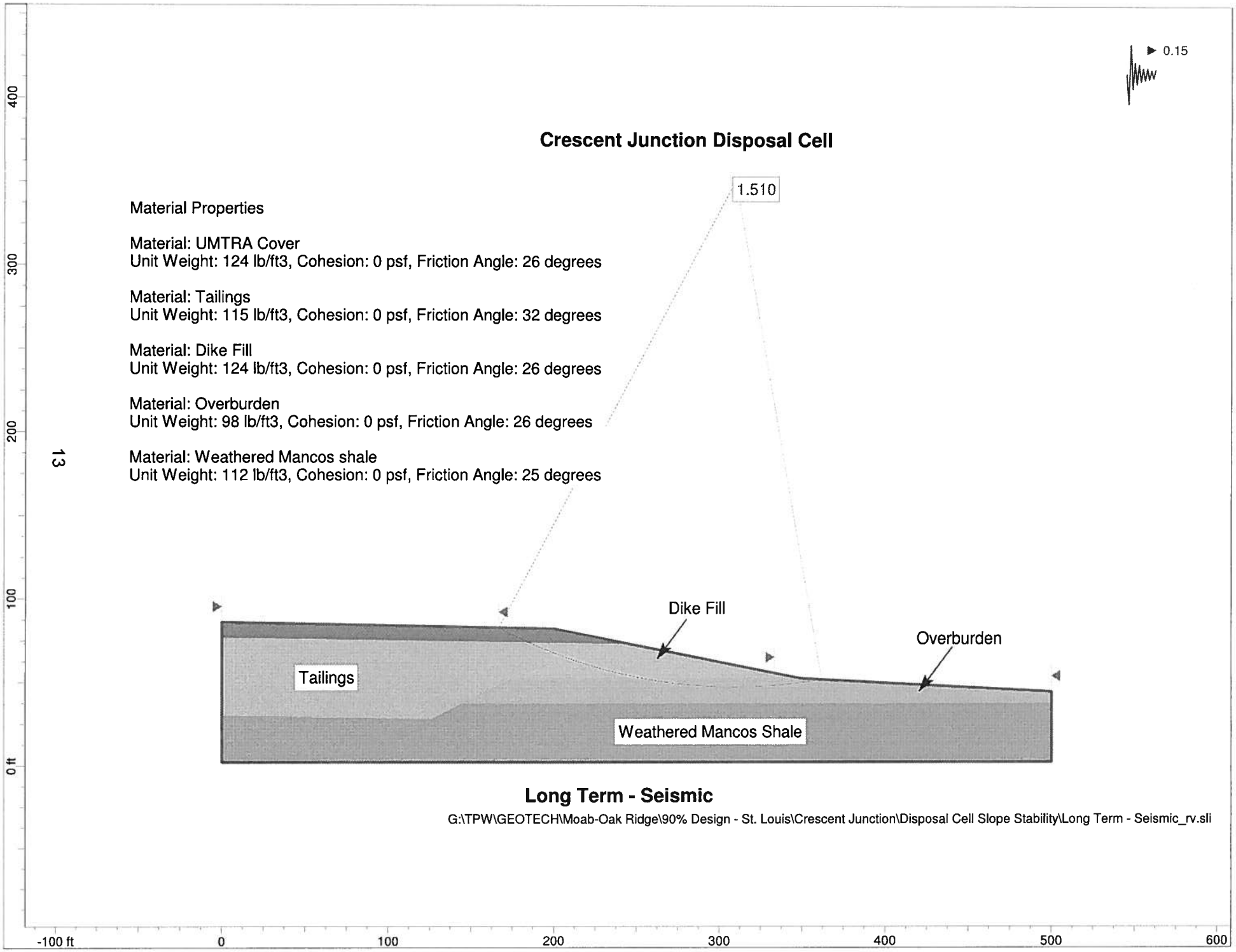

Long Term - Seismic

G:\TPW\GEOTECH\Moab-Oak Ridge\90% Design - St. Louis\Crescent Junction\Disposal Cell Slope Stability\Long Term - Seismic_rv.sli

JACOBS	Calculation No: C-11	Page: 1 of 14
Calculation Cover Sheet	Rev. No.: 1	Revision Date: 4/15/08
(Ref. FOWI 116 Design Calculations)	Previous Revision Date: 1/15/08	Current Revision Date: 4/15/08
Issuing Department: *Federal Operations Design Engineering*	Supersedes: Revision 0 (dated 1/15/08)	
Client: U.S. Department of Energy Project Title: Moab – UMTRA Project Project Number: 35DJ2600 System:	Engineering Discipline: Geotechnical	

Calculation Title: Settlement Analysis of Uranium Mine Tailings at Crescent Junction, UT

Purpose:

Determine the magnitude of settlement for the uranium mill tailings pile to be constructed at the Crescent Junction Disposal site.

The present condition and characteristics of the uranium mill tailings at the Moab repository site are considerably different than what is anticipated to be placed at the Crescent Junction disposal site. Material properties of the existing mine tailings are available for the Moab site. During the course of this project, the mine tailings at Moab will be mixed and dried out to optimum moisture content before being transported to Crescent Junction. There, the tailings will be placed and compacted to 90% of the maximum density per ASTM D698. The settlement analysis is based on the consolidation characteristics of the remolded tailing materials as reported by others. Both primary and secondary settlements are estimated due to loads imposed on each incremental tailing layer by the cover material and the tailing material above. The settlement of the tailings was also assessed by estimating the compression of the tailing by its own weight.

NQA-1 QUALITY LEVEL: 2

Prepared by: Ahmad Hassan Date: 4-15-2008

Checked by: KK Chepkoit Date: 4-15-2008

Engineering Managers Approval: William D. Bates Date: 05/05/2008

The current applicable version of this publication resides on Jacobs' Intranet. All copies are considered to be uncontrolled.
Copyright© Jacobs Engineering Group Inc., 2007

Revision History:

Pages Affected By Revision	Revised/Added/Deleted	Description of Revision
Rev. 1	Revision / Addition Page 3 of 12 Assumptions	Added sentence about procedure to be used to handle, spread and compact the materials for the new tailings pile. Added sentence(s) re: assumptions concerning compression index, Cc. Tailings thickness: 46.7 ft (instead of 38 ft) Cover thickness: 9 ft (instead of 10 ft)
	Revision Page 4 of 12 Design Inputs	Tailings thickness: 46.7 ft (instead of 38 ft) Cover thickness: 9 ft (instead of 10 ft)
	Revision Page 5 of 12 Calculation Section	Compression of tailings: 2% of 46.7-ft = 0.93', or 11 inches (instead of 2% of 38 ft = 0,76' or 9 inches) Secondary settlement: 8 in. (instead of 6 in.) Total settlement: 19 in. (instead of 17 in.)
	Revision Page 6 of 12 Conclusions/Recommendations	Secondary settlement: 8 in. (instead of 6 in.) Total tailings height + cover: 55.7 ft (instead of 48 ft)
	Addition Pages 7 and 8 of 12 Drawings	New plan and detail of section to be analyzed.
	Revisions Pages 10 and 11 of 12 Calculations	Revised hand calculations to account for difference in tailings pile geometry.
	Revisions Page 12 of 12 Spreadsheet calculations	Spreadsheet settlement calculations using revised cover thickness and tailings height.

The current applicable version of this publication resides on Jacobs' Intranet. All copies are considered to be uncontrolled. Copyright© Jacobs Engineering Group Inc., 2007

Description of Calculation:

This section provides calculations for primary settlement and long term (secondary) settlement of uranium tailings placed within the Crescent Junction disposal cell. The settlement is based on results of the consolidation tests performed by others on remolded tailing samples.

Tailings will be placed, spread and compacted in layers for a period of 20 years or until all tailings have been moved. Settlement of the tailings will be due largely to settlement of its own incremental weight and ultimately due to an additional weight of the protective cover. In general, an embankment made up of sand and silty sand type of materials will compress an amount equal to 2 percent of its height due to its own weight. The settlement of the tailings will also be due to consolidation of each incremental layer loaded by the cover material, construction activity and weight of the tailings above.

It is understood that all natural overburden soils will be removed full depth and the excavation for the disposal cell foot print will extend 2 feet deep into the underlying Mancos Shale. Settlement of the foundation soil will therefore be negligible.

Assumptions:

1. Existing tailings at Moab site will be mixed and dried out to optimum moisture content prior to transport to Crescent Junction site. Once there, tailings will be placed in layers per specification and compacted to 90% of the maximum density per ASTM D698. In general, mine tailings will be placed at optimum moisture content plus 2 percent.

2. Consolidation properties of newly placed composite tailings (Cc- compression index, e_0 – Initial air voids) are anticipated to be similar to the ones obtained for this analysis by averaging values for the sand tailings, transition tailings, and slime tailings. The tailings to be deposited at the Crescent Junction site will be thoroughly mixed and dried to optimum moisture content before transport, and then spread and compacted to 90% of ASTM D 698 density. Therefore, it is estimated that the compression index, Cc, of the combined tailings will be more in line with the test values obtained for the sand and transition tailings. In our opinion, the design Cc value for the composite tailings should range between 0.1 and 0.2.

3. Tailings thickness will be 46.7 feet maximum and cover thickness will be 9 feet, See Figures 1 and 2.

The current applicable version of this publication resides on Jacobs' Intranet. All copies are considered to be uncontrolled. Copyright© Jacobs Engineering Group Inc., 2007

Design Inputs:

Cover thickness: 9 feet
Cover Unit Weight: 124 pcf moist

Tailings thickness: 46.7 feet
Tailings Unit Weight: 115 pcf at 17.4 % moisture content when compacted to 90% of the maximum density per ASTM D698.

Consolidation Properties of tailings:
Compression Index, Cc = 0.16 (see calculation sheets)
Initial Air Void, e_0 = 0.87 (see calculation sheets)

Primary Settlement = $\{C_c / 1+ e_0\} \times H \times \log (p_2 / p_0)$
H = layer thickness
p_2 = final stress level($p_0 + \Delta p$)
Δp = stress increase
p_0 = Initial stress level

Secondary Settlement = $C\alpha \times H \times \log (t_2 / t_1)$
$C\alpha$ = secondary compression index
$C\alpha$ = .05 X Cc, From Holtz and Kovacs
t_1 = construction duration
t_2 = cell life

Software:

Title	Developer	Versions	Revision Level

The current applicable version of this publication resides on Jacobs' Intranet. All copies are considered to be uncontrolled. Copyright© Jacobs Engineering Group Inc., 2007

Calculation Section:

Primary settlement due to consolidation = 11 inches

Compression of the tailings = 2% of 46.7-ft = 0.93' or 11 inches

Use either primary settlement value or compression of tailings value.

Secondary settlement = 8 inches

Total settlement = 11 + 8 = 19 inches.

See attached sheets and spreadsheet.

The current applicable version of this publication resides on Jacobs' Intranet. All copies are considered to be uncontrolled. Copyright© Jacobs Engineering Group Inc., 2007

Conclusions/Recommendations:

The results of the analyses indicate that primary settlement of the tailings will be 11 inches and secondary settlement will be approximately 8 inches. For the total height of the tailings and cover of 55.7 feet, the magnitude of total settlement is insignificant. Also, because of the granular composition of the tailings, most of the primary settlement will take place rapidly.

Reference:

Technical Approach Document (December 1989) DOE/UMTRA-050425-0002

Shaw E&I Inc., (2006), Geotechnical test results on tailings samples, March 13 and November 7. Presented in RAP, Attachment 5, Appendix N, Supplemental Geotechnical Properties of Tailings Materials from the Moab Processing Site.

Holtz, R.D. and Kovacs, W.D. (1981) An Introduction to Geotechnical Engineering.

NAVFAC DM – 7.1 (1982) Soil Mechanics

The current applicable version of this publication resides on Jacobs' Intranet. All copies are considered to be uncontrolled. Copyright© Jacobs Engineering Group Inc., 2007

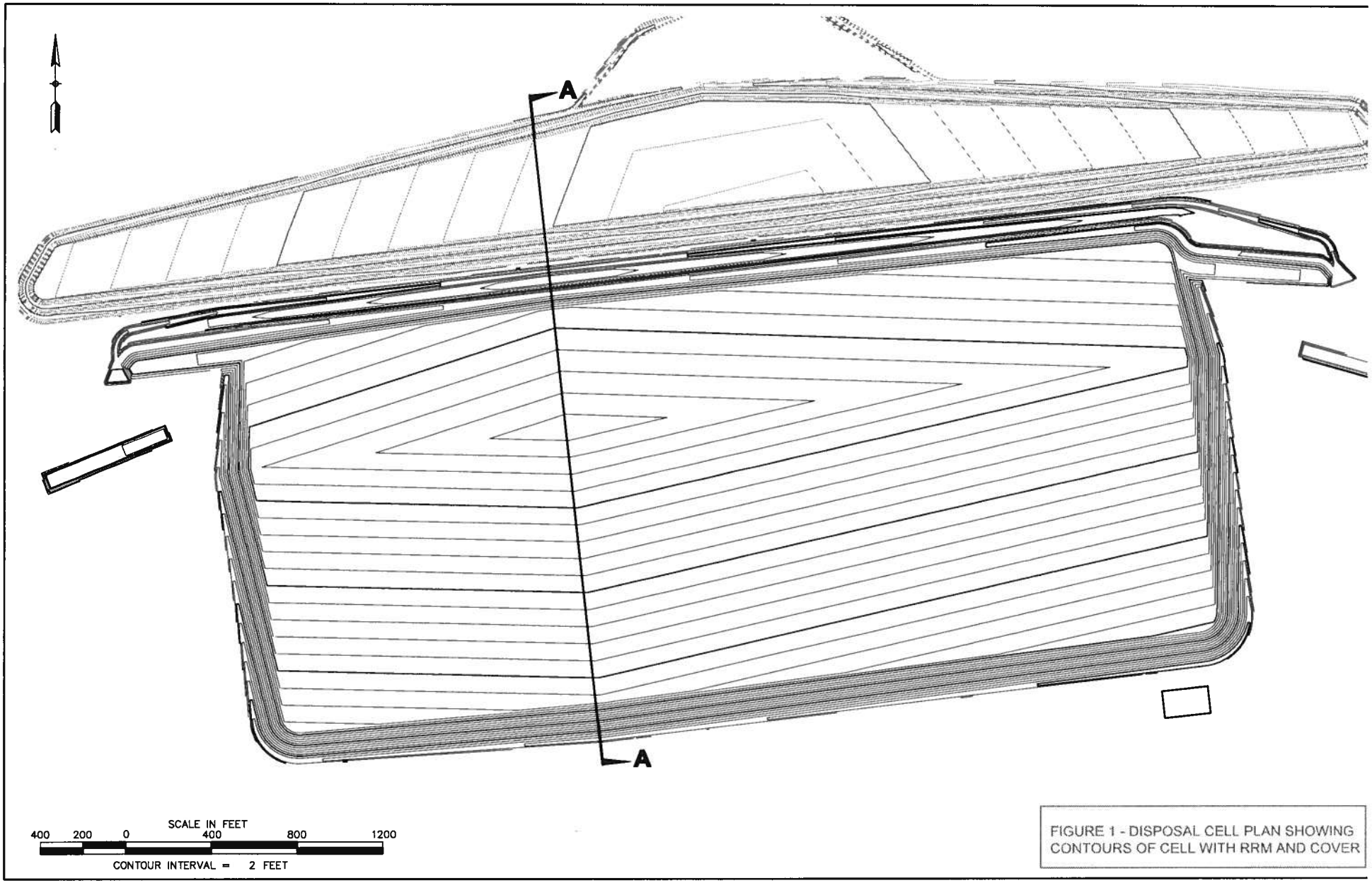

FIGURE 1 - DISPOSAL CELL PLAN SHOWING CONTOURS OF CELL WITH RRM AND COVER

I:\engl\Civil\Documents\FIG-SETTLEMENT-OALO-PLAN.dwg, Layout1, 4/8/2008 6:07:58 PM, DWG To PDF.pc3, ANSI expand B (11.00 x 17.00 Inches), 1:1

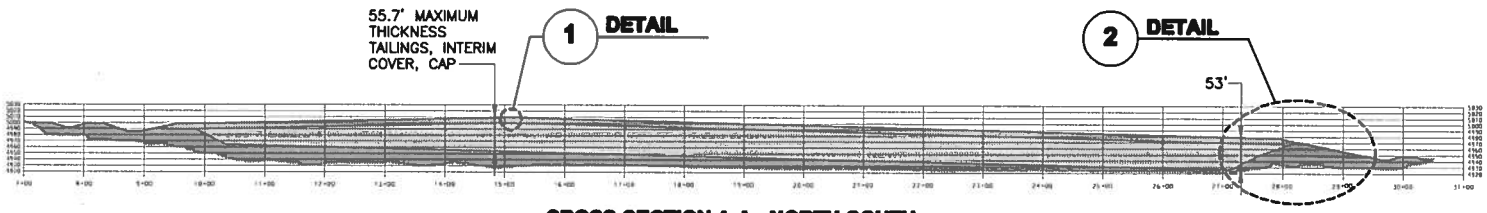

CROSS-SECTION A-A - NORTH-SOUTH
SCALE: HORIZONTAL 1"=200'
VERTICAL 1"=200'

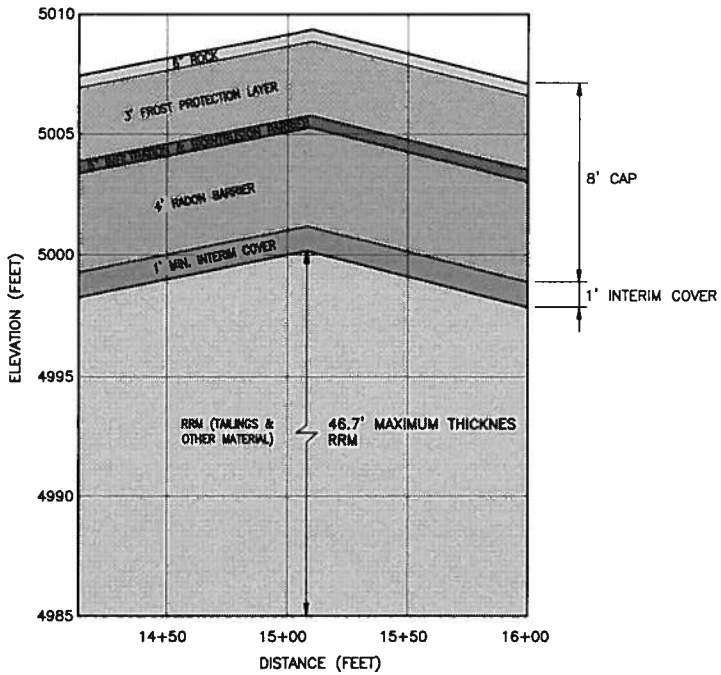

1 **DETAIL**
SCALE: HORIZONTAL 1"=50'
VERTICAL 1"=5'

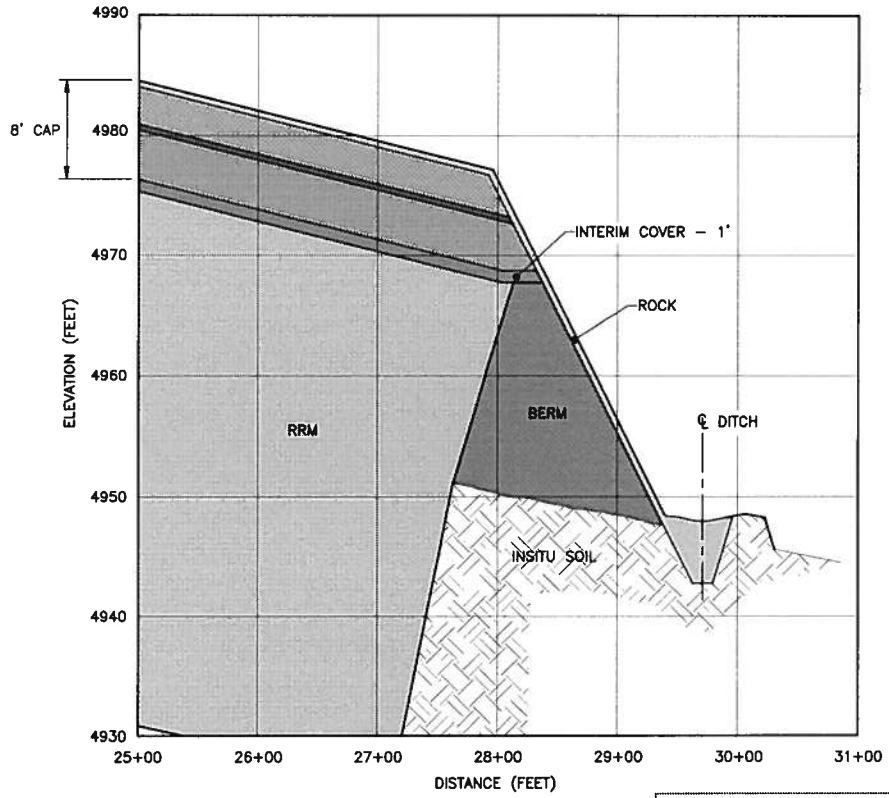

2 **DETAIL**
SCALE: HORIZONTAL 1"=100'
VERTICAL 1"=10'

FIGURE 2 - TAILINGS AND COVER THICKNESS

I:\engCivil\Documents\FIG-SETTLEMENT-CALC-SECTIONS.dwg, Layout1, 4/7/2009 8:57:04 AM, DWG To PDF.pc3, ANSI expand B (11.00 x 17.00 Inches), 1:1.00000

SETTLEMENT ANALYSIS OF LAND CELL

ASSUMPTION:

1) NATIVE OVERBURDEN SOILS' CONSOLIDATION WILL BE INSIGNIFICANT
2) COMPACTED COVER MATERIAL WILL NOT CONSOLIDATE ANY FURTHER AFTER INSTALLATION
3) TAILINGS WILL SETTLE DUE TO ITS OWN WEIGHT AND DUE TO SURCHARGE FROM COVER AND TAILINGS INSTALLED IN STAGES.

TAILING PARAMETERS:

SAND TAILINGS

$MAX\ \gamma_D = (113.3 + 112.8)/2 = 113.05$ PCF

$M/C\ OPT = (12.7 + 13.1)/2 = 12.9\%$

$C_c = (0.15 + 0.07)/2 = 0.11$

$e_0 = (0.88 + 0.638)/2 = 0.76$

TRANSITION TAILINGS

$MAX\ \gamma_D = (107.3 + 107.8)/2 = 107.6$ PCF

$M/C\ OPT = (18.4 + 16.0)/2 = 17.2\%$

$C_c = (0.20 + 0.17)/2 = 0.19$

$e_0 = (0.808 + 0.703)/2 = 0.76$

SLIME TAILINGS

$MAX\ \gamma_D = (101.6 + 101.5)/2 = 101.6$ PCF

$M/C\ OPT = (22.5 + 20.9)/2 = 21.7\%$

$C_c = (0.37 + 0.34)/2 = 0.36$

$e_0 = (1.157 + 1.052)/2 = 1.10$

MIXED TAILING COMPOSITE VALUES

$MAX\ \gamma_D \approx 107.4$ PCF, $M/C\ OPT = 17.3\%$

COMPACTION TO 91% TO ACHIEVE 90% DENSITY

98 PCF @ 17.4% MOISTURE

$\gamma_m = 98 \times 1.17.4 = 115$ PCF

$C_c^* \approx 0.11 + 0.19 + 0.36$
≈ 0.22 *

* ANTICIPATE $C_c \approx \frac{1}{2}(0.11 + 0.19)$
$= 0.15$ SAY 0.16 BECAUSE
TAILINGS WILL BE MIXED, DRIED & COMPACTED
WITH EXPECTED C_c RANGE OF 0.10 TO 0.20

$e_0 \approx 0.76 + 0.76 + 1.10$
≈ 0.87

CALCULATE SETTLEMENT:

$$\rho = \frac{C_c}{1+e_0} \times H \times \log\left(\frac{p_2}{p_0}\right)$$

WHERE, p_0 = INITIAL STRESS

Δp = STRESS INCREASE DUE TO COVER LOADING

$p_2 = p_0 + \Delta p$

UMTRA COVER MATERIAL

$\gamma_m = 124$ PCF

THICKNESS = 9'

$\Delta p = 124 \text{ PCF} \times 9' = 1{,}116$ PSF

TOTAL PRIMARY SETTLEMENT = 11"

JACOBS

Subject: SETTLEMENT OF DISPOSAL CELL
Project: MOAB URANIUM TAILINGS
Sheet No. 3 Of
Authored by: AM Date: 4/15/08
Checked by: WKC Date: 04/15/08

SECONDARY SETTLEMENT

$$\rho_s = C_\alpha H \times \log\left(t_2/t_1\right)$$

WHERE,

$C_\alpha = 0.05 \times C_c$ HOLTZ & KOVACS
$= 0.05 \times 0.16$
$= 0.008$

t_1 = CONSTRUCTION DURATION
= 20 YEARS

t_2 = CELL LIFE
= 1,000 YEARS

$$\rho_s = 0.008 \times 46.7 \times \log\left(1000/20\right)$$

$$= 0.63' = 7.62'' \simeq 8''$$

35DJ2600 Moab Uranium Tailings Relocation
Crescent Junction Disposal Cell

By: Hasan **4/14/2008**
Chkd by: KKC 04/15/08

Primary Settlement Analysis

$$Settl = \frac{C_C * H * Log(p_2/p_0)}{1+e_0}$$

Cc = 0.16
e_0 = 0.87
Moist Unit Weight of Cover = 124 pcf
Moist Unit Weight of Tailings = 115 pcf

Cc and e Based on Consolidation Test Data from Shaw Testing

Layer	Depth		Mid Depth	Thickness	Initial Stress, p_o	Stress Increment,	Final Stress, p_2	C_c	Void Ratio	Settlement	
No.	From (FT)	To (FT)	(FT)	(FT)	(psf)	(psf)	(psf)			(FT)	(INCH)
1	0	4	2.0	4.0	230	1,116	1,346	0.16	0.87	0.26	3.15
2	4	8	6.0	4.0	690	1,116	1,806	0.16	0.87	0.14	1.72
3	8	12	10.0	4.0	1150	1,116	2,266	0.16	0.87	0.10	1.21
4	12	16	14.0	4.0	1610	1,116	2,726	0.16	0.87	0.08	0.94
5	16	20	18.0	4.0	2070	1,116	3,186	0.16	0.87	0.06	0.77
6	20	24	22.0	4.0	2530	1,116	3,646	0.16	0.87	0.05	0.65
7	24	28	26.0	4.0	2990	1,116	4,106	0.16	0.87	0.05	0.57
8	28	32	30.0	4.0	3450	1,116	4,566	0.16	0.87	0.04	0.50
9	32	36	34.0	4.0	3910	1,116	5,026	0.16	0.87	0.04	0.45
10	36	40	38.0	4.0	4370	1,116	5,486	0.16	0.87	0.03	0.41
11	40	44	42.0	4.0	4830	1,116	5,946	0.16	0.87	0.03	0.37
12	44	46.7	45.4	2.7	5215	1,116	6,331	0.16	0.87	0.02	0.23
									Total	0.91	10.96

Note:
UMTRA cover thickness is 9 feet
Tailing is 46.7 feet deep

JACOBS

Subject: Settlement of Disposal Cell

Authored by: A. Hasan Date: 2/11/2008

Project: Moab Mine Tailings
Sheet No: 1 of 1
Checked by: RKC
Date: 12/4/07

CONSOLIDATION TEST DATA			
Sample No	Soil Type	Coefficient of Consolidation	Initial Void Ratio
GABT - 04	Sand Tailings	0.15	0.880
GABT - 06	Sand Tailings	0.07	0.638
GABT - 09	TransitionTailings	0.20	0.808
GABT - 10	TransitionTailings	0.17	0.703
GABT - 11	Slime Tailings	0.38	1.157
GABT - 13	Slime Tailings	0.34	1.052

Reference: Shaw E&I Test Results Dated November 7, 2007

Bench Test Sample No.	Soil Type	Atterberg Limits (LL/PL/PI) ASTM D 4318	Sieve/Hydrometer Analyses				Sample Prep Dry Unit Weight (pcf)/ Water Content (%)/Confining Pressure (psi)	Hydraulic Conductivity (1)	Triaxial Shear Strength (2)		Coefficient of Consol., Cc	Volume Moisture Content at 15-bar (3)	Maximum Dry Density (pcf) (Standard Proctor) (4)	Optimum Moisture Content (Standard Proctor) (4)	Settled Percent Compaction (4)
			% Gravel	% Sand	% Silt	% Clay			c, psf	Eff. Friction Angle, degrees					
GABT-01	Cover Soil	NP	4	73	18	5	106.3 / 7.0% / 2.5	4.7E-06					117.7	11.9%	82.0%
							106.3 / 7.0 / 2.5	7.6E-06							
							106.3 / 7.0 / 2.5	1.1E-05							
GABT-02	Cover Soil	NP	3	80	14	3							109.2	13.8%	85.8%
GABT-03	Sand Tailings	NP	1	83	15	2	90.5 / 14.4 / 2.25	2.7E-04	0	34.5			106.3	12.7%	79.3%
							90.5 / 14.4 / 2.26	3.8E-04							
							90.5 / 14.4 / 2.27	7.9E-05							
GABT-04	Sand Tailings	NP	0	76	21	3	88.2 / 17.5 / 2.25	1.7E-04	0	36.5	0.15	6.1	103.9	15.6%	82.2%
							88.2 / 17.5 / 2.26	1.3E-05							
							88.2 / 17.5 / 2.27	1.8E-05							
GABT-05	Sand Tailings	NP	3	76	17	5	101.7 / 15.3 / 2.25	3.1E-04	0	38.3			113.3	13.1%	90.9%
							101.7 / 15.3 / 2.26	2.2E-04							
							101.7 / 15.3 / 2.27	2.1E-04							
GABT-06	Sand Tailings	NP	1	83	13	4					0.07	24.4	107.3	14.6%	82.6%
GABT-07	Transition Tailings	31/22/9	1	49	42	8	96.3 / 20.5 / 2.5	1.2E-05	0	47.2			107.3	18.4%	78.8%
							96.3 / 20.5 / 2.6	1.4E-05							
							96.3 / 20.5 / 2.7	1.3E-05							
GABT-08	Sand Tailings	NP	7	72	19	9	101.4 / 17.9 / 2.25	3.2E-05	0	37.1			112.8	16.0%	83.3%
							101.4 / 17.9 / 2.26	2.1E-05							
							101.4 / 17.9 / 2.27	7.4E-05							
GABT-09	Transition Tailings	23/20/3	0	42	50	8	91.8 / 23.0 / 2.5	6.4E-05	0	36.3	0.20	24.4	102.0	21.1%	87.9%
							91.8 / 23.0 / 2.6	6.9E-05							
							91.8 / 23.0 / 2.7	7.1E-05							
GABT-10	Transition Tailings	19/17/2	0	70	24	6					0.17	>50.5	107.8	18.7%	94.6%
GABT-11	Slimes Tailings	56/27/29	0	22	53	25					0.38	27.6	96.0	27.8%	68.5%
GABT-12	Slimes Tailings	35/19/16	0	41	47	12	83.6 / 20.9 / 2.5	8.4E-05	0	50.8			101.6	22.5%	39.3%
							83.6 / 20.9 / 2.6	2.1E-05							
							83.6 / 20.9 / 2.7	1.9E-05							
GABT-13	Slimes Tailings	49/23/23	0	12	63	25					0.34	25.1	95.0	28.7%	84.9%
GABT-14	Slimes Tailings	43/22/21	0	16	62	22	81.2 / 22.8 / 3.0	2.7E-06	0	37.6			101.5	20.9%	76.6%
							81.2 / 22.8 / 3.1	1.8E-06							
							81.2 / 22.8 / 3.2	1.8E-06							

(1) Hydraulic Conductivity tests performed at low confining pressures. Tests are currently being reanalyzed at estimated post-construction confining pressures. Data will be presented when available.
(2) Triaxial shear strength tests performed at low confining pressures. Tests are currently being reanalyzed at estimated post-construction confining pressures. Data will be presented when available.
(3) Capillary-Moisture Relationships analyzed with WP4 Potentiometer. Tests are currently being reanalyzed using ASTM D 5298 (filter paper method) Data will be presented when available.
(4) Test results from Golder Associates, Inc. (GAI), 2006. *Results to Bench Scale Testing Program on Cover Soils and Uranium Mill Tailings from the Moab Tailings Impoundment, Grand County, Utah*, Draft technical memorandum, Lakewood, Colorado, April 3.

JACOBS	Calculation No: C-12	Page: 1 of 22
Calculation Cover Sheet	Rev. No.: 2	Revision Date: 4/15/08
(Ref. FOWI 116 Design Calculations)	Previous Revision Date: 2/13/08	Current Revision Date: 4/15/08
Issuing Department: *Federal Operations Design Engineering*	Supersedes: Revision 1 (dated 2/13/08)	
Client: U.S. Department of Energy Project Title: Moab – UMTRA Project Project Number: 35DJ2600 System:	Engineering Discipline: Geotechnical	

Calculation Title: Liquefaction Analysis of Uranium Mine Tailings Repository at Crescent Junction, UT

Purpose:

Assess the liquefaction potential of the uranium mill tailings pile to be constructed at the Crescent Junction Disposal site.

The present condition and characteristics of the uranium mill tailings at the Moab repository site are considerably different than what is anticipated to be placed at the Crescent Junction disposal site. Material properties of the existing mine tailings are available for the Moab site. During the course of this project, the mine tailings at Moab will be mixed and dried out to optimum moisture content before being transported to Crescent Junction. There, the tailings will be placed and compacted to 90% relative compaction. Since Standard Penetration Test data are not available for the "modified" tailings deposited at the Crescent Junction site, it is necessary to use empirical relationships to assume final conditions for liquefaction analysis.

The analysis will focus on the liquefaction potential of the proposed tailings pile instead of the natural subsurface materials since all natural soils will be removed full depth and the excavation extended 2 feet into the underlying Marcos Shale beneath the entire base footprint of the tailings pile. The underlying Mancos Shale is not considered to be liquefiable.

NQA-1 QUALITY LEVEL: 2

Prepared by: Kurt J. Bettger Date: 4-28-2008

Checked by: Ahmad Hans Date: 4-30-2008

Engineering Managers Approval: William D. Bartlett Date: 5/5/2008

The current applicable version of this publication resides on Jacobs' Intranet. All copies are considered to be uncontrolled.
Copyright© Jacobs Engineering Group Inc., 2007

Revision History:

Pages Affected By Revision	Revised/Added/Deleted	Description of Revision
Rev. 2	Revision, Page 4 Section: Design Inputs	Revised tailings pile geometry from 60% to 90% drawings resulted in the following changes to design input: Tailings thickness: 46.7 ft (from 38 ft) Cover thickness: 9 ft (from 10 ft) Total soil thickness: 55.7 ft (from 48 ft) Saturated soil thickness: 46.7 ft (from 38 ft)
	Revision, Page 6 Conclusions/Recommendations	New factor of safety calculations based on revised tailings pile geometry: ..."calculated factor of safety ranged from 1.37 to 2.38 in the tailings containing 17% fines, and from 1.74 to 3.04 in the tailings with 46% fines". (Changed from "1.37 to 1.84 in the tailings containing 17% fines, and from 1.74 to 2.34 in the tailings with 46% fines.")
	Revision Pages 7 & 8 Calculation Page	Revised tailings pile geometry resulted in the following change to calculation input for liquefaction analyses (for both tailings with 17% fines and with 46% fines): Soil thickness: 55.7 ft

The current applicable version of this publication resides on Jacobs' Intranet. All copies are considered to be uncontrolled. Copyright© Jacobs Engineering Group Inc., 2007

Description of Calculation:

Evaluation of soil liquefaction potential using Seed-Idriss Simplified Procedure based on Standard Penetration Test and modified for 1996 NCEER and 1998 NCEER/NSF Workshops on Evaluation of Liquefaction Resistance of Soils.

Design input includes soil property characteristics (soil type, percent passing No. 200 sieve, and unit weight), soil thickness, depth to groundwater, and seismic design properties (earthquake magnitude and estimated peak acceleration at the ground surface for Crescent Valley).

Spread sheet calculates seismic cyclic stress ratio (CSR) and cyclic resistance ratio (CRR) and factor of safety (FS). The factor of safety against liquefaction in a tailings layer can be calculated by dividing the shear stress required to cause liquefaction in the layer by the shear stress generated in that layer by the design earthquake.

Assumptions:

1. Existing tailings at Moab site will be dried out to optimum moisture content prior to transport to Crescent Junction site. Once there, tailings will be placed in layers per specification and compacted to 90% relative compaction. In general, mine tailings should not be saturated.
2. For analysis purposes only, assume tailings are saturated full depth (worst case)
3. Seismic design input as given in Technical Approach Document and RAP Attachment 1, Appendix D for estimated peak acceleration at the ground surface for Crescent Valley.
4. Liquefaction potential will be analyzed using earthquake moment magnitude = 6.5 (see attached paper by Wong & Olig (refers to design earthquake magnitudes at Moab site).
5. SPT blowcounts can be reasonably estimated for the placed and compacted materials based on assumed relative density of the compacted tailings layers.

The current applicable version of this publication resides on Jacobs' Intranet. All copies are considered to be uncontrolled. Copyright© Jacobs Engineering Group Inc., 2007

Design Inputs:

Tailings thickness: 46.7 feet
Cover thickness: 9 feet (per discussion with Jacobs' Oak Ridge personnel)
Total soil thickness: 55.7 feet

Saturated soil thickness: 46.7 feet (tailings saturated)

Cover Unit Weight: 104 pcf dry
112 pcf at 7% moisture content

Tailings Unit Weight: 98 pcf dry
124.1 pcf at 27% moisture content

Tailings Fines Content: 17% minimum (SM)
46% mean (SM-ML)

Seismic Data:

Peak acceleration at ground surface: 0.22 g
(Note: for stability analysis, TAD allows for surface acceleration = 0.11g at end of construction, and 0.66 x 0.22g = 0.15 g for long term conditions)

Earthquake moment magnitude: 6.5

Tailings to be compacted to 90% relative compaction. The equivalent relative density is 50% (Holtz and Kovacs). Based on correlations of SPT blow counts, N, and relative density, an N_{60} of 10 to 15 (at overburden pressure of approximately 20 psi) will be required to achieve 50% relative density. This field N is equivalent to N_{60} = 15 where N_{60} is the corrected blow counts for 60% rod energy ratio and for overburden pressure.

Software:

Title	Developer	Versions	Revision Level
Liquefaction Analysis Spreadsheet	Jacobs		

The current applicable version of this publication resides on Jacobs' Intranet. All copies are considered to be uncontrolled. Copyright© Jacobs Engineering Group Inc., 2007

Calculation Section:

See attached spreadsheets.

Liquefaction analysis has been performed for two cases:

1. Tailings with 17% fines (i.e. 17% passing the No. 200 sieve); and
2. Tailings with 46 % fines (i.e. 46% passing the No. 200 sieve).

The current applicable version of this publication resides on Jacobs' Intranet. All copies are considered to be uncontrolled. Copyright© Jacobs Engineering Group Inc., 2007

Conclusions/Recommendations:

The results of the analyses indicate that liquefaction of the tailings will not occur under the assumed soil and seismic conditions. Furthermore, it is considered likely that field SPT N-counts in 90% relative density material may result in higher blow counts than assumed in this liquefaction analysis.

The Technical Approach Document (TAD) indicates the minimum factor of safety considered acceptable for UMTRA sites is 1.5. The calculated factors of safety ranged from 1.37 to 2.38 in the tailings containing 17% fines, and from 1.74 to 3.04 in the tailings with 46% fines. Due to the extreme (and unlikely) assumption made for saturated conditions to be present full height of the tailings, it is concluded that the tailings at the site are not liquefiable.

Reference:

Technical Approach Document (December 1989) DOE/UMTRA-050425-0002

Wong, I.G. and Olig, S.S., "Earthquake hazards in the Intermountain U.S.: Issues relevant to uranium mill tailings disposal".

Lambe and Whitman (1969), Soil Mechanics.

University of Utah Seismograph Stations – NEHRP. List of Earthquakes in Utah and surrounding areas.

USGS Earthquake Hazards Program
http://eqint.cr.usgs.gov/deaggint/2002/out/Moab_17395_seismogramps.jpg

Seed, H.B. and I.M. Idriss (1971), "Simplified Procedures for Evaluating Soil Liquefaction Potential", American Society of Civil Engineers, Journal of Soil Mechanics and Foundations Division, 97(9).

Shaw E&I Inc., (2006), Geotechnical test results on tailings samples, March 13 and November 7. Presented in RAP, Attachment 5, Appendix N, Supplemental Geotechnical Properties of Tailings Materials from the Moab Processing Site.

Gibbs, H.J. and Holtz, W.G., "Research on Determining the Density of Sand by Spoon Penetration Test," Proceedings, Fourth International Conference Soil Mechanics and Foundations Engineering, vol I, (1957)

Holtz, R.D. and Kovacs, W.D. (1981) An Introduction to Geotechnical Engineering.

The current applicable version of this publication resides on Jacobs' Intranet. All copies are considered to be uncontrolled. Copyright© Jacobs Engineering Group Inc., 2007

EVALUATION OF SOIL LIQUEFACTION POTENTIAL USING SEED-IDRISS SIMPLIFIED PROCEDURE - STANDARD PENETRATION TEST

Jacobs Civil

By: KB
Chkd:
Date: 4/15/2008

Job #: 35DJ2600
File:

Density of water (pcf)	62.4
Water table depth (ft)	10
Peak bedrock acceleration (g)	
Estimated surface acceleration (g)	0.22
Earthquake moment magnitude	6.5
Atmospheric pressure (psf)	2116.2
Borehole diameter (inches)	4.0
SPT hammer efficiency	60%
Split spoon liner	FALSE

soil thickness (ft) 55.7
maximum amplification 1.5

Magnitude Scaling Factor, MSF 1.4
Sloping Ground Correction Factor, K_α 1.0

Soil Boring: Assumed to get N60 = 15

depth (ft)	N_{FIELD}	% passing #200	Soil Type	Strength, Q_u (tsf)	Unit weight (pcf)	Total stress (psf)	effective stress (psf)	Cn	C*	N_{60}	N_{60CS}	K_σ	Cyclic Resistance Ratio (CRR)	r_d	Cyclic Stress Ratio (CSR)	factor of safety	Comment
0.0	0	95	0		1	1	8	1.70	0.90	0.0		3.0	0.05	1.0	0.02	13.76	
5.0	10	95	cl		112	560	560	1.50	0.95	14	22	1.3	0.24	1.0	0.14	3.25	Clay
10.0	12	17	sm		124	1150	1150	1.26	1.01	15	19	1.1	0.20	1.0	0.14	2.38	Okay
15.0	12	17	sm		124	1770	1458	1.16	1.06	15	19	1.1	0.20	1.0	0.17	1.84	Okay
20.0	12	17	sm		124	2390	1766	1.08	1.11	14	18	1.0	0.20	1.0	0.19	1.57	Okay
25.0	13	17	sm		124	3010	2074	1.01	1.17	15	19	1.0	0.21	0.9	0.20	1.52	Okay
30.0	13	17	sm		124	3630	2381	0.94	1.22	15	19	1.0	0.20	0.9	0.20	1.42	Okay
35.0	14	17	sm		124	4250	2689	0.89	1.20	15	19	1.0	0.20	0.9	0.20	1.37	Okay
40.0	15	17	sm		124	4870	2997	0.84	1.20	15	19	0.9	0.20	0.9	0.20	1.38	Okay
45.0	16	17	sm		124	5490	3305	0.79	1.20	15	19	0.9	0.21	0.8	0.19	1.42	Okay
50.0	16	17	sm		124	6110	3613	0.75	1.20	14	18	0.9	0.20	0.8	0.18	1.39	Okay
55.7	16	17	sm		124	6817	3964	0.71	1.20	14	18	0.9	0.19	0.7	0.17	1.38	Okay

Note:
N_{FIELD} - blow counts measured in the field
Q_u (tsf) - soil strength (RIMAC, PP) used in estimating the density for cohesive soil
Cn - factor to normalize blow counts to an effective overburden pressure of approximately 1 atm.
C* correction factor for N taking in account the rod length, split spoon liner, borehole diameter, and hammer efficiency
N_{60} Corrected blow counts (excludes correction for fines).
N_{60CS} Corrected blow counts to equivalent clean sand (correction for fines content).
K_σ - Overburden pressure correction factor [Ref. 1 and 2]
K_α - Sloping ground correction factor [Ref. 1 and 2]
MSF - Magnitude Scaling Factor (applied when design eartquake moment magnitude is not equal to 7.5)[Ref. 1 and 2]
r_d - Stress Reduction Factor [Ref. 1 and 2]

Soil Type - CH, CL & ML are cohesive and should have RIMAC or PP values
Soil Type - SM-ML, SM, SP, SW & GP are cohesionless soils
SM-ML - Very Fine Silty Sand
SM - Fine Sand
SP - Medium Sand
SW - Clean Medium to Coarse Sand
GP - Sandy Gravel

Reference:
1. "Liquefaction Resistance of Soils: Summary Report from the 1996 NCEER and 1998 NCEER/NSF Workshops on Evaluation of Liquefaction Resistance of Soils", by Youd et al., by Youd et by Youd et al., Journal of Geotechnical and Geoenvironmental Engineering, October 2001
2. "Liquefaction Evaluation Procedures", IDOT Bridge Section - Foundation Unit.

EVALUATION OF SOIL LIQUEFACTION POTENTIAL USING SEED-IDRISS SIMPLIFIED PROCEDURE - STANDARD PENETRATION TEST

Jacobs Civil

By: KB
Chkd:
Date: 4/15/2008

Job #: C5X58706
File: G:\TPW\GEOTECH\Moab-Oak Ridge\crescent junction calculations\[crescent junction liquefaction analysis 17% fines-Rv 04-15-2008.xls]46% fines

Density of water (pcf)	62.4
Water table depth (ft)	10
Peak bedrock acceleration (g)	
Estimated surface acceleration (g)	0.22
Earthquake moment magnitude	6.5
Atmospheric pressure (psf)	2116.2
Borehole diameter (inches)	4.0
SPT hammer efficiency	60%
Split spoon liner	FALSE

soil thickness (ft) 55.7
maximum amplificatior 1.5

Magnitude Scaling Factor, MSF 1.4
Sloping Ground Correction Factor, K_α 1.0

Soil Boring: Assumed to get N60 = 15

depth (ft)	N_{FIELD}	% passing #200	Soil Type	Strength, Q_u (tsf)	Unit weight (pcf)	Total stress (psf)	effective stress (psf)	Cn	C*	N_{60}	N_{60CS}	K_σ	Cyclic Resistance Ratio (CRR)	r_d	Cyclic Stress Ratio (CSR)	factor of safety	Comment
0.0	0	95	cl		112	0	0	1.70	0.90	0.0		#DIV/0!	0.05	1.0	#DIV/0!	**#DIV/0!**	
5.0	10	95	cl		112	560	560	1.50	0.95	14	22	1.3	0.24	1.0	0.14	**3.25**	Clay
10.0	12	46	sm-ml		124	1150	1150	1.26	1.01	15	23	1.1	0.26	1.0	0.14	**3.04**	Okay
15.0	12	46	sm-ml		124	1770	1458	1.16	1.06	15	23	1.1	0.25	1.0	0.17	**2.34**	Okay
20.0	12	46	sm-ml		124	2390	1766	1.08	1.11	14	22	1.0	0.25	1.0	0.19	**1.99**	Okay
25.0	13	46	sm-ml		124	3010	2074	1.01	1.17	15	23	1.0	0.26	0.9	0.20	**1.94**	Okay
30.0	13	46	sm-ml		124	3630	2381	0.94	1.22	15	23	1.0	0.26	0.9	0.20	**1.80**	Okay
35.0	14	46	sm-ml		124	4250	2689	0.89	1.20	15	23	1.0	0.26	0.9	0.20	**1.74**	Okay
40.0	15	46	sm-ml		124	4870	2997	0.84	1.20	15	23	0.9	0.26	0.9	0.20	**1.76**	Okay
45.0	16	46	sm-ml		124	5490	3305	0.79	1.20	15	23	0.9	0.26	0.8	0.19	**1.81**	Okay
50.0	16	46	sm-ml		124	6110	3613	0.75	1.20	14	22	0.9	0.25	0.8	0.18	**1.76**	Okay
55.7	16	46	sm-ml		124	6817	3964	0.71	1.20	14	21	0.9	0.23	0.7	0.17	**1.74**	Okay

Note:
N_{FIELD} - blow counts measured in the field
Q_u (tsf) - soil strength (RIMAC, PP) used in estimating the density for cohesive soil
Cn - factor to normalize blow counts to an effective overburden pressure of approximately 1 atm.
C* correction factor for N taking in account the rod length, split spoon liner, borehole diameter, and hammer efficiency
N_{60} Corrected blow counts (excludes correction for fines).
N_{60CS} Corrected blow counts to equivalent clean sand (correction for fines content).
K_σ - Overburden pressure correction factor [Ref. 1 and 2]
K_α - Sloping ground correction factor [Ref. 1 and 2]
MSF - Magnitude Scaling Factor (applied when design eartquake moment magnitude is not equal to 7.5)[Ref. 1 and 2]
r_d - Stress Reduction Factor [Ref. 1 and 2]

Soil Type - CH, CL & ML are cohesive and should have RIMAC or PP values
Soil Type - SM-ML, SM, SP, SW & GP are cohesionless soils
SM-ML - Very Fine Silty Sand
SM - Fine Sand
SP - Medium Sand
SW - Clean Medium to Coarse Sand
GP - Sandy Gravel

Reference:
1. "Liquefaction Resistance of Soils: Summary Report from the 1996 NCEER and 1998 NCEER/NSF Workshops on Evaluation of Liquefaction Resistance of Soils", by Youd et al. by Youd et by Youd et al., Journal of Geotechnical and Geoenvironmental Engineering, October 2001
2. "Liquefaction Evaluation Procedures", IDOT Bridge Section - Foundation Unit.

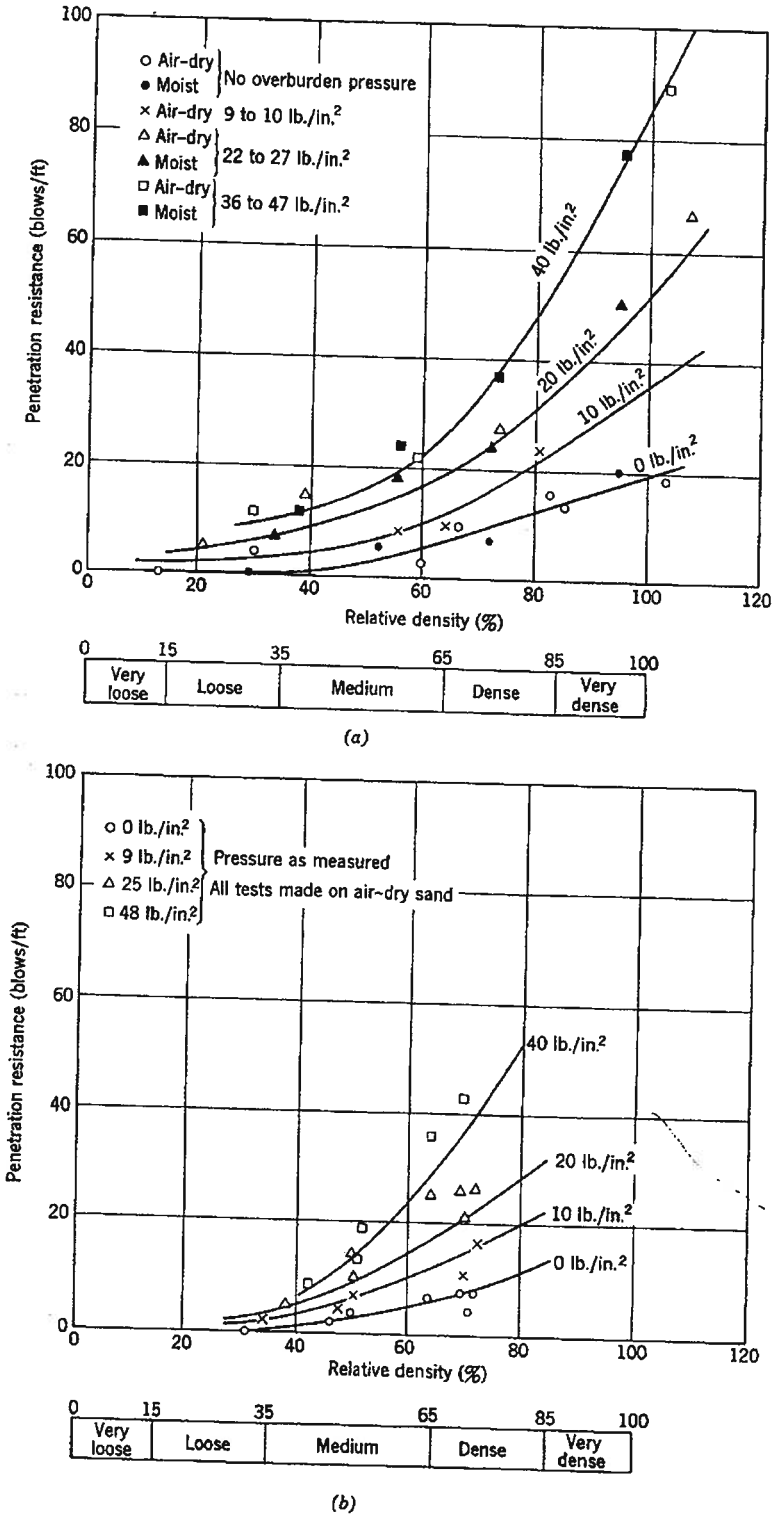

Fig. 7.5 Results of standard penetration tests. (*a*) Coarse sand. (*b*) Fine sand. (From Gibbs and Holtz, 1957.)

Earthquakes Researched for this Project

Click on Common Name for information about that earthquake.
Click here for an explanation of Magnitude or Intensity.

Sorted by Magnitude

Date	Common Name	Magnitude	Intensity
Mar 22, 1876	Moroni, UT	5.0	VI
Jul 18, 1894	Ogden, UT	5.0	VI
Apr 20, 1891	St. George, UT	5.0	VI
Apr 15, 1908	Milford, UT	5.0	VI
Jan 10, 1910	Elsinore, UT	5.0	VI
Jul 15, 1915	Provo, UT	5.0	VI
Jan 20, 1933	Parowan, UT	5.0	VI
Aug 30, 1942	Cedar City, UT	5.0	VI
Sep 26, 1942	Cedar City, UT	5.0	VI
Feb 22, 1943	Magna, UT	5.0	VI
Nov 17, 1945	Glenwood, UT	5.0	VI
Mar 06, 1949	Salt Lake City, UT	5.0	VI
Feb 13, 1958	Wallsburg, UT	5.0	VI
Feb 27, 1959	Panguitch, UT	5.0	VI
Apr 15, 1961	Ephraim, UT	5.0	VI
Sep 05, 1962	Magna, UT	5.2	VI
Oct 04, 1967	Marysvale, UT	5.2	VII
Aug 14, 1988	San Rafael Swell, UT	5.3	VI
Jan 29, 1989	So. Wasatch Plateau, UT	5.4	VI
Aug 01, 1900	Eureka, UT	5 1/2 +/-	VII
Nov 11, 1905	Shoshone, ID	5 1/2 +/-	V
May 22, 1910	Salt Lake City, UT	5 1/2	VII
May 13, 1914	Ogden, UT	5 1/2 +/-	VII
Feb 29, 1928	Helena, MT	5 1/2 +/-	IV
Sep 23, 1945	Flathead Lake, MT	5.5	VI
Mar 31, 1952	Big Fork, MT	5.5	VII
Feb 15, 1929	Lombard, MT	5.6	V
Dec 05, 1887	Kanab, UT	5.7	VII
Jul 21, 1959	Southwest UT	5.7	VI

Aug 30, 1962	Cache Valley, UT	5.7	VII
Jun 12, 1930	Grover, WY	5.8	VI
Sep 02, 1992	St. George, UT	5.8	VII
Feb 03, 1994	Draney Peak, ID	5.9	VII
Nov 17, 1902	Pine Valley, UT	6 +/-	VIII
Oct 05, 1909	Hansel Valley, UT	6 +/-	VIII
Sep 29, 1921	Elsinore, UT	6 +/-	VIII
Feb 13, 1945	Central Idaho	6.0	VI
Mar 27, 1975	Pocatello, ID	6.0	VIII
Jul 12, 1944	Central Idaho	6.1	VII
Jun 30, 1975	Yellowstone, WY	6.1	VII
Oct 18, 1935	Helena, MT	6 1/4	VIII
Nov 23, 1947	Virginia City, MT	6 1/4	VIII
Nov 10, 1884	Bear Lake, ID	6.3	VIII
Nov 13, 1901	Southern UT	6 1/2 +/-	IX
Mar 12, 1934	Hansel Valley, UT	6.6	IX
Jun 27, 1925	Clarkston Valley, MT	6 3/4	VIII
Oct 28, 1983	Borah Peak, ID	7.3	IX
Aug 17, 1959	Hebgen Lake, MT	7.5	X

Note: Date listed in Local Time

University of Utah Seismograph Stations «» 135 South 1460 East, Room 705 WBB
Salt Lake City, Utah 84112-0111 «» Phone 801-581-6274 «» Fax 801-585-5585
E-mail UUSS!

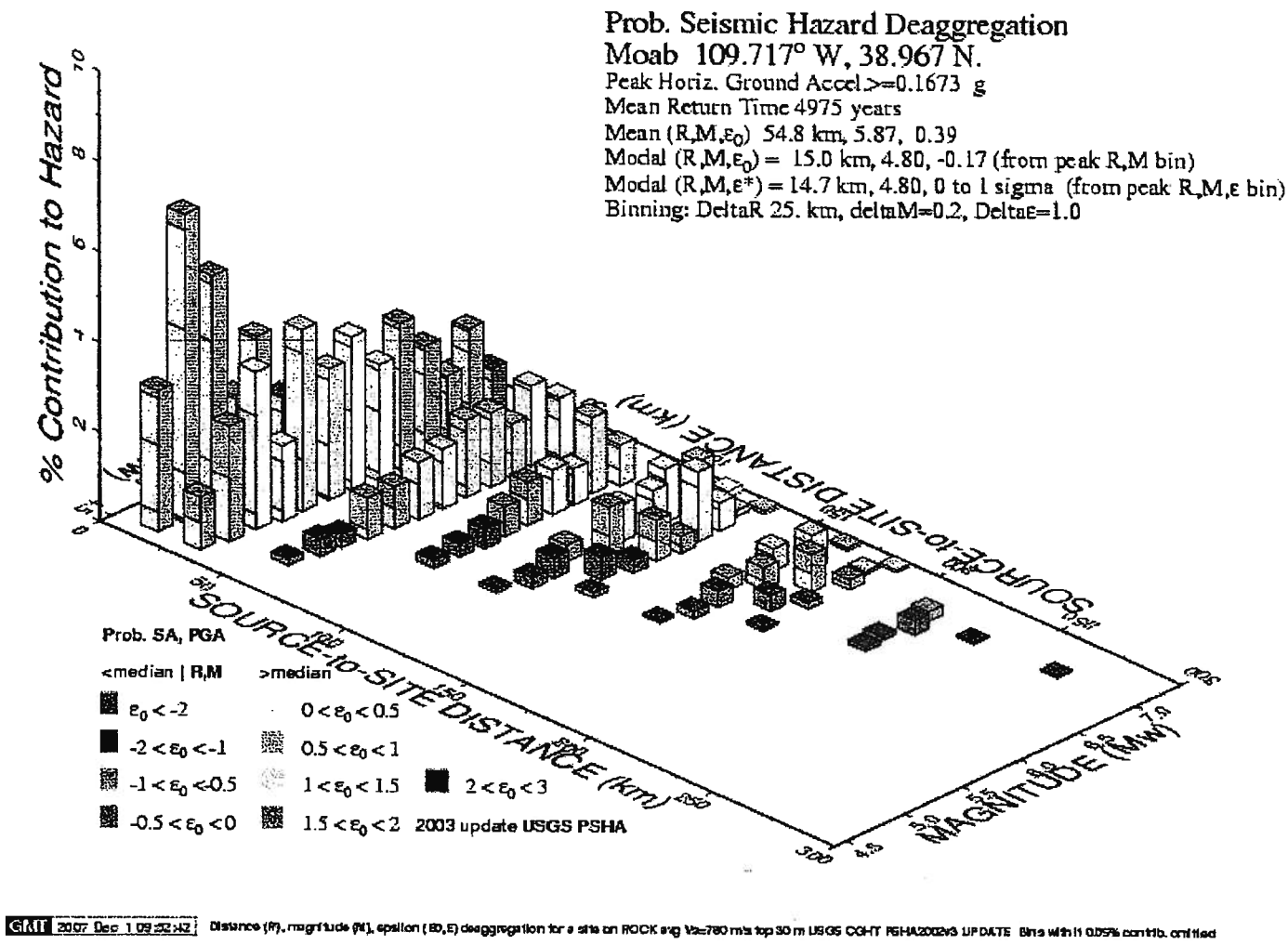

GMT 2007 Dec 1 09:22:42 Distance (R), magnitude (M), epsilon (ε0,ε) deaggregation for a site on ROCK avg Vs=760 m/s top 30 m USGS CGHT PSHA2002v3 UPDATE Bins with lt 0.05% contrib. omitted

Earthquake hazards in the Intermountain U.S.: Issues relevant to uranium mill tailings disposal

Ivan G. Wong and Susan S. Olig
Seismic Hazards Branch, Woodward-Clyde Federal Services, Oakland, CA USA

Bruce W. Hassinger
Smith Environmental Technologies Corporation., Englewood, CO USA

Richard E. Blubaugh
Environmental and Government Affairs, Atlas Corporation, Denver, CO USA

ABSTRACT:

In the past two decades, a tremendous amount of new information and data has emerged on seismic sources in the Intermountain United States and their associated processes of earthquake generation. Consequently, the seismic safety of U.S. uranium mill tailings sites, which are located almost exclusively in this region, are being reviewed by the U.S. Nuclear Regulatory Commission (NRC). Based on a deterministic and probabilistic re-evaluation of potential seismic hazards at a Title II site in southeastern Utah, three significant issues have been raised which will impact other sites in the Intermountain U.S. required to revisit their seismic design criteria by the NRC. These issues are: (1) whether the NRC's required use of a deterministic approach for assessing seismic hazards is appropriate for Title II uranium mill tailings sites in a region such as the Intermountain U.S.; (2) is the alternative approach of probabilistic seismic hazard analysis acceptable to the NRC for uranium mill tailings sites; and (3) what is the appropriate return period that should be used. Based on our evaluation, we conclude that deterministic ground motion approaches such as the NRC's 10 CFR 40 Appendix A can result in overly conservative seismic design criteria for Title II sites in the Intermountain U.S. and that instead, probabilistic seismic hazard analysis should provide the bases for such criteria. Additionally, as in all decisions of this nature, the selection of a return period for a specific site should be based on what is deemed an acceptable level of risk;. Such levels may vary from site to site depending on the consequences of radionuclide release into the environment. However, the values of 200 and 1000 years cited in the Environmental Protection Agency's (EPA) 40 CFR 192.02 and NRC's Appendix A Criterion 6(1) should form the basis for the selected return period.

1 INTRODUCTION

Many portions of the Intermountain region of the western United States (Figure 1) exhibit geologic evidence for large prehistoric earthquakes although they may lack even low levels of historical and/or contemporary seismicity. Such areas are subject to future seismic hazards. Large events such as the 1959 magnitude (M) 7.3 Hebgen Lake, Montana and 1983 M 6.8 Borah Peak, Idaho earthquakes attest to the earth's potential to damage both natural and man-made environments. The recurrence intervals of such large events on a specific fault in the Intermountain U.S., however, may span from a few thousands to more than 100,000 years. Hence, one of the most significant problems

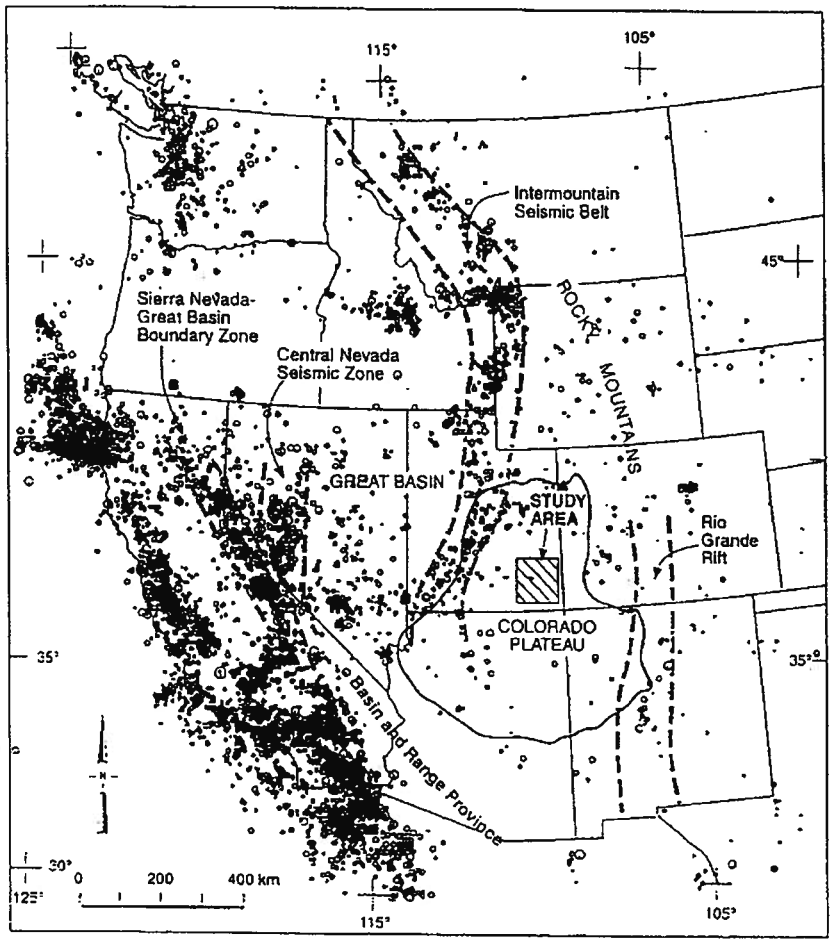

Figure 1. Seismicity of the western U.S. (1808 to 1996) and physiographic provinces and major seismic source zones located in the Intermountain U.S. Also shown is the study area around the Moab site in southeastern Utah. Earthquake data courtesy of the National Earthquake Information Center.

facing the community involved in earthquake hazard mitigation is how to address the hazard from large but infrequent earthquakes. In contrast, there also exist portions of the Intermountain U.S., such as the interior of the Colorado Plateau, where the earthquake potential is low based on both recent geologic and seismologic data.

In 1978, Congress enacted the Uranium Mill Tailings Radiation Control Act (UMTRCA) to provide for the disposal, long-term stabilization, and control of uranium mill tailings. The NRC, which regulates UMTRCA uranium mill tailing sites, has initiated a program of re-evaluating the seismic design criteria of Title II (licensed) sites based on the results of a recent study performed by Lawrence Livermore National Laboratory (LLNL) (Bernreuter et al. 1995). In the LLNL study, "simplified" site-

specific probabilistic seismic hazard analyses were performed for 19 Title II sites located in Utah, Wyoming, South Dakota, and New Mexico based on readily available information. Bernreuter et al. (1995) concluded that at most sites, their estimates of probabilistic peak ground acceleration at return periods of 2,000 years and more were higher than the values used in design.

In a recent re-evaluation of a Title II site in Moab, Utah, three key seismic hazard issues have emerged in our interactions with the NRC. These issues will significantly impact most, if not all, other sites in the Intermountain U.S. This paper describes these issues and our approach to resolving them.

2 EARTHQUAKE HAZARDS IN THE INTERMOUNTAIN U.S.

The Intermountain U.S., as defined in this paper, consists of the states of Idaho, Nevada, Arizona, Utah, Montana, New Mexico, Colorado, and Wyoming. Physiographically, the region consists principally of the Basin and Range province, Colorado Plateau, Rocky Mountains, and Great Plains. Four major seismic zones are located within or border the Intermountain U.S. including: (1) the Sierra Nevada-Great Basin boundary zone; (2) the Intermountain seismic belt including the Centennial Tectonic Belt; (3) the Central Nevada seismic zone; and (4) the Rio Grande rift (Wong et al. 1982) (Figure 1). Elsewhere, away from these zones, the level of historical seismicity is more subdued but there still exists the potential for the occurrence of large but infrequent earthquakes as indicated by the presence of late-Quaternary faults. For example, the 1887 Sonoran earthquake of estimated M 7.4 occurred as a result of rupture along the Pitaycachi fault just south of the Arizona-Mexico border (Bull and Pearthree 1988) in an area characterized by a low level of historical and contemporary seismicity.

Of greatest relevance to the Intermountain Title II sites are the Intermountain seismic belt and Rio Grande rift. The Intermountain seismic belt is one of the most extensive zones of seismicity within the continental United States (Figure 1). It trends 1300 km northward from- northwestern Arizona through central Utah, straddles the Idaho Wyoming border, and turns northwestward through Montana in the vicinity of Yellowstone National Park (Smith and Sbar 1974; Smith and Arabasz 1991) Much of the Intermountain seismic belt is characterized by generally north- to northwest-trending normal faults. Prominent fault zones include the Sevier and Hurricane faults in northern Arizona and southern Utah, the Wasatch fault zone in central Utah, and the Madison and Hebgen faults near Yellowstone. Since the beginning of the historical record in the mid 1800's, about 25 earthquakes of M 6 or greater have occurred along the Intermountain seismic belt (Smith and Arabasz 1991). The largest event in historical time was the 1959 Hebgen Lake earthquake.

The Rio Grande rift extends for approximately 600 hen from south-central New Mexico northward to south-central Colorado (Figure 1). Most of New Mexico's population is concentrated along the Rio Grande rift in cities such as Albuquerque and Santa Fe. The earliest report of earthquake activity was a sequence of 22 events felt in 1849 to 1850 near the town of Socorro (Sanford et al. 1991). The largest earthquakes observed to date are three events that occurred on 12 and 16 July and 15 November 1906 near Socorro. The estimated size of the latter event, the largest of the trio, is about M 6.

3 SEISMIC HAZARD EVALUATION OF THE MOAB SITE

In response to a request by the NRC, an up-to-date seismic hazards evaluation of the Title II Moab site was performed (Wong et al. 1996). This site, owned by Atlas Corporation, consists of a 130-acre pile consisting of 10 1/2 million tons of processed tailings derived from the past operation of the Atlas uranium mill. The tailings were emplaced over alluvial soils and the disposal area was developed from 1956 to 1984. The site is in the process of final closure and the Remedial Action Plan (Reclamation Plan) requires NRC approval.

According to the Standard Review Plan (SRP June 1993), "there are no NRC regulatory guidelines directly applicable to the geologic and seismologic aspects of the UMTRA Program". However, the basic acceptance criteria pertinent to the geologic and seismic stability aspects are provided in the EPA's 40 CFR Part 192, Subpart A and according to section 192.02, "control of residual radioactive materials and their listed constituents shall be designed to be effective for up to 1000 years, to the extent reasonably achievable, and in any case, for at least 200 years". NRC staff has interpreted this standard to mean that certain geologic and seismic conditions must be met in order to have reasonable assurance that the long-term performance objectives will be achieved (NRC 1994).

The SRP states that NRC staff review of seismotectonic stability must conclude whether the information and investigations in the Remedial Action Plan provide an adequate basis for selection of the Maximum Credible Earthquake (MCE) and determination of the resulting vibratory ground motion at the site. The NRC defines the NICE as the "earthquake which would cause maximum vibratory ground motion based upon an evaluation of earthquake potential considering the regional and local geology and seismology and specific characteristics of local subsurface material" (10 CFR 40 Appendix A). The NRC's Appendix A approach, which basically requires the determination of the 84th percentile MCE ground motions, is a deterministic approach. It requires the use of the worst case earthquake with no consideration for its frequency of occurrence. Although Appendix A stipulates that a tailings pile be designed for the MCE, the Introduction to Appendix A allows for alternatives to be proposed by the licensee. These alternatives "may take into account local or regional conditions, including geology, topography, hydrology, and meteorology. The commission may find that the proposed alternatives meet stabilization and containment of the site concerned, and a level of protection for public health, safety, and the environment from radiological and non-radiological hazards associated with the sites, which is equivalent to, to the extent practicable. or more stringent than the level which would be achieved by the requirements of this Appendix and the standards promulgated by the EPA in 40 CFR Part 192." Furthermore, Appendix A Criterion 6(1) specifies that the regulatory standard is "reasonable assurance" of stability of the tailings disposal for the 200 to 1,000 year period.

Moab is located within the interior of the Colorado Plateau which has been generally considered to be seismically inactive and devoid of large earthquakes. Seismological studies performed in the past decade, however, indicate that seismicity is fairly widespread throughout the Plateau interior, albeit at a low to moderate level, and that earthquakes up to M 6 have occurred in historical times (Wong and Humphrey 1989). Although detailed fault studies have not been performed to date within the Colorado Plateau. the available geologic data suggests that only a few significant late-Quaternary

faults may exist in the Plateau interior (Hecker 1993). Thus there appears to be at least a low level of earthquake hazard within the Plateau.

In our seismic hazard evaluation of the Moab site, potentially seismogenic faults and seismic source zones (areal sources) significant to the site were identified, characterized, and considered in the analysis. These seismic sources included 11 faults, a zone of microseismicity along the Colorado River southwest of Moab, and a seismic source zone for the Colorado Plateau which represents unknown earthquake sources having no geologic surficial expression (Figure 2). The closest fault to the site is the Moab fault which trends beneath the northeastern corner of the site. Available geologic and geophysical evidence, however, indicates that the fault is not capable of producing significant earthquakes (Olig et al. 1996). In fact, 10 of the 11 faults considered in our evaluation are associated with salt structures and are probably not seismogenic (Wong et al. 1996).

Based on an Appendix A approach, ground motions, as characterized by peak horizontal acceleration, were estimated for three potential earthquake scenarios: (1) a M 5.0 earthquake at a source-to-distance of 30 km, our proposed largest event along the Colorado River seismicity trend; (2) a M 6 1/2 earthquake along this same zone at a distance of 5 km from the site as proposed by the NRC; and (3) a "floating" earthquake of M 6 1/4 at a distance of 15 km. In the absence of any nearby capable faults, the NRC's policy requires that the MCE be represented by a floating (random) earthquake. For the second scenario, the NRC assumed that half of the seismicity zone along the Colorado River could rupture in a single large earthquake. Based on geological and seismological arguments presented in Woodward-Clyde Federal Services (1996), we consider this scenario to be extremely unlikely.

Given a maximum magnitude and source-to-site distance, empirically-based attenuation relationships can be used to estimate median (50th percentile) and median plus one standard deviation (84th percentile) ground motions for a site. The NRC stipulated 84th percentile peak horizontal accelerations at the Moab site were 0.06 g, 0.63 g, and 0.29 g, respectively for the above earthquake scenarios. Based on this analysis, the MCE for the site would be the NRC's M 6 1/2, earthquake occurring along the Colorado River seismicity trend at a source-to-site distance of 5 km.

As an alternative approach, we evaluated the earthquake hazard at the Moab site probabilistically similar to, but in a more rigorous manner than was done by LLNL. In a probabilistic seismic hazard analysis, levels of ground motions associated with a probability or likelihood of being exceeded in a specified time period (or inversely, return period) can be calculated. This approach also allows for the explicit inclusion of the range of possible interpretations and uncertainties in components of the model including seismic source characterization and ground motion estimation. The probabilistic seismic hazard model used in our study is similar to the hazard model originally developed by Comell (1968) and refined by McGuire (1974).

All seismic sources within a distance of about 150 km from the site were characterized and input into the analysis (Wong et al. 1936). This included the 11 faults such as the Moab fault, the Colorado River seismicity trend, and the Colorado Plateau source zone. Ten of the 1 1 faults were assigned low probabilities of being seismogenic because they show no evidence for Quaternary activity except deformation related to shallow salt dissolution and flowage (Wong et al. 1996). The attenuation of ground motions was addressed through the use of state-of-the-art empirical relationships for peak horizontal acceleration and stiff soil conditions.

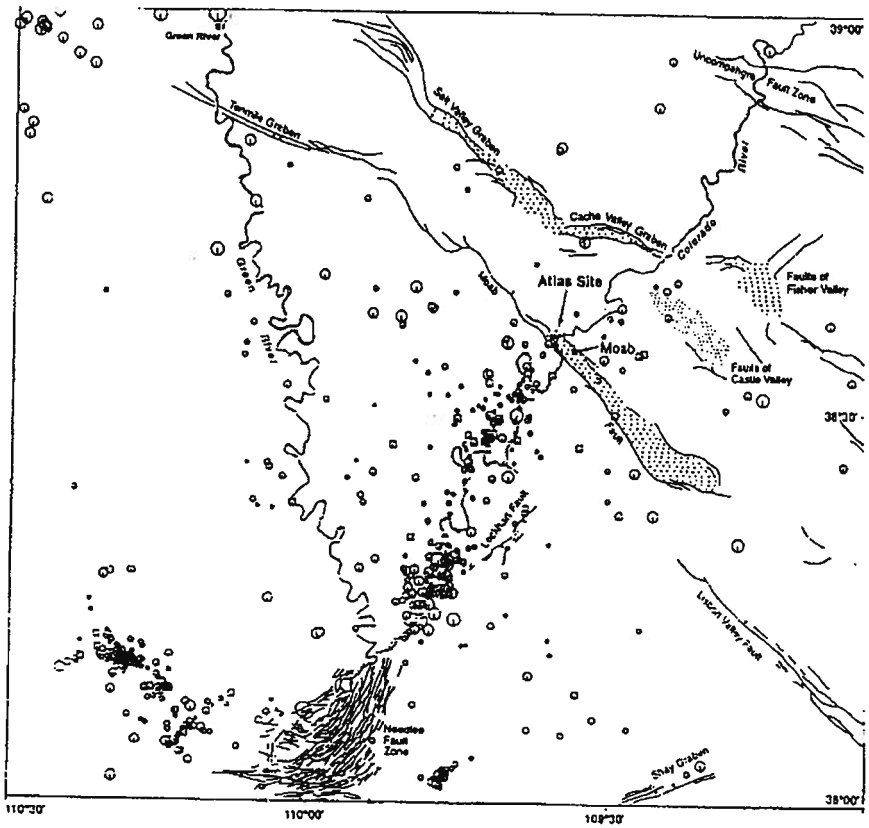

(Source: Wong et al. 1996)

Figure 2. Seismicity (1953 to 1994) and selected Cenozoic faults (after Hecker 1953) in the Moab study area. Stippled areas represent areas of distributed deformation due to salt dissolution. Ball on normal faults is on downthrown side.

The probabilistic seismic hazard analysis resulted in peak horizontal accelerations at the Moab site of 0.05 to 0.18 g for return periods ranging from 500 to 10,000 years (Figure 3). The MCE 84th percentile peak horizontal acceleration of 0.63 g has a return period of about 750,000 years (Figure 3) or 750 times greater than the 1000-year design life stipulated in 40 CFR 192.02 and Appendix A Criterion 6(1). The major contributor to peak: acceleration hazard at 10,000 years is the background earthquake in the Colorado Plateau source zone. The Colorado River seismicity trend and the Moab fault contribute little to the hazard at the Moab site at this return period (Wong et al. 1996).

4 SEISMIC HAZARD ISSUES IN THE INTERMOUNTAIN U.S.

In the seismic hazard evaluation of the Moab site, three significant issues were raised due to NRC regulations governing Title II sites. The first issue stems from the NRC's current

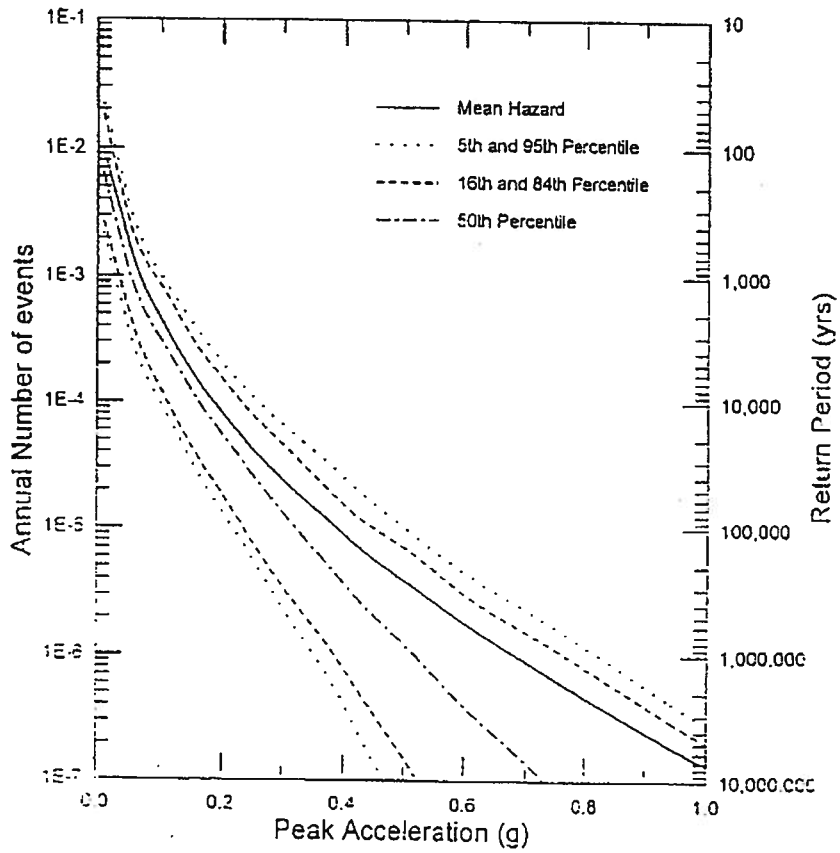

(Source: Wong et al. 1996)

Figure 3. Probabilistic seismic hazard curves for the Moab site. The fractile curves give the range of uncertainty about the mean or median (50th percentile) values. The peak horizontal acceleration of 0.18 g at a 10.000 year return period, our recommended seismic design value, can be read from the mean hazard curve.

position of requiring the seismic design of Title II sites be based on a deterministic Appendix A approach incorporating the concept of the MCE. In such an approach, the 84th percentile ground motions generated by the MCE provide the basis for the Design Basis Earthquake. Intertwined in this issue is also the issue of the reasonableness of the 15 km source-to-site for the floating earthquake in areas of low seismicity.

We believe the MCE peak horizontal acceleration for the Moab site (0.63 g) and even the value estimated for the floating earthquake (0.29 g) are overly conservative for seismic design purposes given the low seismic potential that exists within the interior of the Colorado Plateau. This latter observation is supported by the available seismological and geological data. In particular, the location of the Moab site in the Canyonlands region where many precariously balanced rocks occur throughout the area, some very delicately, suggests that this portion of the Colorado Plateau interior has not been subjected to strong earthquake ground shaking for at least several thousands of years (Wong et al. 1996).

As described earlier, the NRC's policy specifies the 15 km source-to-site distance for the floating earthquake. This distance is rather arbitrary because it is independent of the seismic potential of the region being considered. Thus whether a site is located along the more seismically active Wasatch Front in central Utah or the much less active Moab area, the 15-km distance is fixed. In general, deterministic approaches such as dictated in the NRC's Appendix A can result in overly-conservative seismic design criteria in areas of low earthquake potential. Even for sites in more seismically active areas of the Intermountain U.S., deterministically-based ground motions can also be too high for seismic design because the majority of late-Quaternary faults are characterized by long recurrence intervals far exceeding the lifetimes of engineered structures.

The second issue is whether probabilistic seismic hazard analysis is acceptable to the NRC as an alternative to their Appendix A deterministic approach for developing seismic design criteria at Title II sites. The NRC has endorsed the use of probabilistic risk assessment in nuclear regulatory matters as specified in their final policy statement in the Federal Register (16 August 1995). At this time, however, the NRC has not officially established a policy for Title II sites. Probabilistic analysis has become increasingly used in seismic hazard analysis for a wide range of facilities and structures. It provides the basis for the Uniform Building Code and is now become acceptable for evaluating the potential seismic hazards to nuclear reactors.

Given the uncertainties in seismic source characterization and ground motion estimation in the Intermountain U.S., probabilistic seismic hazard analysis is well suited to addressing these uncertainties. For example, given the observation that the largest known earthquake along the Colorado River is less than M 3, there is considerable uncertainty in the assumption that the maximum earthquake for this zone is M 5 relevant to the Moab site. As previously discussed, the NRC's position that a maximum earthquake of M 6 1/2, could occur within this zone is even more uncertain. Additionally, because the acceptable risk of Title II sites has been defined in terms of time (200 to 1000 years), it is best evaluated through probabilistic analysis which incorporates the recurrence of earthquake sources.
If probabilistic analysis is acceptable for Title II sites, a significant issue is at what return period (or alternatively a probability of nonexceedance) is deemed appropriate by the NRC. It was our recommendation that the seismic design criteria for the Moab site be based on a return period of 10,000 years (corresponds to a 10% chance of exceedance in 1000 years). We selected and recommended this very conservative return period based on the fact that the Moab site is located adjacent to the Colorado River and that radionuclide release into the major water source, if possible, might be considered higher risk than other Title II sites. In the probabilistic seismic hazard analysis performed by Bernreuter et al.(1995) for Title II sites, they calculated peak horizontal accelerations assuming a return period of 10,000 years. They adopted this value because, in their opinion, it satisfied the criteria cited in Appendix A. Furthermore, they stated that such a probability of exceedance may be too conservative for design because of the "relatively low risk posed by the tailings piles." For comparison, the current design life for the proposed underground nuclear waste repository at Yucca Mountain, Nevada is 10,000 years.

Because we considered a 10,000 return period to be very conservative compared to the required 1,000 years cited in 40 CFR 192.02 and Appendix A and because both EPA and NRC considered but explicitly rejected a 10,000 year control period for uranium mill tailings, our recommended seismic design value of 0.18 g for the Moab site provides

"reasonable assurance" of a level of protection "equivalent to, to the extent practicable" stipulated in Appendix A. We believe that selection of longer return periods, which correspond to lower probabilities of exceedance, would certainly result in overly conservative seismic design criteria not consistent with the available geologic, seismologic, and geophysical data pertinent to earthquake hazards in the vicinity of the Moab site and the interior of the Colorado Plateau.

5 CONCLUSIONS

Probabilistic seismic hazard analysis has been increasingly accepted as an approach often superior to deterministic methods alone for evaluating seismic hazards for a wide variety of facilities and structures. The probabilistic methodology is particularly well suited in applications for uranium mill tailings sites because of their generally lower risk and locations in the Intermountain U.S. In this region, large damaging earthquakes are possible but relatively infrequent There are also considerable uncertainties in characterizing seismic sources and estimating ground motions which can be explicitly incorporated into probabilistic seismic hazard analysis. Finally, because the level of acceptable risk for Title II sites has been expressed in a time frame of 200 to 1000 years (40 CFR 190.02), probabilistic seismic hazard analysis is better suited to providing the basis for seismic design criteria than deterministic approaches, which are time independent.

6 ACKNOWLEDGMENTS

The seismic hazard evaluation of the Atlas site was performed by Woodward-Clyde Federal Services for Smith Environmental Technologies on behalf of Atlas Corporation. Our thanks to Jacqueline Bott. Andy Gorton. Ann Becker Clark Fenton. Bob Green, Jeff McCleary, Sue Penn, Doug Wright, Richard Ely, Jim Cooksley, Fumiko Goss. and Sadako NcInerney for assistance in this study. We also benefitted greatly from interactions with NRC staff particularly Phil Justus, Bakr Ibrahim, Joe Holonich, Myron Fliegel, Ted Johnson and Dan Rom We greatly appreciate review of this paper by Tony Thompson.

REFERENCES

Bernreuter D, E. McDermott & J. Wagoner 1995. Seismic hazard analysis of Title II Reclamation Plans. Unpublished report prepared by Lawrence Livermore National Laboratory for the U. S. Nuclear Regulatory Commission.

Buil. W.B. and P.A Pearthree 1988. Frequency and size of Quaternary surface ruptures of the Pitaycachi fault, northeastern Sonora Mexico, Bull Seismol. Soc. Am., 78: 956-978.

Cornell, C.A 1968. Engineering seismic risk analysis, Bull Seismol. Soc Am.. 58:1583-1606.

Hecker, S 1993. Quaternary tectonics of Utah with emphasis on earthquake-hazard characterization. Utah Geol. Survey Bull. 127:157 p

McGuire, RK. 1974. Seismic structural response risk analysis incorporating peak response regressions on earthquake magnitude and distance, Massachusetts Institute of Technology Dept. of Civil Engineering Research Report R74-51.

Olig, S.S., C.H. Fenton, J. McCleary & I.G. Wong 1996. The earthquake potential of the Moab fault and its relation to salt tectonics in the Paradox Basin, Utah. In C. Huffman (ed.) 1996 Symposium and Field Conference on the Geology and Resources of the Paradox Basin (in press).

Sanford, A.R., L.H. Jaksha & D.J. Cash 1991. Seismicity of the Rio Grande rift in New Mexico. In D.B.

Slemmons, E.R Engdahl, M.D. Zoback & D.D. Blackwell (eds.), Neotectonics of North America, Geol. Soc. Am. Decade Map 1 :229-244

Smith, RB. & W.J. Arabasz 1991. Seismicity of the Intermountain seismic belt. In D.B. Slemmons, E.R. Engdahl, M.D. Zoback, M.L. Zoback & D. Blackwell (eds.), Neotectonics of North America, Geol. Soc. Am. Decade Map 1:185-228.

Smith, RB. & M.L. Sbar 1974. Contemporary tectonics of the interior of the western United States with the emphasis of the Intermountain seismic belt. GeoL Soc. Am. Bull. 85:1205-1918.

U.S. Nuclear Regulatory Commission 1994. Final safety evaluation report to license the construction and operation of a facility to receive, store and dispose of 11e(2) byproduct material near Clive, Utah. NUREG-1486.

Wong, I.G. & J.R. Humphrey 1989. Contemporary seismicity, faulting and the state of stress in the Colorado Plateau. Geol. Soc. Am. Bull 101:1127-1146.

Wong, I.G., S.S. Olig, & J.D. Bott 1996. Earthquake potential and seismic hazards in the Paradox Basin, southeastern Utah. In C. Huffman (ed.) 1996 Symposium and Field Conference on the Geology and Resources of the Paradox Basin (in press).

Wong, I.G., F. Swan m & L.S. Cluff 1982. Seismicity and tectonics of the Basin and Range and Colorado Plateau provinces: Implications to microzonation. In Third International Earthquake Microzonation Conference Proceedings 1:53-69.

Woodward-Clyde Federal Services 1996. Evaluation of potential seismic and salt dissolution hazards at the Atlas uranium mill tailings site, Moab. Utah. Unpublished final report prepared for Smith Environmental Technologies and Atlas Corporation.

JACOBS	Calculation No: C-13	Page: 1 of 32
Calculation Cover Sheet	Rev. No.: 1	Revision Date: 4/15/08
(Ref. FOWI 116 Design Calculations)	Previous Revision Date: 1/15/08	Current Revision Date: 4/15/08
Issuing Department: *Federal Operations Design Engineering*	Supersedes: Revision 0 (dated 1/15/08)	
Client: Project Title: MOAB UMTRA Project Project Number: 35DJ2600 System:	Engineering Discipline: Geotechnical	

Calculation Title: Frost Penetration Depth at Crescent Junction Disposal Site

Purpose:

The purpose of the attached calculation is to make an independent computation of the maximum frost penetration depth into the final cover expected to occur at the Moab uranium mill tailings repository in Crescent Junction, Utah. Calculations of maximum frost penetration into the cover had previously been prepared and included in the RAP Attachment 1: Disposal Cell Design Specs, Appendix A.

The objective of this design calculation is to determine the maximum frost penetration at the Crescent Junction repository site assuming a recurrence interval of 200 years for design of the freeze/thaw protective layer. In addition, frost penetration depth for recurrence interval of 1,000 years was performed as per the federal regulations including 10 Code of Federal Regulations Part 40.

NQA-1 QUALITY LEVEL: 2

Prepared by: Kurt J. Better / KK Chelkoit — Date: 12/3/07 / 04/17/08

Checked by: KK Chelkoit / Amal Nasr — Date: 12/3/07 / 04/17/08

Engineering Managers Approval: William D. Boyle — Date: 5/5/08

The current applicable version of this publication resides on Jacobs' Intranet. All copies are considered to be uncontrolled.
Copyright© Jacobs Engineering Group Inc., 2007

Revision History:

Pages Affected By Revision	Revised/Added/Deleted	Description of Revision
Rev. 1	Addition Page 1 of 32 Cover Sheet	Add sentence re: frost depth penetration determined for 1,000 year recurrence interval per federal regulations.
	Addition Page 6 of 32 Calculation Section	Added text description of calculation made to extrapolate frost depth vs. recurrence interval to 1,000 years per requirements of 10 Code of Federal Regulations Part 40 instead of to 200 years as used in the original analysis.
	Revision Page 16 of 32 Calculations	Revised extreme frost penetration calculations: added calculations for 200 yr and 1,000 yr intervals; calculated frost depth penetrations for N = 0.8 and 0.9 for top 5 frost depth penetration conditions.
	Revision Pages 17 and 18 of 32 Graphs	Revised graphics to extrapolate frost depth penetrations extending from 200 to 1,000 year recurrence interval.
	Addition Page 19 of 32 Graph	Added graphical plot of cumulative probability vs. standard variate (Gumbel Probability Function for Frost Penetration).

The current applicable version of this publication resides on Jacobs' Intranet. All copies are considered to be uncontrolled. Copyright© Jacobs Engineering Group Inc., 2007

Description of Calculation:

The Modified Berggren Formula (MBF) will be used to determine maximum frost penetration into the final cover of the Moab uranium mill tailings repository for known climatic and soil conditions at or near Crescent Junction, Utah.

Climatic conditions are based on available climate records for nearby Thompson Springs, Utah (approximately 5 miles from the Crescent Junction Disposal site).

Material properties for the in-situ soils and borrow material have been obtained from the "Geotechnical Properties of Native Materials" calculation set (Attachment 5, Vol. 1, Appendix E) for the Crescent Junction site.

Use the methods described in Smith and Rager (2002) to predict the maximum depth of frost penetration for the Crescent Junction Disposal site. This method includes projection of extreme-value frost depths for the 200-year recurrence interval by extrapolating beyond the available climate records using the cumulative probability distribution of the Gumbel function. Steps included in the analyses are:

1. Determine freeze-index parameters (air-freeze index, duration of freeze, mean annual temperature)
2. Determine surface correction factor
3. Determine thermal properties of the soil
4. Determine annual frost depths
5. Determine extreme frost depth

Assumptions:

Climate: Historical climatic condition records for Crescent Junction are not available.
Historical climatic condition records are available from NOAA and the Western Regional Climate Center for Moab and Thompson Springs (Thompson) Utah, respectively. Thompson Springs is located approximately 5 miles east of the proposed Crescent Junction Disposal site and the weather station elevation is within ±150 feet (El. 5150 vs El. 5,000) of the proposed top of the cell cover elevation at the Crescent Junction site.

Climate data for the frost penetration calculation has been obtained from National Climate Data Center COOP Station #428705 in Thompson, Utah; latitude: 38°58'; longitude: 109°43'; elevation: 5,150 ft AMS. It is assumed that the climatic data presented in RAP, Attachment 1, Disposal Cell Design Specifications, Appendix A "Freeze/Thaw Layer Design", including air-freezing index, length of freezing season, and mean annual temperature is correct.

Soils: Boring log and laboratory test data information of existing materials at the Crescent Junction site has been obtained from the "Geotechnical Properties of Native Materials" calculation set, RAP Attachment 5, Appendix E.

Soil properties: The existing soils which will be used as borrow material at the Crescent Junction site is described as Silt, clayey, sandy (CL). The average dry unit weight is 91.6 pcf and the average moisture content is 6.2%.

The current applicable version of this publication resides on Jacobs' Intranet. All copies are considered to be uncontrolled. Copyright© Jacobs Engineering Group Inc., 2007

Design Inputs:

Air Freezing Index (FI): varies, depending on year. Obtain from RAP Attachment 1, Appendix A and from WRCC data.

Length of Freezing Season (d) : varies, depending on year. Obtain from RAP Attachment 1, Appendix A.

Mean Annual Temperature (T): varies, depending on year. See attached sheets from WWCC; use values from RAP Attachment 1, Appendix A.

Soil: clay-silt type soil (CLAY, sandy, silty (CL)); dry unit weight: 91.6 pcf , moisture content: 6.2%

Thermal Conductivity (K); use chart (attached) for K_f and K_u for frozen and unfrozen silt-clay soils OR

$K_u = 0.0833(0.9 \log w - 0.2)\ (10^{0.01*\text{dry unit wt}}) = 0.352$ and

$K_f = (0.0833)\ [0.01(10^{0.022*\text{dry unit wt}}) + 0.085\ (10^{0.008*\text{dry unit wt}})(w)] = 0.324$; therefore

$K_{ave} = 0.5 * (K_u + K_f) = 0.338$

Volumetric Specific Heat (C) for unfrozen and frozen soil

$C_u = \text{dry unit wt}\ (0.17 + (w/100)) = 21.25\ \text{BTU/ft}^3 \cdot °\text{F}$ and

$C_f = \text{dry unit wt}\ (0.17 + [0.5w/100]) = 18.41\ \text{BTU/ft}^3 \cdot °\text{F}$; therefore

$C_{ave} = (C_u + C_f)/2 = 19.83\ \text{BTU/ft}^3 \cdot °\text{F}$

Latent Heat (L) of a Soil; use equation

$L = [(144\ \text{BTU/lb})\ (w)\ (\text{dry unit wt})]/100 = 818\ \text{BTU/ft}^3$

Surface Correction N-factor for freezing conditions:
N = 1 for snow
N = 0.9 for sand and gravel
N = 0.7 for bare ground (soil)
N = 0.5 for turf

Use N = 1 as worst case for the analysis. An assumed value of N = 0.8 can be used for a silt-clay cover ignoring any rock cover. An assumed value of N = 0.9 should be used for a rock cover.

Modified Berggren formula

$X = \lambda\ \text{sq rt}[(48*\ k_{ave}*\ n*FI)\ /L]$

Where

The current applicable version of this publication resides on Jacobs' Intranet. All copies are considered to be uncontrolled. Copyright© Jacobs Engineering Group Inc., 2007

x = depth of freeze (ft)

λ = dimensionless coefficient which takes into account effect of temperature changes in soil mass.

K_{ave} = thermal conductivity of soil, average of frozen + unfrozen (BTU/hr • ft • °F)

N, FI, and L as defined above.

Determine λ, where $\lambda = f(\mu, \alpha)$ From attached chart.

μ = fusion parameter = $(T_f - T_s)$ (C/L) and $T_f - T_s$ = nFI/d; therefore μ = nFI/d x C_{ave}/L

α = thermal ratio = $T - T_f / T_f - T_s$ where T = mean annual air temperature, T_f = 32°F, and $T_f - T_s$ = nFI/d

The current applicable version of this publication resides on Jacobs' Intranet. All copies are considered to be uncontrolled. Copyright© Jacobs Engineering Group Inc., 2007

Calculation Section:

Annual frost depths were determined for each of the subject years identified in Attachment 1, Appendix A using the Modified Berggren Formula (MBF). Spreadsheets for sample calculations are presented in Appendix A of this calculation, as well as a table summarizing all of the results calculated for the frost years identified in Attachment 1, Appendix A versus the results of this calculation.

The federal regulations including 10 Code of Federal Regulations Part 40 requires an extreme frost depth be determined for 1,000 years where reasonably achievable, but in any case no less than 200 years. Once the annual frost depths were calculated, methods as described in Smith and Rager (2002) were used to determine extreme frost depths for recurrence interval of 200 and 1,000 years using the following sequence:

1. Compile computed frost depths in ascending order.
2. Determine recurrence interval, Tr, where Tr = (n+1)/m, and n = number of observations and m = ordered sequence of frost depth values.
3. Determine Gumbel cumulative probability distribution (F(x)) of each frost depth calculation which is equal to the inverse of the recurrence interval. F(x) = 1/(1-Tr).
4. Determine standard variate, y, where y = -ln[-ln(1-(1/Tr))] for each frost depth calculation.
5. Plot calculated frost depths in relation to recurrence interval on arithmetic graph paper.
6. Determine best-fit line segments through the data with emphasis on the right (upper) distribution of data which represents the higher recurrence intervals.
7. Extrapolate the data to 200 years and 1,000 years to obtain the extreme frost penetration depth estimate.

The graphical results of the extreme-frost depth analysis suggest a maximum frost penetration of 45 inches for a recurrence interval of 200 years with a surface factor of 1.0. Frost depth predictions were also made with surface factor of 0.9 and 0.8 for the three highest frost penetration records, resulting in a maximum frost penetration of about 43 inches and 41 inches, respectively. The analysis was further extrapolated to recurrence interval of 1,000 years to satisfy the requirements of 10 Code of Federal Regulations Part 40. The results indicate an extreme-frost depth of 52, 50 and 48 inches for surface factor of 1.0, 0.9 and 0.8, respectively.

Based on Gumbel probability functions (see chart), designing for recurrence interval of 1,000 years verses 200 years does not add any significant value of risk reduction. In view of this, we recommend a maximum frost depth of 45 inches for a recurrence interval of 200 years should be used in the design of the cover.

The current applicable version of this publication resides on Jacobs' Intranet. All copies are considered to be uncontrolled. Copyright© Jacobs Engineering Group Inc., 2007

Conclusions/Recommendations:

Calculated annual frost depth penetrations were typically in line with results presented in RAP Attachment 1, Appendix A. The method of analysis used for these check calculations resulted in reasonably close results to those originally estimated using a surface correction factor of N = 1. The difference in results ranged from -2 to +0.7 inches, with the overall average difference for all frost years evaluated was less than 0.1 inch greater than previous calculations.

Regional frost depth maps presented in NAVFAC 7.1 suggest a extreme frost penetration depth of approximately 30 inches for the Crescent Junction area based upon state averages. This frost depth magnitude represents a recurrence interval of approximately 3 years. For a 200-year design life for the cover system, the 30 inch penetration is not acceptable.

Based on the results of the freeze/thaw analysis, a maximum frost penetration of 43 inches should be assumed for design of the Moab uranium tailings cover at the Crescent Junction Disposal Site using a rock cover, or 41 inches assuming a vegetation cover.

The current applicable version of this publication resides on Jacobs' Intranet. All copies are considered to be uncontrolled. Copyright© Jacobs Engineering Group Inc., 2007

SUMMARY OF LABORATORY TEST RESULTS
CRESCENT JUNCTION DISPOSAL SITE, UTAH

Natural Moisture (%)	Dry Density (pcf)	Soil Type
4.2	91	Clay, silty, sandy (CL)
4.5	100	Clay, silty, sandy (CL)
6.6	83	Clay, silty, sandy (CL)
6.1	83	Clay, silty, sandy (CL)
7.3	106	Clay, silty, sandy (CL)
8.4	108	Clay, silty, sandy (CL)
13.4	77	Clay, silty, sandy (CL)
8.2	96	Clay, sand, silty (CL/SC)
6.1	90	Clay, silty, sandy (CL)
4.6	84	Clay, silty, sandy (CL)
6	83	Clay, silty, sandy (CL)
5.4	102	Clay, silty, sandy (CL)
3.8	85	Clay, silty, sandy (CL)
12.4	95	Clay, silty, sandy (CL)
4.7	90	Clay, silty, sandy (CL)
4.2	94	Clay, silty, sandy (CL)
5.7	85	Clay, silty, sandy (CL)
2.8	95	Clay, silty, sandy (CL)
6	89	Clay, silty, sandy (CL)
4.7	91	Clay, silty, sandy (CL)
8.2	99	Clay, silty, sandy (CL)
5.7	87	Clay, silty, sandy (CL)
7.7	71	Clay, silty, sandy (CL)
12.2	89	Clay, silty, sandy (CL)
7.1	102	Clay, silty, sandy (CL)
6.5	85	Clay, silty, sandy (CL)
4.8	87	Clay, silty, sandy (CL)
5.6		Clay, silty, sandy (CL)
4.3		Clay, silty, sandy (CL)
2.9		Clay, silty, sandy (CL)
5.5		Clay, silty, sandy (CL)
5.7		Clay, silty, sandy (CL)
4.4		Clay, silty, sandy (CL)
7.6		Clay, silty, sandy (CL)
2.7		Clay, silty, sandy (CL)
7.2		Clay, silty, sandy (CL)
2.7		Clay, silty, sandy (CL)
5.5		Clay, silty, sandy (CL)
5.8	89	Clay, silty, sandy (CL)
4.9	89	Clay, silty, sandy (CL)
7	87	Clay, silty, sandy (CL)
5	93	Clay, silty, sandy (CL)
8.6	98	Clay, silty, sandy (CL)
7.6	103	Clay, silty, sandy (CL)
10	109	Clay, silty, sandy (CL)
6.2	**91.6**	

Source: Geotechnical Engineering Group, Inc. lab test results, December 22, 2005
Attachment 5 Vol. 1, Appendix E

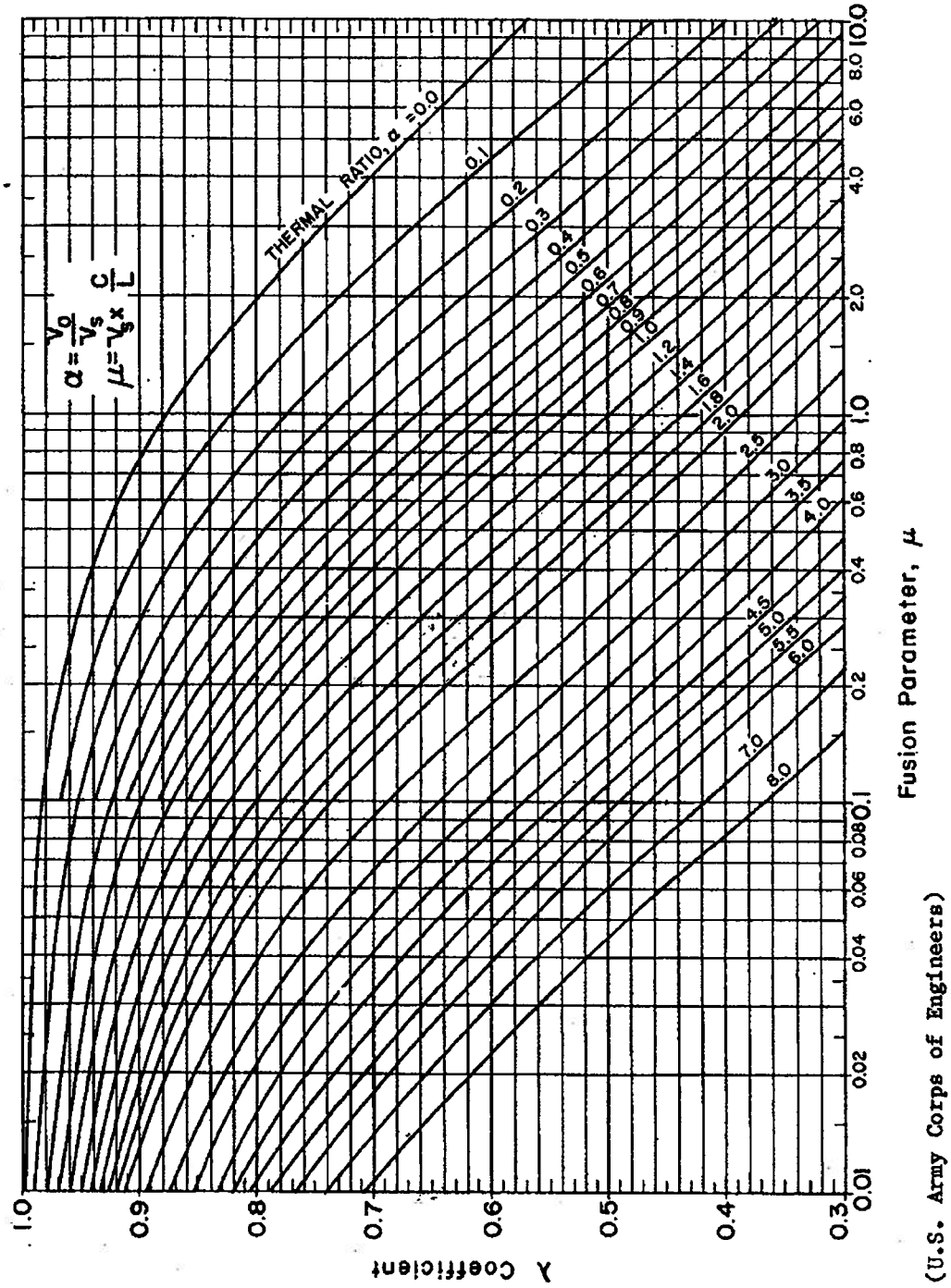

(U.S. Army Corps of Engineers)

Figure 3-1. λ coefficient in the modified Berggren formula.

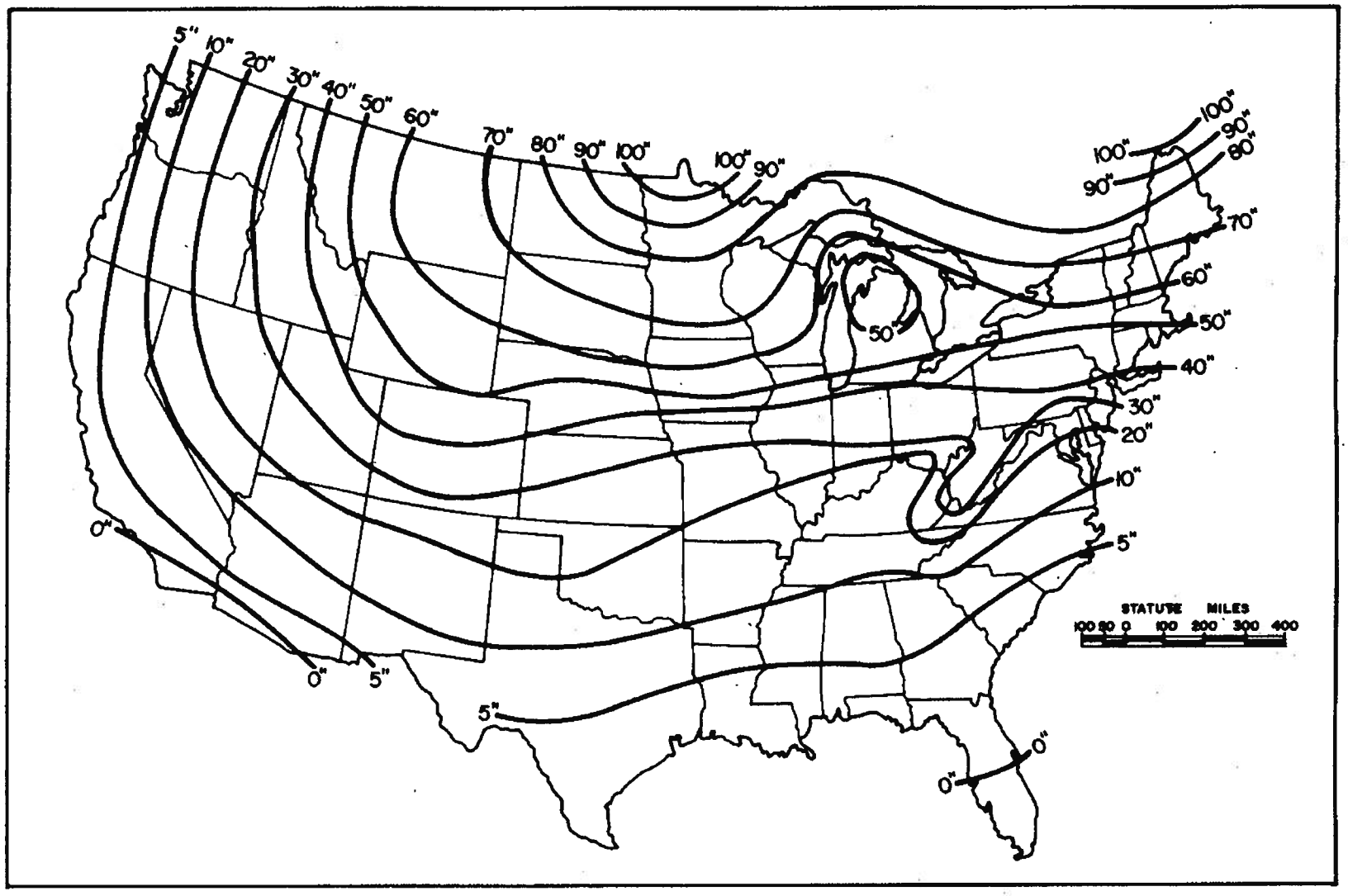

FIGURE 7
Extreme Frost Penetration (in inches) Based Upon State Average

ANNUAL FROST PENETRATION CALCULATION RESULTS
AND
SAMPLE CALCULATION SHEET

CALCULATED ANNUAL FROST PENETRATION DEPTHS
CRESCENT JUNCTION, UTAH

Year	Air Freeze Index (°-days)	Length of Freeze Season (days)	Mean Annual Temperature (°F)	Depth of Frost Penetration (in) - Appendix A	Depth of Frost Penetration, n=1.0 (in)	Difference (in)	Depth of Frost Penetration, n=0.9 (in)	Depth of Frost Penetration, n=0.8 (in)
1933	1141	83	48.8	38.3	39	0.7	37	35
1934	80	42	56.7	6.0	5	-1.0		
1935	124	62	53.3	8.0	6	-2.0		
1937	970	83	50.1	33.9	34	0.1	32	31
1938	177	69	53.5	10.2	10	-0.2		
1939	765	87	52.1	27.7	28	0.3		
1941	765	87	52.1	27.7	28	0.3		
1943	17	5	55.8	2.0	3	1.0		
1944	119	33	55.2	8.8	8	-0.8		
1945	32	9	54.7	4.0	4	0.0		
1946	520	73	53.2	22.0	22	0.0		
1950	501	67	52.5	21.6	22	0.4		
1954	240	45	55.3	13.4	14	0.6		
1955	829	93	51.4	29.7	30	0.3		
1956	45	29	55.3	24.0	3			
1960	338	67	53.8	16.0	16	0.0		
1961	199	60	54.0	11.1	11	-0.1		
1963	735	44	52.9	28.9	29	0.1		
1971	289	29	54.0	16.6	17	0.4		
1974	734	82	53.0	27.0	27	0.0		
1975	403	44	53.3	19.8	20	0.2		
1976	293	45	53.7	15.8	16	0.2		
1977	264	55	54.8	13.6	14	0.4		
1978	177	6	55.0	14.4	14	-0.4		
1979	1132	93	51.3	36.0	36	0.0	33	32
1980	293	48	53.5	15.6	16	0.4		
1982	448	56	53.4	20.4	21	0.6		
1983	92	21	53.3	8.3	8	-0.3		
1986	106	37	54.2	8.0	8	0.0		
1987	225	51	53.7	12.8	13	0.2		
1988	832	74	50.8	30.7	31	0.3		
1989	714	88	53.1	25.9	26	0.1		
1990	255	85	53.6	12.5	12	-0.5		
1991	696	77	52.0	26.8	27	0.2		
1992	718	74	52.0	27.4	27	-0.4		
1994	284	83	52.3	14.3	14	-0.3		
average	**432**	**58**	**53**	**19**	**18**	**0**		

Note:
Air Freeze Index, Length of Freezing Season, Mean Annual Temperature, and Depth of Frost Penetration - Appendix A for each frost year analyzed are obtained from RAP, Attachment 1, Appendix A.

DEPTH OF FROST PENETRATION CALCULATION
CRESCENT JUNCTION, UTAH
FROST YEAR 1933

dry unit wt (pcf)	91.6
moisture content	6.2

thermal conductivity (k)

for unfrozen silt-clay soils, ku = 0.0083(0.9 log w-0.2)*(10^0.01*dry unit weight)

0.0833	0.71315252	0.51315252	0.916	8.24138115	
		ku	0.352		

for frozen silt-clay soils, kf =(0.083)[(0.01(10^0.022*dry unit wt))+0.085(10^0.008*dry unit wt)(w)]

0.0833	2.0152	103.561898	1.03561898	0.7328	5.40505354	2.84846321
		kf	0.324			

for frozen silt-clay soils, kave = (ku+kf)/2

kavg 0.338 **Eq. 1**

volumetric specific heat

for unfrozen soil, Cu = dry unit wt (0.17+(w/100))

Cu 21.25

for frozen soil, Cf = dry unit wt (0.17+(0.5w/100))

Cf 18.41

Cavg 19.83 **Eq. 2**

Latent Heat (L) of a soil

latent heat = [144 BTU/lbxwxdry unit wt]/100

L 817.8048

L 818 **Eq.3**

Freezing Index, (FI) = summation(T-32) and T = 0.5(T1+T2) where T is in days (obtained from other spreadsheet)

T = mean daily temperature = 0.5(T1+T2)

T1 = max daily air temperature

T2 = min daily air temperature

FI 1141 **Eq. 4**

N-factor (N) = surface freezing index / air freezing index.

Typical N values	snow	1
	pavement free of snow	0.9
	sand and gravel	0.9
	soil	0.7
	turf	0.5

N 1 **Eq. 5**

Length of Freeze (d)

Per Utah Climate Center for Thompson, Utah, Freeze-free period= 79 days (short), 176 days (ave.), 211 days (long)

Ave = 365 - 176 = 189 days. Seems to be too long based on 1948-1994 climate data.

Based on daily average temperatures for 1948-1994, days with temp below 32 F = 134

DEPTH OF FROST PENETRATION CALCULATION
CRESCENT JUNCTION, UTAH
FROST YEAR 1933

Based on daily average temperatures when the average of the min and max temp < 32 F, d = 63 days

d **83** **Eq. 6**

modified Berggren Formula, x = λ[((48)(Kavg)(n)(FI))/L)]^1/2

x = depth of freeze (ft)

λ = dimensionless coefficient which takes into account effect of temp changes in soil mass

kave = thermal conductivity of soil, average of frozen and unfrozen (BTU/hr*ft*F)

n = conversion factor for air freezing index to surface freezing index

FI = freezing index (F*days)

L = latent heat (BTU/cu ft)

Determine λ λ= f(μ, ∞) determined from Figure 1 graph

Determine μ, fusion parameter

μ = (Tf-Ts)(C/L)

where
Tf-Ts = nFI/d

Tf-Ts	13.75
Cavg/L	0.024
μ	0.333

Eq. 7

Determine ∞, thermal ratio

∞= (T-Tf)/Tf-Ts

where
T = mean annual temperature, F per Thompson Utah climate records **48.8**
Tf = 32 F
Tf-Ts = nFI/d

∞ 1.2 **Eq. 8**

Determine λ from figure 1

λ **0.68**

Calculate depth of freezing (ft)

x = (λ)*sqrt[((48)(Kave)(n)(FI))/L)]

22.63 4.76

x (ft)	3.23
x (in)	**39**

Eq. 9

RESULTS OF EXTREME FROST DEPTH ANALYSIS

EXTREME FROST PENETRATION CALCULATIONS
GUMBEL EXTREME-VALUE DISTRIBUTION
CRESCENT JUNCTION, UTAH

Frost Depth (in)	Frost Depth (N=1.0) (m)	Rank	Recurrence interval Tr	Standard variate	1-(1/Tr)	y = -LN[-LN(1-(1/Tr))]	Extreme Gumbel Pred. F(x) = e^(-e^(-y))	Regular Gumbel Pred. F(x) = 1 - e^(-e^(y))		Frost Depth (N=0.9) (m)	Frost Depth (N=0.8) (m)
	1.328		1000.0	6.907	0.9990	6.907	0.999	1.000		1.277	1.226
	1.152		200.0	5.296	0.9950	5.296	0.995	1.000		1.101	1.050
39	0.991	1	37.0	3.597	0.9730	3.597	0.973	1.000		0.940	0.889
36	0.914	2	18.5	2.890	0.9459	2.890	0.946	1.000		0.864	0.813
34	0.864	3	12.333	2.470	0.9189	2.470	0.919	1.000		0.813	0.762
31	0.787	4	9.250	2.168	0.8919	2.168	0.892	1.000			
30	0.762	5	7.400	1.930	0.8649	1.930	0.865	0.999			
29	0.737	6	6.167	1.732	0.8378	1.732	0.838	0.996			
28	0.711	7	5.286	1.562	0.8108	1.562	0.811	0.992			
28	0.711	8	4.625	1.412	0.7838	1.412	0.784	0.984			
27	0.686	9	4.111	1.278	0.7568	1.278	0.757	0.972			
27	0.686	10	3.700	1.155	0.7297	1.155	0.730	0.958			
27	0.686	11	3.364	1.042	0.7027	1.042	0.703	0.941			
26	0.660	12	3.083	0.936	0.6757	0.936	0.676	0.922			
22	0.559	13	2.846	0.837	0.6486	0.837	0.649	0.901			
22	0.559	14	2.643	0.744	0.6216	0.744	0.622	0.878			
21	0.533	15	2.467	0.654	0.5946	0.654	0.595	0.854			
20	0.508	16	2.313	0.568	0.5676	0.568	0.568	0.829			
17	0.432	17	2.176	0.486	0.5405	0.486	0.541	0.803			
16	0.406	18	2.056	0.406	0.5135	0.406	0.514	0.777			
16	0.406	19	1.947	0.328	0.4865	0.328	0.486	0.750			
16	0.406	20	1.850	0.251	0.4595	0.251	0.459	0.724			
14	0.356	21	1.762	0.176	0.4324	0.176	0.432	0.697			
14	0.356	22	1.682	0.102	0.4054	0.102	0.405	0.670			
14	0.356	23	1.609	0.029	0.3784	0.029	0.378	0.643			
14	0.356	24	1.542	-0.045	0.3514	-0.045	0.351	0.616			
13	0.330	25	1.480	-0.119	0.3243	-0.119	0.324	0.589			
12	0.305	26	1.423	-0.193	0.2973	-0.193	0.297	0.561			
11	0.279	27	1.370	-0.269	0.2703	-0.269	0.270	0.534			
10	0.254	28	1.321	-0.346	0.2432	-0.346	0.243	0.507			
8	0.203	29	1.276	-0.426	0.2162	-0.426	0.216	0.479			
8	0.203	30	1.233	-0.510	0.1892	-0.510	0.189	0.452			
8	0.203	31	1.194	-0.598	0.1622	-0.598	0.162	0.423			
6	0.152	32	1.156	-0.694	0.1351	-0.694	0.135	0.393			
5	0.127	33	1.121	-0.800	0.1081	-0.800	0.108	0.362			
4	0.102	34	1.088	-0.921	0.0811	-0.921	0.081	0.328			
3	0.076	35	1.057	-1.071	0.0541	-1.071	0.054	0.290			
3	0.076	36	1.028	-1.284	0.0270	-1.284	0.027	0.242			

Tr = recurrence interval = n+1/m, where n = number of observations and
m = ordered sequence of frost depth values.

F(x) = cumulative probability distribution of the Gumbel function, which is equal to the inverse of the recurrence interval.

Thus F(x) = 1/(1-Tr)

y = standard variate = -ln[-ln(1-(1/Tr))].

Frost depths are plotted in relation to the standard variate on arithemetic graph paper.
A best-line fit is drawn through these data swith emphasis on the right tail of the distribution where the higher-recurrence intervals are located.

MOAB - Crescent Junction: Extreme Frost Penetration Extrapolation

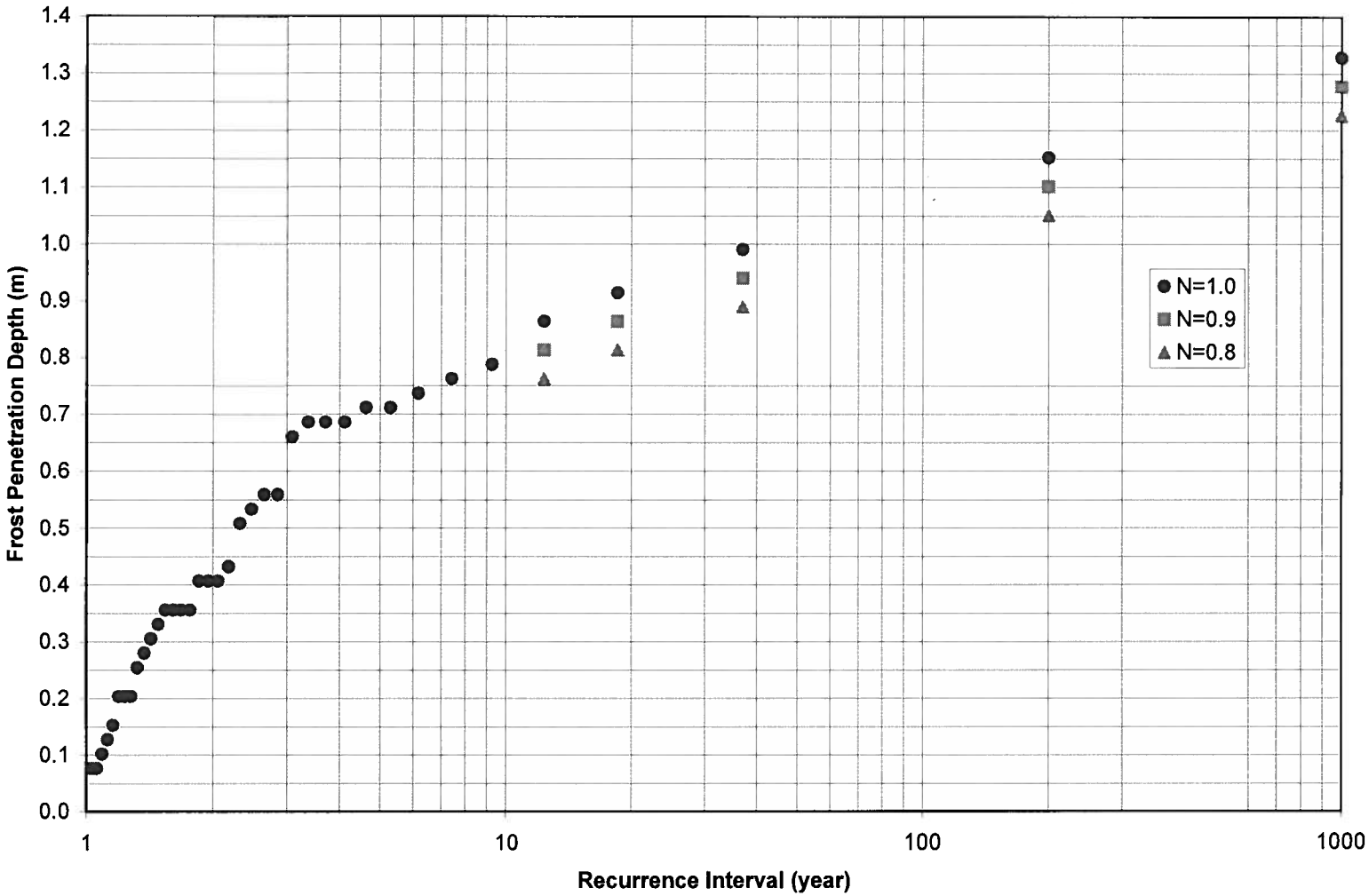

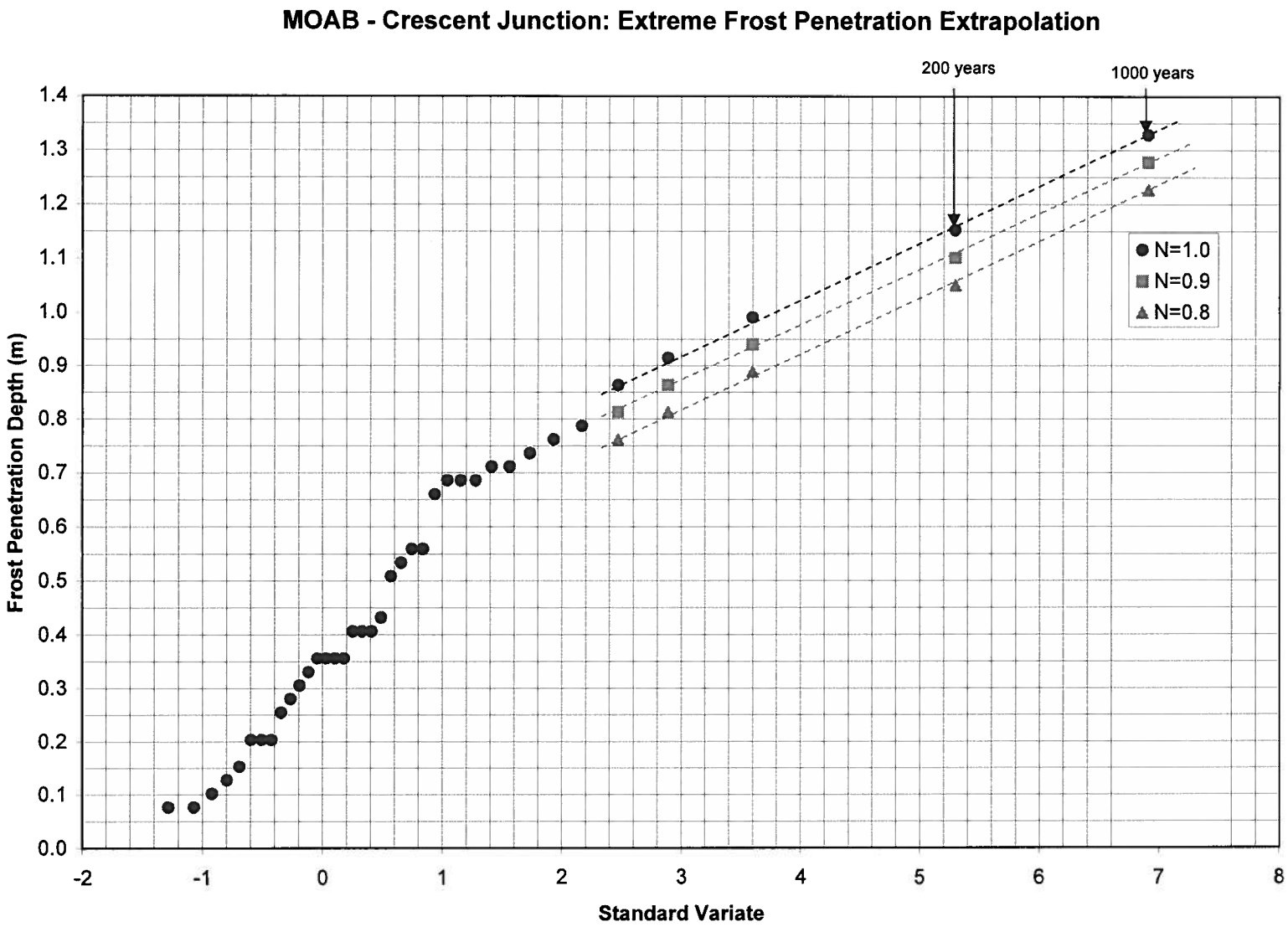
MOAB - Crescent Junction: Extreme Frost Penetration Extrapolation
200 years
1000 years
N=1.0
N=0.9
N=0.8
Frost Penetration Depth (m)
Standard Variate
1.4
1.3
1.2
1.1
1.0
0.9
0.8
0.7
0.6
0.5
0.4
0.3
0.2
0.1
0.0
-2
-1
0
1
2
3
4
5
6
7
8

MOAB - Cresecent Junction: Gumbel Probability Function for Frost Penetration

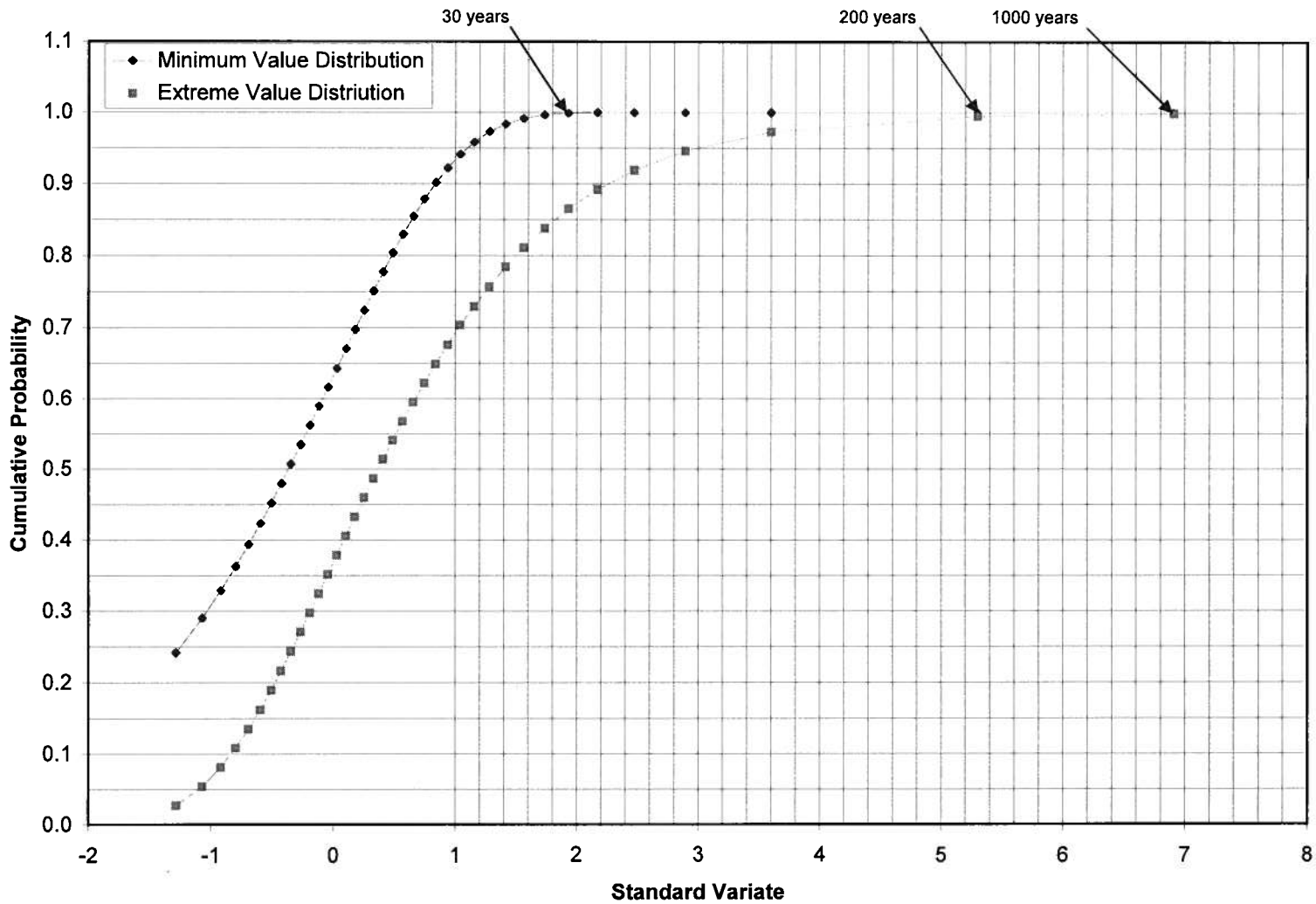

BACK-UP CLIMATIC DATA FOR THOMPSON, UTAH

THOMPSON, UTAH

Period of Record General Climate Summary - Temperature

Station:(428705) THOMPSON													
From Year=1948 To Year=1994													
	Monthly Averages			Daily Extremes				Monthly Extremes				Max. Temp.	
	Max.	Min.	Mean	High	Date	Low	Date	Highest Mean	Year	Lowest Mean	Year	>= 90 F	<= 32
	F	F	F	F	dd/yyyy or yyyymmdd	F	dd/yyyy or yyyymmdd	F	-	F	-	# Days	# Da
January	37.1	14.6	25.9	62	26/1975	-23	13/1963	38.2	1956	13.1	1973	0.0	9
February	45.5	22.3	33.9	68	12/1962	-18	06/1989	43.0	1954	19.7	1955	0.0	2
March	55.3	29.7	42.5	80	27/1953	8	21/1955	51.2	1972	36.3	1952	0.0	0
April	66.0	37.9	52.0	86	20/1989	15	08/1973	57.6	1981	45.9	1975	0.0	0
May	75.6	47.0	61.3	93	31/1994	26	07/1988	67.1	1969	57.4	1975	0.4	0
June	86.9	57.1	72.1	108	25/1990	34	02/1990	76.8	1977	66.8	1965	12.6	0
July	93.1	63.9	78.5	105	06/1985	44	06/1993	81.5	1964	74.6	1993	24.9	0
August	90.4	61.5	75.9	103	19/1986	40	25/1992	80.5	1994	70.6	1968	18.6	0
September	81.6	52.6	67.1	97	15/1990	31	25/1961	72.4	1979	58.0	1961	4.1	0
October	69.5	41.1	55.3	88	01/1963	15	31/1991	60.7	1978	49.7	1994	0.0	0
November	52.1	28.2	40.2	77	09/1958	2	10/1950	46.4	1965	33.3	1979	0.0	0
December	40.4	18.1	29.2	66	06/1958	-12	27/1962	39.4	1980	19.7	1978	0.0	5
Annual	66.1	39.5	52.8	108	19900625	-23	19630113	55.5	1981	50.6	1979	60.6	18
Winter	41.0	18.3	29.7	68	19620212	-23	19630113	38.7	1981	19.6	1979	0.0	17
Spring	65.7	38.2	52.0	93	19940531	8	19550321	54.8	1974	48.5	1975	0.4	0
Summer	90.1	60.8	75.5	108	19900625	34	19900602	78.6	1994	72.4	1993	56.0	0
Fall	67.7	40.6	54.2	97	19900915	2	19501110	57.9	1963	48.6	1961	4.1	0

Table updated on Jul 28, 2006
For monthly and annual means, thresholds, and sums:
Months with 5 or more missing days are not considered
Years with 1 or more missing months are not considered
Seasons are climatological not calendar seasons
Winter = Dec., Jan., and Feb. Spring = Mar., Apr., and May
Summer = Jun., Jul., and Aug. Fall = Sep., Oct., and Nov.

THOMPSON, UTAH

Monthly Average Temperature (Degrees Fahrenheit)

(428705)

File last updated on Oct 18, 2007
*** Note *** Provisional Data *** After Year/Month 199411
a = 1 day missing, b = 2 days missing, c = 3 days, ..etc..,
z = 26 or more days missing, A = Accumulations present
Long-term means based on columns; thus, the monthly row may not
sum (or average) to the long-term annual value.
MAXIMUM ALLOWABLE NUMBER OF MISSING DAYS : 5
Individual Months not used for annual or monthly statistics if more than 5 days are missing.
Individual Years not used for annual statistics if any month in that year has more than 5 days missing.

YEAR (S)	JAN	FEB	MAR	APR	MAY	JUN	JUL	AUG	SEP	OCT	NOV	DEC	ANN
1948	-----z	-----z	-----z	-----z	-----z	-----z	77.35a	74.90a	-----z	52.47n	34.42	32.02f	62.22
1949	29.77r	25.20a	43.08	54.77	60.37	68.28c	76.74	74.98	67.98	50.53	43.47	27.52	53.90
1950	23.41b	32.38g	41.24d	51.68	59.06	68.20h	75.11h	75.08	65.29f	57.33y	-----z	34.33j	50.10
1951	27.65e	38.28j	42.47	51.38	56.67k	72.41h	78.40b	73.03	66.23	53.61	36.27	23.00q	53.63
1952	26.08	30.50	36.29	54.12	62.82	70.09n	77.98	76.32a	69.95	60.38c	-----z	28.75e	52.32
1953	32.80h	35.41f	45.71g	49.22j	58.40k	72.50h	81.02c	75.55	68.58f	57.92	43.83	26.08	56.88
1954	33.21	43.02	41.06	57.45	64.53	72.13	80.68	75.13	67.88	57.32	44.47	27.47	55.36
1955	21.47	19.66	39.32	48.57	60.18l	72.12m	76.56	78.61	71.27	57.68	36.87	36.53	48.65
1956	38.21	32.14	42.95	53.62	65.29	75.77	78.34	74.73	71.80	57.08	-----z	-----z	58.99
1957	-----z	-----z	45.58	50.22	57.68	70.75	77.39	74.84	66.00	53.58	36.83	32.03p	59.21
1958	30.24	40.57	40.34	49.57	61.00v	74.05b	77.60	78.82	68.75	58.58	43.38	38.16	54.55
1959	31.05	37.23	42.73	54.08	61.95u	76.22	79.55	75.19	66.03	54.05	40.03	32.45	53.51
1960	24.05	29.71	44.02	52.83	60.10	73.73	79.66	76.26	68.42	53.37	41.85	29.42	52.78
1961	28.16	36.98	41.03	49.13	61.16	74.50	77.82	73.37	58.03	51.35	36.45	21.15	50.76
1962	22.39	36.04	36.50	56.42	58.28v	71.87	77.16	76.61	68.00	55.39l	45.22	30.21	52.04
1963	13.71	39.66	40.71	48.93	65.34	68.93	79.44	74.22v	68.78	59.95	44.83	30.00	50.94
1964	27.50	31.36	38.65	49.93	61.24	69.75	81.52	78.36q	67.30c	60.16	39.38	31.34	50.74
1965	33.52	34.52	39.76	51.15	58.50	66.78	75.92	76.75s	60.81d	58.06	46.37	31.50	50.63
1966	24.93j	29.62	44.06	52.52	65.94	73.74k	79.26	77.15	68.03	54.03	46.33x	26.64j	58.83
1967	25.26	37.25	47.19	50.38	60.24	67.23	79.44	76.85g	68.79d	57.76	44.75	20.98	50.84
1968	-----z	-----z	-----z	-----z	-----z	-----z	78.25q	70.56	65.25	55.46f	39.33o	29.89m	67.91
1969	32.06f	34.20	36.64c	53.36a	67.06	67.45a	79.89c	79.50	-----z	47.92k	39.32	32.53	54.44
1970	29.97	41.32	40.35	47.62	63.71	71.22	79.48	78.47	64.87	52.37d	42.17	31.50	53.59
1971	29.15	35.80	42.77	52.25	60.81	72.67	81.15	78.40	63.57	57.25w	38.30	26.58	52.86
1972	31.58	40.24	51.21	55.43	64.67p	75.05	80.58	77.69	68.58	47.41o	38.68	24.98	54.40
1973	13.11	27.95	41.82	46.92l	60.37	69.77	77.27	77.29	66.33	56.81	42.32	31.24	51.30
1974	18.92	21.89	47.60a	50.32	66.39	75.92	78.13	75.81	69.47	58.18	41.83	28.85	52.78
1975	22.85	34.39	42.31	45.92	57.35	66.93	78.65	75.74	67.90	54.44	40.13	30.05	51.39
1976	26.76	40.47	40.95	52.05	63.60	71.62	80.95	75.27	67.82	52.94	41.92	30.98	53.78

1977	26.35	39.80	41.43b	56.58	61.45	76.80	78.19	77.76	69.35	57.61	42.63	36.32	55.36
1978	27.47	33.27	47.60	53.32	59.40	73.17	79.32	76.19	68.75	60.74	42.85	19.69	53.48
1979	16.76	22.21	40.06	51.61c	60.03	71.83	78.45	74.66	72.37	58.24	33.32	27.65	50.60
1980	32.35	39.14	39.94	51.08	57.71	72.13	78.92	74.48	66.98	54.35	42.52	39.40	54.08
1981	37.23	39.43	44.03	57.60	60.29	75.42	78.53	76.52	69.07	52.26	43.92	31.69	55.50
1982	23.53	31.61	43.00	49.68	61.00	69.93	75.71	75.66	64.82	49.81	38.12	31.76	51.22
1983	32.24	39.41	43.63	46.60	58.06	70.03	78.16i	80.30i	71.70	55.63p	41.17l	27.63l	51.67
1984	18.87	30.02i	42.98j	49.67j	67.39i	69.05i	79.82l	76.11i	67.61k	49.34i	40.63k	32.03m	18.87
1985	27.60k	32.64j	44.19j	58.83r	64.32n	73.68b	78.85	76.71	61.57a	51.97a	37.54b	30.66	58.71
1986	32.37	39.29	47.95	50.20	59.24	74.60	76.21	77.74	62.38	51.48	40.68	32.23	53.70
1987	25.77	35.89	39.32	54.63	62.36b	74.35	74.97	73.23	66.17	56.71	39.57	27.21	52.52
1988	16.73	27.12	37.84	50.28	59.95	74.02	78.76	74.63	63.65	57.19	40.25	29.16	50.80
1989	17.48a	27.18	45.97	56.58	61.71	70.67	80.31	73.19	65.17	53.53	40.50	28.73	51.75
1990	27.76	34.93	45.82	55.87	59.21	73.57	77.47	75.76	70.73	53.63	41.37	22.79	53.24
1991	21.42	33.38	41.26	47.16a	62.23	71.13	79.10	75.56	67.22	54.89	38.35	24.76	51.37
1992	17.19	34.66	46.42	56.90a	67.50y	-----z	-----z	69.92s	67.43	57.44	34.15	22.56	42.09
1993	27.32	33.27	44.97	48.98	60.97	68.07	74.65	74.44	65.18	51.39	34.57	28.21	51.00
1994	29.74	31.64	45.69	51.43	61.66	75.92	79.32a	80.53	67.37	49.73	33.32	-----z	55.12

Period of Record Statistics

MEAN	25.87	33.90	42.51	52.01	61.34	72.05	78.49	75.91	67.09	55.29	40.17	29.22	52.75
S.D.	6.19	5.74	3.36	3.10	2.57	2.89	1.66	1.96	3.00	3.14	3.51	4.52	1.61
SKEW	-0.22	-0.67	0.28	0.11	0.59	-0.24	-0.34	0.00	-0.77	-0.04	-0.34	-0.01	0.28
MAX	38.21	43.02	51.21	57.60	67.06	76.80	81.52	80.53	72.37	60.74	46.37	39.40	55.50
MIN	13.11	19.66	36.29	45.92	57.35	66.78	74.65	70.56	58.03	49.73	33.32	19.69	50.60
NO YRS	39	39	42	41	35	37	42	40	42	38	40	37	20

THOMPSON, UTAH (428705)

Period of Record Monthly Climate Summary

Period of Record : 7/ 1/1948 to 11/30/1994

	Jan	Feb	Mar	Apr	May	Jun	Jul	Aug	Sep	Oct	Nov	Dec	Annual
Average Max. Temperature (F)	37.1	45.5	55.3	66.0	75.6	86.9	93.1	90.4	81.6	69.5	52.1	40.4	66.1
Average Min. Temperature (F)	14.6	22.3	29.7	37.9	47.0	57.1	63.9	61.5	52.6	41.1	28.2	18.1	39.5
Average Total Precipitation (in.)	0.80	0.53	0.86	0.76	0.88	0.43	0.69	1.00	0.94	1.07	0.64	0.59	9.20
Average Total SnowFall (in.)	4.8	2.4	1.2	0.1	0.0	0.0	0.0	0.0	0.0	0.2	0.6	3.2	12.4
Average Snow Depth (in.)	2	1	0	0	0	0	0	0	0	0	0	1	0

Percent of possible observations for period of record.
Max. Temp.: 92.3% Min. Temp.: 92.1% Precipitation: 95.4% Snowfall: 88.4% Snow Depth: 84.2%
Check Station Metadata or Metadata graphics for more detail about data completeness.

Western Regional Climate Center, wrcc@dri.edu

THOMPSON, UTAH (428705)

1971-2000 Monthly Climate Summary

	Jan	Feb	Mar	Apr	May	Jun	Jul	Aug	Sep	Oct	Nov	Dec	Annual
Average Max. Temperature (F)	36.5	45.2	56.0	65.7	75.4	87.2	92.8	90.4	81.4	68.0	49.7	39.5	65.8
Average Min. Temperature (F)	14.9	22.8	31.5	38.4	47.2	57.2	63.5	61.4	52.5	40.7	27.6	17.7	39.7
Average Total Precipitation (in.)	0.93	0.66	0.95	0.90	0.94	0.37	0.71	0.90	1.04	1.17	0.77	0.72	10.05

Unofficial values based on averages/sums of smoothed daily data. Information is computed from available daily data during the 1971-2000 period. Smoothing, missing data and observation-time changes may cause these 1971-2000 values to differ from official NCDC values. This table is presented for use at locations that don't have official NCDC data. No adjustments are made for missing data or time of observation. Check NCDC normals table for official data.

Western Regional Climate Center, wrcc@dri.edu

THOMPSON, UTAH

NCDC 1971-2000 Monthly Normals

	Jan	Feb	Mar	Apr	May	Jun	Jul	Aug	Sep	Oct	Nov	Dec	Annual Monthly
Mean Max. Temperature (F)	37.7	46.2	56.7	65.7	76.3	87.9	93.8	91.6	82.2	68.9	52.0	40.9	66.7
Highest Mean Max. Temperature (F)	50.7	55.4	65.2	73.7	83.1	94.4	97.8	95.3	87.9	75.5	59.1	51.7	97.8
Year Highest Occurred	1981	1995	1972	1989	1984	1994	1994	1994	1979	1988	1999	1980	1994
Lowest Mean Max. Temperature (F)	24.1	33.5	50.4	59.0	68.5	81.8	91.1	87.8	76.0	61.6	43.8	30.5	24.1
Year Lowest Occurred	1973	1979	1979	1975	1995	1995	1987	1999	1986	1984	2000	1978	1973
Mean Temperature (F)	26.0	34.2	43.5	51.6	61.9	72.4	78.7	76.8	67.6	54.6	40.0	29.3	53.1
Highest Mean Temperature (F)	36.4	41.8	50.3	57.6	68.4	77.0	81.5	80.8	72.4	60.9	44.5	38.8	81.5
Year Highest Occurred	1981	1995	1972	1992	1984	1977	1971	1994	1979	1978	1995	1980	1971
Lowest Mean Temperature (F)	12.3	21.2	38.6	45.4	57.2	66.9	74.9	73.4	62.2	50.1	33.0	19.1	12.3
Year Lowest Occurred	1973	1974	1988	1975	1995	1995	1993	1989	1985	1984	1979	1978	1973
Mean Min. Temperature (F)	14.3	22.1	30.3	37.4	47.4	56.9	63.6	61.9	52.9	40.3	28.0	17.6	39.4
Highest Mean Min. Temperature (F)	23.2	28.2	35.4	42.7	53.6	63.1	67.9	66.6	58.4	47.3	31.4	25.9	67.9
Year Highest Occurred	1980	2000	1972	1981	1984	1972	1972	2000	1998	1978	1998	1980	1972
Lowest Mean Min. Temperature (F)	0.6	7.7	23.6	31.9	43.6	51.8	58.0	57.1	47.4	34.6	20.5	7.7	0.6
Year Lowest Occurred	1973	1974	1988	1975	1975	1993	1993	1988	1989	1982	1979	1978	1973
Mean Precipitation (in.)	1.00	0.56	1.03	0.83	1.00	0.35	0.77	0.88	1.02	1.23	0.68	0.62	9.97
Highest Precipitation (in.)	3.15	2.36	2.49	3.50	3.20	0.90	2.27	1.87	3.68	3.93	2.09	1.65	3.93
Year Highest Occurred	1993	1993	1978	1994	1973	1983	1987	1977	1982	1972	1978	1972	1972
Lowest Precipitation (in.)	0.00	0.00	0.00	0.00	0.00	0.00	0.00	0.00	0.08	0.00	0.00	0.00	0.00
Year Lowest													

Occurred	1976	1972	1994	1982	1974	1994	1994	1975	1978	1976	1976	1989	1976
Heating Degree Days (F)	1209.	864.	667.	410.	151.	18.	0.	0.	54.	332.	749.	1109.	5563.
Cooling Degree Days (F)	0.	0.	0.	8.	54.	241.	424.	365.	131.	11.	0.	0.	1234.

Western Regional Climate Center, wrcc@dri.edu

THOMPSON, UTAH

NCDC 1961-1990 Monthly Normals

	Jan	Feb	Mar	Apr	May	Jun	Jul	Aug	Sep	Oct	Nov	Dec	Annual
Mean Max. Temperature (F)	35.1	44.6	53.5	63.1	74.1	85.0	91.9	88.9	79.7	67.5	51.4	39.0	64.5
Highest Mean Max. Temperature (F)	48.9	52.8	63.4	72.1	79.4	90.5	96.7	92.2	86.1	74.4	57.0	50.0	67.4
Year Highest Occurred	1981	1970	1972	1989	1963	1990	1989	1988	1979	1988	1962	1980	1981
Lowest Mean Max. Temperature (F)	22.3	31.7	46.1	55.9	68.9	77.5	88.3	82.2	71.5	58.6	43.7	28.8	61.7
Year Lowest Occurred	1973	1979	1969	1983	1980	1967	1987	1968	1961	1984	1979	1978	1973
Mean Temperature (F)	24.0	33.0	41.4	50.2	60.7	71.0	78.1	75.3	66.0	54.2	40.0	28.2	51.8
Highest Mean Temperature (F)	35.6	39.9	49.9	56.6	66.5	76.0	81.0	79.5	71.5	59.9	45.2	38.3	54.4
Year Highest Occurred	1981	1970	1972	1989	1984	1977	1964	1983	1979	1978	1965	1980	1981
Lowest Mean Temperature (F)	11.5	20.4	35.2	44.3	56.5	66.0	74.5	69.8	57.2	47.9	32.2	18.6	49.5
Year Lowest Occurred	1973	1974	1962	1975	1975	1965	1987	1968	1961	1969	1979	1978	1979
Mean Min. Temperature (F)	12.8	21.3	29.3	37.2	47.3	57.0	64.3	61.6	52.2	40.8	28.6	17.4	39.2
Highest Mean Min. Temperature (F)	23.3	27.7	36.4	42.7	53.7	63.1	67.9	69.2	58.4	47.2	34.0	26.6	42.6
Year Highest Occurred	1980	1976	1972	1981	1984	1972	1972	1983	1990	1978	1965	1980	1972
Lowest Mean Min. Temperature (F)	0.3	7.8	20.2	31.9	42.9	51.9	60.5	57.1	42.8	34.5	20.6	7.7	35.2
Year Lowest Occurred	1963	1974	1962	1975	1961	1975	1982	1988	1961	1982	1979	1961	1961
Mean Precipitation (in.)	0.75	0.48	0.92	0.75	0.86	0.54	0.76	0.92	0.93	1.02	0.69	0.60	9.22
Highest Precipitation (in.)	2.64	1.79	2.49	1.84	3.20	2.78	3.02	1.91	3.68	3.93	2.09	1.65	14.49
Year Highest Occurred	1978	1962	1978	1985	1973	1969	1965	1961	1982	1972	1978	1972	1965
Lowest Precipitation (in.)	0.00	0.00	0.00	0.00	0.00	0.00	0.00	0.00	0.00	0.00	0.00	0.00	5.41
Year Lowest Occurred	1976	1972	1972	1982	1974	1980	1971	1975	1968	1976	1976	1989	1964

Heating Degree Days (F)	1271.	896.	732.	449.	167.	22.	0.	0.	88.	346.	750.	1141.	5862.
Cooling Degree Days (F)	0.	0.	0.	0.	34.	202.	406.	319.	118.	11.	0.	0.	1090.

Western Regional Climate Center, wrcc@dri.edu

CLIMATOGRAPHY OF THE UNITED STATES NO. 84, 1971-2000

Daily Normals of Temperature, Precipitation, and Heating and Cooling Degree Days

United States Climate Normals 1971-2000

Station Name: THOMPSON UTAH Station Number: 428705

Latitude: 38 58 00 Longitude: -109 43 00 Elevation (feet): 5099

Climate Division: UT 07 Southeast

DECEMBER

Date	MAX	MIN	AVG	HDD	CDD	PRCP
1	45	22	34	31	0	0.02
2	45	22	34	31	0	0.02
3	44	22	33	32	0	0.02
4	44	22	33	32	0	0.01
5	44	21	33	32	0	0.01
6	44	21	32	33	0	0.01
7	43	21	32	33	0	0.02
8	43	20	31	34	0	0.02
9	43	20	31	34	0	0.02
10	42	20	31	34	0	0.02
11	42	19	30	35	0	0.02
12	42	19	30	35	0	0.02
13	41	18	30	35	0	0.02
14	41	17	29	36	0	0.02
15	41	17	29	36	0	0.02
16	41	17	29	36	0	0.02
17	40	17	29	36	0	0.02
18	40	16	28	37	0	0.02
19	40	16	28	37	0	0.02
20	40	16	28	37	0	0.02
21	39	16	28	37	0	0.02
22	39	15	27	38	0	0.02
23	39	15	27	38	0	0.02
24	39	15	27	38	0	0.02
25	39	15	27	38	0	0.02
26	38	15	27	38	0	0.02
27	38	14	26	39	0	0.02
28	38	14	26	39	0	0.02
29	38	14	26	39	0	0.03
30	38	14	26	39	0	0.03
31	38	14	26	39	0	0.03
MTH	40.9	17.6	29.3	1108	0	0.62
WINTER SEASON:			41.6	18.0	29.8	3180	0	2.18

JANUARY

Date	MAX	MIN	AVG	HDD	CDD	PRCP
1	37	14	26	39	0	0.03
2	37	14	25	40	0	0.03
3	37	14	25	40	0	0.03
4	37	14	25	40	0	0.03
5	37	14	25	40	0	0.03
6	37	14	25	40	0	0.03
7	37	14	25	40	0	0.03
8	37	14	25	40	0	0.03
9	37	14	25	40	0	0.03
10	37	13	25	40	0	0.03
11	37	13	25	40	0	0.04
12	37	13	25	40	0	0.04
13	37	13	25	40	0	0.04
14	37	13	25	40	0	0.04
15	37	13	25	40	0	0.04
16	37	13	25	40	0	0.04
17	37	13	25	40	0	0.04
18	37	14	26	39	0	0.03
19	37	14	26	39	0	0.03
20	37	14	26	39	0	0.03
21	38	14	26	39	0	0.03
22	38	14	26	39	0	0.03
23	38	15	27	38	0	0.03
24	38	15	27	38	0	0.03
25	39	15	27	38	0	0.03
26	39	15	27	38	0	0.03
27	39	16	28	37	0	0.03
28	39	16	28	37	0	0.03
29	40	16	28	37	0	0.03
30	40	17	29	36	0	0.03
31	41	17	29	36	0	0.03
MTH	37.7	14.3	26.0	1209	0	1.00

FEBRUARY

Date	MAX	MIN	AVG	HDD	CDD	PRCP
1	41	18	30	35	0	0.02
2	42	18	30	35	0	0.02
3	42	19	30	35	0	0.02
4	42	19	31	34	0	0.02
5	43	19	31	34	0	0.02
6	43	19	31	34	0	0.02
7	44	20	32	33	0	0.02
8	44	20	32	33	0	0.02
9	44	20	32	33	0	0.02
10	45	21	33	32	0	0.02
11	45	21	33	32	0	0.02
12	45	21	33	32	0	0.02
13	46	22	34	31	0	0.02
14	46	22	34	31	0	0.02
15	46	22	34	31	0	0.02
16	47	23	35	30	0	0.02
17	47	23	35	30	0	0.02
18	47	23	35	30	0	0.02
19	48	24	36	29	0	0.02
20	48	24	36	29	0	0.02
21	48	24	36	29	0	0.02
22	49	25	37	28	0	0.02
23	49	25	37	28	0	0.02
24	49	25	37	28	0	0.02
25	50	25	38	27	0	0.02
26	51	25	38	27	0	0.02
27	51	25	38	27	0	0.02
28	51	26	39	26	0	0.02
MTH	46.2	22.1	34.2	863	0	0.56

MARCH

Date	MAX	MIN	AVG	HDD	CDD	PRCP
1	52	27	39	26	0	0.03
2	52	27	39	26	0	0.03
3	53	28	40	25	0	0.03
4	53	28	40	25	0	0.03
5	53	28	40	25	0	0.03
6	53	28	41	24	0	0.03
7	54	28	41	24	0	0.03
8	54	28	41	24	0	0.03
9	55	29	42	23	0	0.03
10	55	29	42	23	0	0.03
11	55	29	42	23	0	0.03
12	56	29	43	22	0	0.03
13	56	30	43	22	0	0.03
14	56	30	43	22	0	0.03
15	56	30	43	22	0	0.04
16	57	30	44	21	0	0.04
17	57	31	44	21	0	0.04
18	57	31	44	21	0	0.04
19	57	31	44	21	0	0.04
20	58	31	45	20	0	0.04
21	58	32	45	20	0	0.04
22	58	32	45	20	0	0.04
23	59	32	46	19	0	0.04
24	59	32	46	19	0	0.04
25	60	32	46	19	0	0.03
26	60	32	46	19	0	0.03
27	60	32	46	19	0	0.03
28	60	33	47	18	0	0.03
29	61	33	47	18	0	0.03
30	61	33	47	18	0	0.03
31	61	33	47	18	0	0.03
MTH	56.7	30.3	43.5	667	0	1.03
SPRING SEASON:			66.2	38.3	52.3	1228	63	2.86

APRIL

Date	MAX	MIN	AVG	HDD	CDD	PRCP
1	62	33	47	18	0	0.03
2	62	34	48	17	0	0.03
3	62	34	48	17	0	0.03
4	62	34	48	17	0	0.03
5	63	35	49	16	0	0.03
6	63	35	49	16	0	0.03
7	63	35	49	16	0	0.03
8	63	35	49	16	0	0.03
9	64	36	50	15	0	0.03
10	64	36	50	15	0	0.03
11	64	36	50	15	0	0.03
12	64	36	50	15	0	0.02
13	65	37	51	14	0	0.02
14	65	37	51	14	0	0.02
15	65	37	51	14	0	0.02
16	66	37	52	13	0	0.02
17	66	38	52	13	0	0.02
18	66	38	52	13	0	0.02
19	67	38	53	12	0	0.03
20	67	38	53	12	0	0.03
21	67	39	53	12	0	0.03
22	67	39	53	12	0	0.03
23	68	39	54	12	1	0.03
24	68	40	54	12	1	0.03
25	69	40	55	11	1	0.03
26	69	40	55	11	1	0.03
27	69	41	55	11	1	0.03
28	70	41	56	10	1	0.03
29	70	41	56	10	1	0.03
30	70	42	56	10	1	0.03
MTH	65.7	37.4	51.6	409	8	0.83

MAY

Date	MAX	MIN	AVG	HDD	CDD	PRCP
1	71	42	57	9	1	0.03
2	72	43	57	8	0	0.03
3	72	43	57	8	0	0.03
4	72	43	57	8	0	0.03
5	72	43	57	8	0	0.03
6	73	44	58	8	1	0.03
7	73	44	59	7	1	0.04
8	74	45	59	7	1	0.04
9	74	45	59	7	1	0.04
10	74	45	60	6	1	0.04
11	74	46	60	6	1	0.04
12	74	46	60	6	1	0.04
13	75	46	61	5	1	0.04
14	75	47	61	5	1	0.04
15	75	47	61	5	1	0.04
16	75	47	61	5	1	0.04
17	76	48	62	5	2	0.03
18	77	48	63	4	2	0.03
19	77	49	63	4	2	0.03
20	77	49	63	4	2	0.03
21	78	49	64	3	2	0.03
22	79	49	64	3	2	0.03
23	79	50	65	3	3	0.03
24	79	50	65	3	3	0.03
25	80	50	65	3	3	0.03
26	80	51	66	2	3	0.03
27	81	51	66	2	3	0.03
28	81	52	67	2	4	0.03
29	81	52	67	2	4	0.02
30	82	52	67	2	4	0.02
31	82	52	67	2	4	0.02
MTH	76.3	47.4	61.9	152	55	1.00

United States Climate Normals 1971-2000

CLIMATOGRAPHY OF THE UNITED STATES NO. 84, 1971-2000

Daily Normals of Temperature, Precipitation, and Heating and Cooling Degree Days

Station Name: THOMPSON UTAH **Station Number:** 428705

Latitude: 38° 58'' 00'' **Longitude:** -109° 43'' 00'' **Elevation (feet):** 5099

Climate Division: UT 07 Southeast

JUNE

Date	MAX	MIN	AVG	HDD	CDD	PRCP
1	83	54	68	2	5	0.02
2	83	54	68	2	5	0.02
3	83	54	68	2	5	0.02
4	84	54	69	1	5	0.02
5	84	55	69	1	5	0.02
6	85	55	70	1	6	0.01
7	85	55	70	1	6	0.01
8	86	55	70	1	6	0.01
9	86	55	70	1	6	0.01
10	86	55	71	1	7	0.01
11	87	55	71	1	7	0.01
12	87	55	71	1	7	0.01
13	87	55	71	1	7	0.01
14	88	56	72	1	8	0.01
15	88	56	72	1	8	0.01
16	88	57	73	0	8	0.01
17	89	57	73	0	8	0.01
18	89	58	74	0	9	0.01
19	89	58	74	0	9	0.01
20	89	58	74	0	9	0.01
21	90	58	74	0	9	0.01
22	90	59	75	0	10	0.01
23	90	59	75	0	10	0.01
24	91	59	75	0	10	0.01
25	91	59	75	0	10	0.01
26	91	60	76	0	11	0.01
27	91	60	76	0	11	0.01
28	92	60	76	0	11	0.01
29	92	60	76	0	11	0.01
30	92	61	77	0	12	0.01
MTH	87.9	56.9	72.4	18	241	0.35

JULY

Date	MAX	MIN	AVG	HDD	CDD	PRCP
1	92	61	77	0	12	0.01
2	93	62	77	0	12	0.02
3	93	62	77	0	12	0.02
4	93	62	77	0	12	0.02
5	93	62	78	0	13	0.02
6	93	63	78	0	13	0.02
7	93	63	78	0	13	0.02
8	93	63	78	0	13	0.02
9	93	63	78	0	13	0.02
10	94	63	79	0	14	0.02
11	94	63	79	0	14	0.02
12	94	64	79	0	14	0.02
13	94	64	79	0	14	0.02
14	94	64	79	0	14	0.02
15	94	64	79	0	14	0.02
16	94	64	79	0	14	0.03
17	94	64	79	0	14	0.03
18	94	64	79	0	14	0.03
19	94	64	79	0	14	0.03
20	94	64	79	0	14	0.03
21	94	64	79	0	14	0.03
22	94	64	79	0	14	0.03
23	95	65	80	0	15	0.03
24	95	65	80	0	15	0.03
25	95	65	80	0	15	0.03
26	94	64	79	0	14	0.03
27	94	64	79	0	14	0.03
28	94	64	79	0	14	0.03
29	94	64	79	0	14	0.03
30	94	64	79	0	14	0.03
31	94	64	79	0	14	0.03
MTH	93.8	63.6	78.7	0	424	0.77
SUMMER SEASON:	91.1	60.8	76.0	18	1030	2.00

AUGUST

Date	MAX	MIN	AVG	HDD	CDD	PRCP
1	94	64	79	0	14	0.03
2	94	64	79	0	14	0.03
3	94	64	79	0	14	0.03
4	94	64	79	0	14	0.03
5	94	64	79	0	14	0.03
6	94	64	79	0	14	0.03
7	93	64	79	0	14	0.03
8	93	64	78	0	13	0.03
9	93	64	78	0	13	0.03
10	93	64	78	0	13	0.03
11	93	63	78	0	13	0.02
12	93	63	78	0	13	0.02
13	93	63	78	0	13	0.02
14	92	62	77	0	12	0.02
15	92	62	77	0	12	0.02
16	92	62	77	0	12	0.03
17	92	62	77	0	12	0.03
18	92	62	77	0	12	0.03
19	91	61	76	0	11	0.03
20	91	61	76	0	11	0.03
21	91	61	76	0	11	0.03
22	91	61	76	0	11	0.03
23	90	61	76	0	11	0.03
24	90	60	75	0	10	0.03
25	90	60	75	0	10	0.03
26	89	60	75	0	10	0.03
27	89	59	74	0	9	0.03
28	89	59	74	0	9	0.03
29	88	59	74	0	9	0.03
30	88	59	74	0	9	0.03
31	88	58	73	0	8	0.03
MTH	91.6	61.9	76.8	0	365	0.88

SEPTEMBER

Date	MAX	MIN	AVG	HDD	CDD	PRCP
1	88	58	73	0	8	0.03
2	87	58	73	0	8	0.03
3	87	58	72	0	7	0.03
4	86	58	72	0	7	0.03
5	86	58	72	0	7	0.03
6	86	58	72	0	7	0.03
7	85	58	71	0	6	0.03
8	85	56	70	1	6	0.03
9	85	55	70	1	6	0.03
10	84	54	69	1	5	0.03
11	84	54	69	1	5	0.03
12	84	54	69	1	5	0.03
13	83	54	69	1	5	0.03
14	83	53	68	1	4	0.03
15	82	53	68	1	4	0.03
16	82	53	68	1	4	0.03
17	82	52	67	2	4	0.03
18	81	52	67	2	4	0.03
19	81	51	66	2	3	0.04
20	81	51	66	2	3	0.04
21	80	51	66	2	3	0.04
22	80	50	65	3	3	0.04
23	79	50	65	3	3	0.04
24	79	49	64	3	2	0.04
25	79	49	64	3	2	0.04
26	78	49	64	3	2	0.04
27	78	48	63	4	2	0.04
28	77	48	63	4	2	0.04
29	77	47	62	5	2	0.04
30	77	47	62	5	2	0.04
MTH	82.2	52.9	67.6	52	131	1.02
AUTUMN SEASON:						
ANNUAL:						

OCTOBER

Date	MAX	MIN	AVG	HDD	CDD	PRCP
1	76	47	61	5	1	0.04
2	76	47	61	5	1	0.04
3	75	47	61	5	1	0.04
4	75	46	60	6	1	0.04
5	75	46	60	6	1	0.04
6	74	45	59	7	1	0.04
7	74	44	59	7	1	0.04
8	73	43	58	8	1	0.04
9	73	43	58	8	1	0.04
10	72	43	58	8	1	0.04
11	72	43	58	8	1	0.04
12	71	42	57	8	0	0.04
13	71	41	56	9	0	0.04
14	70	41	56	9	0	0.04
15	70	40	55	10	0	0.04
16	69	40	55	10	0	0.04
17	69	39	54	11	0	0.04
18	68	39	54	11	0	0.04
19	67	39	53	12	0	0.04
20	67	39	53	12	0	0.04
21	66	38	52	13	0	0.04
22	66	38	52	13	0	0.04
23	65	37	51	14	0	0.04
24	65	37	51	14	0	0.04
25	64	36	50	15	0	0.04
26	64	36	50	15	0	0.04
27	63	35	49	16	0	0.04
28	62	35	49	16	0	0.04
29	62	34	48	17	0	0.04
30	61	34	48	17	0	0.04
31	60	34	47	18	0	0.03
MTH	68.9	40.3	54.6	333	11	1.23
AUTUMN SEASON:	67.7	40.4	54.1	1135	142	2.93
ANNUAL:	66.7	39.4	53.1	5561	1235	9.97

NOVEMBER

Date	MAX	MIN	AVG	HDD	CDD	PRCP
1	60	34	47	18	0	0.03
2	59	34	46	19	0	0.03
3	59	34	46	19	0	0.03
4	58	33	45	20	0	0.03
5	57	33	45	20	0	0.03
6	57	32	44	21	0	0.03
7	56	32	44	21	0	0.03
8	55	31	43	22	0	0.03
9	55	31	43	22	0	0.02
10	54	30	42	23	0	0.02
11	54	30	42	23	0	0.02
12	53	29	41	24	0	0.02
13	53	29	41	24	0	0.02
14	52	29	41	24	0	0.02
15	52	28	40	25	0	0.02
16	51	28	40	25	0	0.02
17	51	27	39	26	0	0.02
18	50	27	39	26	0	0.02
19	50	26	38	27	0	0.02
20	50	26	38	27	0	0.02
21	49	25	37	28	0	0.02
22	49	25	37	28	0	0.02
23	48	25	37	28	0	0.02
24	48	24	36	29	0	0.02
25	47	24	36	29	0	0.02
26	47	23	35	30	0	0.02
27	47	23	35	30	0	0.02
28	46	23	35	30	0	0.02
29	46	22	34	31	0	0.02
30	46	22	34	31	0	0.02
MTH	52.0	28.0	40.0	750	0	0.68

CLIMATOGRAPHY OF THE UNITED STATES NO. 84, 1971-2000

Daily Normals of Temperature, Precipitation, and Heating and Cooling Degree Days

United States Climate Normals 1971-2000

Station Name: THOMPSON UTAH **Station Number:** 428705

Latitude: 38° 58' 00" **Longitude:** -109° 43' 00" **Elevation (feet):** 5099

Climate Division: UT 07 Southeast

PRECIPITATION PROBABILITIES

Probability	JAN	FEB	MAR	APR	MAY	JUN	JUL	AUG	SEP	OCT	NOV	DEC	ANNUAL
0.005	0.00	0.00	0.00	0.00	0.00	0.00	0.00	0.00	0.02	0.00	0.00	0.00	5.19
0.010	0.00	0.00	0.00	0.00	0.00	0.00	0.00	0.00	0.03	0.00	0.00	0.00	5.55
0.050	0.00	0.01	0.00	0.10	0.00	0.00	0.00	0.06	0.11	0.06	0.08	0.00	6.63
0.100	0.20	0.05	0.00	0.21	0.12	0.00	0.06	0.15	0.18	0.18	0.17	0.12	7.26
0.200	0.41	0.12	0.35	0.34	0.30	0.11	0.19	0.29	0.32	0.36	0.29	0.25	8.07
0.300	0.57	0.20	0.53	0.46	0.46	0.17	0.31	0.42	0.47	0.55	0.38	0.34	8.70
0.400	0.72	0.29	0.70	0.58	0.62	0.23	0.44	0.55	0.62	0.74	0.48	0.44	9.26
0.500	0.88	0.39	0.87	0.71	0.80	0.29	0.59	0.70	0.79	0.95	0.59	0.54	9.80
0.600	1.05	0.52	1.07	0.85	1.00	0.36	0.75	0.87	1.00	1.21	0.70	0.65	10.37
0.700	1.25	0.68	1.31	1.02	1.25	0.45	0.96	1.08	1.25	1.52	0.84	0.77	10.99
0.800	1.52	0.90	1.61	1.24	1.58	0.55	1.24	1.37	1.60	1.94	1.03	0.94	11.76
0.900	1.95	1.29	2.10	1.60	2.12	0.73	1.71	1.83	2.17	2.64	1.32	1.21	12.88
0.950	2.35	1.67	2.56	1.93	2.64	0.89	2.17	2.28	2.73	3.33	1.60	1.47	13.85
0.990	3.23	2.55	3.58	2.68	3.82	1.26	3.21	3.30	4.00	4.87	2.22	2.03	15.81
0.995	3.59	2.92	4.01	2.99	4.31	1.42	3.65	3.73	4.54	5.53	2.48	2.26	16.57

PRECIPITATION QUINTILES

Level	JAN	FEB	MAR	APR	MAY	JUN	JUL	AUG	SEP	OCT	NOV	DEC
0 <	0.00	0.00	0.00	0.00	0.00	0.00	0.00	0.35	0.00	0.00	0.00	0.00
1	0.00	0.00	0.00	0.00	0.00	0.00	0.00	0.35	0.00	0.00	0.00	0.00
	0.13	0.31	0.23	0.05	0.00	0.00	0.73	0.97	0.15	0.30	0.03	0.13
2	0.14	0.32	0.24	0.06	0.01	0.00	0.74	0.98	0.16	0.31	0.04	0.14
	0.42	1.06	0.61	0.28	0.28	0.06	1.58	1.84	0.89	0.58	0.39	0.29
3	0.43	1.07	0.62	0.29	0.29	0.07	1.59	1.85	0.90	0.59	0.40	0.30
	1.19	1.43	1.19	0.47	0.59	0.15	2.07	2.43	1.68	1.01	0.64	0.72
4	1.20	1.44	1.20	0.48	0.60	0.16	2.08	2.44	1.69	1.02	0.65	0.73
	1.71	2.19	2.05	0.88	0.86	0.80	3.11	3.35	2.53	1.38	1.85	1.79
5	1.72	2.20	2.06	0.89	0.87	0.81	3.12	3.36	2.54	1.39	1.86	1.80
	4.82	4.27	4.22	2.29	2.25	2.62	6.49	7.90	8.60	7.10	3.81	3.19
6 >	4.82	4.27	4.22	2.29	2.25	2.62	6.49	7.90	8.60	7.10	3.81	3.19

Abbreviations:

MAX = Maximum Temperature (degrees Fahrenheit)
MIN = Minimum Temperature (degrees Fahrenheit)
AVG = Average Temperature (degrees Fahrenheit)

NOTES

HDD = Heating Degree Days (base 65)
CDD = Cooling Degree Days (base 65)
PRCP = Precipitation Amount (inches)

MTH = Monthly Means / Totals
SEASON = Seasonal Means / Totals
ANNUAL = Annual Means / Totals

This publication presents daily temperature, precipitation, and heating and cooling degree day normals for stations based on the 1971-2000 record *adjusted* to the present station location. Stations contained in the monthly normals (Climatography of the United States No. 81) are included. Precipitation-only stations have no data in the temperature and degree day fields on Pages 1 and 2. Latitude and longitude values are presented in DD MM SS, where DD=Degrees, MM=Minutes, and SS=Seconds. Small differences between monthly values in this publication and the monthly normals presented in Climatography of the United States No.81 are attributable to smoothing techniques applied to this data set, as described below.

Daily Normals Tables:

The daily values presented in these tables are not simple means of the observed daily values. They are interpolated from the much less variable monthly normals by use of the natural spline function. The procedure involved constructing a cumulative series of monthly sums from the monthly normals. The cumulative series was for a 24-month period (July, August, ..., December, January, ..., December, January, ..., June), so that the interpolating function could adequately fit the end points in the annual series. This process was applied independently to all six elements. No normal values for February 29 are included; in common practice, the normal values for the 28th are used for the 29th in each leap year. Thus, for leap years, the February monthly total degree days or precipitation are calculated by adding the daily value for the 28th to the monthly total. February temperature averages are likewise not adjusted for leap years. For most stations, the monthly heating and cooling degree day normals (base 65 degrees Fahrenheit) are derived from monthly normal temperature using an estimation technique developed by H.C.S. Thom. An asterisk (*) for a daily degree day value indicates a daily normal of less than one degree day, but not equal to zero. Seasonal means / totals correspond to the three months listed immediately above.

Precipitation Probabilities and Quintiles Tables:

The precipitation probabilities are the monthly precipitation totals that correspond to the indicated probability levels. The probability levels are based on the 1971-2000 historical sequential monthly precipitation. The historical precipitation data are the adjusted values from the monthly normals (Climatography of the United States No. 81).

When historical climate data are accumulated and examined, they generally follow a certain pattern called a statistical distribution. While temperature usually follows a Gaussian or bell-shaped distribution, precipitation does not because it is zero-bounded. Precipitation generally follows a Gamma distribution, where most values are near zero with rapidly diminishing higher values. Thus, the Gamma distribution was used to estimate the precipitation values in the probability and quintile tables published above. The probability table shows the amount of precipitation expected at fifteen probability levels (0.005, 0.01, 0.05, 0.10, 0.20, 0.30, 0.40, 0.50, 0.60, 0.70, 0.80, 0.90, 0.95, 0.99, and 0.995) for each month of the year and for the annual total. For example, if 1.77 inches corresponds to the 0.20 probability level, that means that on average, 2 out of 10 years will have 1.77 inches *or less* of precipitation in that month. It also means that, on average, 8 out of 10 years will have *more than* 1.77 inches of precipitation in that month.

The precipitation quintiles show the expected precipitation values at the five quintile levels for each of the twelve months: 1. First Quintile (0-20%); 2. Second Quintile (20-40%); 3. Third Quintile (40-60%); 4. Fourth Quintile (60-80%); 5. Fifth Quintile (80-100%). For example, if 2.91 and 4.07 inches are the bounds for the second quintile (level 2), then a monthly total precipitation amount for that month falling in the range 2.91 to 4.07 would be classified as a second quintile precipitation amount and that month would be considered relatively dry. The first line (level 0 <) in the table shows the minimum precipitation value derived from the historical record. Quintile level 0 would be used if a future precipitation observation is less than the 1971-2000 value. Level 6 > would be used if the observed value is more than the 1971-2000 maximum.

Release Date: December 1, 2001 **National Climatic Data Center/NESDIS/NOAA, Asheville, North Carolina**

JACOBS	Calculation No: C-15	Page: 1 of 8
Calculation Cover Sheet	Rev. No.: 3	Revision Date: 7/11/08
(Ref. FOWI 116 Design Calculations)	Previous Revision Date: 6/9/08	Current Revision Date: 7/11/08
Issuing Department: *Federal Operations Design Engineering*	Supersedes: Revision 2 (dated 6/9/08)	
Client: Project Title: MOAB UMTRA Project Project Number: 35DJ2600 System:	Engineering Discipline: Geotechnical	

Calculation Title: Analysis for Cover Cracking of the Crescent Junction Disposal Cell

Purpose:

The uranium mill tailings which will be placed at the Crescent Junction Disposal Site are to be stabilized and controlled by placement in an encapsulated disposal cell. The cover of the disposal cell serves to prevent the escape of radon from the tailings pile as well as to inhibit infiltration to the tailings. Cracking of the disposal cell cover can adversely impact the ability to achieve those two purposes.

Calculations for potential cracking of the disposal cell cover had previously been prepared by others for the preliminary design of the Crescent Junction disposal cell and included in the RAP Attachment 1: Disposal Cell Design Specs, Appendix D.

The purpose of the attached calculation is to make an independent assessment of the potential for cracking of the Crescent Junction disposal cell cover to occur, given the anticipated materials to be used, the most recent proposed disposal cell geometry configuration, and the calculated total and differential settlements of the cell cover.

NQA-1 Quality Level - 2

Prepared by: AHMAD HASAN (Per Verbal Approval) Date: 7-30-08

Checked by: KURT BETTGER (Per Verbal Approval) Date: 7-30-08

Engineering Managers Approval: [signature] for BILL BARTON Date: 7-30-08

The current applicable version of this publication resides on Jacobs' Intranet. All copies are considered to be uncontrolled.
Copyright© Jacobs Engineering Group Inc., 2007

Revision History:

Pages Affected By Revision	Revised/Added/Deleted	Description of Revision
Rev. 1	Revision Page 4 of 13 Assumptions	Due to changes in the tailings pile geometry from the 60% to the 90% drawings, the following assumptions were changed: Tailings thickness: 46.7 ft (instead of 38 ft) Cover thickness: 9 ft (instead of 10 ft) 2(H):1(V) slope for the lower 27 ft of tailings (instead of lower 18 ft of tailings) Total settlement: 19 in. (instead of 17 in.)
	Revision Page 5 of 13 Design Input	Tailings thickness: 46.7 ft (instead of 38 ft) Total Settlement: 19 in. (instead of 17 in.) Length between differential settlement: 114 ft (instead of 96 ft)
	Revision Page 6 of 13 Calculation Section	Distortion (Δ/L) = 0.014 (instead of 0.015)
	Revision Page 7 of 13 Hand-Written Calculation Sheet	Same changes to tailings pile geometry as listed above.
Rev. 2	Revision Page 7 of 13 Hand-Written Calculation Sheet	Revised conclusion statement for clarification. "Maximum cover strain is less than allowable (0.014% < 0.065%)".
Rev. 3	Revision Page 7 of 13 Hand-Written Calculation Sheet	Revised conclusion statement to read: Maximum covered strain calculated for a distortion of 0.014 is less than the allowable strain.

The current applicable version of this publication resides on Jacobs' Intranet. All copies are considered to be uncontrolled.
Copyright© Jacobs Engineering Group Inc., 2007

Description of Calculation:

Depending on actual amounts occurring at a given site, total and differential settlement of a tailings pile can lead to cracking of the disposal cell cover (EPA, 1991). Settlement analyses have already been performed to determine total settlement (primary and secondary) of the cover for the current disposal cell design. The potential for cracking is assessed by comparing the horizontal tensile strains computed for the estimated total settlement of the cover to the strains required to cause cracking in the cover materials. Magnitude of differential settlement will be between zero (0) and the computed value for maximum total settlement.

This calculation evaluates the potential for cracking to occur due to differential settlement in the low permeability earthen layer of the disposal cell cover.

Evaluation of the allowable strain for the earthen cover material is based on the premise that there is an empirical relationship between the plasticity of the soil layer and the allowable strain for that material (Claire et al, and Caldwell and Reith):

$e_f = 0.05 + 0.003\ PI$,

where PI = plasticity index of the cover soil; and

e_f = allowable cover strain at failure (in percent)

Given the plasticity characteristics of the material, a lower bound limit for tensile strain that would result in failure can be calculated and the results compared with an established range of maximum tensile strain at failure for that type of material.

Evaluation of the strain required to cause cracking in the cover material is based on the premise that there is a relationship between distortion, which is defined as the differential settlement between two points divided by the horizontal distance between the two points (Δ/L), and the tensile strain in the cover materials. As the distortion increases, the tensile strain in the cover also increases.

Design input for these calculations includes the type of soil, the plasticity index of the soil, the differential settlement along the inside slope of the embankment, and the horizontal distance between the toe and crest of the inside slope of the embankment.

The current applicable version of this publication resides on Jacobs' Intranet. All copies are considered to be uncontrolled.
Copyright© Jacobs Engineering Group Inc., 2007

Assumptions:

1. Relationship between allowable cover strain at failure and plasticity index of soil exists per references as follows: $e_f = 0.05 + 0.003$ PI, where PI = plasticity index of the cover soil and e_f = allowable cover strain at failure.

2. Current disposal cell design includes a tailings thickness of 46.7 ft; a 9 ft thick cover; an embankment with an inside slope of 3(H):1(V) for the upper 20 ft of tailings and slope of 2(H):1(V) for the lower 27 ft of tailings.

3. The location of maximum differential settlement is along the inside slope of the embankment (horizontal distance along inside slope from top to bottom of tailings).

4. Design calculations for the current disposal cell geometry indicate a total settlement of 19 inches (1.58 feet).

5. For compacted clayey soils, the maximum tensile strain at failure range from 0.1 to 1 percent (Gilbert and Murphy).

The current applicable version of this publication resides on Jacobs' Intranet. All copies are considered to be uncontrolled.
Copyright© Jacobs Engineering Group Inc., 2007

Design Inputs:

Soil Type 1: Silty clay (alluvial)
Plasticity Index: 5

Soil Type 2: weathered Mancos Shale
Plasticity Index: 10

Tailings Thickness: 46.7 feet (tailings saturated)

Total Settlement: 19in. (= 1.58 ft)
Differential Settlement: 0 to 19 in., assume 19 in. (= 1.58 ft) as worst case

Length between differential settlement: 114 ft (see sketch on calculation page)

Software:

Title	Developer	Versions	Revision Level
Not Applicable			

The current applicable version of this publication resides on Jacobs' Intranet. All copies are considered to be uncontrolled.
Copyright© Jacobs Engineering Group Inc., 2007

Calculation Section:

See attached calculations.

For comparison of allowable cover strain at failure for the cover materials, it was assumed that the alluvial material properties (worst case) would govern.

Based on published ranges of maximum tensile strain at failure for clayey soils, taking the lower value with a factor of safety of 2 results in an allowable tensile strain of 0.05%.

The allowable tensile strain for the proposed alluvial cover material (worst case) is 0.065%.

For the given embankment inside slope configuration, the distortion, (Δ/L) = 0.014.

From Figure 2-16 in EPA/625/4-91/025, the graphical relationship between distortion and tensile strain indicates the tensile strain for a distortion of 0.014 is < 0.1%.

The current applicable version of this publication resides on Jacobs' Intranet. All copies are considered to be uncontrolled.
Copyright© Jacobs Engineering Group Inc., 2007

EVALUATION OF DISPOSAL CELL COVER CRACKING

CHECK FOR ALLOWABLE STRAIN FOR COVER MATERIAL

FOR CLAYEY SOILS, MAXIMUM TENSILE STRAIN AT FAILURE 0.1% TO 1.0%

(GILBERT & MURPHY)

USE LOWER VALUE WITH FACTOR OF SAFETY OF 2 FOR THIS ANALYSIS

ALLOWABLE TENSILE STRAIN = 0.1%/2 = 0.05%

ALLOWABLE STRAIN = 0.05 + 0.003 PI (CLAIRE, KUO & WANKET)
FROM RAP, ATTACHMENT 1, APPENDIX E.

PI FOR SILTY SAND CLAY (CL) = 5
PI FOR MUNCOS SHALE = 10
USE PI = 5

ASSUME PI = 5

ALLOWABLE STRAIN = 0.05 + 0.003×5 = 0.065%

CHECK FOR STRAIN DUE TO DIFFERENTIAL SETTLEMENT OF COVER

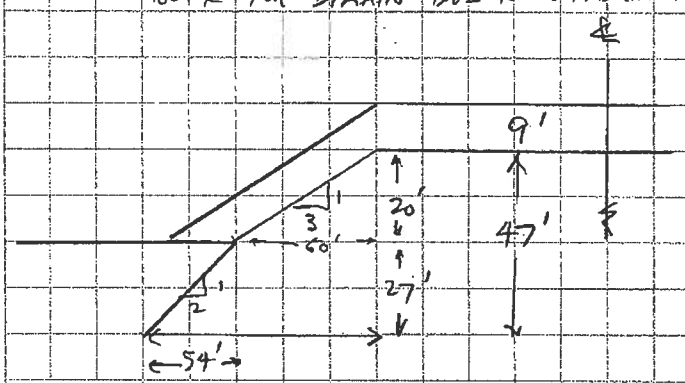

L = 114'

Δ = TOTAL SETTLEMENT
= 19" = 1.58', FROM EARLIER CALCS

$\Delta/L = \frac{1.58}{114} = 0.014$

FROM EDA FIG 2-16
FOR $\Delta/L \approx 0.014$, TENSILE STRAIN 0.01 - 0.1

MAXIMUM COVER STRAIN CALCULATED FOR A DISTORTION OF 0.014 IS LESS THAN THE ALLOWABLE STRAIN.

BASED ON CALCULATED SETTLEMENT, COVER IS NOT ANTICIPATED TO CRACK

Conclusions/Recommendations:

The results of the cover cracking analysis show that the maximum calculated tensile stresses in the cover due to differential settlement are less than or equal to the allowable stresses for the cover earthen materials. Calculations were made for the worst case where differential settlement is equal to the total settlement.

The results of the analyses indicate that cracking of the cover layer will not occur due to differential settlement of the tailings.

Reference:

United States Environmental Protection Agency, Office of Research and Development, (May 1991) EPA/625/4-91/025, "Design and Construction of RCRA/CERCLA Final Covers." Seminar Publication.

Caldwell, J.A., Wathen, T.R., and D'Antonio, J.R., "Criteria for Remedial Work at Inactive Uranium Mill Tailings Piles".

U.S. Army Corps of Engineers Technical Letter No. ETL 1110-1-162, "Engineering and Design, Checklist for Hazardous Waste Landfill Cover Design", September, 2001.

Claire, Robert F., Kuo, Jason C., and Wanket, Daniel R. (1994), "Evaluation of the Cover Cracking Potential Due to Ground Subsidence at UMTRA Project Disposal Cells."

Gilbert, P.A. and W.L. Murphy (1987). "Prediction/Mitigation of Subsidence Damage to Hazardous Waste Landfill Covers." EPA/600/2-87/025 (PB87-175386), Cincinnati, Ohio: U.S. EPA.

The current applicable version of this publication resides on Jacobs' Intranet. All copies are considered to be uncontrolled.
Copyright© Jacobs Engineering Group Inc., 2007